



City Research Online

City, University of London Institutional Repository

Citation: Yiallouras, C. (2015). Design of a 2D MRI compatible robot for performing prostate cancer treatment using therapeutic ultrasound. (Unpublished Doctoral thesis, City University London)

This is the accepted version of the paper.

This version of the publication may differ from the final published version.

Permanent repository link: <https://openaccess.city.ac.uk/id/eprint/14485/>

Link to published version:

Copyright: City Research Online aims to make research outputs of City, University of London available to a wider audience. Copyright and Moral Rights remain with the author(s) and/or copyright holders. URLs from City Research Online may be freely distributed and linked to.

Reuse: Copies of full items can be used for personal research or study, educational, or not-for-profit purposes without prior permission or charge. Provided that the authors, title and full bibliographic details are credited, a hyperlink and/or URL is given for the original metadata page and the content is not changed in any way.



**Design of a 2D MRI compatible robot for
performing prostate cancer treatment using
therapeutic ultrasound.**

Christos Yiallouras

This dissertation is submitted for the degree of Doctor of Philosophy

Department of Electrical, Electronic Engineering
City University London

January 2015



**THE FOLLOWING PART OF THIS THESIS HAS BEEN
REDACTED FOR COPYRIGHT REASONS:**

p 12: **Fig 2.3.** Zones of the prostate gland image.

Abstract

Therapeutic ultrasound is a promising treatment method for many common cancers, including prostate cancer. Magnetic resonance image (MRI) guidance of therapeutic ultrasound permits targeting and monitoring of therapy. In this thesis a prototype MRI compatible positioning device for the treatment of prostate cancer using therapeutic ultrasound is presented. The accuracy, MRI compatibility and functionality of the positioning device was evaluated in in vitro experiments (using gel phantoms and in vitro). The MRI was used as the imaging guidance technique. The proposed device incorporates a portable electronic system and operates in two PC controlled stages, linear and angular ($X - \Theta$) and one manual driven stage Z (height of the probe). The device is small and portable and can be placed on the patient's table to any commercial MRI scanner. The proposed device was tested on two clinical MRI scanners of different manufacturers. Additionally, in this thesis a software that controls an MRI guided focus ultrasound system is presented. The software was written in C sharp and consists of the following options: a) connection with DAQ device, b) tab that controls 2D device, c) tab that controls 3D device, d) tab that controls ultrasound protocol and e) operation command history list, g) MRI compatible camera, h) open and control the DICOM images captured from the MRI scanner during the therapy, i) temperature reading of the HIFU focal point.

The proposed positioning device offers approximately $20\mu\text{m}$ accuracy on linear and angular stages. It incorporates MRI compatible optical encoders as mechanical motion feedback. The accuracy measurements were taken using a digital calibre. The positioning device has range of 111mm in linear stage, $\pm 90^\circ$ on angular stage and 50mm on Z stage. The design was based on measurements that were taken by a 100 patients. The MRI compatibility and motion accuracy images were taken by scanning gel phantoms using T2W FSE on 1.5T and 3T MRI scanner.

Acknowledgments

I thank in advance all the people that helped to implement all the tasks during this research. Especially, I thank my advisors, Prof. Christakis Damianou and Prof. Panayiotis Kyriacou, for their guidance during my research studies at City University. Also I thank them for their co-operation to the completion of my research work. They were positive and ready to help me during of my research.

List of Contents

ABSTRACT	I
ACKNOWLEDGMENTS.....	II
LIST OF CONTENTS.....	III
LIST OF FIGURES	VIII
LIST OF TABLES	XII
ABBREVIATIONS	XIII
1. CHAPTER: INTRODUCTION.....	1
1.1. Introduction to the proposed application.....	1
1.2. Aim and Objectives	6
1.3. Chapters Outline	6
2. CHAPTER: ANATOMY, PHYSIOLOGY AND PATHOLOGY OF THE PROSTATE GLAND	9
2.1. Introduction	9
2.2. Prostate Gland	9
2.3. Prostate Functionality	10
2.4. Anatomy of the prostate gland.....	11
2.5. Surrounding functions of the prostate.....	12
2.6. Pathology - Prostate cancer.....	15
2.7. Prostate cancer symptoms	15
2.8. Prostate Cancer Statistics	16
3. CHAPTER: THERAPIES FOR PROSTATE CANCER	17
3.1. Introduction	17

3.2.	Diagnostic methods of prostate cancer	17
3.2.1.	Active surveillance	20
3.3.	Therapies of prostate cancer	21
3.3.1.	Hormonal Therapy	21
3.3.2.	Radical prostatectomy	22
3.3.3.	Laparoscopic prostatectomy	22
3.3.4.	Brachy therapy.....	23
3.3.5.	Cryotherapy	24
3.3.6.	Photodynamic therapy	26
3.3.7.	Microwave thermal therapy	27
3.3.8.	Transurethral ultrasound therapy	28
3.3.9.	HIFU	28
3.4.	Conclusion	29
4.	CHAPTER: HIGH INTENSITY FOCUS ULTRASOUND	30
4.1.	Introduction	30
4.2.	History of HIFU	30
4.3.	Physical Principles of HIFU	31
4.4.	Prostate Cancer – Clinical trials using HIFU devices	33
4.5.	HIFU – Image Guidance.....	35
4.5.1.	Ultrasound Imaging.....	35
4.5.2.	Magnetic Resonance Imaging – MRI.....	36
5.	CHAPTER: THE CURRENT STATE OF ART IN MRI COMPATIBLE ROBOTIC SYSTEMS.....	37
5.2.	MRI Compatible Materials.....	37
5.3.	MRI Compatible Actuators and Sensors.....	38
5.4.	MRI Compatible positioning sensors	39
5.5.	MRI guided HIFU positioning devices	39
5.6.	MRI guided devices - Other applications	46
5.7.	Conclusion.....	49
6.	CHAPTER: DESIGN AND DEVELOPMENT OF THE POSITIONING DEVICE FOR PROSTATE CANCER TREATMENT USING HIFU.....	50
6.1.	Introduction	50

6.2.	Measurements of the prostate size	50
6.3.	Mechanical system of the positioning device	53
6.4.	Design and development of the 2D MRI compatible robot positioning device	54
6.5.	Conclusion and discussion	62
7.	CHAPTER: CLOSE – LOOP FEEDBACK USING MRI COMPATIBLE ENCODERS	64
7.1.	Introduction	64
7.2.	Optical Encoders – Control of linear and angular motion	64
7.3.	Close - loop control system design	66
7.4.	Design of the close loop feedback control system of Θ axis motion	67
7.5.	Design of the close loop feedback control system of X axis motion	68
7.6.	Control of Optical Encoders using software platform	70
7.7.	Conclusion	73
8.	CHAPTER: ELECTRONIC SYSTEM OF THE MRI COMPATIBLE POSITIONING DEVICE	74
8.1.	Piezoelectric Ultrasonic Motors (PUM) and Their Drivers	74
8.2.	Robot drivers	78
8.3.	Parts and Specifications of Drivers	80
8.4.	Development of Drivers for the Positioning Device	82
9.	CHAPTER: DESIGN AND DEVELOPMENT OF SOFTWARE FOR CONTROLLING AN MRI GUIDED FOCUS ULTRASOUND ROBOT ASSISTED SYSTEM	91
9.1.	Introduction	91
9.2.	System Architecture	91
9.2.1.	Architecture Design	91
9.2.2.	Decomposition Diagram	92
9.2.3.	Data Flow Diagram	94
9.3.	Human Interface Design	95
9.3.1.	Design of Ultrasound control panel interface (GUI)	95
9.3.2.	Design of MRI compatible camera control panel - GUI	96

9.3.3.	Design of MRI images control panel – GUI	97
9.3.4.	Design of Select directory panel - GUI	98
9.3.5.	Design of robot control panel – GUI	98
9.3.6.	Design of command history panel – GUI	99
9.3.7.	Design of Patient’s Data Form (GUI).....	100
9.3.8.	Design of single software platform.....	101
9.4.	Development of Software Platform using MATLAB (Version One).....	102
9.5.	Ultrasound Control Panel	103
9.6.	Implementation of the ultrasound control panel	103
9.7.	Parameters needed for implementing ultrasound control panel	104
9.8.	Functions developed for implementing ultrasound panel	105
9.9.	Agilent Generator commands for ultrasound control panel	107
9.10.	Display information about the selected transducer.....	109
4.5.3.	Ultrasound Control Panel - GUI Test.....	110
9.11.	Timer	111
9.12.	MRI Compatible Camera Control Panel	113
9.12.1.	Parts for implementing camera control panel.....	113
9.12.2.	Parameters needed for implementing the camera control panel.....	114
9.12.3.	Functions developed for implementing the camera control panel.....	114
9.13.	MRI images.....	116
9.13.1.	Parameters needed for implementing MRI images panel.....	117
9.13.2.	Functions used for implementing this MRI images panel	117
9.14.	Parts for implementing robot movement actuation	119
9.14.1.	Data acquisition board.....	119
9.15.	Functions used for implementing robot movements	120
9.15.1.	Date acquisition Register Command	120
9.15.2.	Motor Movements (X – Θ axes).....	121
9.15.3.	Motor – Get Counter Value	123
9.15.4.	Robot initial and current position.....	126
9.16.	Application Command History.....	127
9.16.1.	Functions used for implementing command history.....	127
9.17.	Interconnection between the electronic devices	127
9.18.	Patient Data Form	128
9.18.1.	Data files	129
9.18.2.	Design of Patient Data GUI	130
9.18.3.	OLEDB Connection	131

9.18.4.	Query Database	131
9.18.5.	Query Language – SQL.....	133
9.19.	Development of software platform using C Sharp	134
9.20.	Control of the devices using C Sharp.....	135
9.21.	Control of HIFU Generator RFG 1000	135
9.22.	Temperature readings using thermocouple.....	137
9.23.	Final Version of the software platform	139
9.24.	Discussion and Conclusion.....	146
10.	CHAPTER: EVALUATION OF 2D MR COMPATIBLE POSITIONING DEVICE FOR GUIDING A FOCUSED ULTRASOUND SYSTEM FOR TRANS- RECTAL TREATMENT OF PROSTATE CANCER.	148
10.1.	Introduction.....	148
10.2.	Materials and Methods.....	148
10.2.1.	Focused ultrasound system	148
10.2.2.	MRI processing.....	148
10.2.3.	In vitro experiments.....	149
10.2.4.	Experiment setup (Lab).....	150
10.3.	Results	151
10.3.1.	MRI Compatibility Tests	153
10.3.2.	Positioning Device Accuracy Tests	158
10.4.	Conclusion and discussion	163
10.	CHAPTER: CONCLUSION AND FUTURE EXPANSIONS.....	164
10.1.	Conclusion	164
10.2.	Future Expansions.....	167
	APPENDIX.....	168
	REFERENCES	219

List of Figures

Figure 2.1: Prostate gland and surroundings organs [25] 10

Figure 2.2: Prostate Lobes [26] 11

Figure 2.3: Zones of the prostate gland [25]..... 12

Figure 2.4: Cancerous cells are divided uncontrollably [26]..... 15

Figure 3.1: A doctor performs a rectal exam [54]..... 18

Figure 3.2: Ultrasound prostate examination [57]..... 19

Figure 3.3: MRI prostate examinations [58]..... 19

Figure 3.4: Robotic assisted laparoscopic radical prostatectomy [38]..... 23

Figure 3.5: Ice is placed on cancerous cells [59]..... 25

Figure 3.6: Cryotherapy guided by ultrasound and computer [60]..... 26

Figure 4.1: Spherical focused ultrasound transducer [61]..... 32

Figure 4.2: MRI scanner machine 36

Figure 5.1: Illustration of the first prototype used to utilize focus ultrasound inside the MRI scanner which was developed by GE..... 40

Figure 5.2: The positioning device developed by InSightec which is used predominantly to treat fibroids 41

Figure 5.3: The exablate 4000 transcranial Magnetic Resonance guided focus ultrasound surgery system from InSightec Israel..... 42

Figure 5.4: MRI compatible ultrasonic intersial applicators operating from 6-10 MHz for prostate interventions 42

Figure 5.5: Sonalleve by Philips MRI-HIFU system for the treatment of fibroids 43

Figure 5.6: MRI compatible ultrasonic transurethral applicator for prostate interventions..... 44

Figure 5.7: MRI compatible positioning device for animal experiments for brain applications by MEDSONIC LTD..... 46

Figure 6.1 A. Anterior face of the prostate. B. Apex base of the prostate..... 51

Figure 6.2 A: Posterior Left - Right. B: Anus - Apex base of the prostate..... 51

Figure 6.3A: Anus base of the prostate. B: Posterior of the prostate. H: Rotate Angle. 52

Figure 6.4 A: CAD design (isometric view) of the Z axis control system. B: photograph of the system zooming on the rack and pinion mechanism used to elevate the robot positioning device. The pinion can be rotated though a cylindrical handle attached on it. Moreover there is a handle on the pinion in order to asset the movement. 55

Figure 6.5 A: CAD design (isometric view) of the robot base. B: photograph of the robot base with piezoelectric ultrasonic motor and the two cables that are needed to operate the motor. Additionally, there is a support of the probe enclosure on the robot base. The optical encoder for linear motion control is placed on the left hand side. 55

Figure 6.6 A: CAD design (isometric view) of the elevating system (Z axis) and robot base. B: a photograph of the manufactured parts. C: In the circular photo, the plastic pinion inserted into the Z axis guide. 56

Figure 6.7 A: CAD design (isometric view) of the X plate together with the Θ axis motor, linear encoder. B bottom view of the X plate and rack is visible in this view. C and D photographs of the manufactured part..... 57

Figure 6.8 A: CAD design of the robot with the robot base, Z axis and X plate together with the angular motion control mechanism. B: a photograph of the robot base, Z axis, X plate and angular motion control mechanism. Additionally, optical encoder modules covers are placed on the robot. A probe has been attached for demonstration purposes. 58

Figure 6.9 A: CAD design of the probe enclosure. Image shows the way that probe with HIFU transducer will be inserted into the probe enclosure. B: A photograph of the manufactured part.....	59
Figure 6.10A CAD design (isometric view) of the robot positioning device. B A photograph of the manufactured positioning device.	60
Figure 6.11 CAD design of the positioning device placed on patient's table of an MRI scanner. Also, legs support structure is presented.	61
Figure 6.12 A: A shows a photograph of the robot inside the MRI scanner. B shows the cables that are passed out of the MRI room through a hole on the side wall.....	61
Figure 7.1 Angular EM1 Optical Encoder (US Digital Corporation, USA).....	64
Figure 7.2 Linear EM1 Optical Encoder (US Digital Corporation, USA).....	65
Figure 7.3 X1 Encoding Waveform Diagram (National Instruments - Manual)	66
Figure 7.4 X2 Encoding Waveform Diagram (National Instruments - Manual)	66
Figure 7.5 X4 Encoding Waveform Diagram (National Instruments - Manual)	66
Figure 7.6 A: Angular motion control System Design, B: Encoder Base Design - Angular.....	67
Figure 7.7 Photograph of the developed angular encoder module and strip.	68
Figure 7.8 CAD design of linear strip base for control of X motion of the transducer.	68
Figure 7.9 CAD design of linear encoder module cover.....	69
Figure 7.10 A photograph of the installation of the linear encoder module an strip	69
Figure 7.11 C Sharp interface for testing the close loop feedback control system.....	72
Figure 8.1 Piezo Systems Ultrasonic Motor by Shinsei.	75
Figure 8.2 Traveling Wave Formation.	75
Figure 8.3 Diagram of the Mechanism of the Ultrasonic Motor. The Diagram Above Was.....	75
Figure 8.4 Inside Structure of Ultrasonic Motor by Shinsei. (http://www.shinsei-motor.com/English/techno/ultrasonic_motor.html).....	76
Figure 8.5 A Photo of Piezoelectric Ultrasonic Motor by Shinsei USR60E3N.....	77
Figure 8.6 A Photo of Dedicated Driver for Shinsei USR60 Series, Shinsei D6060E.....	77
Figure 8.7 Basic Connection Diagram of the Dedicated Driver for Shinsei USR60 Series, Shinsei D6060E.....	78
Figure 8.8 The Wiring Diagram of the Driving Electronics and Computer-Controlled Interface.	79
Figure 8.9 Euro Case 42 TE A0234670 by OKW.	80
Figure 8.10 A Photo of Power Supply by Mean Well, S-72-24.	81
Figure 8.11 A. the Schematic of the Main Switch and B. the Schematic of the Switch That Used to Control Manually the Robot.	82
Figure 8.12 A The Drawing of the Front Panel. B. A Photo of the Front Panel After the Implementation.	83
Figure 8.13 Connector Diagram	83
Figure 8.14 A. The Drawing of the Rear Panel. B. a Photo of the Rear Panel After the Implementation.....	84
Figure 8.15 Front Panel With Components Installed.	85
Figure 8.16 Rear Panel With Components Installed.	85
Figure 8.17 Enclosure Box With Front and Rear Panel (Top - Inside View).	86
Figure 8.18 A Photo That Illustrates the Wiring Connection (Top – Inside View). B the Corresponding Circuit Diagram.	88
Figure 8.19 A Photo of the First Version Drivers	90
Figure 8.20 A. a Photograph of the Front Panel and B. a Photograph of the Rear Panel of the New Version Drivers.....	90
Figure 9.1 a schematic of the compete MRI compatible HIFU system.....	92
Figure 9.2 Diagram of software	93

Figure 9.3 Data flow diagram for level one of decomposition diagram.....	94
Figure 9.4 Design of interface for controlling the signal generator.....	95
Figure 9.5 Design of software that control the MRI camera.....	96
Figure 9.6 Design of software that control the MRI images A:the file names listed in a list box B: MRI images slide show.....	97
Figure 9.7 Design of software that control the platform's directory.....	98
Figure 9.8 Design of the robot control interface.....	99
Figure 9.9 Design of robot position display and initialization.....	99
Figure 9.10 Design of command history interface.....	100
Figure 9.11 Design of patient data form.....	101
Figure 9.12 Main GUI of the software.....	101
Figure 9.13 Agilent Signal Generator.....	103
Figure 9.14 Computer Software that controls the signal generator.....	104
Figure 9.15 Flowchart of turning ON and OFF.....	105
Figure 9.16 Flowchart for pulsed operation.....	106
Figure 9.17 Pulsed paradigm, Three Cycle Waveform.....	109
Figure 9.18 Software that sends continuous signal to the generator.....	110
Figure 9.19 Software that sends pulsed signal to the generator.....	111
Figure 9.20 Flowchart that controls the time that the generator is ON.....	112
Figure 9.21 A: picture of MR Camera. B: Filter Box. C: Video crapper. D: Block diagram of MRI compatible camera.....	113
Figure 9.22 Recording Operation.....	116
Figure 9.23 Open DICOM images in series of figures.....	118
Figure 9.24 Function to move the motor in one direction.....	123
Figure 9.25 Flowchart for the Get Counter Value.....	125
Figure 9.26 Edge Counter value compare with Voltage value.....	126
Figure 9.27 Wiring diagram of all electronic devices.....	128
Figure 9.28 Patient Data Form (Sample data).....	130
Figure 9.29 Main windows of the final version of the software platform.....	140
Figure 9.30 Main windows of the software platform (X – Y – Z tab enabled).....	141
Figure 9.31 Main windows of software– ultrasound control panel tab enabled (Agilent signal generator).....	142
Figure 9.32 Main windows of software platform – third tab enabled (RFG_1000 generator).143	143
Figure 9.33 Temperature Readings Form. Gathering temperature measurements and creating real time graph chart.....	144
Figure 9.34 Explanation of main menu – Submenu: Settings and Options.....	145
Figure 9.35 Explanation of main menu – Sub menu: Signal Generator Type.....	145
Figure 9.36 Explanation of main menu – Sub menu: DICOM Images.....	145
Figure 10.1 complete setup of the MRgFUS ultrasound system used for the experiments in vitro on dead tissues and gel phantoms.....	150
Figure 10.2 A line graph of the measured distance versus the number of cycles covered by the optical encoder. Graph demonstrates the linearity of the motor movement on X stage.....	151
Figure 10.3 A line graph of the measured distance versus the number of cycles covered by the optical encoder (overhead time). Graph demonstrates the non-linearity (below 10 degrees) of the overhead time on Θ stage. From 10 degrees and above the overhead is standard.....	152
Figure 10.4 A photograph of the robot positioning device placed on the table of the MRI scanner.....	153

Figure 10.5 A. Image of the MRI compatible liquid phantom capture with the present of the robot positioning device. 10.5B image of the MRI compatible liquid phantom with the present and activation of the robot positioning device.	154
Figure 10.6: A photograph of the experiment setup on 3T MRI scanner. B. A photograph the liquid marker attached to the 2D positioning device, probe reception point.....	154
Figure 10.7: Image was taken with power supply OFF using 1.5Tesla. B. Image was taken with power supply ON using 1.5Tesla. The use of power supply was causing some artefacts on the image.....	155
Figure 10.8: A. Image of a linear mark using 1.5Tesla. B. Image of a linear mark using 1.5Tesla.....	155
Figure 10.9: Image of a Θ mark using 1.5Tesla. B. Image of a Θ mark using 1.5Tesla.....	156
Figure 10.10: An image of Θ movement in water. B another image of Θ movement in water using 1.5Tesla.....	156
Figure 10.11: Image of the marker using 1.5Tesla (top view).	156
Figure 10.12: A and B shows two arcs were created using Θ movement using 3Tesla.....	157
Figure 10.13: A and B shows images of the liquid marker using 3Tesla.	157
Figure 10.14 Thermal lesions created in the gel phantom using the linear stage of the positioning device. The seven lesions proof the excellent repeatability of the positioning device.....	158
Figure 10.15 Thermal lesions created in the turkey dead tissue using the linear stage of the positioning device. The nine lesions proof again the excellent and robust repeatability of the positioning device.....	159
Figure 10.16A and B Thermal lesions created in the pork tissue using linear stage of the positioning device. Overlapping lesions were created successfully.....	159
Figure 10.172A Gel phantom (top view) B A photograph of the gel phantom (side view), demonstration of Θ stage functionality. Some lesions caused by reflected beam are shown.....	160
Figure 10.18 Photograph of the overlapping thermal lesions created in pork tissue in vitro using both linear and angular stages of the positioning device. The ablation grid was 5x5 with spacing between lesions of 2 mm for the linear stage and 3° for the angular stage.	160
Figure 10.19A A photograph of the gel phantom (top view), B photograph of the gel phantom (side view).....	161
Figure 10.20 A. MRI compatible robot with test transducer holder and gel phantom demonstrates the transducer to gel coupling. B. MRI image of transducer to gel coupling.	161
Figure 10.21 A T2W FSE image of the gel phantom (top view). B T2W FSE image of the gel phantom (side view).....	162

List of Tables

<i>Table 6:1 Prostate measurements from 100 patients</i>	53
<i>Table 6:2: Synopsis of the positioning device specifications</i>	62
<i>Table 7:1 Encoder Module Pin-out (National Instruments - Manual)</i>	70
<i>Table 8:1 Specifications of the power supply.</i>	81
<i>Table 8:2 List of the Components.</i>	89
<i>Table 9:1 Parameters and Measurements Units of signals</i>	104
<i>Table 9:2 MATLAB functionalities for controlling Data acquisition tool box</i>	120
<i>Table 9:3 MS Access Patient's Data</i>	129
<i>Table 9:4 String commands were used to control the HIFU generator. The X, Y, and Z are integer parameter values</i>	137

Abbreviations

Abbreviation	Explanation
1.5T	1.5 Tesla
ABS	Acrylonitrile Butadiene Styrene
AIO	Analogue Input Output
BPH	Begin Prostate Hyperplasia
BW	Bandwidth
CAD	Computer Aided Design
CAM	Computer Aided Manufacture
CCW	Counter Clock Wise
CE	European Commision
CW	Clock Wise
DAQ	Data Acquisition
DC	Direct Current
DICOM	Digital Imaging and Communications in Medicine
DIO	Digital Input Output
DOF	Degrees of freedom
DPI	Dots per inch
EBRT	External beam radiation therapy
ETL	Echo Train Lenght
FDA	Food and Drug Administration
FLASH	Fast Low Angle Shot
FOV	Field of View
FSE	Fast Spin Echo
HIFU	High Intensity Focus Ultrasound
kHz	Kilohertz
LED	Light Emitting Diode
mm	Millimeters
MRC	MRI Compatible Camera
MRgFUS	Magnetic Resonance guided focused Ultrasound Surgery
MRI	Magnetic Resonance Imaging
NEX	Number of excitations

PC	Personal computer
PDT	Photodynamic therapy
PFI	Programmable Function Interface
PSA	Prostate Specific Antigen
PUM	Piezoelectric Ultrasonic Motor
px	Pixels
RF	Radio Frequency
ST	Signal Time
T1	Longitudinal Relaxation Time
T2	Transverse Relaxation Time
TE	Echo Time
TR	Repetition Time
TTL	Transistor-Transistor logic
USB	Universal Serial Bus
μm	Micrometers

1. CHAPTER: INTRODUCTION

1.1. Introduction to the proposed application

Prostate is a gland in the male reproductive system found below the bladder and in front of the rectum. As part of the male reproductive system, the prostate glands primary function is to secrete a slightly alkaline fluid that forms part of the seminal fluid, a fluid that carries sperm. During the male orgasm, the muscular gland of the prostate helps to propel the prostate fluid, in addition to the sperm that was produced in the testicles, into the urethra. The semen then leaves the body out through the tip of the penis during ejaculation. Prostate gland can be affected by cancer, with high probability of death, during the male human lifetime.

Prostate cancer is one of the most dangerous tissues that can affect the male humans all over the world. Prostate cancer usually occurs in older men. In Cyprus for instance, research that was carried out in the year of 2012 shows that the number of people that are affected by this disease has reported at 204.73 per each 100.000 [1]. Currently in the United States of America, the number of cases reported is 317.97 per each 100.000 [1], [2]. The current United Kingdom statistics show that the number of cases is 272.9 per each 100.000 [1], [3].

Throughout the years, a number of therapies have been promoted and tested. Hormonal therapy, also known as androgen deprivation therapy, is the use of drugs or surgery to decrease the production of, androgens, in order to stop or limit the expansion of prostate cancer [4]. Prostate cancer is hormone-sensitive or hormone-dependent, meaning that prostate cancer growth depends on androgens, particularly testosterone. The goal of hormone therapy is to dramatically reduce testosterone levels in the blood, thus slowing the rate of growth of prostate cancer cell. Hormone therapy is the primary treatment for prostate cancer that has spread beyond the prostate gland to distant sites, including lymph nodes, bone and other organs [4]. Another therapy is the prostate surgery or prostatectomy [5]. The aim of prostatectomy is to remove the prostate gland. By removing the prostate gland, the case of

metastasis is eliminated. The adjacent functions of the prostate are reattached after the prostatectomy. The part of the urethra travelling through the gland's transition zone is also removed. The two ends of remaining urethra are reattached in a connection called the anastomosis [5].

Nowadays, because of the technological progression, scientists investigate and apply alternative therapies. Once diagnosed with prostate cancer, a patient must make an informed decision on which mode of treatment to pursue. This decision is made more difficult by the varied modalities, invasiveness, outcomes, and return to baseline function after treatment. Moreover, treatment type depends on clinical stage, Gleason grade, patient preference, and other coexisting conditions.

These sorts of therapies are categorized into two groups, the whole gland therapy and the focal therapy. Therapies which belong to the category of the whole gland therapy are active surveillance, radical prostatectomy [6], brachytherapy (external and internal therapy) [5], laparoscopic robotic prostatectomy [5], and cryotherapy [6]. Therapies which belong to the category of the focal therapy are photodynamic therapy [51], microwave therapy [51], transurethral therapy [6] and high intensity focus ultrasound (HIFU) [6, 7, 8, 9, 10, and 11]. Focal therapy has the advantage over whole gland therapy in that the probability of causing damage to adjacent functions during the operation is minimized [6].

Focal therapy of the prostate in patients with low-risk cancer characteristics is a proposed treatment approach in development that aims to eradicate all known foci of cancer while minimizing damage to adjacent structures necessary for the preservation of urinary, sexual, and bowel function. Prostate focal therapy is a promising and emerging treatment strategy for men with a low risk of cancer progression or metastasis. Evaluation in formal prospective clinical trials is essential before this new strategy is accepted in clinical practices. Adequate trials must include appropriate end points, whether absence of cancer on biopsy or reduction in progression of cancer, along with assessments of safety and longitudinal alterations in the quality of life. 3

HIFU has been proposed to treat the prostate [4]. HIFU also has been proposed for different therapeutic applications [4, 5, 6, 7, and 8]. It is presently used for prostate cancer therapy and for the treatment of benign hypertrophy of the prostate [5]. High Intensity focused ultrasound, or HIFU, is a therapy that destroys tissue with rapid heat elevation, which essentially "cooks" the tissue. Ultrasound energy, or sound waves, is focused at a specific location and at that focal point the temperature rise above 70 degrees Celsius in a matter of seconds. HIFU is a 2-3 hour, one-time procedure performed on an out-patient basis under spinal or epidural anesthesia. Unlike radiation, HIFU is not ionizing so it can be repeated if necessary without damaging healthy tissue. This means that HIFU can also be used as a salvage technique if other prostate cancer treatments fail.

Experimental results have shown that it is possible to treat precise zones in tissues by focusing an ultrasound high energy beam in a target volume. In just a few seconds, HIFU causes the temperature to rise above 70°C in the focal zone of the transducer [11]. The rapidity of this phenomenon induces a localized elementary coagulation necrosis lesion. Complete tumors can be treated using multiple elementary lesions placed side by side, so that the coagulated volumes (sonication) overlap [12]. HIFU systems are operated by special design robotic positioning devices.

Currently, there are two commercially available ultrasound guided trans-rectal devices used for the treatment of prostate cancer [12]. The machines are the following: Ablatherm (EDAP TMS, Lyon, France) and the Sonablate 500 (Focus Surgery, IN, USA) [11]. These devices are approved in the treatment of localized prostate cancer in Europe and Asia. Also, these devices are used for clinical treatment in the USA. Both HIFU devices do not cause damage between the probe and the target area of tissue. The Ablatherm device has three versions. The original devices have two probes to perform the operation; the new version has one probe with two transducers, the one transducer used for the imaging and the second transducer used for the treatment. Also, the newest version of the Ablatherm has the ability to perform three different treatment scenarios. The second commercially available machine named Sonablate 500 has higher mobility and customization of the treatment than 4

Ablatherm. Sonablate 500 has better control of HIFU beam as far as adjustment of focal length is concerned, which provides energy and power delivered to the target. Also it has the ability to perform tailor made treatment, based on the particular characteristics of the patient prostate. Additionally the Sonablate 500 is smaller than the Ablatherm and needs more manual manipulation of the probe.

The Sonablate 500 device equipment consists of ultrasound power generator, multiple transrectal probes of different focal depth, the probe positioning system, and the cooling system [11]. The transrectal HIFU probes use proprietary transducer technology with low energy ultrasound (4 MHz) for imaging of the prostate and for delivery of high energy ablative pulses (site intensity, 1300-2200 W/m²). The single piezoelectric crystals alternate between the high energy ablative and low energy ultrasound for total cycles of 7 to 16 seconds [12].

The Ablatherm device is a combination of various components: 1) a specially designed bed for the patient to lie on during the treatment. 2) An ultrasound generator. 3) An integrated ultrasound imaging system, which allows the visualization of the prostate by the surgeon. 4) An end rectal head consisting of the imaging probe and the treatment transducer which emits the focused ultrasound. These two elements are placed in a latex balloon filled with a cooled liquid. 5) A computer which controls and aims the shots according to the treatment plan established by the surgeon.

The technology of both systems is basically the same, but there are a few technical differences between these two devices [13]. The Ablatherm has both the imaging (7.5 MHz) and therapeutic (3 MHz) transducers included in a unique endorectal probe focused at 40 mm. The Sonablate uses a single transducer (4 MHz) for both imaging and treatment. Several probes are available with many focal lengths (from 25 to 45 mm). The Ablatherm requires a specific bed with a patient on a lateral position, whereas the procedure is conducted in a dorsal position, while the Sonablate requires the patient to lie on a regular operating table. The Ablatherm includes three treatment

protocols with specifically designed treatment parameters, depending on the 5 clinical use (standard, HIFU re-treatment, and radiation failure). The Sonablate uses a single treatment protocol in which the power is manually adapted by the operator. This “visually directed” HIFU treatment is based on grey-scale ultrasonographic changes observed during treatment that allow the operator to change the power level for each HIFU pulse. Both devices offer a real-time ultrasonic monitoring of the treatment.

Although the existing systems are quite mature regarding therapeutic ultrasound, they have the disadvantage that they are using ultrasonic systems for imaging of the prostate during the procedure (tissue to necrosis contrast is very poor). MRI (Magnetic Resonance Imaging) was used as the monitoring method in this thesis. The use of MRI implies that the robot has to be MRI compatible. Therefore, the aim of this research is to design and manufacture a 2-D MR compatible robot for performing prostate cancer treatment using therapeutic ultrasound.

The incentive of this study has been the two commercial systems that use HIFU for the treatment of prostate cancer using ultrasonic imaging [14], [15]. Despite the fact that ultrasonic imaging does not provide adequate feedback regarding temperature and thermal damage, the results of these two technologies were very promising. So the aim of this study was to design and fabricate a 2D MR compatible robot device for performing prostate cancer treatment with therapeutic ultrasound and use the MRI instrument for guiding the robot device for imaging the prostate area during the procedure.

The use of MRI gives the advantage that we have better quality images than diagnostic ultrasound. Consequently all the components must be non ferromagnetic materials. MRI compatible robotic system refers to a system that is not hazardous in any way and does not generate any interference to the MRI scanner. Furthermore, it is not affected by the strong electromagnetic field of the MRI scanner [15, 16, 17, 18]. During the last decade the concept and the development of MRI compatible robots is moving at an accelerated pace and the number of the groups involved, as well as funding, is increasing

[19]. The positioning device has to be small to fit the gantry of a typical MR scanner 6

with a diameter of 55 cm-70 cm. In addition the device has to be small in order to fit under the legs of the patient.

1.2. Aim and Objectives

According to the above mentioned, the goal and objectives of this thesis are the following:

- design and develop a 2D MRI compatible positioning device for guiding a HIFU transducer for trans-rectal treatment of prostate cancer that can be used in any commercial MRI scanner.
- Design and develop the robot positioning device that can be fitted under the legs of the patients.
- The robot positioning device incorporates an additional stage, which is manually driven in order to access rectums of different heights.
- Design and develop a software platform using C Sharp. The MRI guided focus ultrasound system is guided by a software platform. The platform includes windows for displaying MRI images, a window for displaying the movement of the transducer, a window for messaging, a window for controlling the HIFU protocol and a window for monitoring the robot movement using an MR compatible camera.
- In vitro experiments for testing the accuracy of the robot positioning device.
- In vitro experiments for testing the MRI compatibility of the robot positioning device in real MRI scanner.
- In vitro experiment for virtual testing of the operation of the robot positioning device in real MRI scanner.

1.3. Chapters Outline

The first chapter is an introductory note to my thesis including some important information about this thesis. Also some statistical information about the prostate cancer world-wide is presented.

The second chapter consecrates on the anatomy, pathology and physiology of the prostate gland. In this chapter, the functionality and the zones of the prostate are presented. Also, the pathology of the prostate cancer is discussed.

The third chapter includes some literature review of the current prostate cancer therapies (invasive and non-invasive).

The fourth chapter discusses about the high intensity focus ultrasound treatment therapy. Important principles of the technique are presented. Also, 7

clinical trials on prostate cancer using high intensity focus ultrasound are presented.

The fifth chapter presents the current state of the art in MRI compatible robotics including not only robots that manipulate HIFU transducers but also for other applications and purposes. Commercial and research devices are presented here. This chapter shows that MRI compatible robotics has investigated in varieties of application in a lot of functions and parts of the human body.

The sixth chapter presents mechanical design of the MRI compatible positioning device for the treatment of prostate cancer using therapeutic ultrasound. The positioning device was design using measurements was taken by 100 patients.

The seventh chapter presents the close loop feedback system of the positioning device. The chapter shows how the positioning device uses the mechanical motion feedback of the MRI compatible optical encoders in order to move a HIFU transducer accurate and robust.

The eighth chapter presents the electronic system of the positioning device. The portable electronic system incorporates two drivers for each of the PUM motors and one 24DC power supply. The front panel supply switches on/off/on for the manual driven of the 2 stages and a DAQ interface port for the PC controlled of the 2 stages.

The ninth chapter presents the software that controls the MRgFUS system. The software was written in C. The software has the following options: a) MRI imaging, b) transducer movement (the user may move the robot manually or automatically by specifying the pattern, the step and the number of steps), c) messaging (starting time, treatment time left etc), d) Camera control, e) Patient data (age, weight, etc), f) Controlling the parameters and activation of a signal generator.

The tenth chapter presents the evaluation of the positioning device. The device was evaluated for its motion accuracy, MRI compatibility and motion functionality. The device was evaluated in experiments in vitro on gel 8 phantoms and dead tissues. The device was used to create overlapping and desecrate lesions on gel phantoms and dead tissues using both linear and angular stages.

The eleventh chapter is a conclusion and discussion about the future expansions of the proposed system.

2. CHAPTER: Anatomy, Physiology and Pathology of the prostate gland

2.1. Introduction

Prostate gland is a part of the male reproductive system. It communicates and operates with the association of its surrounding organs. When the prostate gland is affected by a disease like cancer, functionality of the surrounding organs may be affected also, therefore the quality of life suffers. The aim of this research is to design and develop a robot positioning device that navigates a focus ultrasound transducer, for non-invasive surgery of prostate gland, guided by MRI scanners. The device will destroy tumor cell generated by the cancerous cells on prostate gland, using focus ultrasound ablation. As a result of this, the enlargement of the prostate will be eliminated.

In this chapter the prostate anatomy and the prostate functionalities are presented, as well as the pathology of the prostate gland [24]. In addition, the prostate and all surrounding organs of this gland are described [20, 21, and 24].

2.2. Prostate Gland

The prostate is a gland in the male reproductive system located just below the bladder, the organ that collects and empties urine, and in front of the rectum, the lower part of the intestine. It is about the size of a walnut or about 3-5 cm in width and surrounds part of the urethra, the tube that empties urine from the bladder. The prostate gland produces fluid that makes up part of the semen [23]. Figure 2.1 shows all the organs near the prostate gland.

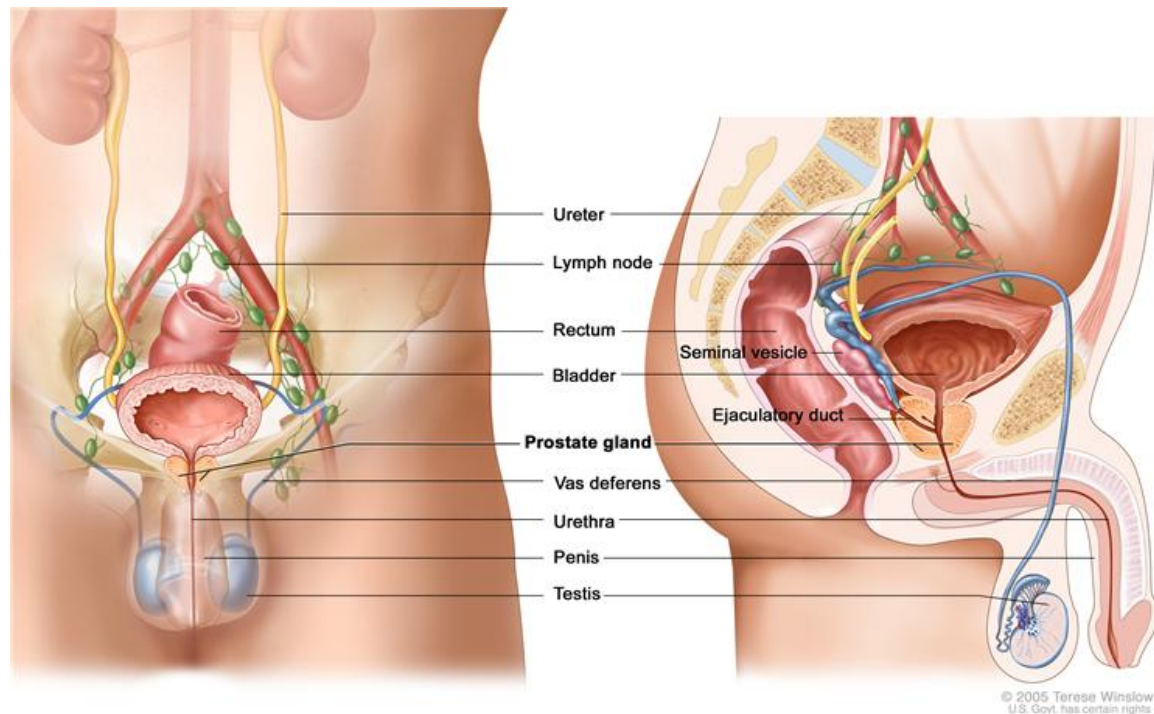


Figure 2.1: Prostate gland and surroundings organs [25]

2.3. Prostate Functionality

The main function of the prostate is to produce much of the liquid that accompanies sperm during ejaculation. This liquid is slightly alkalized to help the sperm survive against the high acidity of the vaginal tract. The alkalizing helps neutralize the acid, which helps the sperm survive longer. The prostate fluid is also what gives semen its milky colouring. The prostate also contains 30 percent smooth muscle tissue. This muscle tissue helps propel the sperm out of the penis during ejaculation. This effectively transports the sperm, as well as the seminal fluid, from the prostate and testicles and out of the body [23], [24].

The prostate works using androgens simply referred to as male hormones. The most important of these hormones is testosterone, more specifically dihydrotestosterone. The secretion of this hormone into the body helps regulate prostate function, and keeps the prostate working properly.

2.4. Anatomy of the prostate gland

As mentioned above, the prostate gland is located just below the bladder and at the top of the penis. The prostate gland is divided into a number of lobes (See figure 2.2).

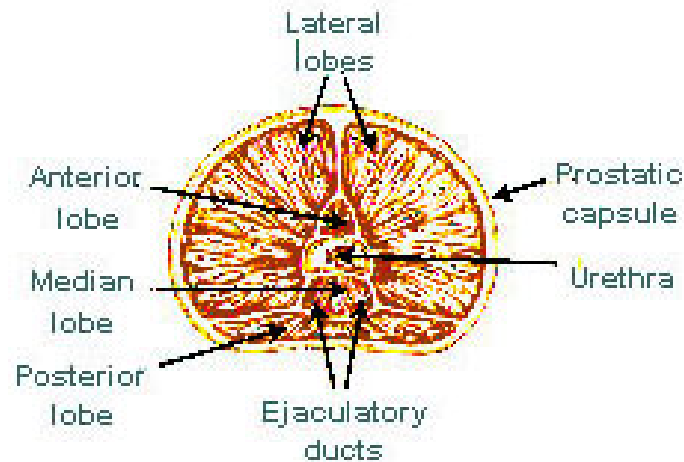


Figure 2.2: Prostate Lobes [26]

The anterior lobe is used to describe the anterior portion of the gland lying in front of the urethra. It is devoid of glandular tissue being formed completely of fibro muscular tissue (See figure 2.2).

The median lobe is the cone-shaped portion of the gland situated between the two ejaculatory ducts and the urethra (See figure 2.2). The lateral lobes (right and left lobes) form the main mass of the gland and are continuous posterior. They are separated by the prostatic urethra (See figure 2.2). The posterior lobe is used by some to describe the posterior medial part of the lateral lobes that can be palpated through the rectum during digital rectal exam (DRE) (See figure 2.2). The prostate is separated into three zones [24]: (See figure 2.3): a) Peripheral zone, b) Central zone and c) Transition zone

The anatomy of the prostate gland shows the three glandular regions: peripheral zone (PZ) making up 70% of the gland and surrounding the urethra; central zone (CZ) making up 25% of the gland and surrounding the ejaculatory ducts; transition zone (TZ) making up 5% of the gland surrounding the proximal urethra.



Figure 2.3: Zones of the prostate gland [27]

The peripheral zone [20] comprises all the prostatic glandular tissue at the apex as well as the entire tissue located posterior near the capsule (See figure 2.3). In this zone, carcinoma, chronic prostatitis, and post-inflammatory atrophy are relatively more common than in the other zones. The central zone is a cone-shaped area of the adult gland, with the apex of the cone at the confluence of the ejaculatory ducts and the prostatic urethra at the verumontanum (See figure 2.3). The transition zone [20] consists of two equal portions of glandular tissue lateral to the urethra in the middle of the gland (See figure 2.3).

2.5. Surrounding functions of the prostate

The surrounding functions and organs of the prostate are the following: 1) ureter, 2) lymph node, 3) rectum, 4) bladder, 5) vas deferens, 6) epididymis, 7) urethra, 8) penis, 9) semen, 10) testicles. Below you can see some explanation of the functions that are mentioned above [24].

Ureter is a function of the prostate nearby. When urine exits the kidney, it enters a long tube known as a ureter. There is one ureter in each kidney, and

the purpose of this organ is to channel the urine down into the bladder. They are about 10 to 12 inches in length and the urine moves downward by gravity and peristalsis.

Lymph node is a tiny bean-shaped gland, located in many different areas of the body. Each lymph node is an important part of our immune system. Our lymph node filters fluids, catching viruses, bacteria, and other unknown materials. Then our unique white blood cells destroy the unwanted materials.

Rectum: The Purpose of the Rectum is to act as an impermanent space site for fecal substance before it is removed from the body over the anal canal. The rectum is a muscular ring that is at the end of the large intestine.

Bladder is a hollow organ in the pelvis with flexible, muscular walls. Its main function is to store urine before it leaves the body.

Vas deferens is a long, muscular tube that travels from the epididymis into the pelvic cavity, to just behind the bladder. The vas deferens transports mature sperm to the urethra in preparation for ejaculation.

Epididymis is a long, coiled tube that rests on the backside of each testicle. It functions in the transport and storage of the sperm cells that are produced in the testes.

Urethra is also a part of the male reproductive system and it is separated into three parts. At about 8-9 inches (200 mm) long, the adult *male urethra* is longer than the adult female urethra (of approx. 1.5 inches 35 mm). It has three portions (the prostatic urethra, the membranous urethra, and the spongy urethra) and extends from the neck of the bladder (shown in the figure above 2.1) to the meatus urinarius at the end of the male penis/urethra.

Penis is the male organ for sexual intercourse. It has three parts: the root, which attaches to the wall of the abdomen; the body, or shaft; and the glans, which is the cone-shaped end of the penis.

The body of the penis is cylindrical in shape and consists of three internal chambers. These chambers are made up of special, sponge-like erectile

tissue. This tissue contains thousands of large spaces that fill with blood when the man is sexually aroused. As the penis fills with blood, it becomes rigid and erect, which allows for penetration during sexual intercourse. The skin of the penis is loose and elastic to accommodate changes in penis size during an erection.

Testicles: The testes are responsible for making testosterone, the primary male sex hormone, and for generating sperm.

2.6. Pathology - Prostate cancer

Cancer occurs when cells in the body (in this case prostate cells) divide without control or order. Normally, cells are divided in a regulated manner. If cells keep dividing uncontrollably (See figure 2.4) when new cells are not needed, a mass of tissue forms, called a growth or tumour [22]. The term cancer refers to malignant tumours, which can invade nearby tissue and spread to other parts of the body. A benign tumour does not invade or spread.

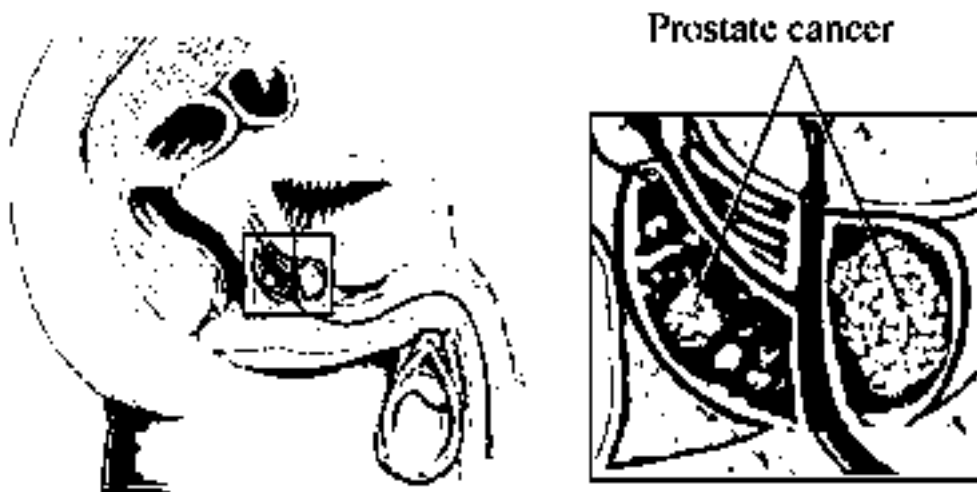


Figure 2.4: Cancerous cells are divided uncontrollably [28]

2.7. Prostate cancer symptoms

As all diseases, prostate cancer has some symptoms. Symptoms can help us recognize that we may be facing a case of prostate cancer. There are often no symptoms associated with early-stage prostate cancer. However, most cases of prostate cancer are diagnosed before symptoms develop through screening. A few of these symptoms are the following [22]: a) Inability to urinate, b) Discontinuous or weak urine flow, c) Difficulty in starting or stopping urine flow, d) Frequent urination, especially at night, e) Blood in

urine, f) Pain or burning with urination, and g) Continuous back, pelvis, and upper thigh pain.

2.8. Prostate Cancer Statistics

Prostate cancer is the second most frequently diagnosed cancer and the sixth leading cause of cancer death in males, accounting for 14% (903,500) of the total new cancer cases and 6% (258,400) of the total cancer deaths in males in 2008 [2]. Incidence rates vary by more than 25 fold worldwide, with the highest rates recorded primarily in the developed countries of Oceania, Europe, and North America (See Table 1, Appendix), largely because of the wide utilization of prostate-specific antigen (PSA) testing that detects clinically important tumours as well as other slow-growing cancers that might otherwise escape diagnosis. In contrast, males of African descent in the Caribbean region have the highest prostate cancer mortality rates in the world, which is thought to reflect partly difference in genetic susceptibility.

3. CHAPTER: Therapies for prostate cancer

3.1. Introduction

In this chapter, the way of prostate cancer is diagnosed and how it progresses is demonstrated. Also in this chapter the existing prostate therapies are explained. The existing therapies of the prostate are the following:

- a) Hormonal therapy [24, 29]
- b) Active surveillance [31, 32, 24]
- c) Radical prostatectomy [34, 35]
- d) Laparoscopic robotic prostatectomy [36, 37]
- e) Brachy therapy(external and internal therapy) [39, 40, 41, 42, 43]
- f) Cryotherapy [44, 45]
- g) Photodynamic therapy [46, 47, 48, 49, 50],
- h) Microwave thermal therapy [51, 52],
- i) Transurethral ultrasound therapy [52] and
- j) HIFU [53, 54, 55, 62, 63, 64 and 65]

3.2. Diagnostic methods of prostate cancer

There are a lot of ways to diagnose prostate cancer. One way is the rectal exam, also known as digital rectal exam, usually together with PSA¹ blood test. The rectal exam is performed by a doctor or other healthcare staff as follows: The patient undresses, then is placed in a position where the anus is accessible (lying on the side, squatting on the examination table, bent over the examination table, or lying down with feet in stirrups).

The physician spreads the buttocks apart and will usually examine the external area (anus and perineum) for any abnormalities such as hemorrhoids, lumps, or rashes. Then, as the patient relaxes, the physician slips a gloved and lubricated finger into the rectum through the anus and palpates the insides for approximately sixty seconds (See figure 3.1).

¹ Prostate specific antigen

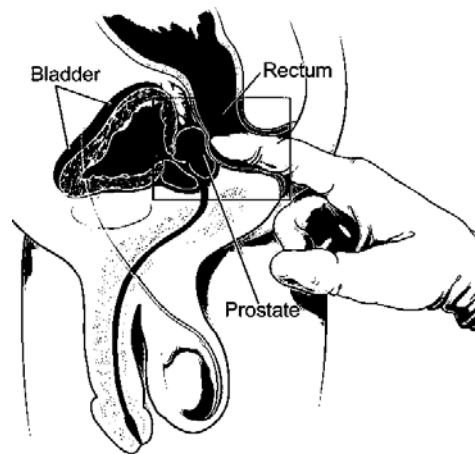


Figure 3.1: A doctor performs a rectal exam [56]

Prostate specific antigen (PSA) is a protein produced by cells of the prostate gland. The PSA test measures the level of PSA in the blood. The doctor takes a blood sample, and the amount of PSA is measured in a laboratory. Because PSA is produced by the body and can be used to detect disease, it is sometimes called a biological marker or a tumor sign.

It is normal for men to have a low level of PSA in their blood; however, prostate cancer or benign (not cancerous) conditions can increase a man's PSA level. While men are becoming older, both benign prostate conditions and prostate cancer become more common. The most frequent benign prostate conditions are prostatitis (inflammation of the prostate) and benign prostatic hyperplasia (BPH) (enlargement of the prostate). There is no evidence that prostatitis or BPH causes cancer, but it is possible for a man to have one or both of these conditions and to develop prostate cancer as well.

Nowadays, technology progression allows the doctors to use other ways that prostate cancer can be diagnosed. The x-rays, the Ultrasound and the MRI imaging are three ways of diagnosing prostate cancer efficiently and accurately.

X-Rays produces an image of the cross section of the body. This image gives the ability to check for swollen or enlarged lymph nodes, which might mean that cancer has spread.

Ultrasound is another way to diagnose the prostate cancer. A probe, very similar to a finger, is inserted into the rectum. This probe produces safe high-frequency sound waves, inaudible to the human ear, that bounce off the surface of the prostate. The sound waves are recorded and transformed into video or photographic images of the prostate gland. Images coming from the probe are produced by different angles that help to estimate the size of the prostate.

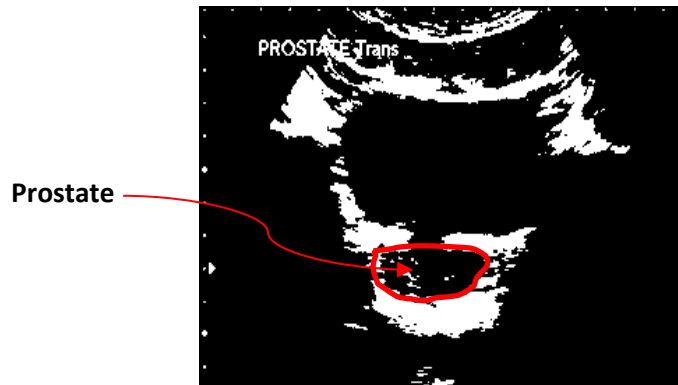


Figure 3.2: Ultrasound prostate examination [57]

MRI is a system that produces high quality images of the human body in 3D mode. MRI may be used to examine the prostate (see figure 3.3) and nearby lymph nodes and distinguish between benign (noncancerous) and malignant (cancerous) areas. This examination will approximately take 45 – 60 minutes.

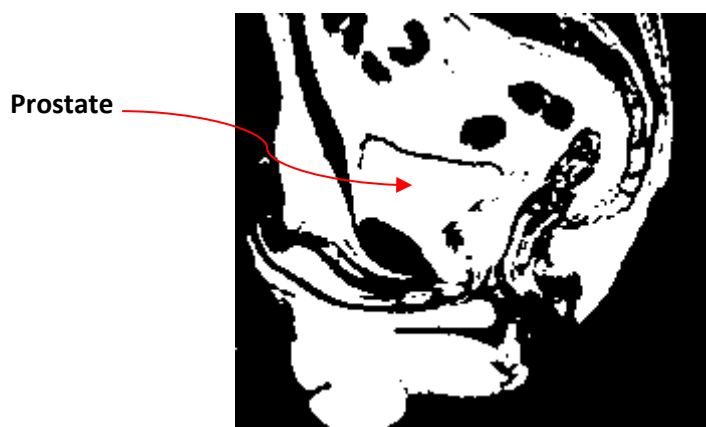


Figure 3.3: MRI prostate examinations [58]

3.2.1. Active surveillance

Active surveillance is actually related to hormonal therapy. Active surveillance [31] therapy is a way of monitoring prostate cancer. It aims to avoid or delay needless treatment in men with low risk cancers. As mentioned above, a way of diagnosing prostate cancer is using the prostate specific antigen (PSA) test. The PSA [32] test measures the level of testosterone in the blood and if this is done at an early stage of the cancer, the active surveillance treatment method will be used. Also, this method can be used on patients who have a low count of cancerous cells found in a biopsy. Prostate cancer can be slow growing and, for many men, the disease may never progress or cause any symptoms. Active surveillance involves monitoring the prostate cancer with regular test rather than treating the cancer. The monitoring of cancer is done in the following ways:

- a) PSA testing every three months for two years, then every six months from then on.
- b) Digital rectal examinations (DRE) every three to six months for two years, then every year.
- c) Repeat prostate biopsies every few years, depending on your treatment centre.

To measure the PSA level in the blood, PSA density could be found by dividing the PSA level by the volume of prostate gland. The following equation demonstrates how PSA density can be found [24]:

- d) Prostate volume = 100 ml
- e) PSA level = 14 ng/ml
- f) PSA Density =?

$$PSA\ Density = \frac{PSA\ Level}{Prostate\ Volume} = \frac{14}{100} = 0.14$$

3.3. Therapies of prostate cancer

3.3.1. Hormonal Therapy

Because the prostate is a hormone sensing gland of the male reproductive system, the first way to treat the prostate is the hormone therapy [24]. As mentioned above the level of the hormone in the blood is a way to diagnose prostate cancer. The hormone that is related to this is testosterone. Testosterone is a steroid hormone from the androgen group that is primarily secreted in the testes. It is the principal male sex hormone and is largely responsible for male growth and development [24]. Men care about testosterone because deficiencies in the hormone can lead to muscle weakness or sexual disorders. Testosterone keeps the prostate gland healthy. The testicles make most of the body's testosterone. However, to make testosterone, the testicles must first receive the "start" signal from special messenger hormones that come from the brain. The testosterone levels in blood [29] (See Table 2 - Appendix) are dependent on the age, sexual live, lack of morning erections, less intensity during ejaculation, less hard erections and irritability. Testosterone is responsible for the enlargement of the prostate cells. As mentioned above, the enlargement of the prostate happens by the division of the uncontrollable cancerous cells.

Prostate cancerous cells need testosterone and other male hormones to grow. These hormones act like fuel to feed the cancer cells and keep them active. Hormone therapy works by lowering the testosterone being made in our body. When testosterone is taken away from cancer cells, they will either die or slow down and stop growing [29]. There are two ways of lowering testosterone levels. Firstly by the removal of testicles that produce the testosterone hormone through surgery, and secondly by using drugs. The drugs, known as Orchiectomy [29], will stop the testicles from producing testosterone, and the drugs, known as Diethylstilbestrol [29], will stop the action of testosterone. (This depends on the kind of medicines which will be used.) Hormonal therapy does not treat prostate cancer permanently. To treat the prostate cancer permanently other therapies must be used.

3.3.2. Radical prostatectomy

A radical prostatectomy is an operation to remove the prostate gland and some of the tissue around it. It is done to remove prostate cancer [34, 35]. This operation may be done by open surgery. Or it may be done by laparoscopic surgery through small incisions. In open surgery, the surgeon makes an incision to reach the prostate gland. Depending on the case, the incision is made either in the lower belly or in the perineum between the anus and the scrotum.

When the incision is made in the lower belly, it is called the retropubic approach. In this procedure, the surgeon may also remove lymph nodes in the area so that they can be tested for cancer.

When the incision is made in the perineum, it is called the perineal approach. The recovery time after this surgery may be shorter than with the retropubic approach. If the surgeon wants to remove lymph nodes for testing, he or she must make a separate incision. If the lymph nodes are believed to be free of cancer based on the grade of the cancer and results of the PSA test, the surgeon may not remove lymph nodes. A Study of Anna Bill-Axelsson et. al. [34] shows that incidence of distant metastasis was 10.2 percentage points lower in the surgery than in the watchful-waiting..

3.3.3. Laparoscopic prostatectomy

For laparoscopic surgery, the surgeon makes several small incisions in the belly. A lighted viewing instrument called a laparoscope is inserted into one of the incisions. The surgeon uses special instruments to reach and remove the prostate through the other incisions.

Robotic-assisted laparoscopic radical prostatectomy [36, 37] is surgery done through small incisions in the belly with robotic arms (See figure 3.4) that translate the surgeon's hand motions into finer and more precise action. This surgery requires specially trained doctors.

The main goal of either open or laparoscopic surgery is to remove all the cancer. Sometimes that means removing the prostate and the tissues around

it, including a set of nerves to the penis that affect the man's ability to have an erection. Some tumours can be removed using a nerve-sparing technique. This means carefully cutting around those nerves to leave them intact. Nerve-sparing surgery sometimes preserves the man's ability to have an erection.



Figure 3.4: Robotic assisted laparoscopic radical prostatectomy [38]

3.3.4. Brachy therapy

Brachy (the term is derived from the Greek word brachys, which means brief or short and belongs to the whole gland therapies) therapy is a procedure that involves placing radioactive material inside the patient's body. Brachy therapy is a type of radiation therapy that is used to treat cancer. Brachy therapy is sometimes called internal radiation. This type of therapy allows doctors to deliver higher doses of radiation to more-specific areas of the body, compared with the conventional form of radiation therapy (external beam radiation) that projects radiation from a machine outside the body [39, 40, 41]. Brachy therapy may cause fewer side effects than does external beam radiation, and the overall treatment time is usually shorter.

In Brachy therapy, a piece of radioactive material called a source is put close to the cancer or, if the patient had surgery carried out, the area where it was before being removed. The source is placed inside hollow plastic or metal tubes called applicators, which are positioned at the top of the prostate. These keep the source in place. Sometimes only one tube is used. The applicators are placed inside the prostate while patients are under a general anaesthetic or sedation in the operating room. Internal radiotherapy may be given either as a low dose rate treatment or as a high dose rate treatment. Both low dose

rate and high dose rate treatment give the same total dose of radiotherapy but do so over different time periods. Once the source is in place, the patient must stay in bed so that the applicators don't move out of position. Brachytherapy has existed since 1970 [24] and it had two problems: the first was technical inability to accurately implant the sources and second the relative paucity of objective dissymmetric criteria by which to analyze the radiation dose in that period.

According to the review study by Hazel Templeton [42], there may be difficulties establishing uniform seed distribution with brachytherapy. Brachytherapy has also been associated with complications such as recto urethral fistula, irritative voiding symptoms, urethral stricture and rectal bleeding [42, 43].

3.3.5. Cryotherapy

Cryotherapy, also known as cryosurgery is part of all gland therapies. It has been used for the treatment of prostate cancer for a number of years, and since the early 1990s a trans-perineal approach has been in use. Tissue destruction is caused by very cold temperatures that destroy tissue via a number of mechanisms (direct cytolysis via ice crystal formation, intracellular dehydration, pH changes, vascular injury, induction of apoptosis, and activation of immune response). Endothelial damage leads to platelet aggregation and micro-thrombosis. It is usual to use at least two freeze thaw cycles of three min freezing at -40°C , to eradicate tumour. The cryotherapy probes are inserted with the aid of trans-rectal ultrasound, often using a trans-perineal template. The advent of third generation gas based probes, with urethral warming and other technical modifications, which can include hydro-dissection of the space between rectum and denonvilliers fascia, have led to a reduction in the morbidity associated with whole gland cryotherapy [44].

With cryotherapy, an ultra-thin metal probe or needle is inserted into the prostate gland. This is done through an incision made between the anus and scrotum. To protect the urethra from the procedure's icy temperatures, a warm saline solution flows through a catheter.

The surgeon uses visual information imaged by ultrasound as a guide during the process. A freezing liquid, such as liquid nitrogen or argon gas, is infused through the probe into the prostate gland. The intense cold freezes the prostate and destroys any cancerous tissue it contains (See figure 3.5).

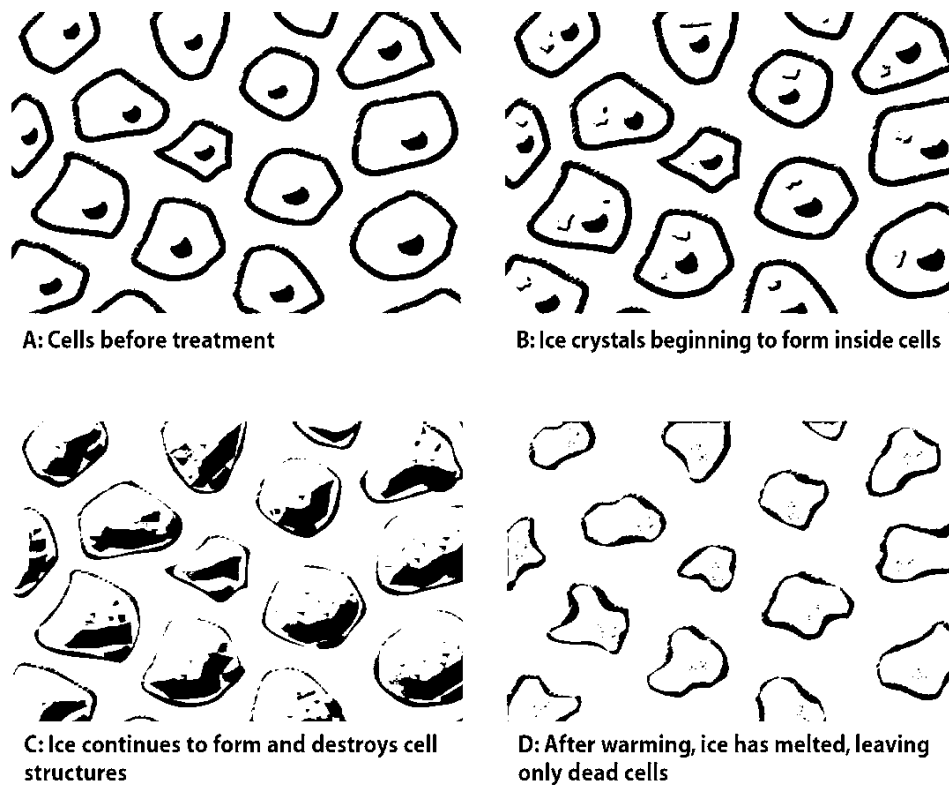


Figure 3.5: Ice is placed on cancerous cells [59]

Using the images from the ultrasound (See figure 3.6) to identify the cancer tissue, the surgeon can limit damage to normal prostate tissue. No living tissue (healthy or unhealthy) can tolerate extreme cold (See figure 3.6). Infusing nitrogen or argon gas into the prostate gland rapidly extracts heat from the gland. As heat is drawn out, there is an instantaneous swell of ice crystals or ice balls. This results in the rupture of cell membranes. That's followed by tissue damage and, ultimately, cell death. After the cancer cells are destroyed, white blood cells clean up the dead cells and tissue. Some studies show that during this process, the immune system strikes out and attacks cancer cells that still remain [45].



Figure 3.6: Cryotherapy guided by ultrasound and computer [60]

Cryotherapy is best used in situations where the PSA is less than 15 and the Gleason grade of the pathology is grade 7 or below. Patients who have severe urinary symptoms or those who have had previous prostatic surgery may not be suitable for this therapy.

According to the review study by Hazel Templeton [42], erectile dysfunction is a common complication of cryosurgery, with the incidence reported as 53–95% followed by urinary incontinence. Pelvic pain, urinary retention and tissue sloughing are reported complications with cryosurgery. Advantages include low morbidity, shorter hospital stay and decreased blood loss.

3.3.6. Photodynamic therapy

Photodynamic therapy, which belongs to the focal therapies, uses laser or other light sources, combined with a light-sensitive drug to destroy cancer cells. A photosensitizing agent is a drug that makes cells more sensitive to light. The drug is attracted to cancer cells. It does not become active until it is exposed to a particular type of light. When the light is directed at the area of the cancer, the drug is activated and the cancer cells are destroyed. Some healthy, normal cells in the body will also be affected by photodynamic therapy, but these cells will usually heal after the procedure [46].

Photodynamic therapy has emerged as a minimally invasive regimen for the treatment of cancers and pre- or non-cancerous conditions and as such,

offers an attractive alternative or complement to conventional therapies. The therapeutic action of photodynamic therapy is based on the generation of reactive oxygen species (ROS) that are formed upon light activation of a photosensitizer such as a porphyrinic pigment [47]. The resulting excited PS (Photosensitizer) transfers its energy to molecular oxygen in tissue to generate ROS. Singlet oxygen is assumed to be the key cytotoxic ROS responsible for localized oxidative cell damage and death [48]. However, PDT is not yet an integral part of clinical practice due, in part, to the lack of selectivity for target cells and concomitant potential for systemic damage.

In order to transform PDT (photodynamic therapy) into a clinically relevant treatment option for prostate cancer a considerably greater selectivity is required in the targeting of the PS to tumour cells in order to limit photosensitivity of non-target tissues while enhancing drug accumulation in tumours.

3.3.7. Microwave thermal therapy

Microwave thermal therapy is an experimental treatment for prostate cancer with the goal of curing the disease, while causing fewer complications than standard treatment options [6]. Microwave thermal therapy uses microwaves radiating helical antennae, can be single or multiple antennae, which is inserted percutaneous under trans-rectal ultrasound guidance. This therapy belongs to the focal therapy.

A study of Blana et. al. [6], patients with proven prostate cancer were candidates for treatment when prostate specific antigen (PSA) was 15 ng/ml. or less and prostate volume was 50 cc. or less. Follow-up included PSA measurement, digital rectal examination, urinalysis, and documentation of adverse events in 4, 8, 12 and 24 weeks. Sextant biopsy was performed in week 24.

3.3.8. Transurethral ultrasound therapy

Transurethral ultrasound therapy can be performed by inserting a probe into the rectum. This therapy can be also performed guided by MRI. Thermal coagulation within a targeted region of the prostate is achieved by generating temperatures of approximately 55 °C along a prescribed target boundary by continuous rotation of the urethral applicator, producing ultrasound fields extending radially [52].

3.3.9. HIFU

HIFU can be performed by inserting a probe into the human male rectum. HIFU therapy can be guided either by using diagnostic ultrasound or MRI as imaging technique. The advantage of HIFU is the trans-rectal approach that HIFU transducer can be navigated through the rectum without affecting the rectum. By combining a precise control of the position of the transducer within the rectum and an active cooling of the rectal mucosa, the risk of rectal injury is minimized [53, 54, 55].

HIFU produces ultrasound waves that are generated by a spherical transducer. The ultrasound energy is focused on a fixed point. An elementary sonication creates a lesion on the prostate gland. The whole gland is treated by creating repeatable and overlapping lesion until the whole gland is covered [62, 63, 64, 65].

A study [66] shows that complications such as recto urethral fistula can be observed after a second HIFU treatment in a patient with a history of hemi colectomy and recurrent anal fistulas can appear. Occasionally underwent transurethral resection after HIFU because of bladder outlet obstruction-related symptoms. An advantage of HIFU is the repeatability of this treatment. It is also noted that external beam radiotherapy (EBRT) and surgery can be performed after HIFU.

3.4. Conclusion

During the past decades, a number of therapies have been applied to prostate cancer. All therapies which have been applied so far have both advantages and disadvantages. HIFU has been proposed and applied on a number of therapies connected with different human organs such as brain, liver, kidney, and prostate. As it has already mentioned, two commercially available machines have treated prostate cancer on more than 10.000 patients worldwide using HIFU [11]. Recently, it has been recognized that HIFU can operate within an MRI scanner [111]. MRI produces better quality images than diagnostic ultrasound so the tissue necrosis contrast will be better.

4. CHAPTER: High Intensity focus Ultrasound

4.1. Introduction

High intensity focus ultrasound known as HIFU has been proposed for different therapeutic applications during the past decades. HIFU has been applied in number of therapies such as brain [67, 68], prostate cancer [11, 12, 13, 14, 15], kidney [74], liver [75], breast cancer [68], and ablation of cardiac valves [76]. An ultrasound beam can be transmitted into the human body by converting the mechanical energy into thermal sound waves. This eliminates the needs for surgery. However, ultrasound therapy required precise targeting and monitoring. In order to achieve this, an imaging device can be employed for the purpose of high intensity focus ultrasound therapy.

By comparing the open surgery and ultrasound therapy, several advantages of the ultrasound therapy can be realized. The advantages are: a) The surgery time can be reduced, b) The damage cause to the cancerous cells is the same with surgery, c) Require before the surgery during the diagnosis and the risk are very low.

HIFU guide systems transmit the ultrasound beam from outside or inside the body and it has the ability to treat the pathological cells without surgery. A lot of machines have been developed and clinically tested for treatment of various parts of the human body for abdominal tumours [77]. Also HIFU used various imaging techniques such as diagnostic ultrasound and MRI. Those machines have been designed according to the imaging technique will operate.

4.2. History of HIFU

High intensity focus ultrasound was initially started in the 1940 [78] as potential modality for the non-invasive treatment of the focal disease in tissue organs. Focal disease sites of essentially any size and shape were considered potential targets for ablation, provided an adequate acoustic window was available for introducing the focused beam from the entry area to the site to be ablated in body. At 1955, the ultrasonic threshold doses to

produce functional and structural irreversible effects in the mouse, rat, cat, monkey, and human central nervous systems [79] were investigated for a wide range of the pertinent parameters. After years of investigations, HIFU has been used for different therapeutic application. HIFU in neurosurgery continued during the 1950s and 1960s [80, 81, 82, and 83], but practical and technological limitations restricted their progress.

In 1956, Burov suggested that HIFU could be used for the treatment of cancer [90], and in the following years several studies looked at the effects of ultrasound on tissues. The specific properties of focused ultrasound conduction and modes of destruction in normal tissues were investigated further during the 1970s and 1980s [82], and studies using HIFU to irradiate experimental tumours followed [83].

The liver has been a target for HIFU since the early days of animal experimentation. Initially, the ability to create lesions was established in small animal models [84, 85], and the thresholds for liver tissue destruction with varying exposure parameters were established in the 1970s and 1980s [86]. Normal tissue studies continued in the 1990s [87, 88, 89, 90].

HIFU also has been used to treat brain tumours during 1990's. The aim of brain tumour surgery is to target, access, and remove intracranial lesions without damaging normal functioning brain tissue, thus preserving essential neurological function [91].

4.3. Physical Principles of HIFU

Ultrasound wave release is based on transducer vibration. Alternation of positive and negative electrical voltage on both sides of the transducer results in alternation of transducer thickness (dilatation and contraction) and therefore acoustical pressure in the coupling medium. This acoustical pressure creates tissue movement (dilatation and contraction), the amplitude of which is directly related to the pressure level. As the tissue response is not perfectly elastic, energy is lost and converted into heat. The heat is homogeneously distributed along the ultrasound path if the transducer is not focused. By using a spherical-shaped transducer, the ultrasound beam is concentrated on the

transducer focus point, resulting in a maximum of pressure concentrated at this point. As tissue heating is directly related to pressure maximum, the lesion is formed at the transducer focus (Figure 4.1).

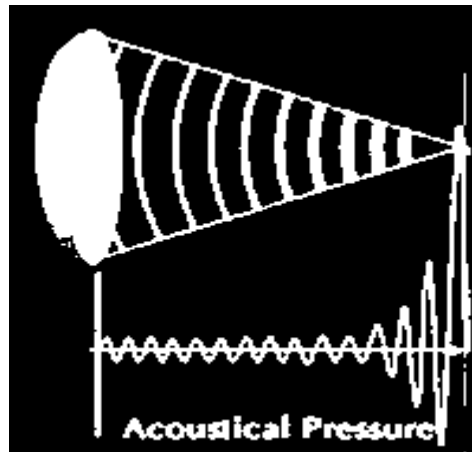


Figure 4.1: Spherical focused ultrasound transducer [61]

The spherical focused ultrasound transducer (Figure 4.1) is targeting the tissue. The tissue damage become from the high temperature is created by HIFU transducer in 1 up to 10 seconds. The temperature is raised up 70o – 90o Celsius. This will generally lead to instantaneous and irreversible cell death via coagulation necrosis in most tissues, which is the primary mechanism for tumour cell destruction in HIFU therapy. The creation of the lesion involves two main effects: a thermal effect directly related to the tissue temperature and a cavitation effect (presence of air bubbles in front of the transducer focus) due to alteration of large positive and negative acoustical pressure. The air bubbles pulsation absorbs acoustical energy and increases the tissue heating.

Using HIFU, the intensity at the focus is much higher than outside the focus. If the temperature elevation is large enough and is maintained for a period of time (seconds), the exposure will result in tissue damage. When ultrasonic energy passes through a viscous medium, such as human soft tissue, the intensity of the beam is attenuated. This attenuation depends on both the energy that is absorbed by the medium and the energy that is scattered from interfaces or in homogeneities within the tissue. Because most of the attenuation is related to tissue absorption, it can be assumed that almost all of the energy from the primary ultrasound beam results in tissue heating.

At high intensity levels, the biological effects are sometimes associated with the formation of small gas bubbles or the oscillation of those small bubbles already present. This type of interaction is called cavitation [91], and it can cause complete destruction of the tissue located next to the gas bubble. Cavitation occurs when the negative component of the acoustic wave causes liquid components to fail under tension, resulting in the formation of gas or bubbles. These bubbles will oscillate at large displacement amplitudes if the acoustic field is continued. The mechanically driven bubbles cause damage to their surroundings, particularly if they oscillate near tissue interfaces. Cell death may occur owing to acoustic cavitation if the oscillating bubble disrupts the cell membrane. Cavitation damage tends to be more random than thermally mediated cell death because cavitation requires the existence of a nucleation site.

When a bubble is solicited at its resonance frequency it may intercept and radiate energy, thereby absorbing much more acoustic power than would pass through normal tissue of its geometrical cross-section. This type of bubble oscillation is called stable cavitation and can cause microstreaming of the fluids around the bubble. When stable cavitation occurs, it can significantly increase the power attenuation and thus cause unexpected temperature elevations in tissue layers through which the tumour is sonicated. Cavitation in tissues depends largely on ultrasound intensity and the frequency used by the device. The higher the frequency, the higher the intensity required to initiate cavitation.

4.4. Prostate Cancer – Clinical trials using HIFU devices

HIFU devices for clinical use are separated into three main categories: 1) extracorporeal [92], 2) trans-rectal [92], and 3) interstitial [63]. Extracorporeal transducers are used for targeting organs that are readily accessible through an acoustic window on the skin, whereas trans-rectal devices are used for the treatment of the prostate and interstitial probes are being developed for the treatment of biliary duct and esophageal tumours. Prostate cancer clinical trials show that, HIFU can achieve tissue damage. Table 4.1 demonstrates several clinical trials using various devices on prostate cancer using HIFU.

Name	Method	Results
Foster et al. [88]	Trans-rectal Device	15 Patients successful treatment
Vallancien et al. [91]	Extracorporeal Device	10% burned skin
Gelet et al. [93]	Trans-rectal Device	Create Prostate Lesions
Koehrmann et al. [94]	Extracorporeal Device	4% burned skin
Uchida et al. [95]	Sonablate 200	Treat patients
Toyoaki et al. [96]	Sonablate 200	Treat 41 Patients
Chaussy et al. [97]	Ablatherm	271 Patients HIFU and HIFU – TURP 25% and 4% success respectively
Gelet et al. [98]	Ablatherm	14 Patients and 50% success
Gelet et al. [99]	Ablatherm	80 Patients and 68% success
Chaussy et al. [99]	Ablatherm	184 Patients and 80% success
Uchida et al. [99]	Sonablate 500	181 Patients and 80% success
Blana et al. [99]	Ablatherm	223 Patients and 49% success
Blana et al. [99]	Ablatherm	146 Patients with high rate negative biopsy after treatment
Vallancien et al. [99]	Ablatherm	30 Patients and 100% success
Lee et al. [99]	Ablatherm	Treat high risk patients with 47% success
Turkerich et al. [100]	ExAplate 2000	Low risk patients with normal biopsy after treatment
Chai et al. [101]	ExAplate 2000	Successful treatment on one patient

Table 4.1: Clinical Trials using HIFU devices

4.5. HIFU – Image Guidance

An integrated imaging component is just as important as the HIFU transducer in focused ultrasound therapy. It is crucial to have some means of assessing the treatment location, tracking the position of the focal point, and verifying that power is being delivered to the proper location. It is also necessary to determine when the critical thermal dose has been reached at each location and to what extent. This feedback allows lesion formation to be controlled and confined to areas planned for tissue destruction. Post treatment imaging for mapping the treated region is also necessary for treatment follow up or continued therapy.

4.5.1. Ultrasound Imaging

Ultrasound is the modality of choice for HIFU treatment visualization. Ultrasound is inexpensive compared to MRI, and with advance in miniature systems, has the potential to provide portable imaging guidance. Transrectal devices such a Sonablate 500 and Ablatherm are using ultrasonography systems as imaging guidance technique. The primary ultrasound modality for detecting lesion formation is B-mode (brightness mode); in which lesions appear as hyper echoic spots on the ultrasound image. Also, it is used to monitor the temperature and tissue property changes to allow more accurate and reliable therapy guidance. Although as mentioned in the introduction, the systems are quite mature regarding therapeutic ultrasound, they have the disadvantage that the monitoring of the heating by diagnostic ultrasound is poor (tissue to necrosis contrast is very poor).

4.5.2. Magnetic Resonance Imaging – MRI

MRI is a way of getting pictures of various parts of your body without the use of x-rays, unlike regular x-rays pictures. A MRI scanner consists of a large and very strong magnet. The patient lies in a table inside the bore of the magnet. A radio wave antenna is used to send signals to the body and then receive signals back. These returning signals are converted into pictures by a computer attached to the scanner. These radio wave signals are actually a varying or changing magnetic field that is much weaker than the steady, strong magnetic field of the main magnet. Because of the strong magnetic field our robot must be MRI compatible and it manufacture with non-ferromagnetic materials.

MRI (figure 4.2) has emerged as an effective tool for monitoring HIFU therapy [112]. MRI offers good tissue contrast for localization of the target volume and can characterize temperature (diffusion of thermal energy), perfusion, and blood flow in tissue. This enables the detection of tissue damage induced by thermal ablation. Experimental results show that the MRI imaging technique gives excellent contrast between lesion and normal tissue [95] on kidney, liver, brain, heart and pancreas. The disadvantage of the using MRI is that, the MRI is more expensive imaging tool than x-rays and ultrasonic systems.



Figure 4.2: MRI scanner machine

5. CHAPTER: The Current State of art in MRI compatible robotic systems

5.1. Introduction

High intensity focused ultrasound (HIFU) has the potential to induce thermal changes in tissue and therefore it is used extensively for medical applications. Today HIFU is utilized to selectively heat biological tissues for oncological applications with minimal invasiveness by using MRI to provide, high resolution images of the heated region necessary for the operator performing the procedure [102].

In order to treat large areas by creating tissue necrosis the HIFU transducer should be maneuverer to create overlapping lesions of a diameter 1 to 3 mm. The positioning device is responsible for this motion of the HIFU transducer and has to be placed inside the MRI scanner. Furthermore the use of the positioning device inside MRI scanner may interfere with the RF field and as a result the quality of the images captured could be harmed. Therefore all the components must be non-magnetic materials. The positioning device has to be small to fit the gantry of a typical MR scanner. MRI safe robotic system refers to a system that is not hazardous in any way and does not generate any interference to the MRI scanner and is not affected by the strong electromagnetic field of the MRI scanner [103, 18]. During the last decade the concept and the development of MRI compatible robots is moving with an accelerated pace and the number of the involved groups and funding is increasing [19]. Recently, a common name for this ultrasonic technology if guided by MRI is called MRI guided focused ultrasound surgery (MRgFUS).

5.2. MRI Compatible Materials

The use of the positioning device inside a MRI scanner may interfere with the magnetic field and deteriorate the MRI images. Therefore all the components of the positioning device must be made from non-ferromagnetic materials.

Materials selected for use inside the MRI scanner room depend greatly on the location of the element, but will generally be either diamagnetic or slightly

paramagnet. There are materials such as nylon, wood, copper, alumina ceramics, acetyl, copolymers and many other engineering plastics that could be used inside the MRI scanner with no magnetic susceptibility artifacts [106]. Other materials that have higher magnetic susceptibility artifacts, such as aluminum, titanium and magnesium will present artifacts, but they may be acceptable if the artifacts location and extent do not deteriorate the image [107]. In any case it is important that if any artifact appears due to the presence of a certain material, it does not cover the region of interest of the scan. Non-magnetic stainless steel has a higher susceptibility difference to that of air, but can also be acceptable at a small distance from the region of interest. During and after the robot manufacture, evaluations of the robot have to take place inside an MRI scanner in order to evaluate the quality of the images coming from the MRI.

5.3. MRI Compatible Actuators and Sensors

There are three different actuation methods in MRI compatible robotics. These methods affect the entire design of the system. The location of the actuator depends on with the material of the actuator is manufactured from. The three methods generally used are: a) generating motion using traditional EM actuators located outside the scanner room; b) having a piezoceramic actuator inside the scanner room but located at a distance from the scanner centre to ensure MR compatibility; and c) placing the actuator inside or close to the scanner centre.

The first method is based on placing an actuator outside the scanner room and as a result removing the restrictions imposed by the MRI environment allowing the use of regular electromagnetic actuators. Motion is transmitted into the scanner room through a waveguide via mechanical transmissions like a cable or belts. Gassert et. al. system [107] motion were produce using two DC motors in the control room. Transmission to the scanner room was done using tubes to a slave manipulator just outside the scanner bore.

The second method is based on pneumatic cylinders. This method allows slow and continuous movement of the robot. Pneumatic cylinders are designed to produce movement between two points. The main limitation of

this method is the accurate movement, on intermediate locations due to the compressibility of the air [108].

The third method is based on ultrasonic motors [109]. Such a motor produce movement based on resonant vibrations of non-magnetic piezoceramic materials, so electromagnetic materials is not required. These actuators are placed inside the MRI scanner room.

5.4. MRI Compatible positioning sensors

In any robotic system, the precise movement is an important thing. In order to produce a precise movement from one point A to another point B a feedback is required from a special hardware named sensor. Also these sensors have to be MRI compatible.

Damianou et. al. [109] used timing belts in order to produce precise movement. The robot employs three timing belts one of each degree of freedom. The robot performs three degrees of freedom. The robot manufactured for ablating brain tumours.

Newly developed optical encoders are manufactured using only non-magnetic materials. Such an optical encoder can be placed inside the MRI scanner. This type of sensor consists of an optical encoder that produces the light, a strip, angular or linear, with high resolution for more accurate movements. The optical encoder consists of a lenses led source and monolithic detector IC enclosed in small polymer package. The resolution is depends on the tracks per inch. Both modules are manufactured using plastic in order to be MRI compatible.

5.5. MRI guided HIFU positioning devices

The combination of ultrasound and MRI was first cited by Jolesz and Jakab [110] in 1991 who demonstrated that an ultrasonic transducer can be used inside a MRI scanner. The idea of using MRI to guide HIFU transducer to achieve necrosis on a tissue was originally introduced in the early nineties by Hynynen et al. [111], [106] and these studies showed that lesions produced by HIFU beams on a canine muscle *in vivo* inside the gantry of an MRI were

clearly visible. Therefore the idea of using MRI to guide a real time non-invasive surgery with HIFU proved to be feasible. Several studies followed this concept [107], [114], [115] and showed that the contrast between necrotic tissue and normal tissue is superior when compared with ultrasound technology. Additionally, it has been shown that MRI is an excellent tool for HIFU guidance. Figure 5.1 shows the first prototype used to utilize focused ultrasound inside the MRI scanner which was developed by GE [115].

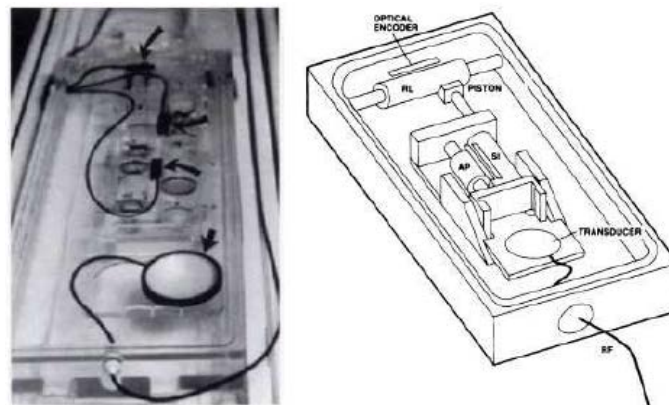


Figure 5.1: Illustration of the first prototype used to utilize focus ultrasound inside the MRI scanner which was developed by GE

The positioning devices developed in the subsequent years [116], [117] used hydraulic principles to move the transducer. These systems place the transducer directly beneath the targeted tumour. The principle for the movement of the various stages at that moment was achieved using hydraulic techniques (pressure was applied against water which is placed in plastic tubes, thus causing movement of a certain stage). The reason that hydraulic principles were used at that time was attributed to the lack of awareness of the potential of piezoelectric motors. The hydraulic positioning systems had serious repeatability and reliability problems, and have never reached the clinics. The motors used in the hydraulic positioning systems interfered with the MRI scanner, and therefore were placed far from the MRI scanner, thus requiring the use of long motor drive shafts, which results to a large and complicated positioning system.

The robotic system of Insightech [118] uses piezoelectric motors to move the transducer inside an MRI scanner. InSightec's system ExAblate 2000 was the

first commercial MRgFUS for the treatment of uterine fibroids received the Food and Drug Administration (FDA) approval in 2004. The system has been used predominantly for the treatment of uterine fibroids [118, 102, 120], Leiomyomata [121, 122, 123] and adenomyosis [124, 125]. Furthermore, the InSightec's systems can also be used to treat prostate cancer [126, 127], breast cancer [128, 129, 130, 131, 132, 133, 134], liver [135, 136] and for pain palliation of bone metastases [137, 138, 139, and 140]. The ExAblate 2000 MRgFUS system is embedded on the patient's table which is compatible with the bore of both 1.5 Tesla and 3 Tesla MRI Systems. Figure 5.2 shows the positioning device developed by InSightec which is used predominantly to treat fibroids.



Figure 5.2: The positioning device developed by InSightec which is used predominantly to treat fibroids

Recently, InSightec developed a transcranial Magnetic Resonance-guided Focused Ultrasound Surgery system which is a promising new technology for the non-invasive treatment of various brain disorders. Figure 5.3 shows the exablate 4000 system of InSightec. The system has the potential for treating functional disorders and brain tumors, and stroke. One recent application of this system is the treatment of essential tremor [141]. The challenge with this technology is that the ultrasonic transducer which is made out of hundreds of elements occupies substantial area around the patients head. Therefore, there is no space to place a head coil around the head of the patient. Therefore, currently the body coil is used. The company is currently looking means for placing both the ultrasonic transducer and imaging coil. Another disadvantage of using phased array technology is the high cost, but since the

application involves therapy for life threatening diseases, the high cost can be justified.



Figure 5.3: The exablate 4000 transcranial Magnetic Resonance guided focus ultrasound surgery system from InSightec Israel

Diederich et al 2004 [142, 143, 144, 145, and 146] proposed an MR compatible transurethral ultrasound applicator for prostate treatment. The prototype catheter-like device which has several ultrasound transducers are designed to deliver ultrasound energy from within the urethra, heating it to a lethal temperature. Figure 5.4 shows MRI compatible ultrasonic interstitial applicators operating from 6-10 MHz for prostate interventions.



Figure 5.4: MRI compatible ultrasonic interstitial applicators operating from 6-10 MHz for prostate interventions

Sonallev MR-HIFU is also a commercial MRgFUS by Philips Healthcare Philips Healthcare, Netherland [148]. This MR guided robotic system is 5 DoF positioning system and is integrated with the HIFU transducer on the patient's table. Sonallev MR-HIFU, which received CE (Certified Europe) mark for clinical use in December, 2009, can be used with either the 1.5 Tesla or 3.0 Tesla versions of the Philips Achieva MRI scanners. The HIFU transducer is integrated into the underside of the gurney thanks to a circle cut into the middle of the table top to expose the parabolic face of the HIFU transducer against the patient's abdomen. A shield is strapped onto the back of the

patients that houses the Philips' SENSE Pelvis coil as well as the sensors for temperature monitoring. The HIFU transducer is integrated into the underside of the gurney thanks to a circle cut into the middle of the table top to expose the parabolic face of the HIFU transducer against the patient's abdomen. Sonalleve MR-HIFU system has received CE Marking for non-invasive palliative pain treatment of bone metastases in 2011. Philips Sonalleve MR-HIFU marketed since 2009 and as of now, Philips has installed around 22 of its Sonalleve MR-HIFU systems worldwide with most of the systems in Asia and Europe. Figure 5.5 shows the Sonalleve MRI-HIFU system by Philips for the treatment of fibroids. The technical approach of the Philips system and the application is similar to the Insightech's system. What is different is the exposure protocol. Philips is using a spiral trajectory for creating thermal lesions. Regarding fast MRI imaging Philips is using echo planar imaging (EPI) techniques.



Figure 5.5: Sonalleve by Philips MRI-HIFU system for the treatment of fibroids

Chopra et al [149, 150] has developed a prototype system for MRI-guided transurethral ultrasound therapy. The ultrasound heating applicator described in this study incorporates a planar transducer and is capable of producing high intensity ultrasound energy in a localized region of tissue. This MRI-compatible ultrasound transducer delivers controlled thermal therapy to the regions of the prostate gland via a trans-urethral approach. This system is using very small transducers (not focused) aligned on a probe introduced through the urethra. Figure 5.6 shows the MRI compatible ultrasonic transurethral applicator [151] for prostate interventions. The advantages of this technology is simplicity and low cost. One possible disadvantage is that

heating originates from the urethra and propagates through prostate tissue until the targeted tissue is reached. This is a drawback, because if a target is away from urethra, all the tissue in front of the target is heated. A focused ultrasound system does not suffer from such issue.

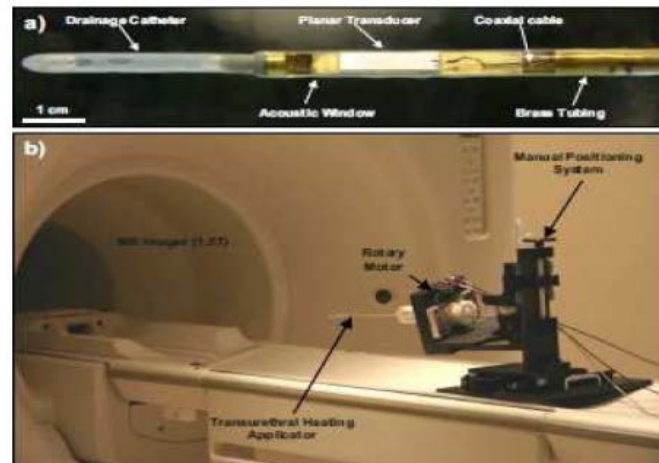


Figure 5.6: MRI compatible ultrasonic transurethral applicator for prostate interventions

Chopra et al 2009 [151] developed an MRI-compatible, computer-controlled three-axis positioning system that delivers focused ultrasound in small animals for high-throughput preclinical drug delivery studies. Each axis was constructed from custom-made nonmagnetic linear ball stages driven by piezoelectric actuators and optical encoders. The main challenge with this system was that all the moving parts had to be immersed in water, and thus water sealed means had to be established.

The study by McDannold et al. 2009 [152] and by Yiallouras et al. [153] evaluated a transrectal MRgFUS system which was tested in a canine prostate model. The main challenge with this system was that all the moving parts had to be immersed in water, and thus water sealed means had to be established. Focal volumes in each half of the prostate were targeted, with high energy in one half of the gland for ablation and in the other with lower-energy sonications to test the ability to localize the focal spot before causing thermal tissue damage.

The positioning device proposed in these two articles can be placed on the table of the MRI scanner. Since the positioning device is placed on the table of the MRI scanner, this device can be used in all the available MRI scanners.

Another issue with this technology is the use of imaging coils. For example in the Yiallouras et. al. [153] the lumbar spine coil was used. A more optimised approach is to use a coil that is placed around the transducer holder. The challenge here is the limited space on the transducer holder. Another choice could be a surface coil that is used externally and proximal to the rectum.

This positioning device can host a single element transducer (least expensive choice) [153] or a phased array (expensive choice) [152]. The phased array technology has the advantage of varying the depth of the focal beam. However the space in the transducer shaft is limited and maybe the number of elements to be used can be limited due to the space needed for wiring all these elements. The current systems which are modular can easily be modified to explore other applications. One of these applications could be the treatment of gynaecological tumors using an endovaginal approach. This application can be achieved either by scaling the system (down) and by modifying the transducer holder.

The MR guided HIFU robotic system proposed by Damianou et al. [154] has three degrees of freedom and is small and portable and it can be placed on the table of any MRI scanner. The intended application of this positioning device is to treat brain tumours. This prototype positioning device is made out of discrete components (brass rods, polyethelyne plastic, timing belts, pulleys). This positioning device was predominantly used for animal experiments. Later this positioning device [155] was improved. The system is manufactured automatically using a rapid prototyping system (FDM400, Stratasys, 7665 Commerce Way, Eden Prairie, Minnesota, 55344, USA). The proposed system could be used to treat targets in the brain (brain cancer or ischemic stroke). This positioning device incorporates only MRI compatible materials such as piezoelectric ultrasonic motors (Shinsei USR60E3N), Acrylonitrile Butadiene Styrene (ABS) plastic, and brass screws. The motion of the X, Y, and Z plates is accomplished with brass racks and pinions. Figure 5.7 shows the MRI compatible positioning device for animal experiments for brain applications.

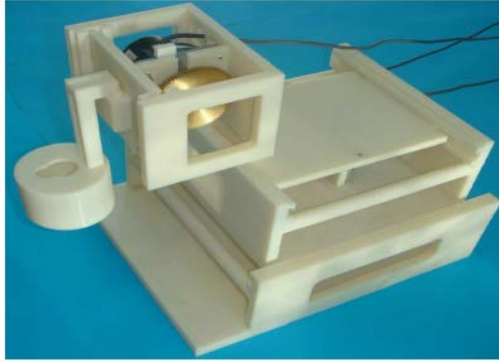


Figure 5.7: MRI compatible positioning device for animal experiments for brain applications by MEDSONIC LTD

Another company that developed an MRgFUS system for small animal experiments is the French company Image Guided Therapy [156]. Finally another positioning device is the fully MR-compatible robotic assistance system InnoMotion (InnoMedic GmbH, Herxheim, Germany) which was originally designed for MR-guided interventions with needles [157]. This system has five pneumatically driven degrees of freedom and can be moved over a wide range within the bore of the magnet. The robotic system was combined with a fixed-focus US transducer.

5.6. MRI guided devices - Other applications

The development of MRI guided HIFU was inspired by the development of MRI compatible positioning devices for other applications such as biopsy, interventional surgery and other engineering therapies. MR compatible robotic systems are very attractive for non-invasive surgeries where the physician will get continuous feedback from the MRI in order to have full control over the procedure.

In 1999 Chinzei et al. [158] deliver a study on the criteria to design MR compatible mechatronic devices and in the year 2000 a five degree of freedom (DoF) MR compatible surgical assist robot [159] was developed by Chinzei et al. at National Institute of Advanced Industrial Science and Technology. This robot is placed outside the bore of the General Electric signa SP double-doughnuts intraoperative MRI, is actuated by ultrasonic motors and used for prostate biopsy.

Another commercial robotic device for precise needle insertion during MR-guided therapy of spinal diseases [160] was developed by Hempel et al. in 2003. This MR-guided robotic system was commercialized by the start-up company Innomedic. This MR guided robotic system was made to perform biopsy, insertion of cannula and probes, drainage, drug delivery and energetic tumour destruction [161, 162]. This MR-compatible interventional robotic system received the CE mark in 2005 and is commercially available under the name of Innomotion, a German company. In 2008 Mazilu et al. use this MR guided robotic system of Innomotion for aortic valve replacement (AVR) [163]. Innomotion MR guided robotic arm with 6 DoF is moving along an arch which is mounted on the MRI patient table. An arm sitting on the arch takes advantage of the clearance between the patient and the bore.

Another positioning system developed by Tsekos et al. [164], also utilizes piezoelectric motors in order to guide a biopsy needle. MR-guided biopsy techniques are becoming more and more available, but there is no current consensus on the optimal technique [165, 166]. Several different types of biopsy robots [167] exist. Target regions are determined using different MRI techniques. Some physicians use a transrectal approach, whereas others prefer a transperineal methodology. Movement of the prostate during the biopsy procedure is one of the biggest challenges in taking biopsies of the prostate [168, 169]. Several solutions for this problem have been suggested, from fixation using needles to rendering real-time images [170].

Stoianovici *et al.* were the first group of researchers to develop a pneumatically actuated MRI-compatible robot designed for transperineal interventions in the prostate [171]. The robot, known as MRBot, has 6 degrees of freedom (three linear and three angular) and can be configured for use in biopsy, thermal and radiofrequency ablation or brachytherapy [172].

The Radboud University Nijmegen Medical Centre (Nijmegen, The Netherlands) developed a MR-compatible transrectal prostate biopsy actuator. The controller unit includes a computer, motion control elements, and electro-pneumatic and electronic interfaces, which are located outside the MRI room. Plastic hoses are used to connect the actuator to the control unit.

The actuator is constructed of nonmagnetic and dielectric materials to achieve MRI compatibility. The actuator uses pneumatic motors; pressured air used in these motors is generated in the controller unit and is transmitted through the plastic hoses. With five degrees of freedom, the needle guide can be manipulated in the desired position. The average in-plane error in a phantom study was 0.35 mm (range: 0.0–4.0 mm) [173, 174].

5.7. Conclusion

Although in the beginning of the deployment of MRI guided Focused ultrasound systems [111], [107] there was significant concern related to MRI compatibility issues. That's why the next prototype was in the early millennium [118]. Recently, due to the significant experience gained in the area, not only from MRgFUS area, but also from other areas MR compatible systems for needle insertion for example [163] or prostate interventions [170], the concern have subsided and the deployment of positioning devices is faster. There is deployment for brain applications [141], prostate [127], [151], breast [130], fibroids [120], and liver [136]. It is amazing what will be manufactured in ten years from now. In our opinion for any organ accessible to ultrasound, there will be a least one positioning device for clinical therapy. Advancements in robotic and MRI technology will enhance the capabilities of MRI guided HIFU, and thus it is possible in the future that for many diseases this technology will become the gold standard. The main reasons are that: a) is minimally invasive and b) the procedure and therapy can be monitored by MRI.

6. Chapter: Design and development of the positioning device for prostate cancer treatment using HIFU

6.1. Introduction

The proposed positioning device is an MRI compatible robot for treating prostate cancer using HIFU. This trans-rectal positioning device was designed and constructed using materials compatible with the strong MRI magnetic field. The positioning device was developed using only MRI compatible materials such as piezoelectric ultrasonic motors by Shinsei USR603N, plastic optical encoders and strips by (US Digital Corp, Vancouver, WA 98684, USA), ABS (Acrylonitrile Butadiene Styrene) plastic, brass screws, and brass pinion (Sterling instrument, NY, USA).

A major challenge when designing and developing of a positioning device compatible with MRI scanners is that the positioning device should be placed on the patient's table in the bore space. Another challenge is the mounting method of the positioning device in order to have access to the rectum and to reduce the space which is necessary for its placement. As a result, the robot positioning device has to be as small as possible and should be positioned in front of the rectum in order to access the patient. In this set-up the patient's legs are placed on a special design support. The available space remaining under the patient's legs was taken into account during the design of the positioning device.

6.2. Measurements of the prostate size.

The positioning device was designed and developed using measurements of a sample of one hundred patients. The measurements were taken from different faces of the prostates using MRI: apex - base, anterior, left – right, anus – apex, anus – base, and table - posterior prostate and rotate angle from 100 patients. Figure 6.1 shows the different faces of the prostate. Figure 6.1A shows the anterior – posterior face of the prostate with the maximum and minimum value is 50.8mm and 25mm respectively and figure 1B shows the

apex – base face with the maximum and minimum value 70.1mm and 37.1mm respectively. Figure 6.2A shows the left and right face of the prostate and figure 2B shows the apex – base face of the prostate.

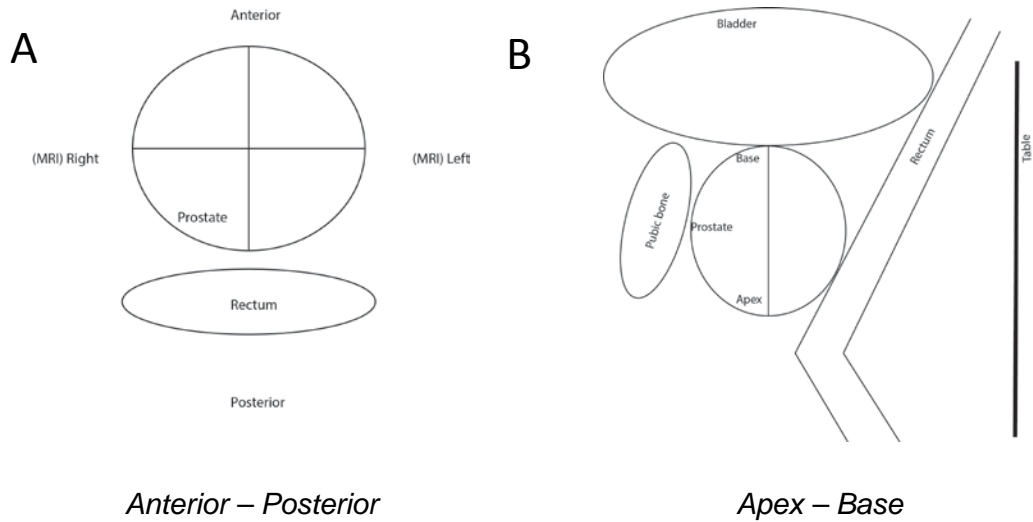


Figure 6.1 A. Anterior face of the prostate. B. Apex base of the prostate

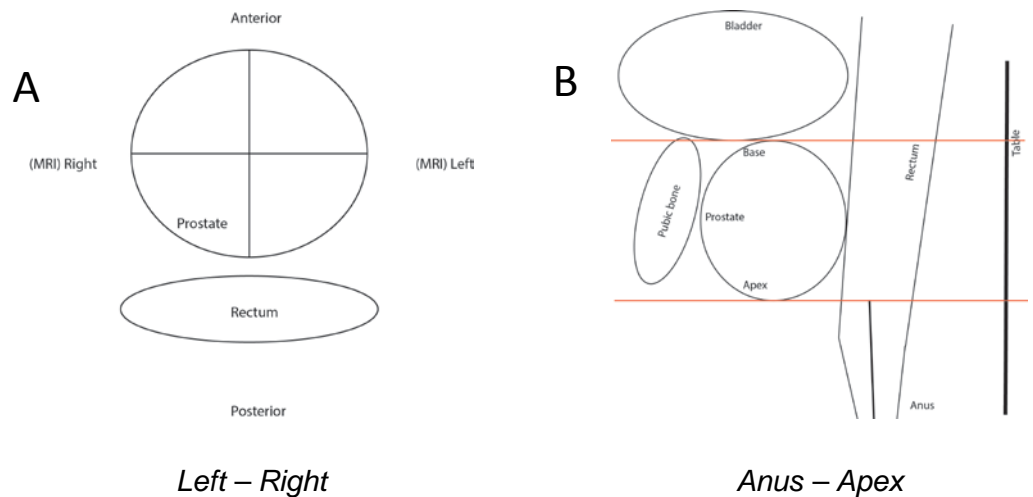


Figure 6.2 A: Posterior Left - Right. B: Anus - Apex base of the prostate

Figure 6.3A shows the anus – base measurement of the prostate. This provides the maximum movement on X plate needed to perform the operation in any prostate. Figure 6.3B shows the distance between the patient's table and the bottom face of the prostate. Figure 3C shows the rotate angle of the transducer is required to cover the prostate. This provides the maximum value of Θ angle rotation in order to treat any patient.

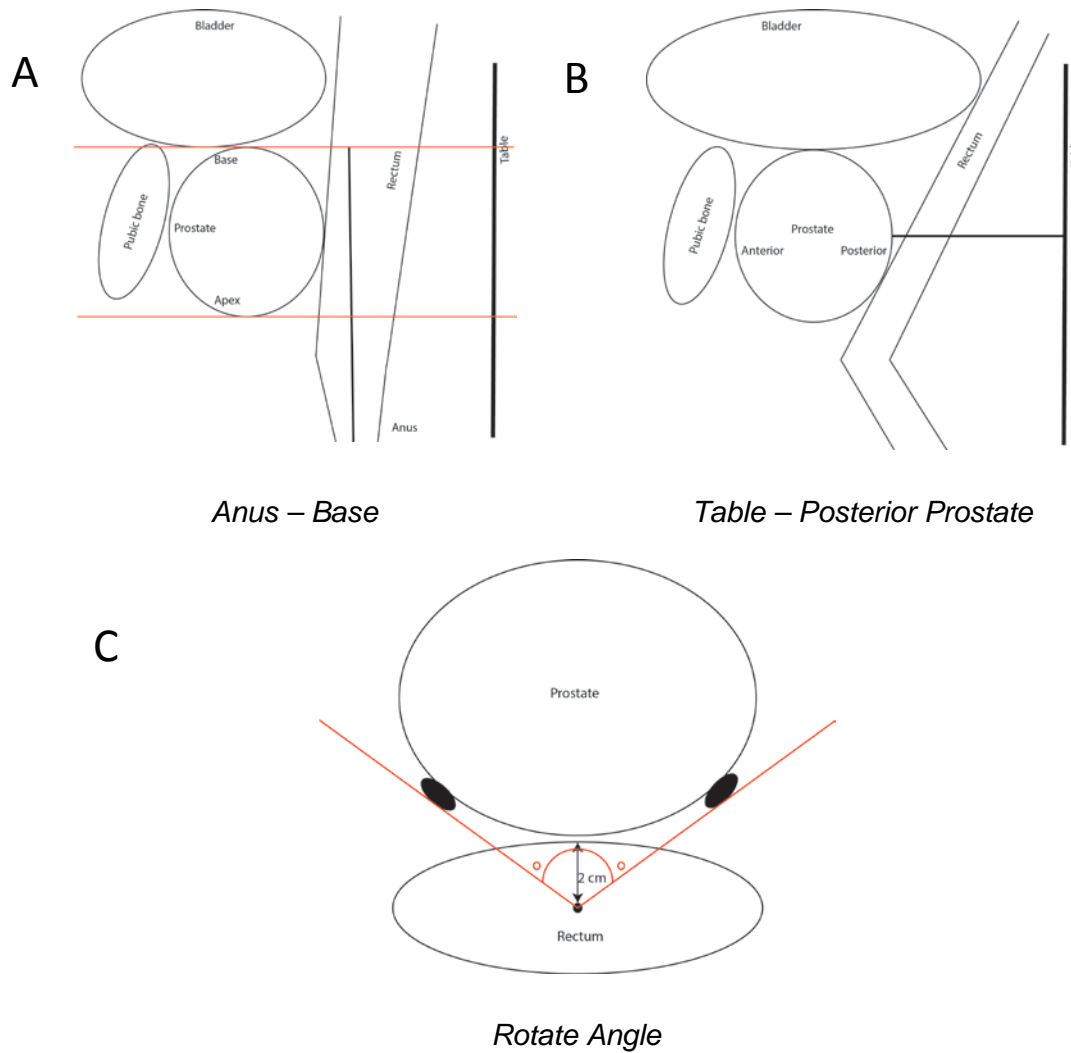


Figure 6.3A: Anus base of the prostate. B: Posterior of the prostate. H: Rotate Angle.

Table 6.1 shows the statistics of the measurements of the difference faces of the prostate. In table 6.1, the mean, maximal and minimal values of 100 patients are presented. For complete data you can see the Appendix 3.3. According to the results, the maximum rotation of the Θ angle is 130° . The minimum rotation is 74° and the mean value of all 100 patients is 99° . The probe rotation must satisfy the maximum value. X motion of the probe must satisfy the maximum value of the Anus – Base measurement which is 118 mm length. Also, the opening at the top of the enclosure of the probe must be 80 mm. The minimum value of the Anus – Base is 56 mm. The mean value is 95 mm. The maximum value from the beginning of the probe up to the exit of the rectum is 64 mm. The minimum value is 55.5 mm and the mean value is 118 mm. The maximum value from the table to posterior prostate is 108 mm.

The minimum value is 89 mm and the maximum value is 146 mm. The table to posterior prostate measurement determines the height of the probe which must be 118mm.

Table 6:1 Prostate measurements from 100 patients

Mean

Volume prostate (cc)	Anterior - Posterior (mm)	Apex - Base (mm)	Left - Right (mm)	Anus - Apex Prostate (mm)	Anus - Base Prostate (mm)	Table - Posterior Prostate (mm)	Rotate angle (°)
50.8	36.2	52.4	52.8	44.8	94.7	107.7	99.1

Maximal

Volume prostate (cc)	Anterior - Posterior (mm)	Apex - Base (mm)	Left - Right (mm)	Anus - Apex Prostate (mm)	Anus - Base Prostate (mm)	Table - Posterior Prostate (mm)	Rotate angle (°)
60	50.8	70.7	66	63.4	118	146.2	130

Minimal

Volume prostate (cc)	Anterior - Posterior (mm)	Apex - Base (mm)	Left - Right (mm)	Anus - Apex Prostate (mm)	Anus - Base Prostate (mm)	Table - Posterior Prostate (mm)	Rotate angle (°)
45	25	37.1	41.8	20.7	55.5	89.1	74.1

6.3. Mechanical system of the positioning device

The 2D MRI compatible robot was designed using CAD (Computer Aided Design) software (Microstation V8, Bentley Systems, Inc.) and was exported to CAM (Computer Aided Manufacture) software (Insight V. 6.4.1, Stratasys Inc.). Then, the model was sent to the 3D printer which builds the robot (Stratasys FDM400 7665 Commerce Way Eden Prairie, MN 55344 U.S.A.). This positioning device is a completely reproducible device.

In order to convert the rotation motion of the piezoelectric motors (USR60-S3N, Shinsei Kogyo Corp., Tokyo, Japan) into a linear motion for the X axis motion a brass pinion (Sterling instrument NY USA) and ABS plastic rack were used. The angular motion was enabled by attaching an ABS plastic cylindrical part to the motor axis. Additionally, the use of two plastic optical encoders and strips (US Digital Inc., EM1, Vancouver, USA) provides feedback control of the motion for the linear and angular stages. The positioning device is controlled by a user friendly interface, developed in C Sharp (Microsoft Corporation, USA). 55

The positioning device has the following dimensions: 250 mm length, 150 mm width, and 100 mm height. The HIFU transducer was attached on an enclosure that has 200 mm length. The dimensions of the device are resizable. The system includes a manual stage (Z axis) which can change the height of the robot. The probe is inserted into the rectum and the transducer is moved on Θ and X stages. The effective range of the robot is 120 mm on X axis, 90 degrees on Θ axis. The minimum height of the probe is 70mm and the maximum 120 (i.e. 50 mm on Z stage). Generally, this is a light weight 2D robot positioning device that can be placed on any commercial MRI scanner patient's table (universal). Also the robot is of low cost and easy to assemble.

6.4. Design and development of the 2D MRI compatible robot positioning device

The proposed device has 3 stages, computer controlled (X - Θ), and manual (Z). In this section all the parts of the positioning device are described. The measurements stated are in mm.

A manual Z axis stage is designed for the purpose of accurate variable rectum height. The Z axis system elevates the positioning device in order to place the probe on the height of the patient's rectum. The elevating system is a rack and pinion mechanism (figure 6.4A). The effective range of elevating system is 50 mm. There are guides on each side of the structure. Two pins are used to fix the system to the proper height. Figure 6.4A shows the CAD design of the elevating system and figure 6B shows a photograph of the manufactured part. The robot Z axis dimensions are 245 mm X 195 mm. The height of the two guides is 102 mm. The diameter of the pinion is equal to 66 mm. The distance between the two guides is 150 mm.

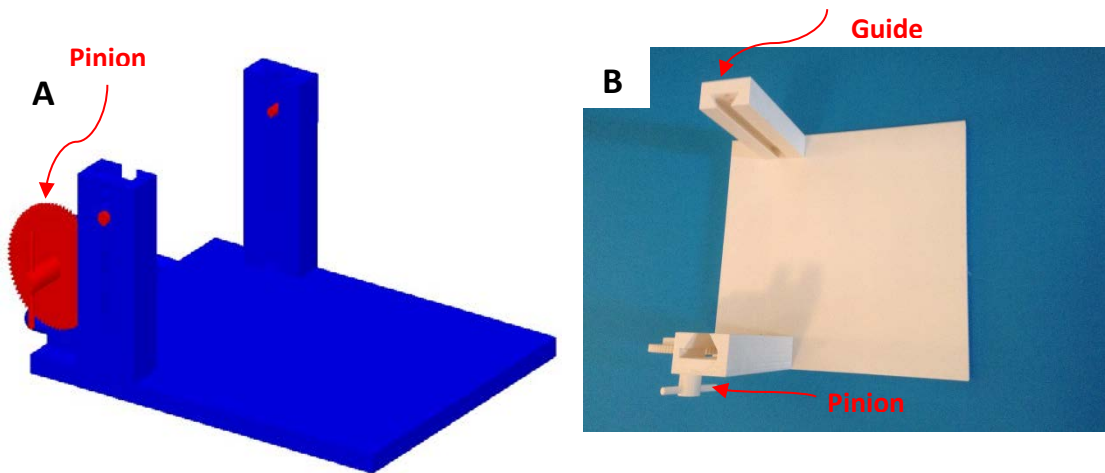


Figure 6.4 A: CAD design (isometric view) of the Z axis control system. B: photograph of the system zooming on the rack and pinion mechanism used to elevate the robot positioning device. The pinion can be rotated through a cylindrical handle attached on it. Moreover there is a handle on the pinion in order to assist the movement.

The robot base is responsible for hosting the X axis stage. There is a mounting holder for the PUM (Piezoelectric Ultrasonic Motor) and two sliding guides for the X plate. Additionally, the robot base has two windows which allow the motor to be fixed on the mounting base using brass screws. The base includes two circular holes for the motor cables. The robot base length is equal to 200 mm, the width is 150 mm and the height is 100 mm (figure 6.5A). A photograph of the manufactured part is presented in figure 6.5B.

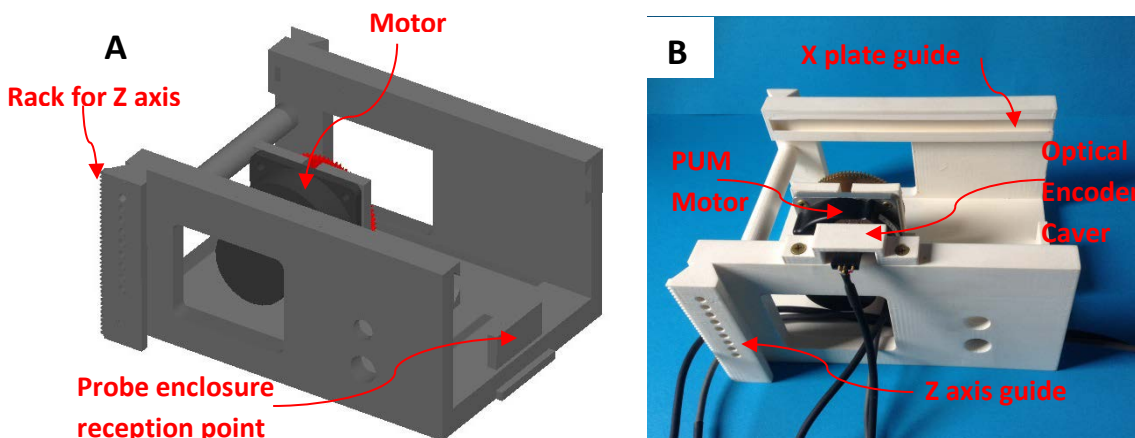


Figure 6.5 A: CAD design (isometric view) of the robot base. B: photograph of the robot base with piezoelectric ultrasonic motor and the two cables that are needed to operate the motor. Additionally, there is a support of the probe enclosure on the robot base. The optical encoder for linear motion control is placed on the left hand side.

The robot base has two vertical guides which are attached on the Z axis. A rack is attached to the right hand side guide for coupling to the frame mechanism of the Z axis. Also, there are holes in both sliding guides in order to fix a stopper when the system is adjusted to the right height.

Additionally, a reception support for the rectal probe enclosure was placed on the robot base. A probe, equipped with the HIFU transducer, will pass within the probe enclosure in order to move the X and Θ axis during the treatment. The probe enclosure will be filled with de-gassed water. As mentioned above, the robot base has 150 mm width, so it is fitted exactly between the two guides of the Z axis system base (figure 6.6A).

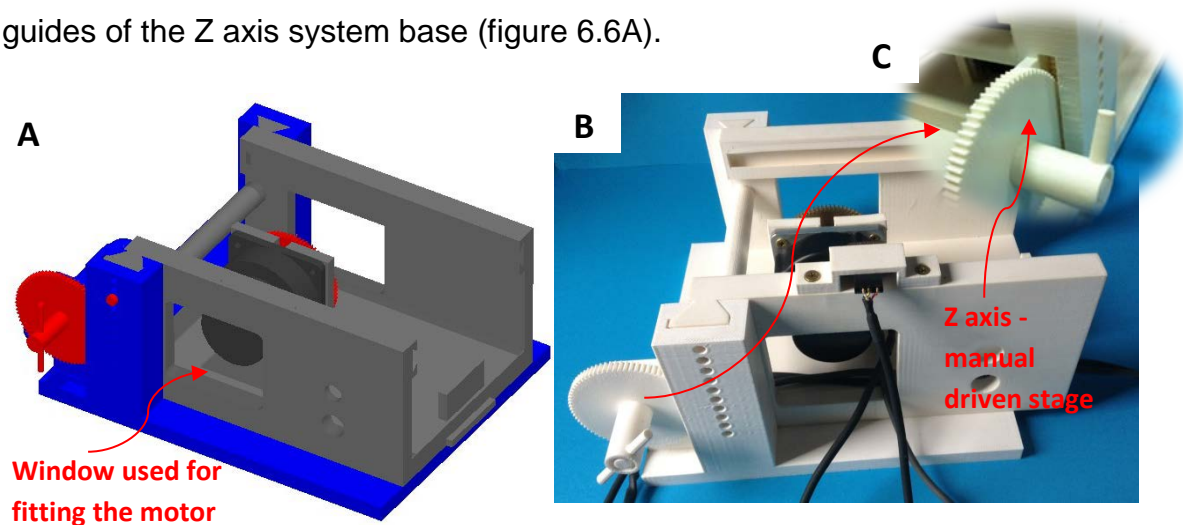


Figure 6.6 A: CAD design (isometric view) of the elevating system (Z axis) and robot base. B: a photograph of the manufactured parts. C: In the circular photo, the plastic pinion inserted into the Z axis guide.

The X plate is responsible for moving the rectal probe along the X axis. Also, on X plate there is an embedded plastic rack. It is used by the brass pinion, fitted on motor base, to move the X plate. The effective range of this stage is 90 mm which is large enough for treating any prostate size (figure 6.6B).

At the front of the X plate, there is a support for mounting the EM1 optical encoder and a hole large enough to fit the motor that controls the Θ axis movement. Also at the top of it, there is an optical encoder strip base responsible for controlling the linear motion. The X plate dimensions are 118 mm width and 168 mm height. (Figure 6.7A)

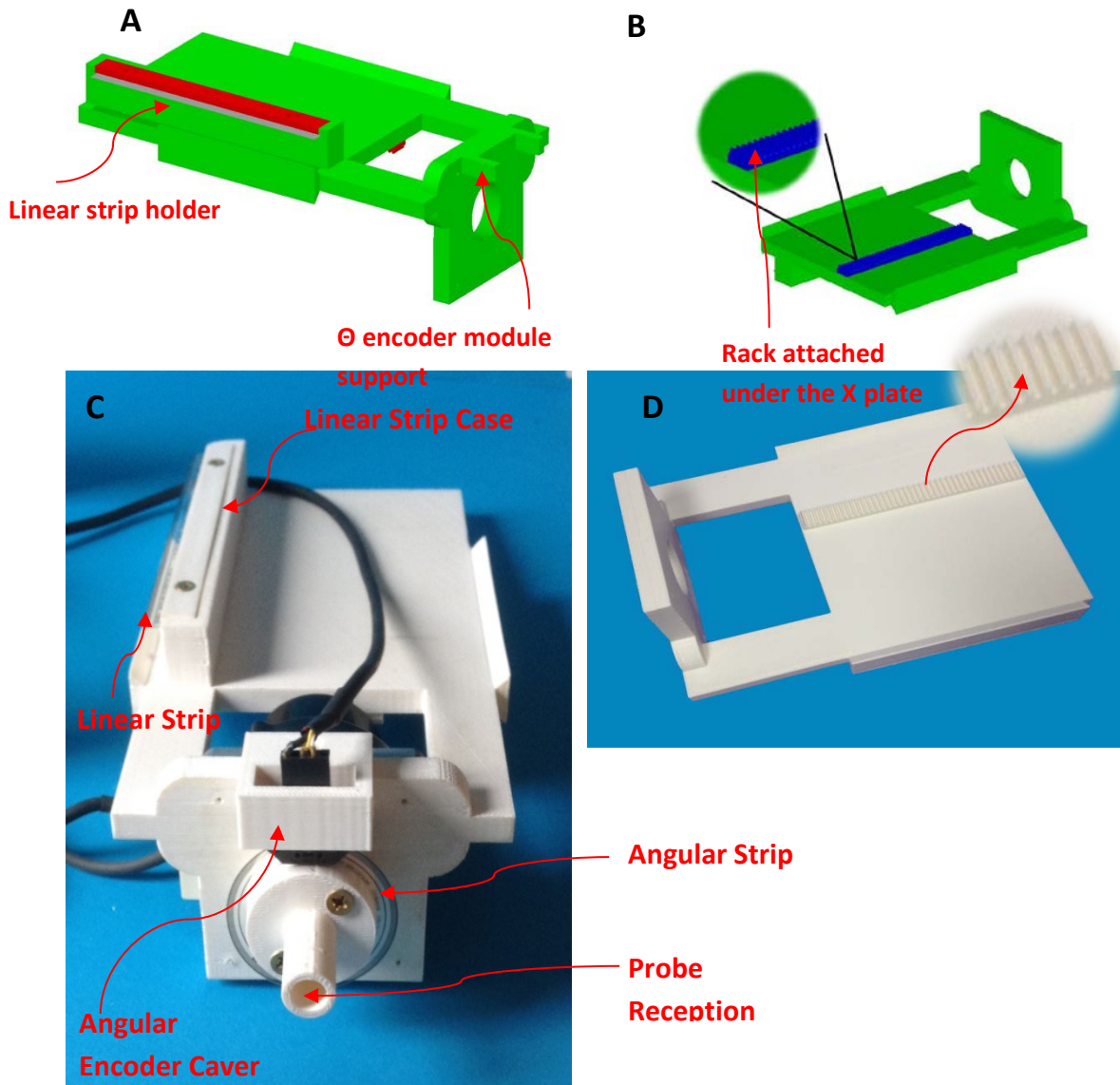
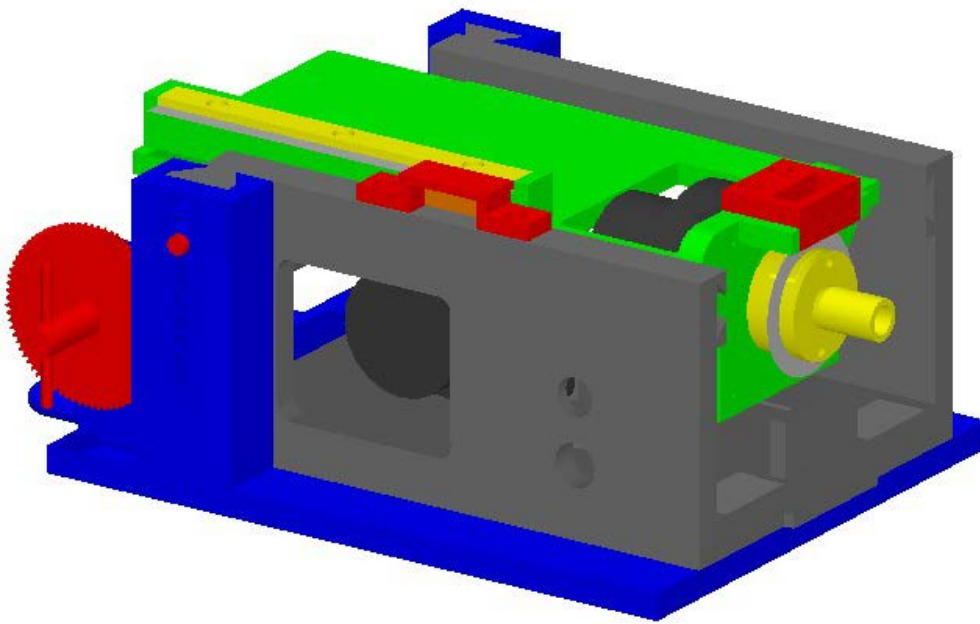


Figure 6.7 A: CAD design (isometric view) of the X plate together with the Θ axis motor, linear encoder. B bottom view of the X plate and rack is visible in this view. C and D photographs of the manufactured part.

The mechanism that rotates the rectal probe on Θ axis consists of two parts. The first part is a cylinder with a hole of 8.1 mm diameter in order to host the motor shaft. The second part is attached to the first part and between the two cylinders plates the angular optical encoder strip is placed. The second part includes a cylindrical space hosting the rectal probe. The angular motion control mechanism is attached to the motor on the X plate (figure 6.7C and 6.7D). Figure 6.8A and 6.8B shows the positioning system, CAD and photograph of the manufactured parts.

A



B

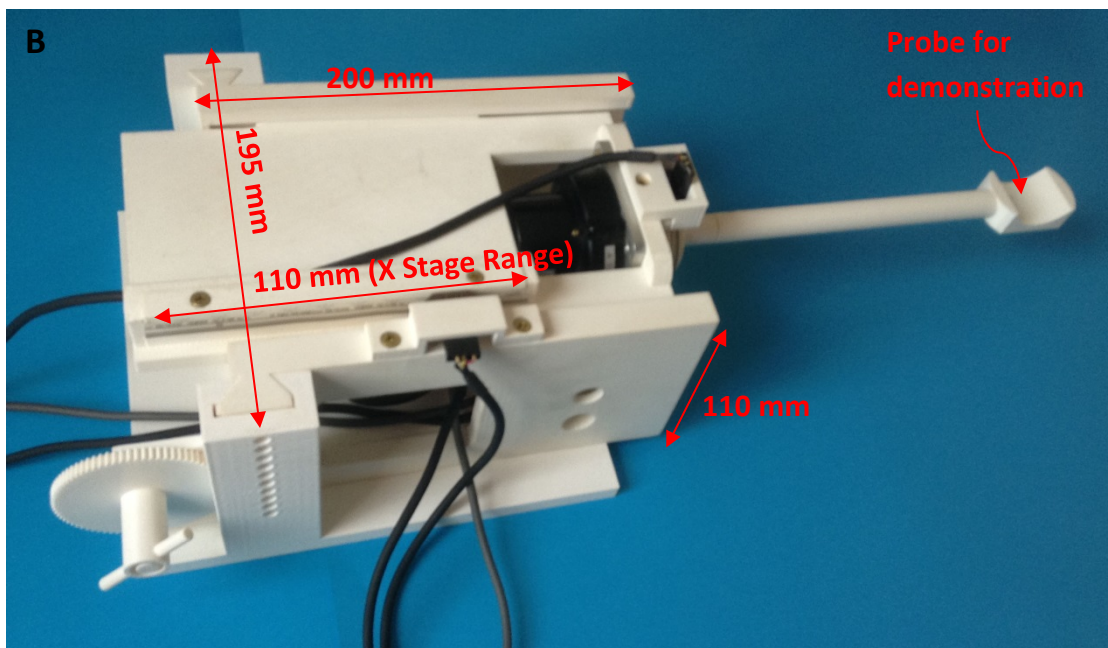
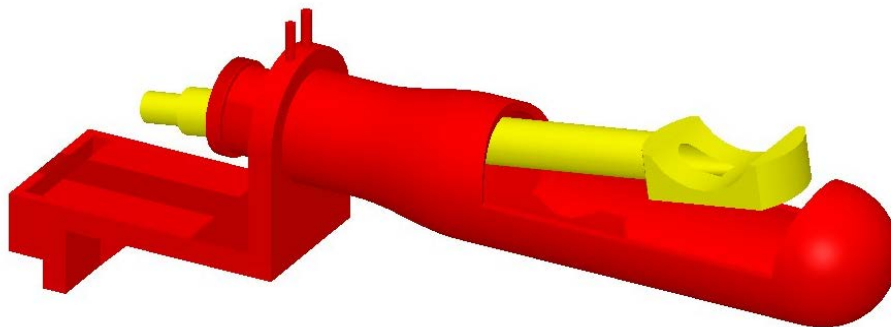


Figure 6.8 A: CAD design of the robot with the robot base, Z axis and X plate together with the angular motion control mechanism. B: a photograph of the robot base, Z axis, X plate and angular motion control mechanism. Additionally, optical encoder modules covers are placed on the robot. A probe has been attached for demonstration purposes.

The need of precise motion is required for any medical application and generally in any robotic system. The close loop feedback system of the robot positioning device consists of optical encoders and strips. Two optical encoder modules and two strips are responsible for controlling the two axes. Figure 6.8A shows the optical encoders and strips placed on base and X plate. Figure 6.9A shows the probe enclosure. The probe enclosure has 200 mm length and 40 mm diameter. The diameter of the probe enclosure is dependent on the size of the transducer that it will be used for the therapy. There is an opening at the top for accessing the prostate using the HIFU transducer. There are two pipes at the top of the enclosure base. The pipes are used for circulating the degassed water. The circulation helps for cooling the rectum. A condom is used in order to seal the enclosure. A plastic balloon is used in order to seal the enclosure at the point of the insertion of probe.

A



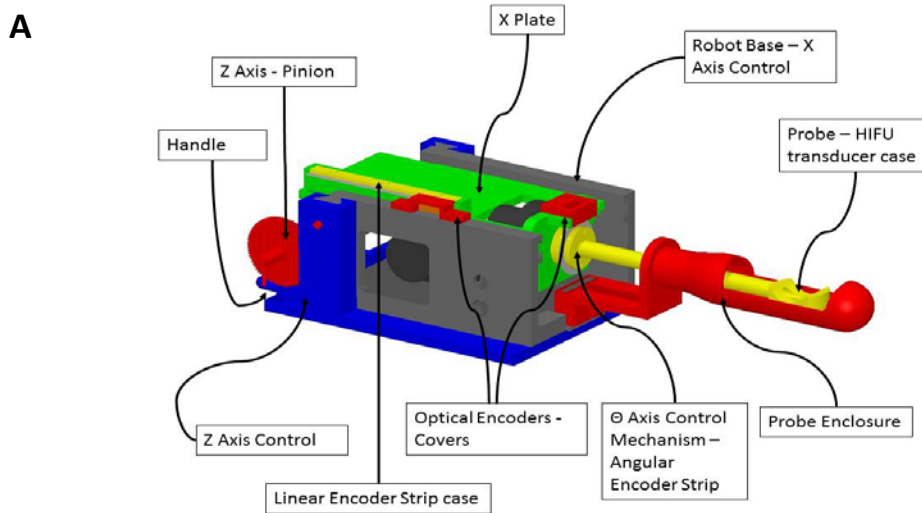
B



Figure 6.9 A: CAD design of the probe enclosure. Image shows the way that probe with HIFU transducer will be inserted into the probe enclosure. B: A photograph of the manufactured part.

Figure 6.10A and 6.10B shows the complete proposed system of the positioning device. Figure 6.10B shows how the Z system elevates the

positioning device to the up to the height of the rectum. The X plate was manufactured finally using gray model, which provides contrast between the different parts of the device. Optical encoder connectors are supplied by the US Digital in order to ensure the better reliability of the encoders operation. Additionally, figure 6.10B shows how the probe enclosure is fitted on robot base and how is inserted into the probe reception point on the angular motion system.



B

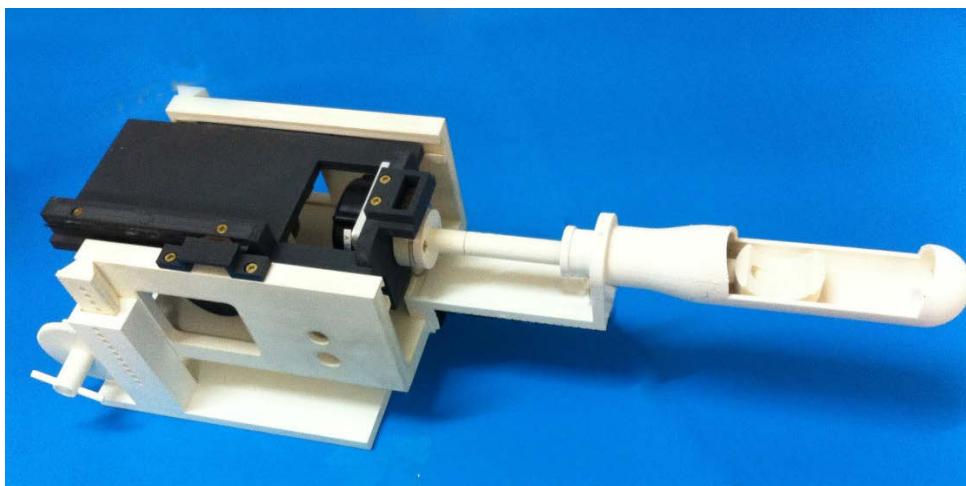


Figure 6.10A CAD design (isometric view) of the robot positioning device. B A photograph of the manufactured positioning device.

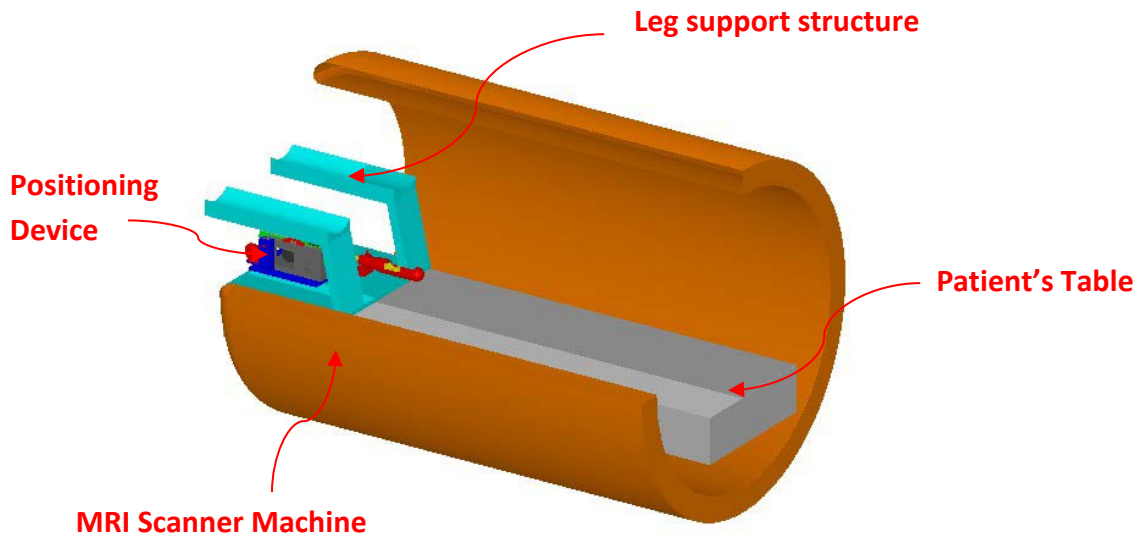


Figure 6.11 CAD design of the positioning device placed on patient's table of an MRI scanner. Also, legs support structure is presented.

Figure 6.11, shows a complete design of the positioning device on a patient's table inside an MRI scanner. Figure 6.11, shows the legs support structure. The positioning device is placed under the legs support. The legs support structure covers only the patient's table under the legs, so there is a space for placing the positioning device directly on the table. The leg support structure size can be changed according to the size of the legs of any patient. Figure 12A shows the positioning device placed on the patient's table of a real clinical MRI scanner. The cables of the device were passed out of the MRI room through a hole on the wall (Figure 12B).

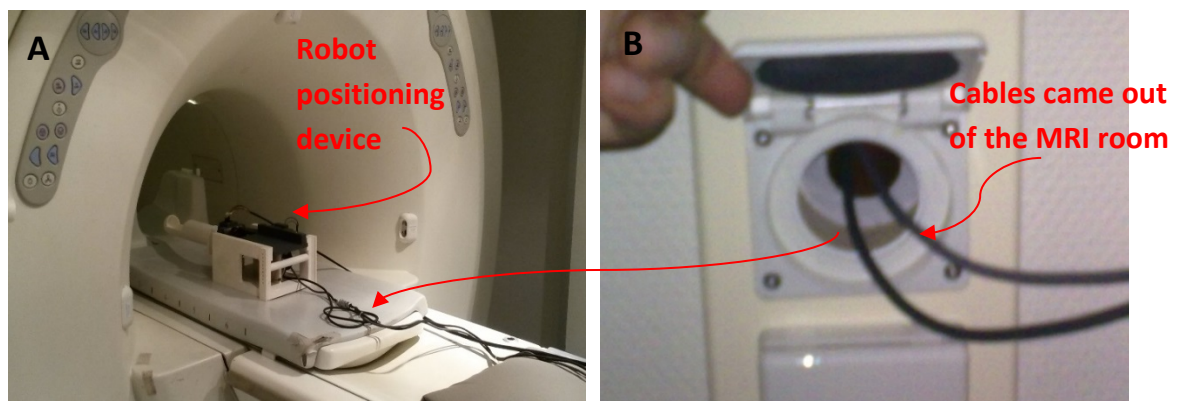


Figure 6.12 A: A shows a photograph of the robot inside the MRI scanner. B shows the cables that are passed out of the MRI room through a hole on the side wall.

6.5. Conclusion and discussion

This chapter, described the design and development of a novel MRI compatible trans-rectal robot positioning device, for heating cancerous cells on prostate gland using therapeutic ultrasound. The robot parts were designed using a CAD software and were manufactured using 3D printer, Stratasys FDM400. The positioning device employs 2 axes (X - Θ), which are PC controlled using software, and one manual axis (Z). The positioning device is responsible to move the rectal probe on X and Θ axis. The presented positioning device incorporates two piezoelectric ultrasonic motors for steering the system and optical encoders for controlling the accuracy of the system. The synopsis of the specifications of the positioning device is shown on table 6.2.

Table 6:2: Synopsis of the positioning device specifications

Positioning device specifications	
<i>Z axis system in mm</i>	
Length	245
Width	195
Height	111
<i>Robot Base in mm</i>	
Length	200
Width	150
Height	101
<i>Accuracy in μm</i>	
X stage	20
Θ stage	13
<i>Range in mm</i>	
X stage	110
Θ stage	$\pm 90^\circ$
<i>Weight in Kg</i>	
Weight	2

The probe on the current device, is 80 mm height from the patients table. This provides a limitation regarding the height of the rectum, where the minimum height of a rectum that can be accessing by the current device is 80 mm. In the future, an improved design of the current device can overcome this limitation by fixing the X – plate at lower height than the current design. The

proposed device could be modified for guiding HIFU transducer for the treatment of various gynecological diseases.

7. Chapter: Close – loop feedback using MRI compatible encoders

7.1. Introduction

Optical quadrature encoders are used for several different applications to provide closed-loop feedback. The goal in this chapter is to design close loop feedback system that establish accurate movement of the robot. The encoder module reads a strip full of dots and it returns the number of dot per inches which is covered by the encoder to the computer. Also this chapter includes, a subprogram which was developed in C Sharp a language of Microsoft Visual Studio 2010 Express Edition (Microsoft Corporation, USA) to control the EM1 optical encoders (US Digital Corporation, Vancouver, WA 98684, USA).

7.2. Optical Encoders – Control of linear and angular motion

The encoder used was the EM1 (US Digital Corporation, USA) trans-missive optical encoder module. The purpose of using optical encoders is to accurate control the linear and angular motion of the positioning device. Optical encoders provide the necessary hardware feedback for controlling the motor movement. For the needs of the 2D MRI compatible robot, two types of encoders were used, angular (figure 7.1) and linear (figure 7.2).

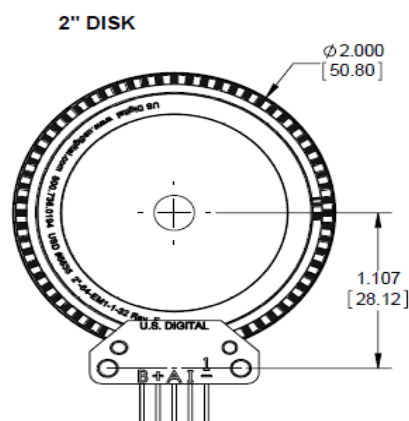


Figure 7.1 Angular EM1 Optical Encoder (US Digital Corporation, USA)

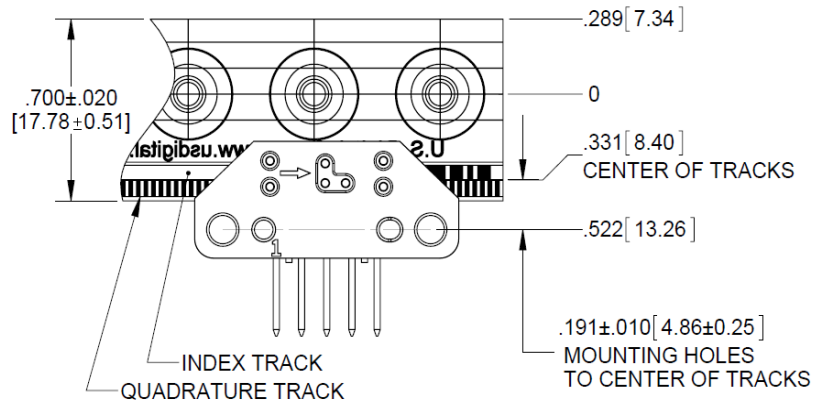


Figure 7.2 Linear EM1 Optical Encoder (US Digital Corporation, USA)

EM1 optical encoders are manufactured, using materials selected for compatibility, with high magnetic fields and fast switching magnetic field gradients encountered inside MRI scanners. The EM1 optical encoders are developed using polymer plastic materials and they use LED (Light Emitting Diode) source and a monolithic detector.

Quadrature encoders typically consist of a spoked pickup wheel attached to the mechanical input. The spokes pass through a pair of optical interruption sensors, consisting of one LED and one light sensor, one LED and two light sensors, or one light sensor and two modulated LEDs. The device generates a pair of phase shifted output streams. The direction of movement can then be determined whether the A or B signal stream is leading. The EM1 come with a third channel, the index channel, that is used to establish an absolute mechanical reference position within one encoder count of the 360° encoder rotation (in case of angular motion).

Three types of encoding can be used on the quadrature encoders: X1, X2, and X4. The basic difference between the schemes is that X1 (figure 7.3) encoder counts once per cycle, X2 (figure 7.4) counts twice per cycle, and X4 (figure 7.5) counts four times per cycle. By counting more times per cycle, X4 is appropriate for high resolution applications. X1 encoding on the other hand, is less susceptible to noise, because the count is only executed once per cycle.



Figure 7.3 X1 Encoding Waveform Diagram (National Instruments - Manual)



Figure 7.4 X2 Encoding Waveform Diagram (National Instruments - Manual)



Figure 7.5 X4 Encoding Waveform Diagram (National Instruments - Manual)

7.3. Close - loop control system design

The close-loop system communicates with external systems through a data acquisition board (USB 6221 NI, Austin, USA). In general, the steering system receives angular and linear position commands from a PC through the NI card device. The system includes the use of a National Instruments (NI) card real time controller; piezoelectric ultrasonic motor, motor driver, EM1 optical quadrature encoder with linear and angular strips, and 24V DC power supply. EM1 optical positioning encoders were connected to the digital input/output port of the NI card device. NI card device was connected to the motor driver and also with the PC through a USB interface. The NI card device supports two counters in digital input/output port.

7.4. Design of the close loop feedback control system of Θ axis motion

The first part of the control system of the MRI compatible robot is the rotation of the Θ axis. An angular strip and an EM1-2-2500-I encoder were used to control this axis (figure 7.6A and 7.6B). So in order to rotate the probe for one degree, rotation equals to 7 DPI (dots per inches) is required. This is because one degree is equals to 7 tracks (dots per inches).

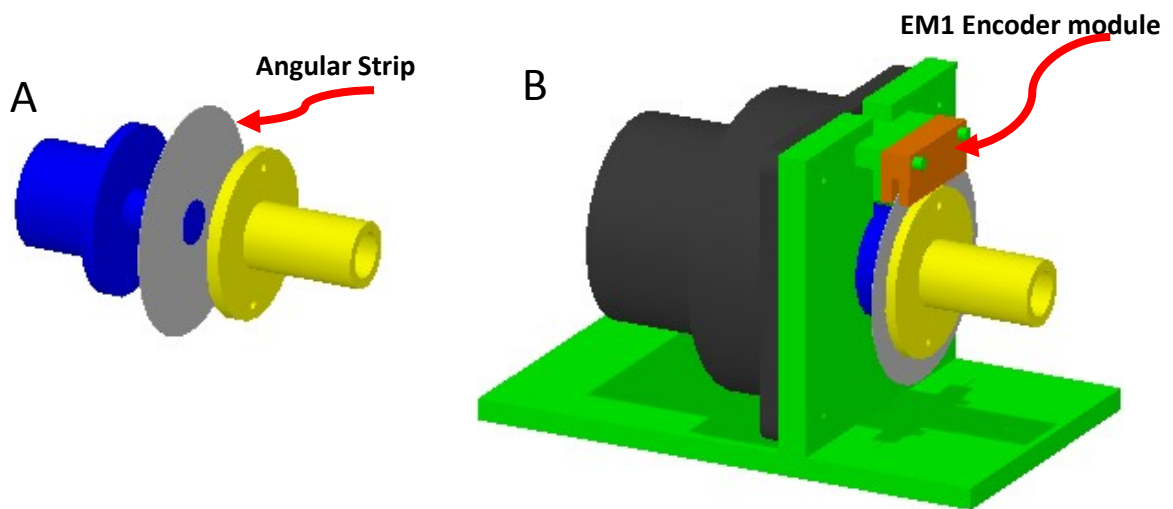


Figure 7.6 A: Angular motion control System Design, B: Encoder Base Design - Angular

According to the design in figure 7.6A and 7.6B, a cylindrical structure was inserted into the shaft of the piezoelectric motor. In one end of the cylindrical structure, there is a circular plate, and within this plate the angular strip is added. Another similar plate is placed on the other side. In order to ensure the origin of the motion, there is a hole in the middle of the strip. This strip hole was enlarged enough to fit on a small cylinder added at the top of the cylindrical plate as shown in figure 7.6A blue part of the drawing. Another circular plate was placed on the angular strip so the strip was placed within the two circular plates. Another cylinder was placed at the top of the second plate. On the second cylinder there is a hole in which the rectal probe will be fitted on (Yellow part in figure 7.6A). The distance between the origin of the angular strip and the origin of the mounting holes of the encoder module was chosen according to the specifications of the US Digital Cop encoder (28.12 mm).

EM1 encoder module was placed at the top of the plate. There are two pins that were placed on a rectangle. The mounting holes of the encoder module were placed on these pins (figure 7.6B). The photograph of complete angular motion control system is shown in figure 7.7.

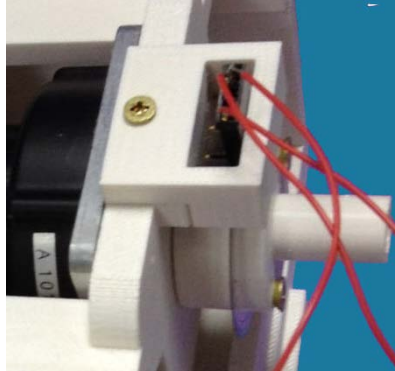


Figure 7.7 Photograph of the developed angular encoder module and strip.

7.5. Design of the close loop feedback control system of X axis motion

In order to control the motion on the X axis, a linear optical encoder (EM1-0-500-I, US Digital Cop, USA) was used. Linear optical encoder has 500 DPI resolution. In order to perform a movement of one millimetre, a 20 dpi linear motion is required. This is because one inch is equals to 24.5 millimeters.

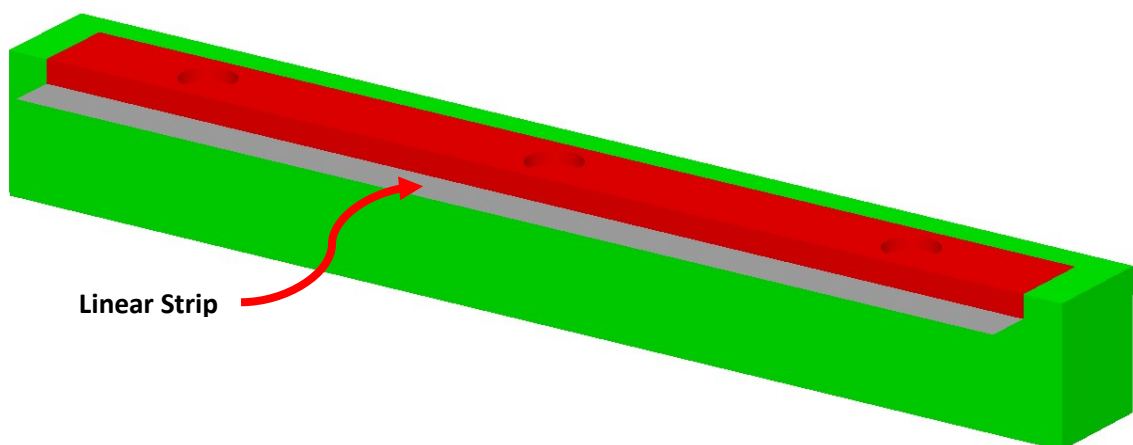


Figure 7.8 CAD design of linear strip base for control of X motion of the transducer.

In figure 7.8, the linear strip was placed on a base attached on the X plate for controlling the linear motion of the system. The linear optical encoder module

was placed on the robot base by using a plastic enclosure (figure 7.9A and 7.9B).

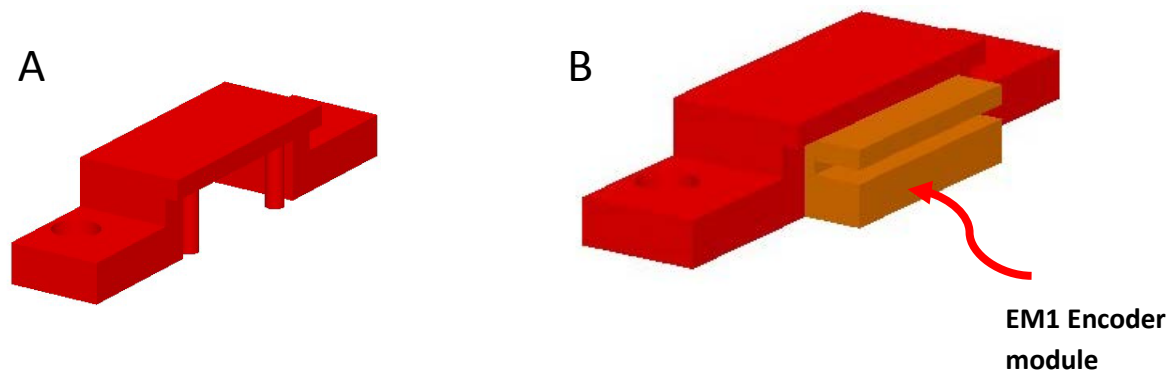


Figure 7.9 CAD design of linear encoder module cover

In figure 7.9A, there are two mounting pins that were fitted on mounting holes that exist on the optical encoder module (figure 7.9B). Also, there are two holes for fitting the cover on the robot base using brass screws. The distance between the middle of the linear strip and the origin of the mounting holes of the encoder module was 13.26 mm (figure 7.2). The photograph of the manufactured parts of the system is shown in figure 7.10.



Figure 7.10 A photograph of the installation of the linear encoder module on a strip

7.6. Control of Optical Encoders using software platform

According to the NI card device manual, there are two counters on Digital I/O part of the pin-outs card. One counter pin was used for each one of the encoder module. An EM1 optical encoder module has the following pin out:

Table 7:1 Encoder Module Pin-out (National Instruments - Manual)

Pin	Five pin signal ended	Pin on NI DAQ device
1	Ground	92/94
2	Index	
3	A Channel	81/76
4	5V DC power supply	96
5	B Channel	

The A Channel of each one of the modules was used for acquiring the edge counter value for the data acquisition board. The edge counter value indicates how many changes from black to transparent have measured by the encoder during the motion. Pin 1 and 4 were used for the power supply (5V DC). The NI DAQ card supplies the encoder 5 volts by connecting the pin number 5 of encoder to pin number 96 of NI card digital I/O part. Pins number 94 and 92 of NI card were connected with the ground pin of the encoder modules. Channel A of the linear and angular encoders were connected with pin 81 and 76 respectively of the NI card device.

A subprogram has been developed, in C Sharp under the Visual Studio .NET 2010 Express Edition platform (Microsoft Corporation, USA), to control the optical encoders (linear and angular). The name of the function is '*getEdgeCounterValue*' and accepts two parameters: the number of the DPI needed to move for each particular axis and the direction of the motion. The function can be called by using the following command:

```
getEdgeCounterValue(Convert.ToInt32(mm), 1);
```

The function is called by passing two parameters. The first parameter is name 'mm' (max value X) which represents the number of DPIs needed to be moved by the encoder module. The second parameter is an integer number representing the direction of the motion.

The communication between the software and the NI card device was established using a session base interface. The following code creates a session by using counter reader task:

```
CounterReadTask.CIChannels.CreateCountEdgesChannel("Dev1/ctr0",  
"", edgeType, Convert.ToInt64("0"), countDirection);
```

The name of the device is the first parameter to this function. Edge type parameter is initialized to 'rising' and the count direction is initialized to 'up', that means the counter will increments while goes up. Also, the initial count number was passed as parameter and it set to zero. The next statement shows how the timing parameters are added to the current task.

```
CounterReadTask.Timing.ConfigureSampleClock("/Dev1/PFI8",  
Convert.ToDouble("10000.00"), SampleClockActiveEdge.Rising,  
SampleQuantityMode.FiniteSamples, Convert.ToInt32("10000"));
```

The function name '*ConfigureSampleClock*' was called by passing five parameters using the counter read task object. The first parameter is the device ID and the digital I/O pin name, the second parameter is the rate of the acquired samples, the third parameter is set to rising, the counter counts when the digital wave is on up edge. The fourth parameter is for setting the sample mode to finite. The last parameter is for setting the number of sample to acquire. The following statement shows how the new instance of the counter reader was constructed:

```
myCounterReader = new CounterReader(CounterReadTask.Stream);
```

The above function was called using the class constructor name '*counterReader*'. The instance created on the above statement is used to acquire an integer value of how many lines are read from the encoder. The value was stored to the variable name 'data'.

```
data = myCounterReader.ReadSingleSampleInt32();
```

The above code was called within a loop until the required value was reached. While the counter value becomes equal to the required value, the loop terminates the function and the motors are turned off.

The following test panel was developed to control the EM1 optical encoder module through the NI 6221USB card device. The test panel consists of four parts: the motion control system of X and Θ axis, an automated motion control system that helps to check the repeatability of the system on grid operation, a part that displays the acquired edge counter value, and a part that helps the end user to set the initial point of the motion in both stages (figure 7.11).

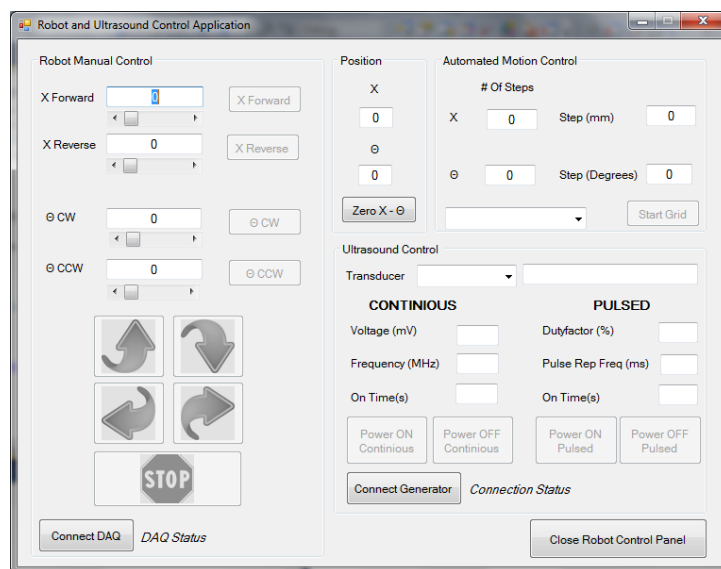


Figure 7.11 C Sharp interface for testing the close loop feedback control system.

Figure 7.11 shows the motion control subprogram of the software with four text boxes and four buttons one for each computer controlled stages of the positioning device. Moreover, there is a subprogram that enables the end user to create an automated motion using both stages. This subprogram consists of two text boxes for entering the steps for X axis (number of steps and distance for each step) and two text boxes for entering the steps for the Θ stage. The current position of the transducer was displayed on two text boxes. Before the motion starts, the starting point has to be set to zero. This is done by pressing the command button named 'Zero X - Θ '.

7.7. Conclusion

The main concern is the accuracy of the motion especially when dealing with devices that are used for medical applications. The hardware feedback gives the ability of excellent repeatability of the motions in both stages, X and Θ (see a sample of measurements in the Appendix). Moreover, the accuracy control system of the positioning device has the ability of accurate control of the transducer and therefore the whole HIFU treatment process.

The presented close loop feedback system consists of EM1 optical encoder module, angular and linear strips and precise design of the bases of the encoder modules and strips based on the US Digital manual. EM1 optical encoders can be controlled by using the NI 6221 USB card device form digital I/O part of the pin-out panel of the card. A special design software function was developed in C Sharp in order to test the control of the EM1 optical encoders.

8. Chapter: Electronic System of the MRI Compatible positioning device

8.1. Piezoelectric Ultrasonic Motors (PUM) and Their Drivers

The actuators of the robot apart from being non magnetic in order to be used in the MRI, must accurately be controlled to guide the HIFU transducer precisely to cover the targeted lesion area avoiding healthy tissues. It must also be small to save space inside the gantry of the MRI and must also be light to contribute to the portability of the robot.

Piezoelectric ultrasonic motors (PUM) have several advantages for space-based robot applications. These motors are MRI compatible, small, light in weight, accurately driven and mechanically simple. Therefore PUM motors are well-suited for these requirements. PUM motor can achieve high precision as a result of low speed, lack of gears and transmissions, and freedom from backlash. They are quite simple mechanically, consisting of a single moving part that provides the same functionality as motor, transmission, and brake in a conventional motor-driven system.

A typical piezoelectric ultrasonic motor (Figure 8.1.) consists of a toothed piezoelectric disk (stator) in contact with a metal disk (rotor). Time-varying electric fields applied to the piezoelectric stator induce a travelling wave which is mechanically rectified, causing the rotor to rotate (Figure 8.2.). This mechanism (Figure 8.3.) produces relatively high torque at low rotor angular velocities, obviating the need for gearing. The friction between rotor and stator provides a passive holding torque typically larger than the rotating torque, eliminating the need for mechanical brakes or active holding torque. These motors can be built such that they neither produce nor are affected by magnetic fields, making them useful in highly magnetic environments and applications in which magnetic fields are harmful.

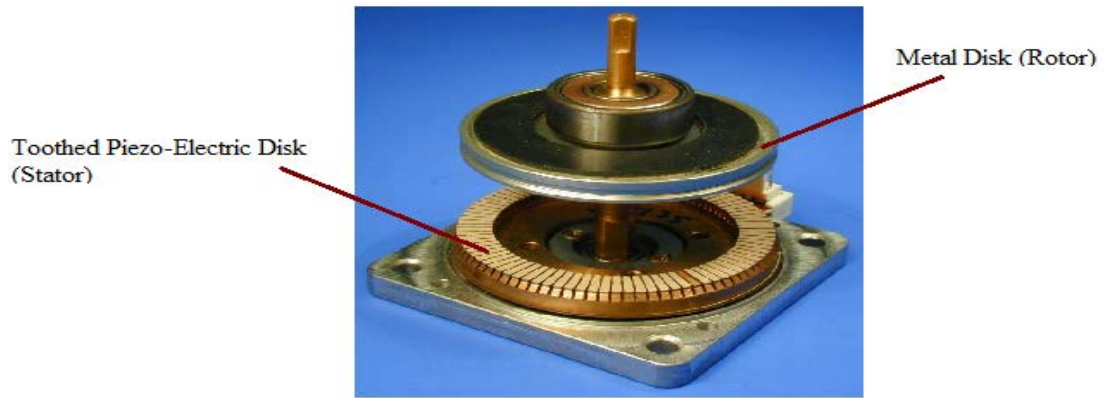


Figure 8.1 Piezo Systems Ultrasonic Motor by Shinsei.

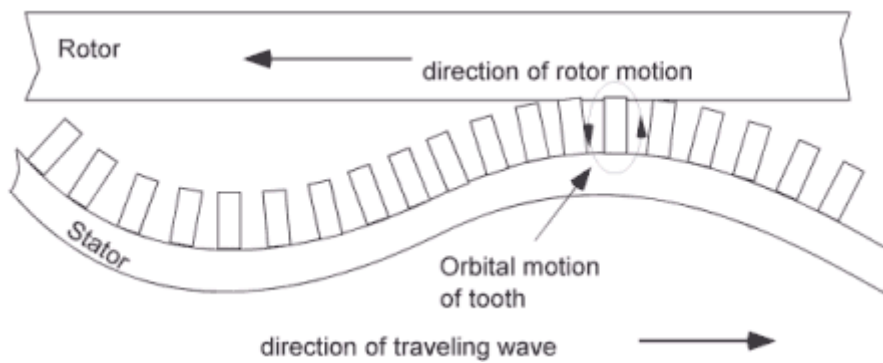


Figure 8.2 Traveling Wave Formation.

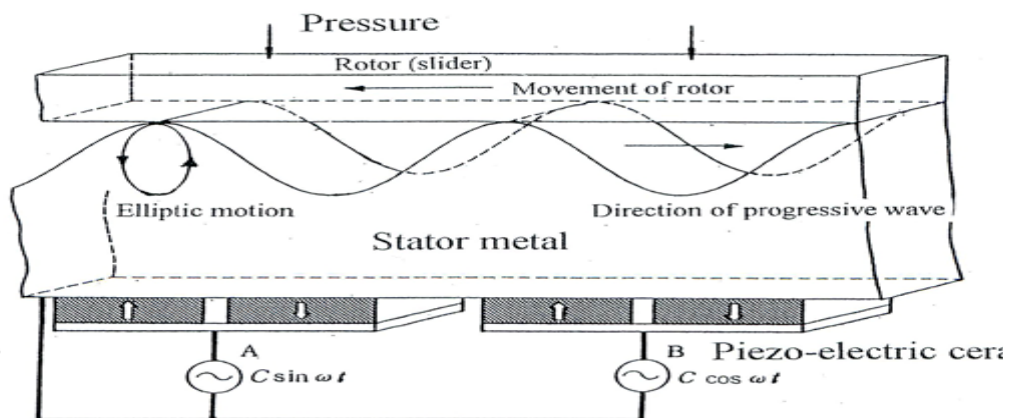


Figure 8.3 Diagram of the Mechanism of the Ultrasonic Motor. The Diagram Above Was

The main structure of ultrasonic motor consist of: a) the stator part which transmits the vibration, b) the rotor which is a rotation part, c) the shaft which transmits the rotation and d) the bearing. Furthermore, the structure of a stator part is the piezo-electric ceramics which generate vibration, the stator metal which makes vibration amplify and the friction material which contacts with a rotor in order to rotate it (Figure 8.4.).

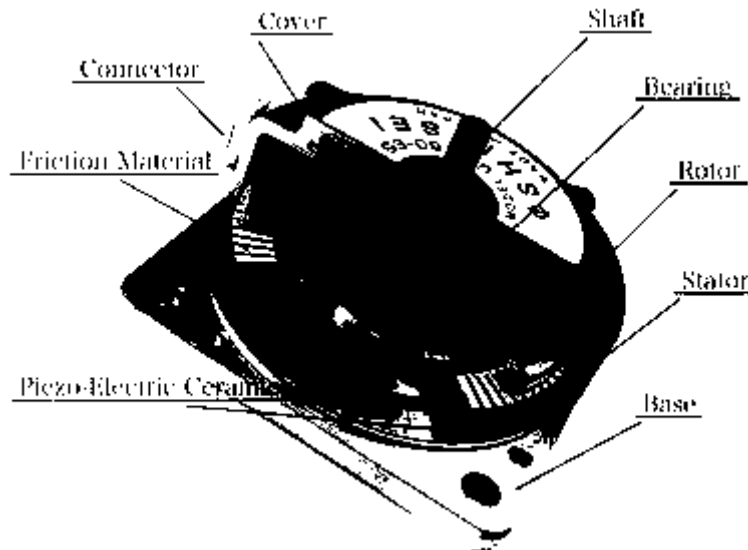


Figure 8.4 Inside Structure of Ultrasonic Motor by Shinsei. (http://www.shinsei-motor.com/English/techno/ultrasonic_motor.html)

The production of drive signals for the PUM motor requires special circuitry that produces a pair of phased sinusoidal signals of variable frequency. The motor was supplied with a standard commercial driver (Piezo Systems/Shinsei D6060E described below) [175] that permits open-loop speed control via an analogue input signal and direction control via a pair of discrete input signals. Figure 8.5 shows a photo of piezoelectric ultrasonic motor by Shinsei USR60E3N and Figure 8.6 a photo of dedicated driver for Shinsei USR60 series, Shinsei D6060E.



Figure 8.5 A Photo of Piezoelectric Ultrasonic Motor by Shinsei USR60E3N.

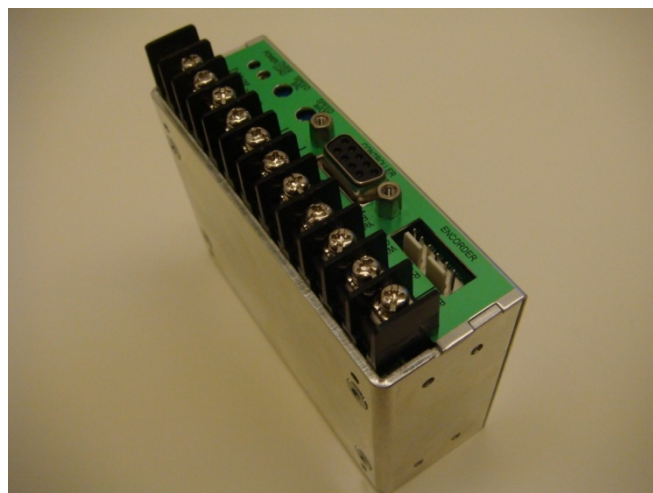


Figure 8.6 A Photo of Dedicated Driver for Shinsei USR60 Series, Shinsei D6060E.

D6060E is the driver for ultrasonic motor USR60 series, it has the function of auto speed control by the encoder signals. By adopting D6060E, users can build the system which stabilized the speed of the ultrasonic motor USR60 series. By using transistor-transistor logic (TTL) voltage levels signal (0 V, 5 V), D6060E can change the direction of rotation to clock-wise (CW), counter-clock-wise (CCW) or stop the rotation. By using analog voltage DC 0 V ~ 3.2 V, D6060E can change the speed of the ultrasonic motor USR60 series. Also a basic connection diagram of the dedicated driver for Shinsei USR60 series, Shinsei D6060E is shown in Figure 8.7.

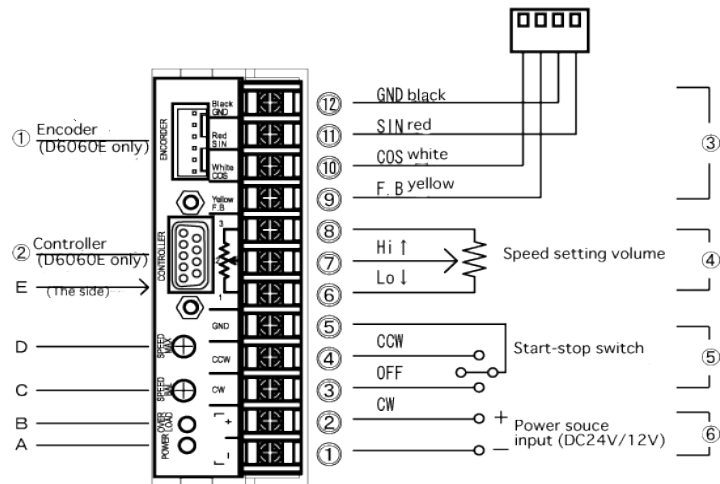


Figure 8.7 Basic Connection Diagram of the Dedicated Driver for Shinsei USB60 Series, Shinsei D6060E.

8.2. Robot drivers

The box hosting the motor drivers is placed outside the MRI room since magnetic materials are involved. Figure 8.8 shows the wiring diagram of the driving electronics and computer-controlled interface.

A DC supply (24 V, 3 A) is used to drive the Shinsei drivers. Wires from the Shinsei drivers are connected to a USB 6221 interface card (National Instruments, Austin, Texas, USA). The USB 6221 interface card includes timing and digital I/O modules. The interface is connected in a portable PC. As it is now the drivers have the ability to drive up to 3 motors.

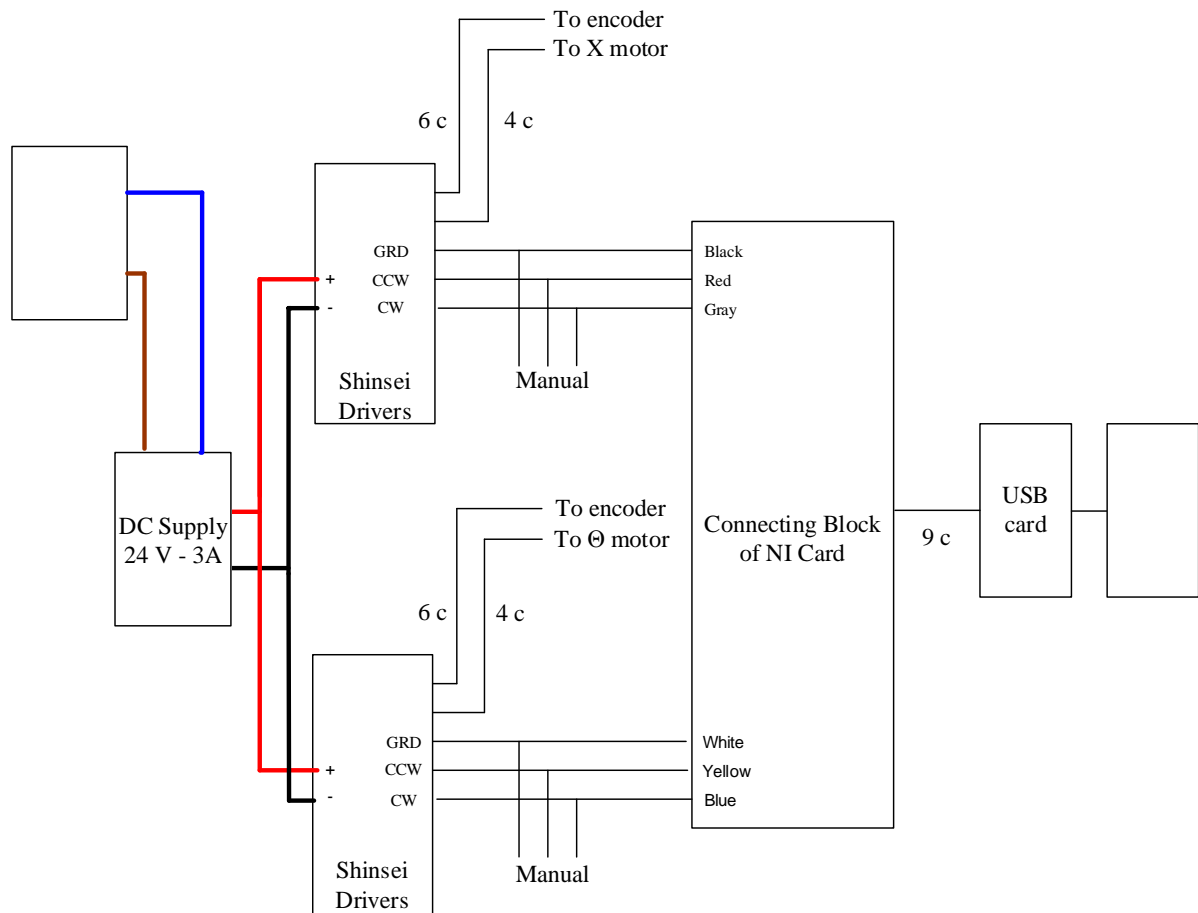


Figure 8.8 The Wiring Diagram of the Driving Electronics and Computer-Controlled Interface.

The motors are driven when the ground and clockwise terminals of the Shinsei drivers are connected (clockwise rotation) or when the ground and anti-clockwise terminals of the Shinsei drivers are connected (anti-clockwise rotation). This is achieved by initiating a command from the software which places 2 digital output terminals of the USB card (for example ground and clockwise) in the same potential. Movement of a certain axis can be achieved also manually by means of an ON-OFF-ON switch.

8.3. Parts and Specifications of Drivers

The parts of the drivers which have been used for the positioning device have been selected to be suitable for the enclosure box (A0234670 EURO CASE 42 TE, see figure 8.9) [176]. This enclosure box will host 2 drivers (Shinsei D6060E, described above), power supply (see Figure 8.10 and Table 8.1 for specifications), the front panel (A0334270 42 TE 3 HE) which mount the main AC switch ON-OFF (CANG WANG, KCD-2, 16A-260V), three switches ON-OFF-ON which control manually the motion of the PUM motor (CW, CCW, stop) and screw-locking mountable receptacles (9 contacts D 104A055, 6 contacts D 104A056, 4 contacts D 104A053). Figure 8.11.A shows the schematic of the main switch and the schematic of the switch that used to control manually the motion (figure 8.11.B). Also cables included, whose specific color is used for proper identification. The weight of the robot drivers is only 3 kg.

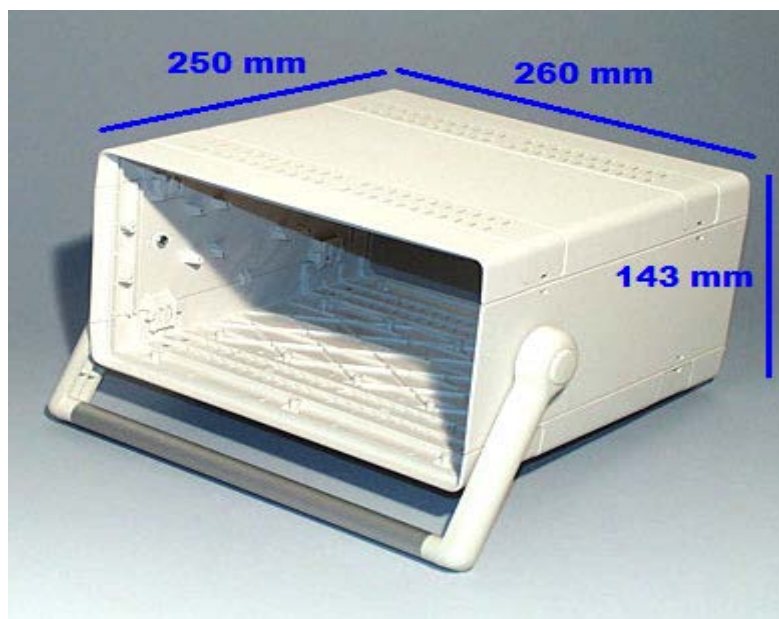


Figure 8.9 Euro Case 42 TE A0234670 by OKW.



Figure 8.10 A Photo of Power Supply by Mean Well, S-72-24.

Table 8:1 Specifications of the power supply.

Specification	Value
Family	S-72-24
Minimum Operating Temperature	-10°C
Maximum Operating Temperature	60°C
Maximum Input Current	4A
Input Frequency	47Hz to 63Hz
Output Connector Type	Screw Terminal Block
Minimum Isolation Voltage	3000V
Number of Outputs	2
Output Voltage	24V DC
Type	Auto Switching
Style	Enclosed
Product Type	AC to DC Power Supply
Maximum Output Current	3A
Maximum Output Power	60W
Input Voltage	90-132V / 180-264V AC
Product Height	42mm
Product Length	159mm
Product Width	97mm
Efficiency	80%

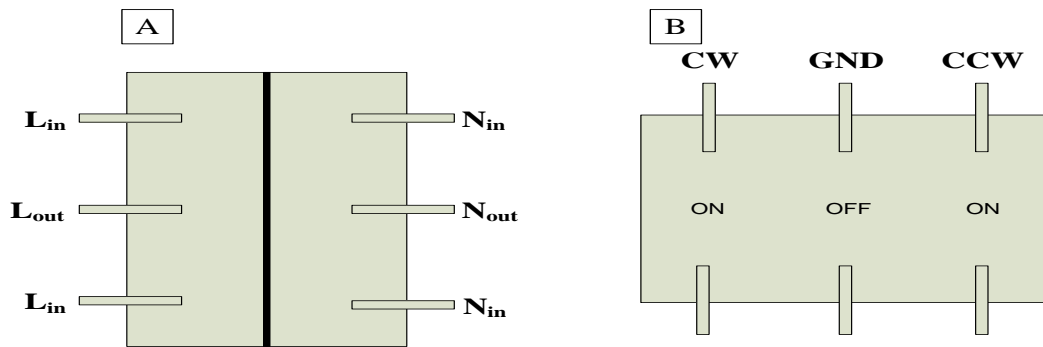


Figure 8.11 A. the Schematic of the Main Switch and B. the Schematic of the Switch That Used to Control Manually the Robot.

8.4. Development of Drivers for the Positioning Device

The drawing of the front panel of the enclosure box is shown in figure 8.12.A and figure 8.12.B shows a photo of the front panel after the implementation. The front panel includes the AC switch, 3 switches for manual control, the interface receptacle (9 pin) and one 4 pin and one 6 pin receptacle for each axis. The details of the receptacle connection are shown in figure 8.13. The length of the front panel is 25 cm and its height is 13.5 cm. Furthermore, the drawing of the rear panel of the enclosure box is illustrated in figure 8.14.A. and a photo is shown in figure 8.14.B. The rear panel includes a receptacle for receiving AC voltage from the mains.

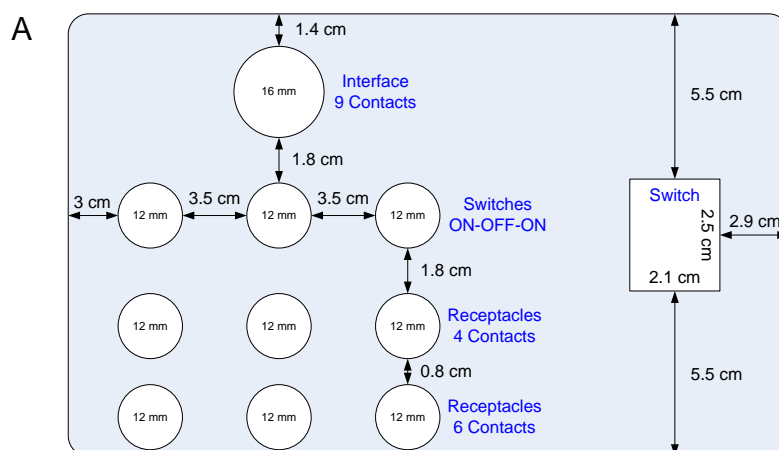




Figure 8.12 A The Drawing of the Front Panel. B. A Photo of the Front Panel After the Implementation.

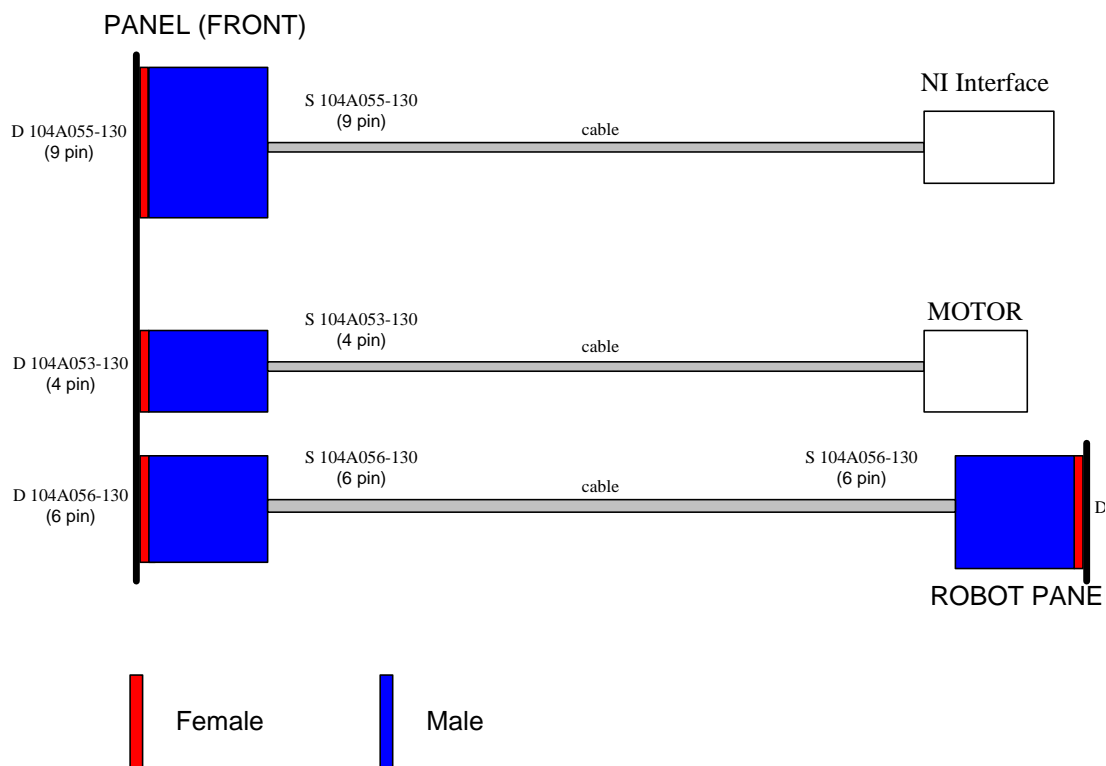


Figure 8.13 Connector Diagram

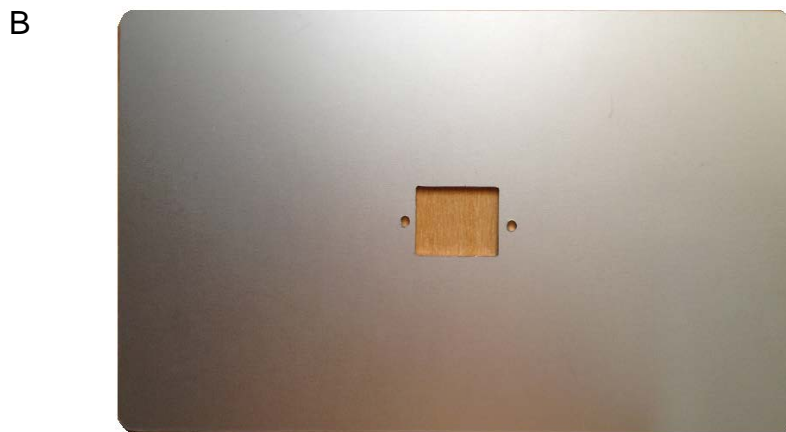
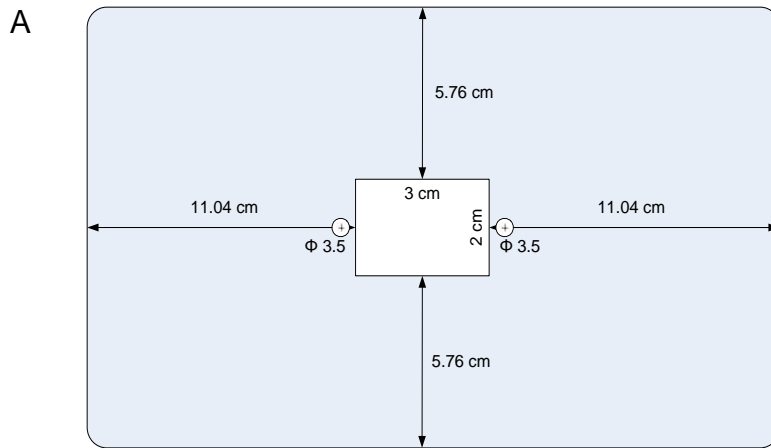


Figure 8.14 A. The Drawing of the Rear Panel. B. a Photo of the Rear Panel After the Implementation

Figures 8.15 and 8.16 show the front and rear panel with the various components installed. Figure 8.17 illustrates the enclosure box when the front and rear panel have been placed. Moreover in figure 8.17 is shown a holder which accommodates the two drivers (Shinsei D6060E) and the power supply (Mean Well, S-72-24) [177]. The power supply has been tested for providing the right voltage since is adjustable and the output voltage has been regulated to 24V which is the proper voltage to feed the drivers.



Figure 8.15 Front Panel With Components Installed.



Figure 8.16 Rear Panel With Components Installed.

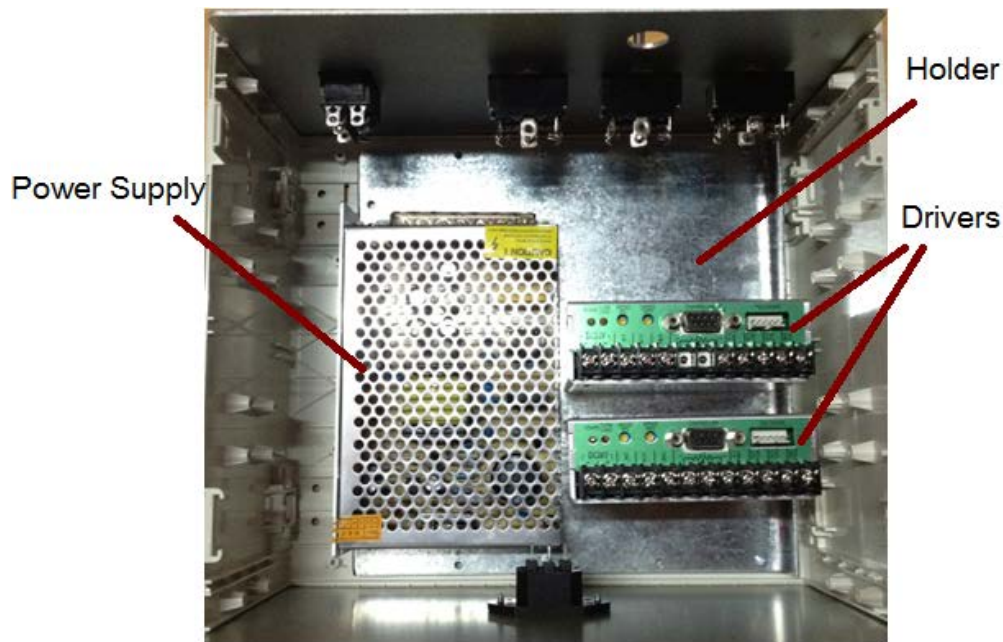
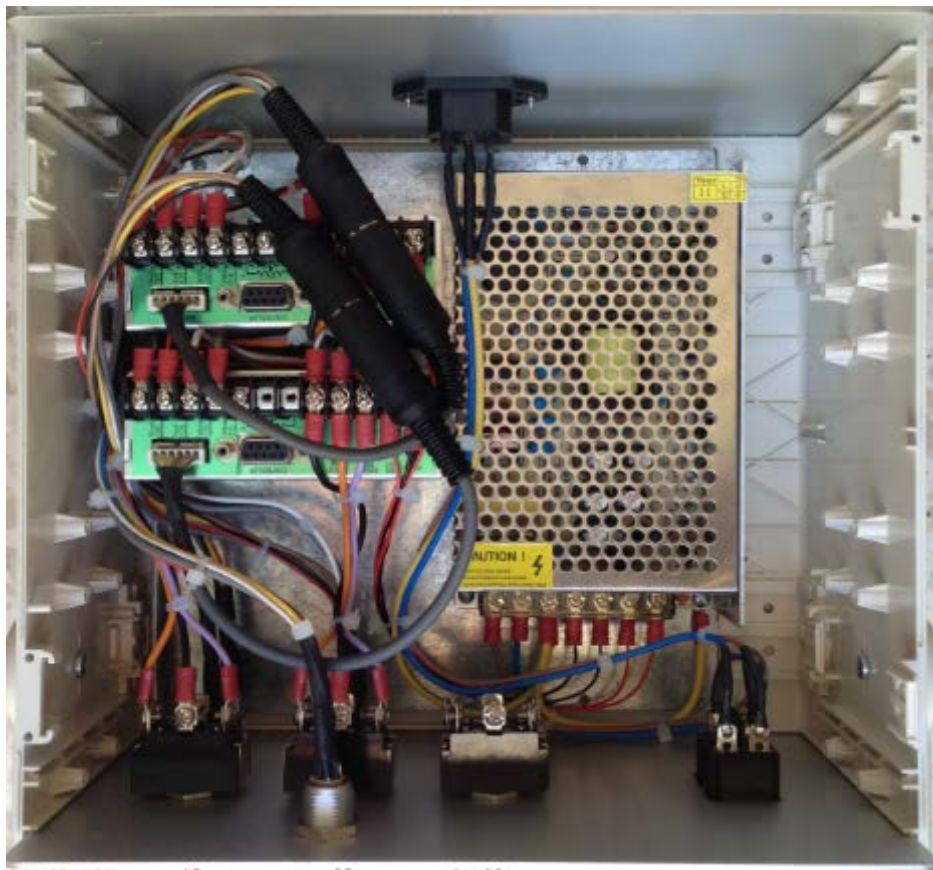


Figure 8.17 Enclosure Box With Front and Rear Panel (Top - Inside View).

Figure 8.18.A shows a photo that illustrates the wiring connection of the components. The corresponding full circuit schematic is illustrated in figure 8.18.B. The AC plug has been connected through wires to the input of the main switch to provide break to the overall system. Then the output of the main switch is connected to the DC power supply in order to convert the 230V AC to 24V DC since the drivers are compatible with 24V DC. For the connection of the power supply to the Shinsei driver D6060E the selected colours for cables was the red and black for live and ground respectively. The switches that control manually the motion of the PUM motor have been connected through wires. The selected colours of cables were the purple for clock-wise (CW) motion, the orange for counter-clock-wise (CCW) motion and the black for ground. Also the screw-locking mountable receptacle that will be used for interface (9 contacts) was connected to the drivers in the same point where the switches (ON-OFF-ON) have been connected previously. The selected colours of the cables that correspond to the driver of the X-motion are the following: grey, red and black for CW, CCW and ground respectively. However for the driver which is responsible for the Θ -motion the chosen colors are blue for CW, yellow for CCW and white for ground. From the drivers (motor connection terminal) to screw-locking mountable receptacles (4 contacts) and then to the motors, the selected colors for cables are the black,

red, grey and white. In order to stabilize the speed of a motor, the drivers use the encoder signals from a motor. The connection from the driver (encoder terminal) to the screw-locking mountable receptacles (6 contacts) and then from the motor back to the screw-locking mountable receptacles to receive the encoder signals the chosen colors of cables are black, red, grey, white, yellow and brown.

A



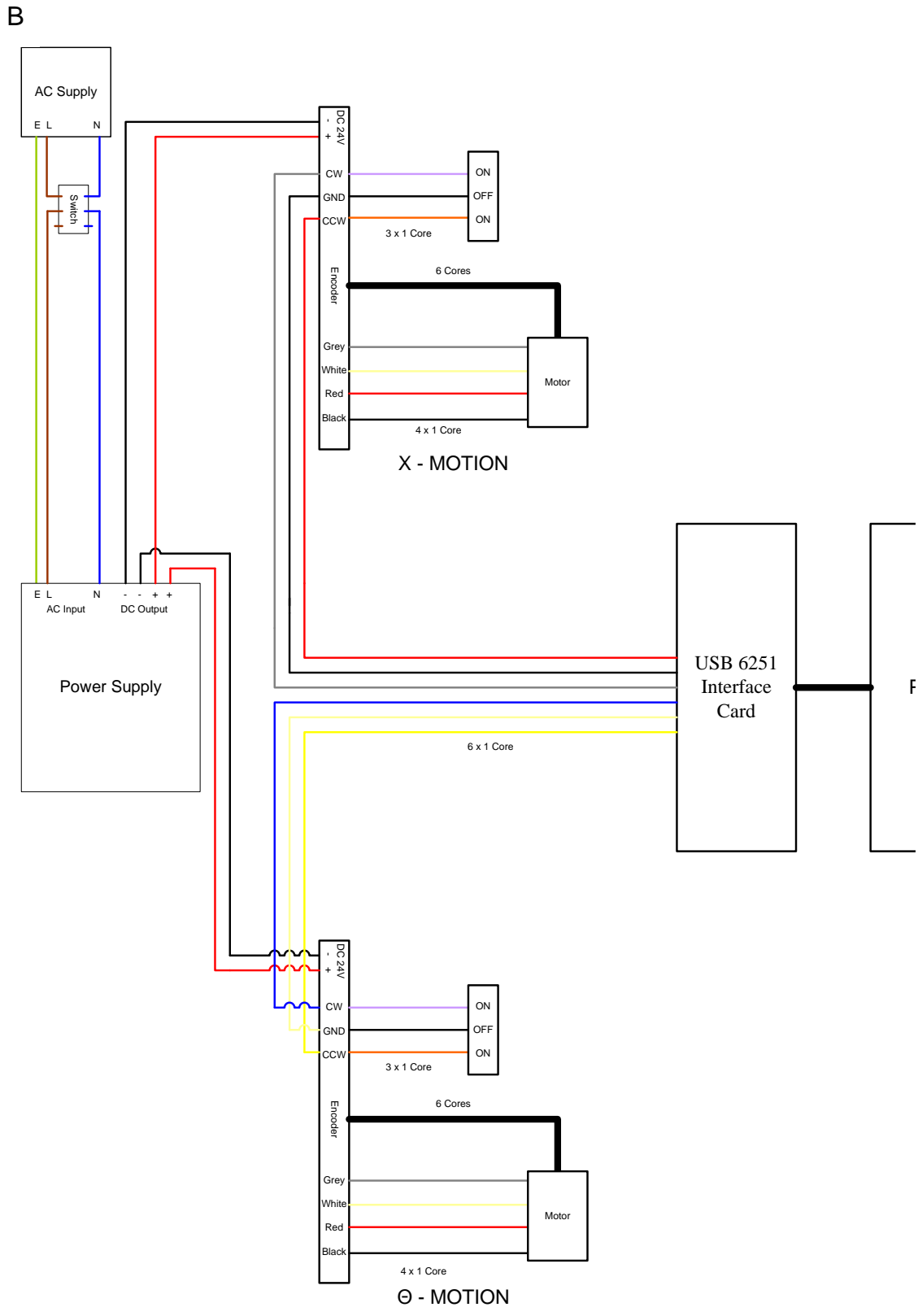


Figure 8.18 A Photo That Illustrates the Wiring Connection (Top – Inside View). B the Corresponding Circuit Diagram.

In table 8.2, it can be seen all the components used for the construction of the positioning device driver and their brand and type.

Table 8:2 List of the Components.

BRAND NAME	ITEM	TYPE	QUANTITY	CONTACTS
OKW Gehäuse Systeme	<u>EURO CASE 42 TE. with handle</u>	<u>A0234670</u>	1	-
OKW Gehäuse Systeme	Front / rear panel 42 TE 3 HE	A0334270	2	-
OKW Gehäuse Systeme	Self-tapping screws 3 x 6 mm	A0306031	20	-
Fischer Connectors	Rear receptacles (female)	D 104A055	1	9
Fischer Connectors	Rear receptacles (female)	D 104A056	3	6
Fischer Connectors	Rear receptacles (female)	D 104A053	3	4
Fischer Connectors	Straight plugs (male)	S 104A055	1	9
Fischer Connectors	Straight plugs (male)	S 104A056	3	6
Fischer Connectors	Straight plugs (male)	S 104A053	3	4
MEAN-WELL	Power Supply	S-72-24	1	-
Shinsei Corporation	Driver	D6060E	2	-
Shinsei Corporation	Ultrasonic Motor	USR60-E3N	2	-
CANG WANG	Switch (on-off)	KCD-2	1	6
FBELE Switch	Switch (on-off-on)	KN3(B)-202	3	6
All Electronics Corporation	AC Plug	CAT ACS-48	1	3

In figure 8.19 is illustrated a photo of the previous version of the driver that had been used to control the positioning device for the treatment of prostate cancer. It can be seen that the power supply (Shenzhen Mastech, HY3003D-3) is out of the enclosure box and this makes the system difficult to its portability rather than in the new version where the power supply is in the

enclosure box. So, the new version needs less space than the previous one and hence the new system is more portable. Also the existing solution is quite more expensive. On the front panel of the previous version there are three switches and a DC plug and on the rear panel one can see the screw-locking mountable receptacles for the motor, encoder and interface. In the new version the front panel includes the main switch, three switches for manual control, screw-locking mountable receptacles for the motor, encoder and interface. A figure 8.20.A shows the front panel and figure 8.20.B shows the rear panel (whole driving electronic system for the new version of driver).

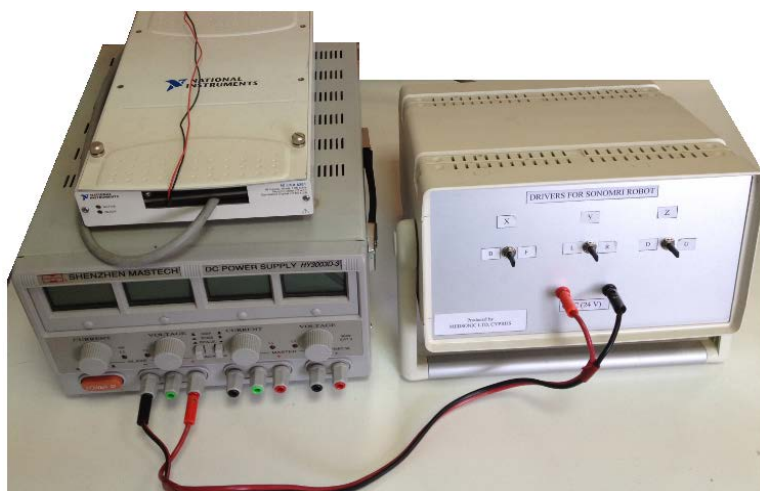


Figure 8.19 A Photo of the First Version Drivers

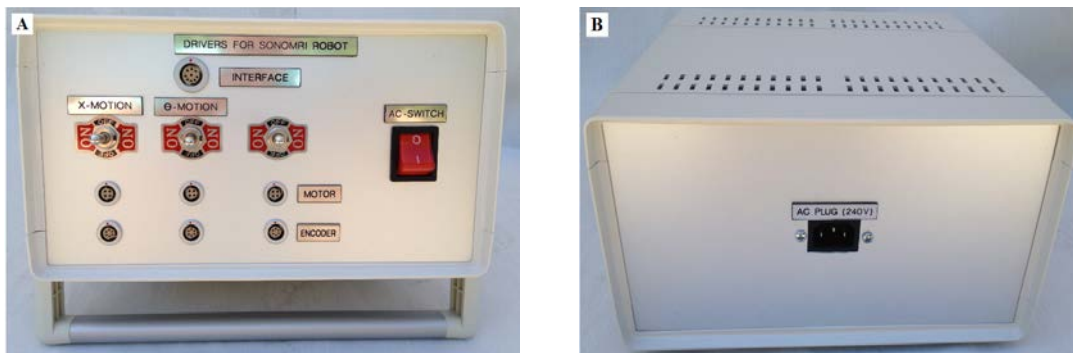


Figure 8.20 A. a Photograph of the Front Panel and B. a Photograph of the Rear Panel of the New Version Drivers

9. CHAPTER: Design and development of software for controlling an MRI guided focus ultrasound robot assisted system.

9.1. Introduction

The software serves seven main tasks: a) MRI imaging, b) transducer movement (the user may move the robot manually or automatically by specifying the pattern, the step and the number of steps), c) messaging (starting time, treatment time left etc), d) Camera control, e) Patient data (age, weight, etc), f) Controlling the parameters and activation of a signal generator, h) Temperature reading of HIFU focal point. The software is responsible to control the entire operation from outside the MRI scanner room.

The design of the software was designed using Microsoft Office Visio 2010 (Microsoft Corporation, USA). The software was designed to fulfill all the needs of MRI compatible HIFU robot assisted system. The software was designed in subprograms that merged in one single platform.

9.2. System Architecture

9.2.1. Architecture Design

The main goal of the software platform is to control the MRI compatible robot that performs HIFU treatment on prostate gland. In order to archive this, the software platform has to control a number of devices. Therefore, the design of the software was divided into different subprograms. The software was divided into the following tasks: a) control of the HIFU protocol, b) control of the robot movement, c) control of the MRI compatible camera, d) control of the MRI images, and e) command history list.

In order to implement the above task, the following devices are required (figure 9.1): a) data acquisition board, b) signal generator, c) MRI compatible camera, d) MRI compatible robot.

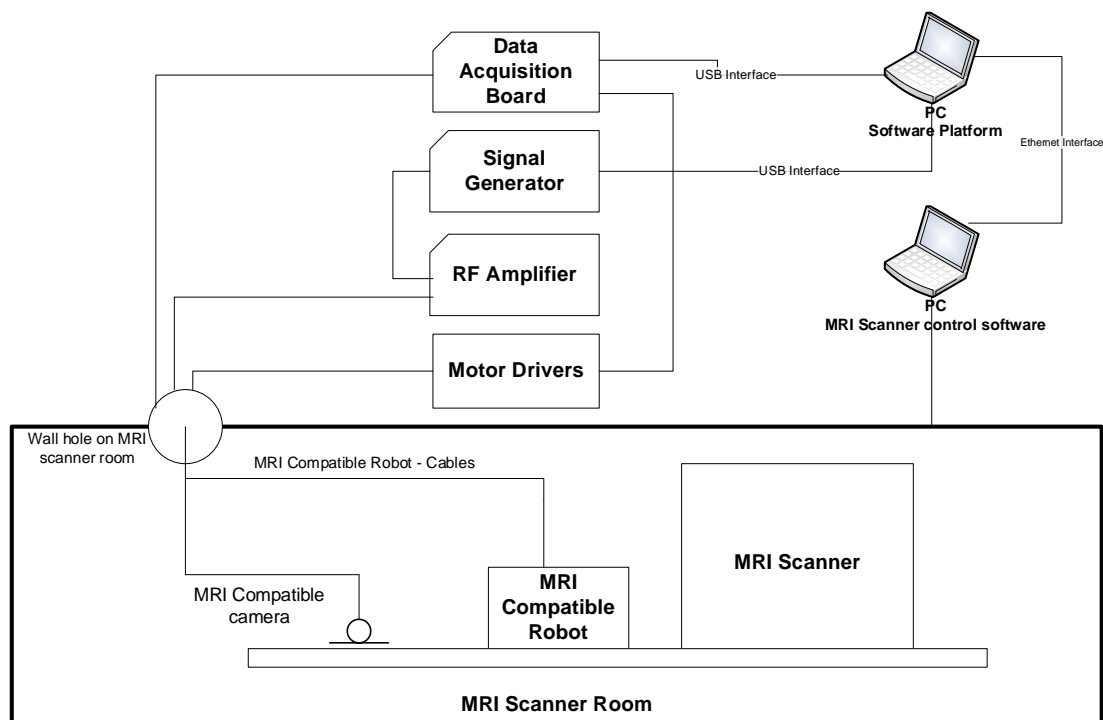


Figure 9.1 a schematic of the complete MRI compatible HIFU system

In figures 9.1 the components that were placed inside the MRI scanner room had to be MRI compatible because of the strong magnetic field. Therefore, the robot chassis, actuators, sensors and camera must be MRI compatible. The robot holds an MRI compatible HIFU piezoelectric transducer.

9.2.2. Decomposition Diagram

Figure 9.2 shows that the software has been separated into subprograms of the software.

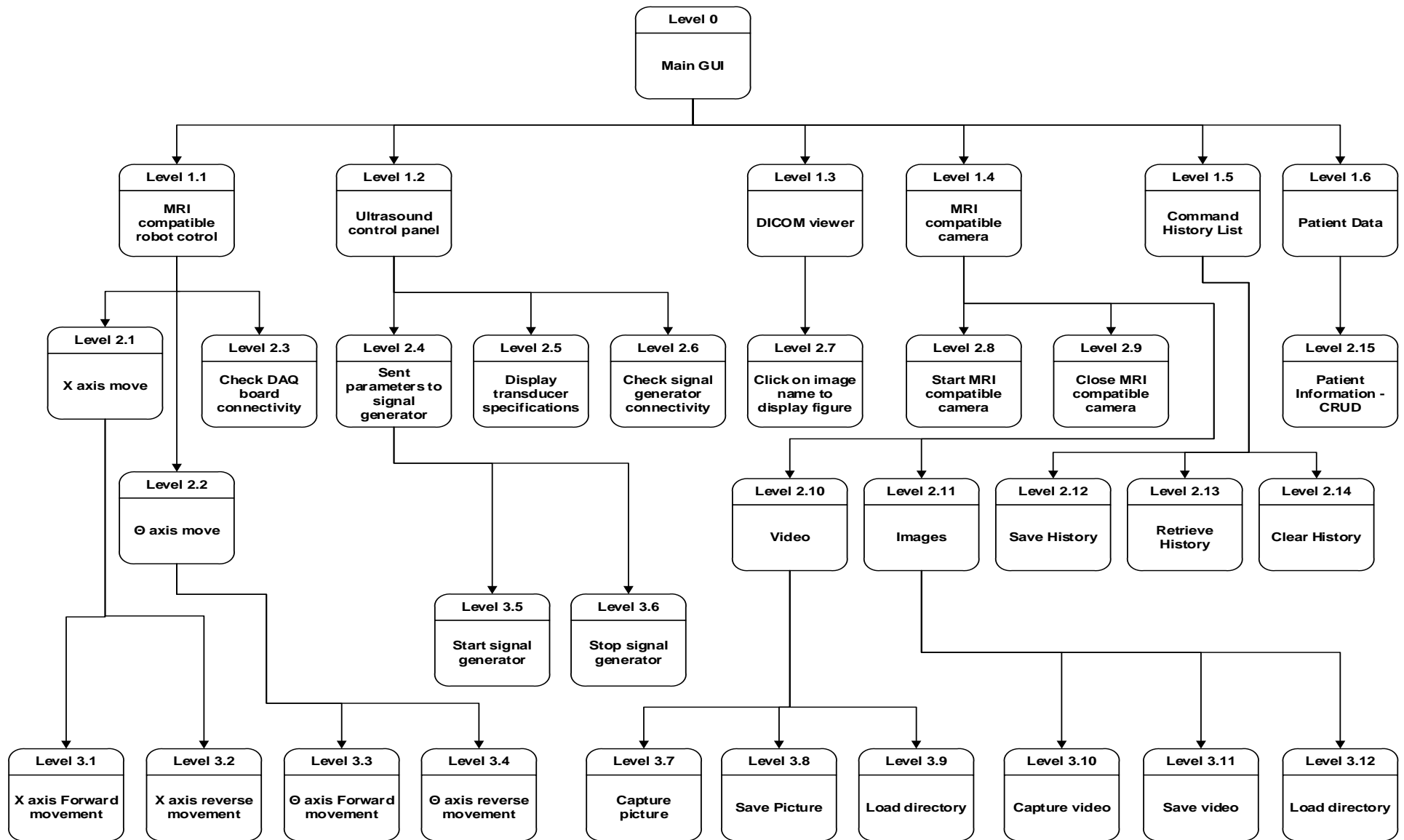


Figure 9.2 Diagram of software

In figure 9.2, the software platform was decomposed into six subprograms. At level zero or context level is the system. At the level one, the software was decomposed into six main functionalities. At the second level, the main functionalities have been separated into sub process one by one. Moreover, all main functionalities at level two have been divided into sub process at level three.

9.2.3. Data Flow Diagram

In figure 9.3, the flow of data is presented. The data flow is analyzed at level one of the decomposition diagram. In this diagram is the flow of data through the various parts of the MRI compatible HIFU system. The arrows show the flow of data from the subprogram to the controlled electronic part and vice versa (in case that is needed).

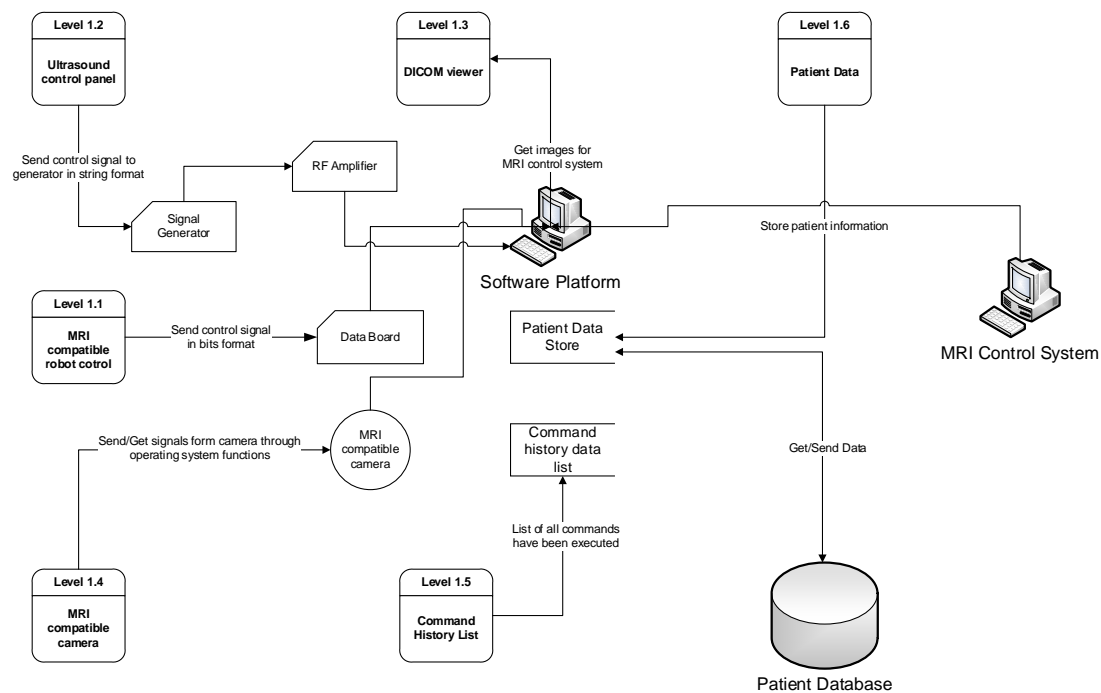


Figure 9.3 Data flow diagram for level one of decomposition diagram

Sub program 1.1 (robot control panel) sends control signal to data board in bits format. This signal is responsible to control the MRI compatible actuator.

Sub program 1.2 (ultrasound control panel) sends signal to generator in string format. The signal generator understands data in string format. Sub program 1.3 (DICOM viewer) gets the dicom file images from the MRI control system in order to display the images from the software platform, to the users. Sub program 1.4 (MRI compatible camera control panel) sends and gets signals from camera by using the operating system's functionalities. The camera returns the captured images to the software platform. Sub program 1.5 (command history panel) stores the commands executed by the software in a list. Finally, sub program 1.6 (patient data) stores useful information about a particular patient into a database file. The software can also retrieve back information for display.

9.3. Human Interface Design

9.3.1. Design of Ultrasound control panel interface (GUI)

The point of using GUI (Graphical User Interface) in all programs is to help the end user that runs the program in an easy and friendly manner. Each parameter can be inserted by the user easily and fast. Figure 9.4 shows the ultrasound control panel GUI.

The screenshot displays a GUI for controlling a signal generator. At the top, there is a 'Transducer' label followed by a dropdown menu showing 'Enter Text' and a small blue arrow icon, and an empty text input field. Below this, the interface is divided into two columns: 'Continuous' on the left and 'Pulsed' on the right. Each column contains three text input fields with corresponding labels: 'Voltage (mV)', 'Frequency (MHz)', and 'ON Time (s)' for the Continuous mode; and 'Duty factor (%)', 'Pulsed Repetition Frequency (ms)', and 'ON Time (s)' for the Pulsed mode. At the bottom of each column, there are two buttons: 'Power ON' and 'Power OFF', with the mode name (Continuous or Pulsed) written below them. At the very bottom of the interface, there is a 'Connect' button and the text 'Agilent Generator Status'.

Figure 9.4 Design of interface for controlling the signal generator

There are six textboxes helping the users to provide the correct parameters to the signal generator. Also, buttons of turning ON and OFF the power were created. Labels that describe what each text box is doing. Additionally, all text boxes are grouped according to the mode of operation. The signal generator

interface is separated into two groups, continuous and pulsed. At the top of the interface a combo box is placed. This combo box is filled up by the list of HIFU transducers. The user has the ability to select a transducer and the specifications of the selected transducer is demonstrated to a text box next the combo box. Additionally, there is a button named Generator. Generator button checks whenever the generator is connected to the computer or not. The resulting message is presented to a label next to that button.

9.3.2. Design of MRI compatible camera control panel - GUI

Figure 9.5 shows the design of the interface. There are six buttons. The first button is used to start the MRI camera, the second button is used to stop the MRI camera, the third button is used to start the recording, and the fourth button is used for taking snapshot images from the camera. The remaining buttons are used for saving the captured images to the selected directory.



Figure 9.5 Design of software that control the MRI camera

The snapshot image object is used for displaying the image computed by the MRI camera. Also, while the camera records a movie, the movie is displayed like a live streaming video.

9.3.3. Design of MRI images control panel – GUI

After the MRI scans the patient, images are saved in series of *dicom* format files on the computer that controls the MRI scanner. The software platform has the ability of getting the images and also it can display the images in two ways: a) the user can load the images all together, and b) the user can display the images one by one by clicking on the image file name.

Figure 9.6A shows the two buttons, the list box, and the text box. The user has the ability of selecting the correct directory and the file names of the images listed on the list box. The user can see the images by clicking on the file name. Images are placed on the screen on series of 1, 2, 3, 4..... n according to the parameter passed by the activation on text box labeled '*Number of Figures*'. The button named '*Close all*' closes all figures that are opened

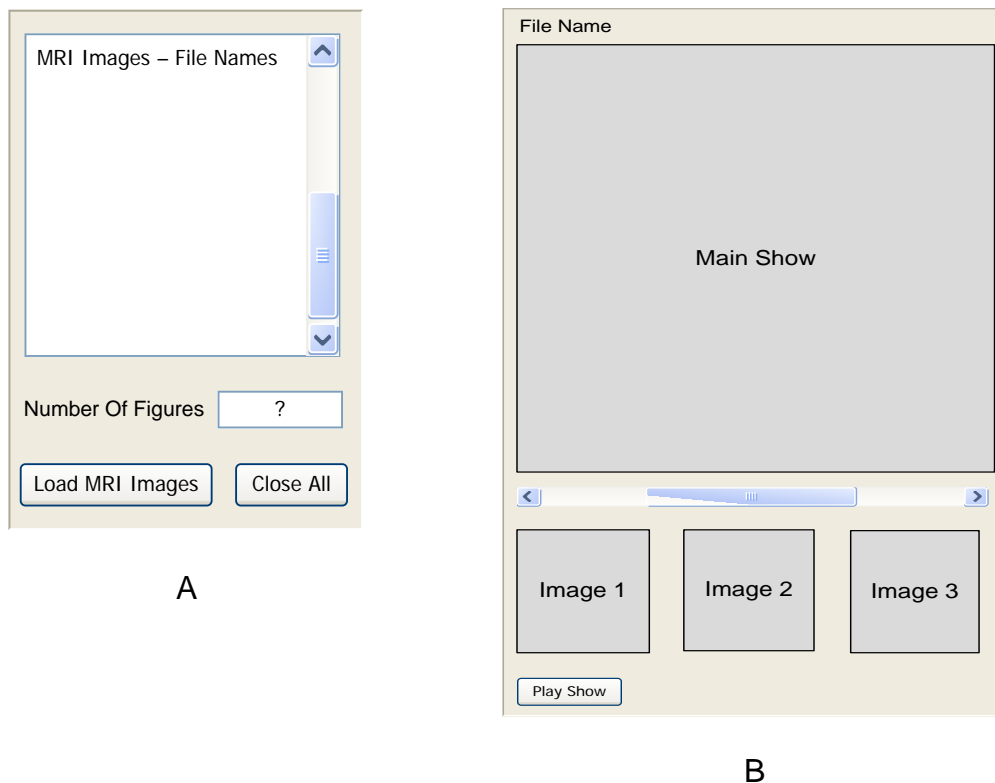


Figure 9.6 Design of software that control the MRI images A:the file names listed in a list box

B: MRI images slide show

In figure 9.6B, the second part of the MRI images panel is shown. This part of the interface consists of four axes controls, one button and one scroll bar. The images loaded from the MRI scanner machine are displayed in a slide show of three thumbnails. In addition the user has the ability to display the images one by one on an axis control named 'main show' by moving the scroll bar right or left. The file name of the current image is displayed on a label at the top of the interface.

9.3.4. Design of Select directory panel - GUI

The software platform has the ability to manipulate images and videos. In order to do that, user has to be able to open the correct directory. This done by clicking the button named 'Load Directory'. Also, the selected directory is displayed on the label next to the button load directory (figure 9.7).



Figure 9.7 Design of software that control the platform's directory

9.3.5. Design of robot control panel – GUI

This part of the software platform controls the robot movement during the treatment. The HIFU transducer has been maneuver in two stages X and Θ . Two text boxes and labels are shown in figure 9.8. The first four buttons are used to move the robot forward and backward in two stages. The last one checks whenever the data acquisition board is connected to the computer or not. The resulting message is displayed in a label next to that button.

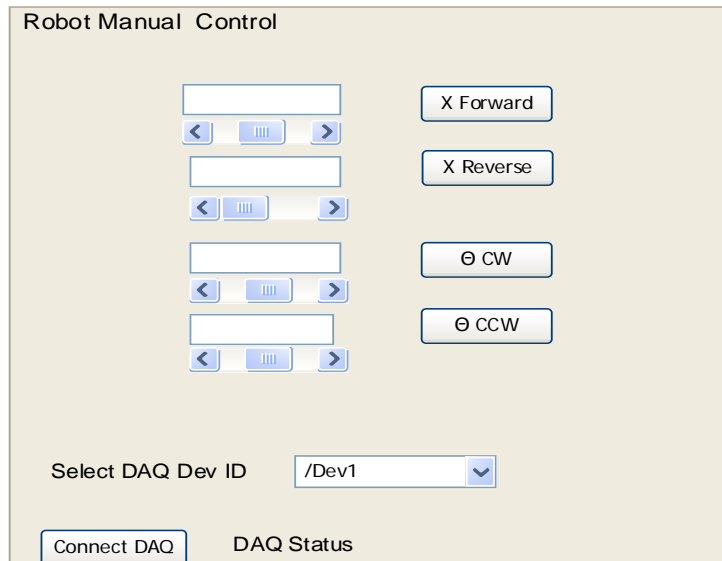


Figure 9.8 Design of the robot control interface

Figure 9.9 shows that the user is able to set the initial position of the robot to zero and also the user can visualize the position of the robot at any instance. At the beginning of the operation, the user must set the initial value to zero by pressing the button 'Zero'.

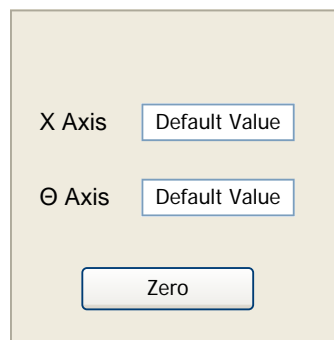


Figure 9.9 Design of robot position display and initialization

9.3.6. Design of command history panel – GUI

The command history interface consists of one list box. The user has the ability to follow the commands that are executed by the software at any individual step of the operation. Figure 9.10 shows the history information consists of command name, time that command executed, and time elapse in order to complete its operation. The software has the ability of save and retrieving from a text file.

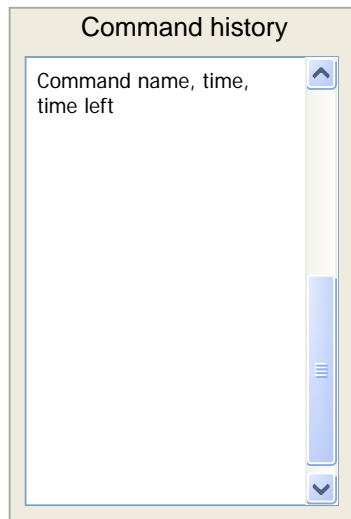


Figure 9.10 Design of command history interface

9.3.7. Design of Patient's Data Form (GUI)

In figure 9.11, the design of patient's data form is shown. This form was designed to give the ability to the user of entering and manipulating the patient's information. By using the form of figure 9.11, the user stores the patient's information to an Access database file. Also, the form offers the main operations that are necessary for manipulating the patient's information. The form can perform the following actions: a) save data, b) update (correct, change) data, c) search for information, d) delete unnecessary information, and d) record navigation.

Additionally, the user has the ability of retrieving the operations of the selected patient and displays them into a data grid. The operations can be modified by the user.

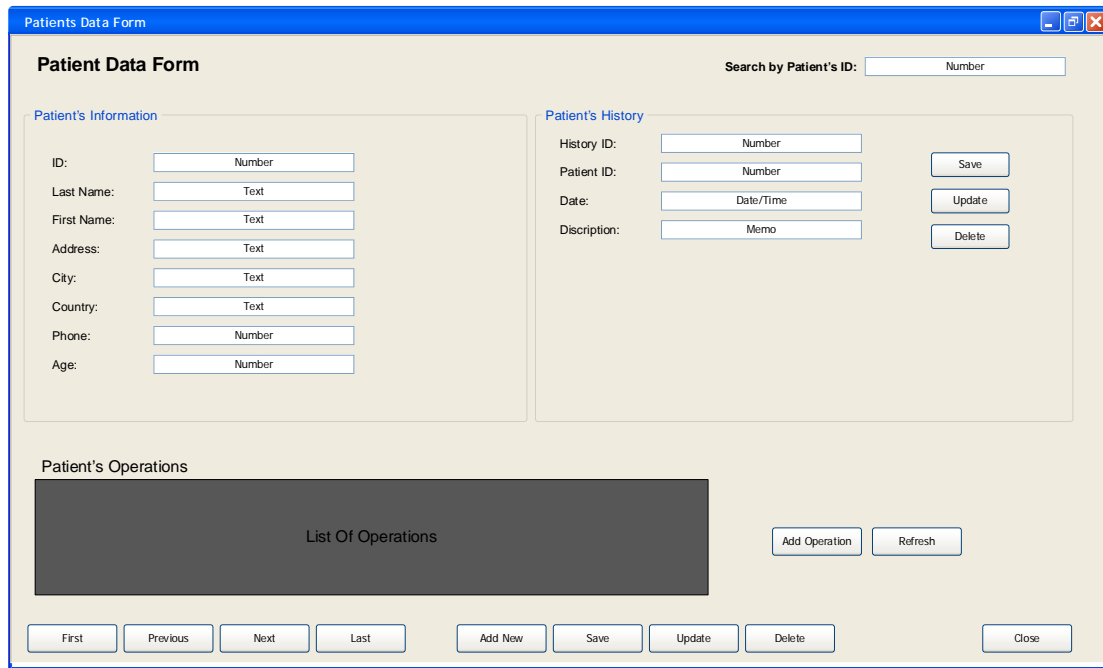


Figure 9.11 Design of patient data form

9.3.8. Design of single software platform

Figure 9.12 shows the design of the software platform. In the form, the six subprograms have been combined into a single platform. The last one task was designed to a separate window form. The main window has the ability of calling the remaining tasks forms. The user has the ability to access the main operations of the platform in the same form.

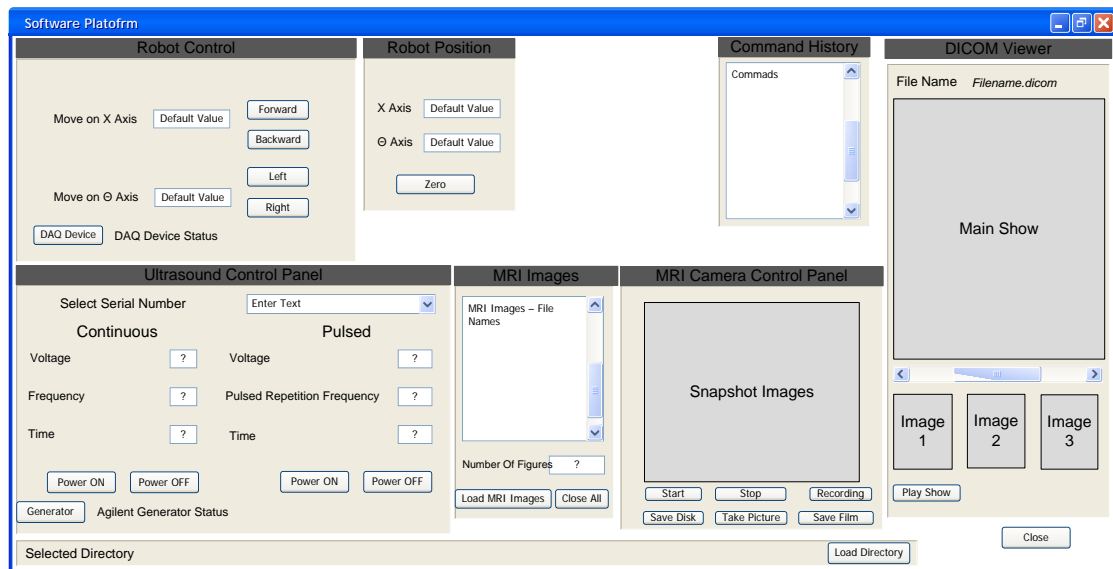


Figure 9.12 Main GUI of the software

9.4. Development of Software Platform using MATLAB (Version One)

This software splits into two main categories, therapy delivery and medical informatics. The patient data and MRI images belong to the medical informatics category and the remains software belongs to the category of therapy delivery. This is because the software will control the robot that delivers HIFU therapy to the prostate gland.

In this chapter, the software that will control the MRI compatible robot is demonstrated. The software is developed to fulfill all the needs of a MRI compatible HIFU robot assisted system. The software was developed using MATLAB (The Mathworks Inc., Natick, MA). MATLAB has compatibility with all the components that are used to implement this system. The development of the following parts is presented:

- a) Ultrasound control panel
- b) MRI Compatible camera control panel
- c) MRI images
- d) Control of MRI compatible motor
- e) Application command history
- f) Patient Data Form

What follows is sample codes together with explanation and interfaces of the various driver components of the system (such as Agilent Generator, NI Instruments card, etc.). Also, flowcharts are used to describe various functions of the system.

9.5. Ultrasound Control Panel

In this section, the software control of the signal generator is presented. This part of the software will control and send the correct parameters to the signal generator in order to provide the signals to the amplifier. The MATLAB programming language is used to develop the functions and the graphical user interface needed to control the Agilent signal generator (Model: 33220A, USB-6221, National instruments, Austin, Texas, USA) as shown in figure 9.13 [178]. The Agilent generator has the ability to interface with the computer using a USB (Universal Serial Bus) interface. In order to develop this part, it was required to design the functions that will send the parameters, in string format, to the signal generator.

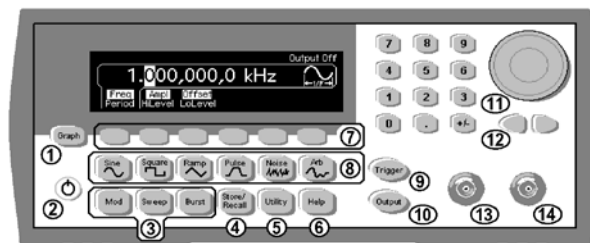


Figure 9.13 Agilent Signal Generator

9.6. Implementation of the ultrasound control panel

In figure 9.14, the computer is connected to the signal generator via a USB interface. The signal generator sends the signals via a coaxial cable to the oscilloscope. The oscilloscope will help us visualize the signal send to generator. Before the generator is connected with the computer, the proper software drivers need to be installed [178]. The drivers are provided by the manufacturer. When the USB interface is connected to the computer, the driver automatically will give us the hardware address of the USB interface. This address will be used to establish a connection line between the computer and the generator. This line will be used to open and close the connection while sending the parameters to the generator. The signal generator is connected automatically and no further action is needed.

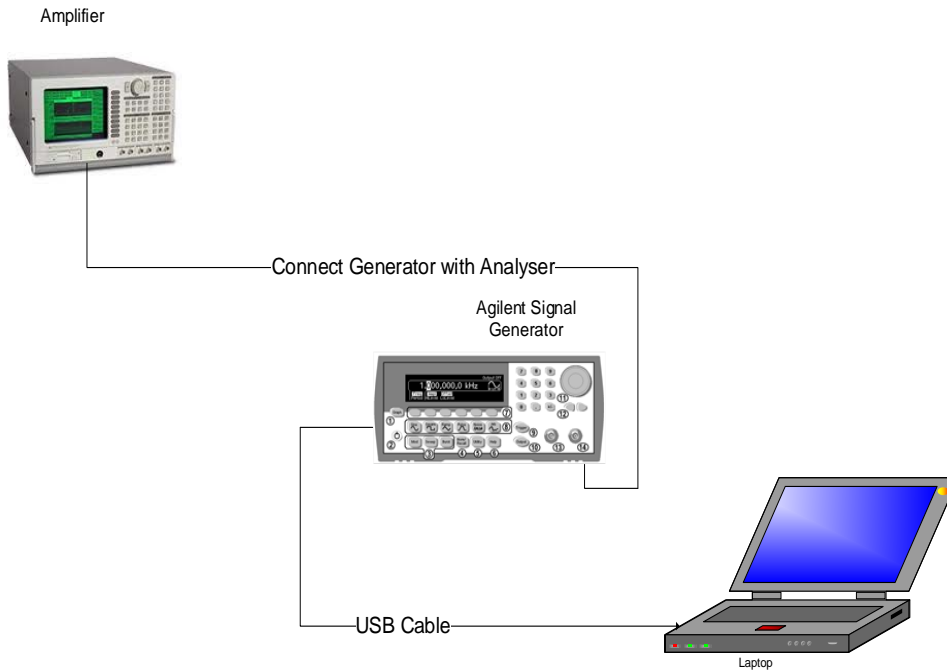


Figure 9.14 Computer Software that controls the signal generator

9.7. Parameters needed for implementing ultrasound control panel

The program needs to have the ability to generate two types of operations: *continuous* and *pulsed*. The parameters are needed to continuous signal are: voltage and frequency. Also, the total time is needed as an additional parameter. The second type operation is pulsed ultrasound. The parameters that are needed to generate this type of operation are: voltage, frequency, duty factor, and pulse repetition frequency. In order to achieve this, the function 'burst' is required to be used [179]. The parameters and the measurement units for each function are shown in table 9.1. The function output will be enabled after sending the correct.

Table 9:1 Parameters and Measurements Units of signals

Parameters	Measurement Units
Voltage	mV
Frequency	MHz
Duty Factor	%
Pulse Repetition Frequency	ms
Cycles	Cycles
Time	s

9.8. Functions developed for implementing ultrasound panel

The program needs to have the ability to generate two types of signals: continuous and pulsed. Continuous signals will send 3 parameters, frequency, voltage, and the time ultrasound to be on. The work is separated into two functions named *turnONcontinuous* and *turnOFFcontinuous* (figure 9.15).

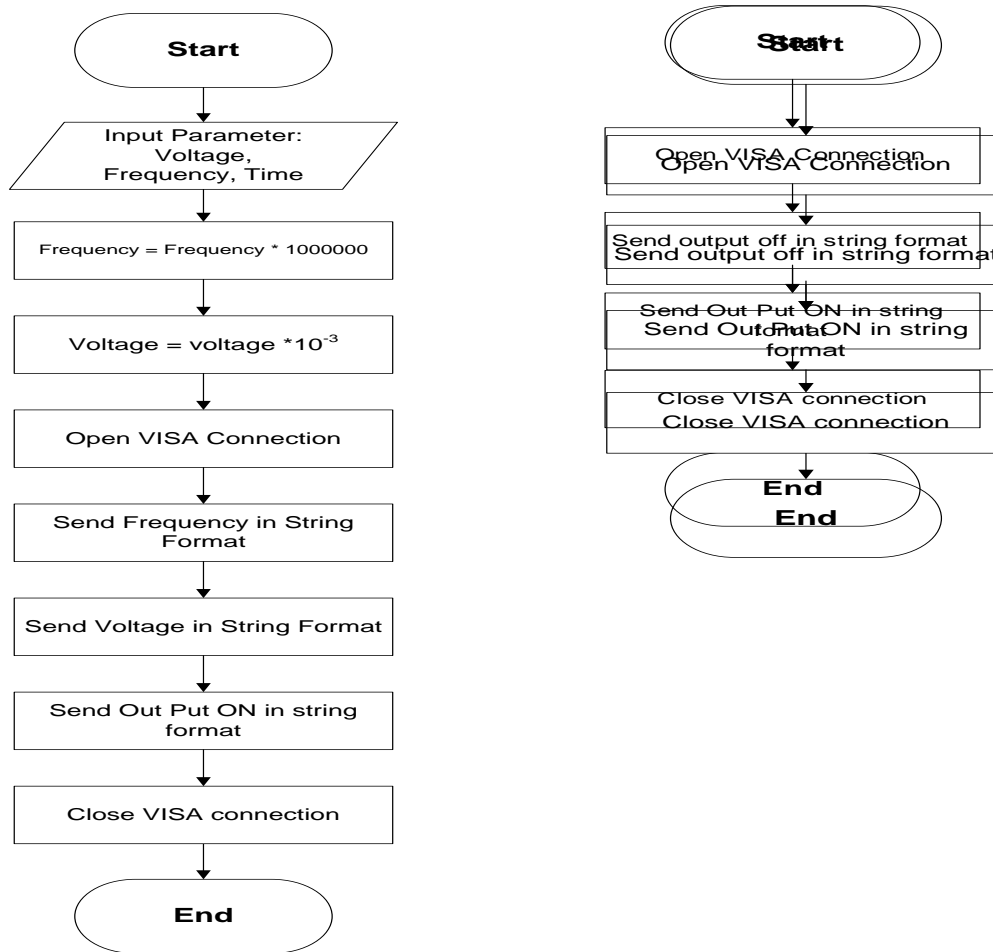


Figure 9.15 Flowchart of turning ON and OFF

From the flowcharts you can notice that all parameters sent to the signal generator are in string format.

Pulsed signal needs five parameters to operate, voltage, frequency, duty factor, and pulsed repetition frequency. The parameter 'Time' is needed in order to determine the time the traducer is ON. Pulsed operation is separated

into two functions named *turnONPulsed* and *turnOFFPulsed* (figure 9.16). Parameters are send in string format, as in the case of continuous.

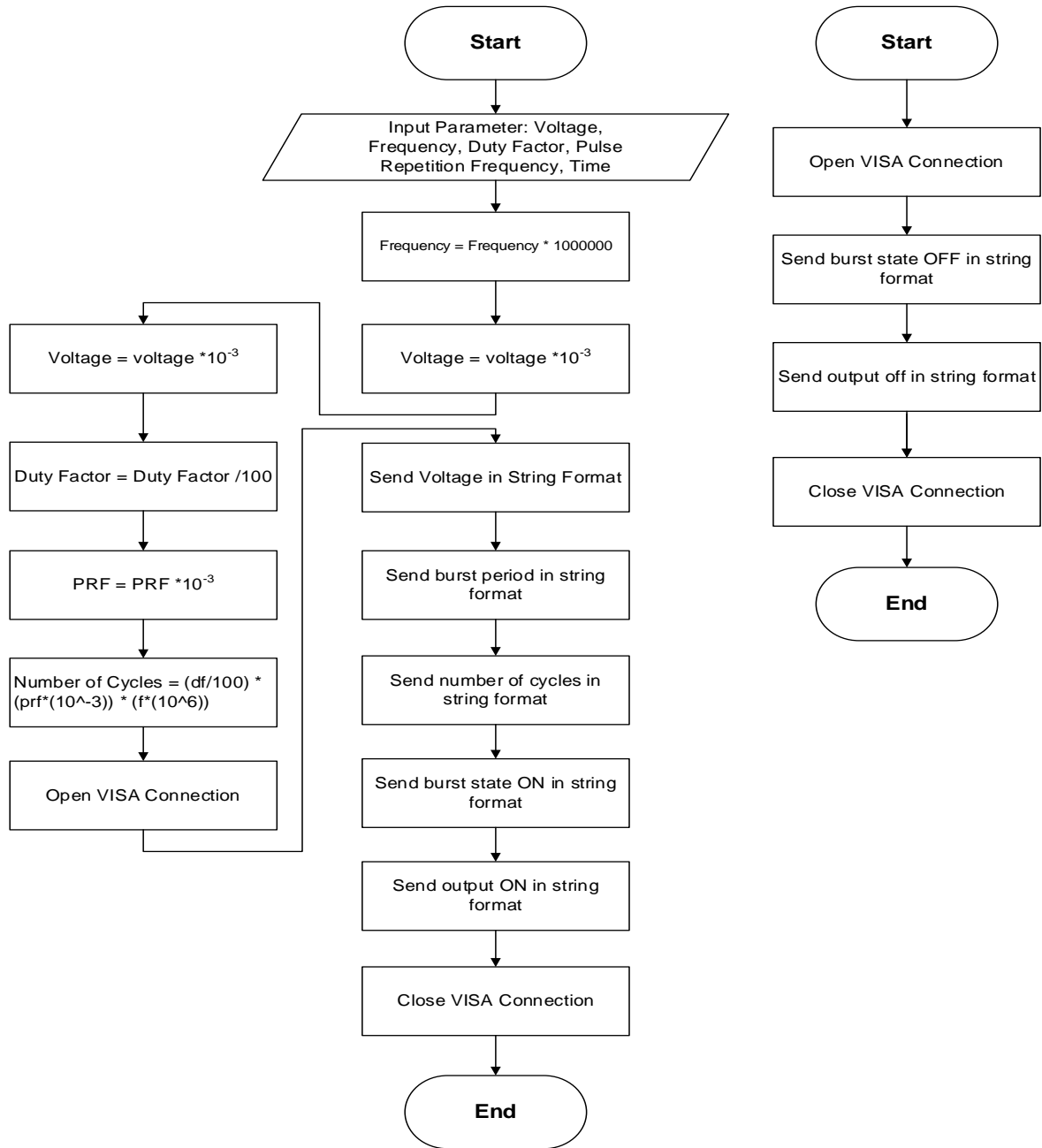


Figure 9.16 Flowchart for pulsed operation

9.9. Agilent Generator commands for ultrasound control panel

The statements needed to operate the above functions are presented. In order to send any statement to the signal generator, a connection between the generator and the computer must be opened. Only one connection can be handled by the generator at a time. The command required by the Agilent generator to open the connection [178] is the following:

'agilent', 'USB0::2391::1031::MY44006721::0::INSTR'

This command is separated into two parts. The first part is the name of the generator and the second part is the hardware address. The hardware address is fixed. The string command required by the Agilent generator to send the frequency [179] is the following:

'frequency ', '1000000'

Also this is a two-part command. The first part is the name of the parameter and the second part is the value to be sent out of this function call. In order to set the parameter voltage, the following command is needed:

'VOLTage ', '200', 'E-3'

This command is separated into three parts. The first part is the name of the command, the second part is the value received by the interface and the third part is the unit needed to convert the parameter into the correct format. The command required by the generator to turn ON the burst mode is the following:

'BURSt:INTernal:PERiod ', '0.01'

The command is separated into two parts. The first part is the function call and the second part is the parameter pulsed repetition period value in ms which is passed to the generator. The following command sends the number of cycles needed to generate a burst signal.

'BURSt:NCYCles ', '1000'

The first part is the name of the function and the second part is the parameter needed by the function (number of cycles). The next command is to enable the burst mode:

'BURSt:STATe ', 'ON'.

This command accepts two parts, the name of the function and the parameter value needed. To close the burst mode the following command will be sent to generator

'BURSt:STATe ', 'OFF'.

This command accepts two parts, the name of the function and the parameter value needed. Generator needs the following command to generate the signal:

'OUTPut ', 'ON'.

The name of the function and the parameter needed to operate the function is required by this command. To close the signal generation mode the following command has to be sent.

'OUTPut', 'OFF'.

The above commands are sent using MATLAB to the generator in string format. Moreover the above commands have to be send to the generator in a specific order [178]. The order needed by the generator to operate the two types of signal is provided below:

1. Continuous:
 - a) VISA Connection
 - b) Frequency
 - c) Voltage
 - d) Output ON
 - e) Close VISA Connection
2. Pulsed:
 - a) VISA Connection
 - b) Voltage

- c) Burst: internal period
- d) Burst: number of cycles
- e) Burst: State ON
- f) Output ON
- g) Close VISA Connection

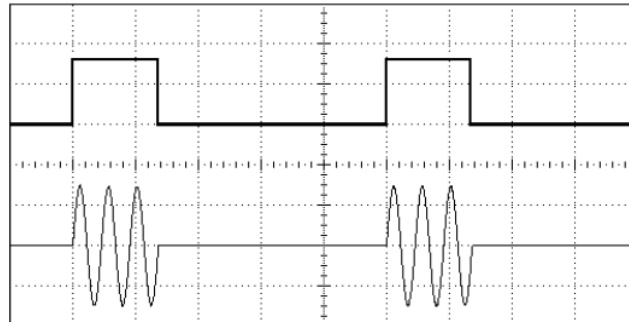


Figure 9.17 Pulsed paradigm, Three Cycle Waveform

Figure 9.17 shows a three wave pulse signal in analogue and digital format. The continuous straight line shows that the power is OFF and the cycle's wave show the time that the power is ON. Pulsed signal is used to avoid overheating in the target focal point.

9.10. Display information about the selected transducer

Based on the design, inside the ultrasound control panel, there is a combo box that enables the user to select and display useful information about the transducer used by the robot [179]. The combo box is filled by the serial numbers of all available transducers stored in an excel file. MATLAB has the ability to open and read column data from a Microsoft Excel file:

[ndata, text, alldata] = xlsread('transducerlist.xls', 'A1:A25');

The line of code above demonstrates the use of MATLAB function named *xlsread*. This function accepts two parameters. The name of the excel file in string format and the range of data that is going to be read.

The information of the selected transducer is displayed in a text box next to the combo box; the selected serial number index row is compared until the appropriate row of the information is found Appendix.

4.5.3. Ultrasound Control Panel - GUI Test

Figures 9.18 and 9.19 show the graphical user interface test of ultrasound control panel. Figure 9.18 shows that ultrasound control panel interface sends a continuous signal with 200 volts to the signal generator, 1 MHz frequency for 10 seconds. Also the software recognizes if the Agilent generator is connected with the computer or not by displaying the proper message. The correctness of the signal is demonstrated on the amplifier's monitor.

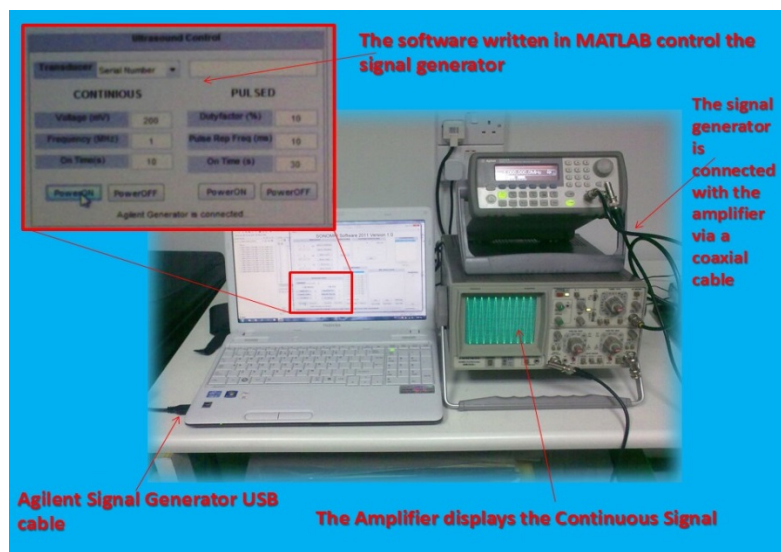


Figure 9.18 Software that sends continuous signal to the generator

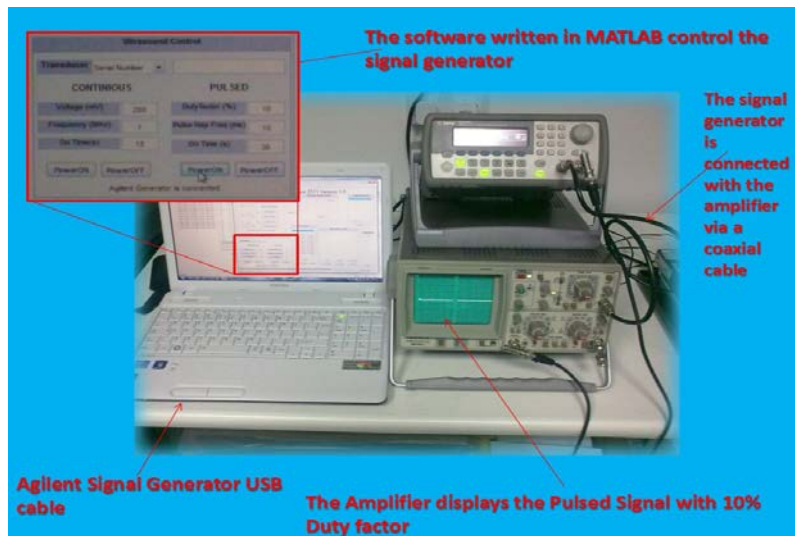


Figure 9.19 Software that sends pulsed signal to the generator

Figure 9.19 shows that ultrasound control panel commands the signal generator to establish a pulsed signal with 10% duty factor, 10ms pulsed repetition pulsed with duration of 30 seconds.

9.11. Timer

Another important aspect in the GUI is the timer [179]. The timer is used to determine the time that a specific signal will be ON. MATLAB programming language has embedded a function called timer. Time can be passed as parameter to the timer object. Timer object works on the background. When the parameter time has expired, the software sends a message to terminate the operation. Alternatively, if the user force stops command (pressing the button power OFF), the timer object and the signal operation stops (figure 9.20).

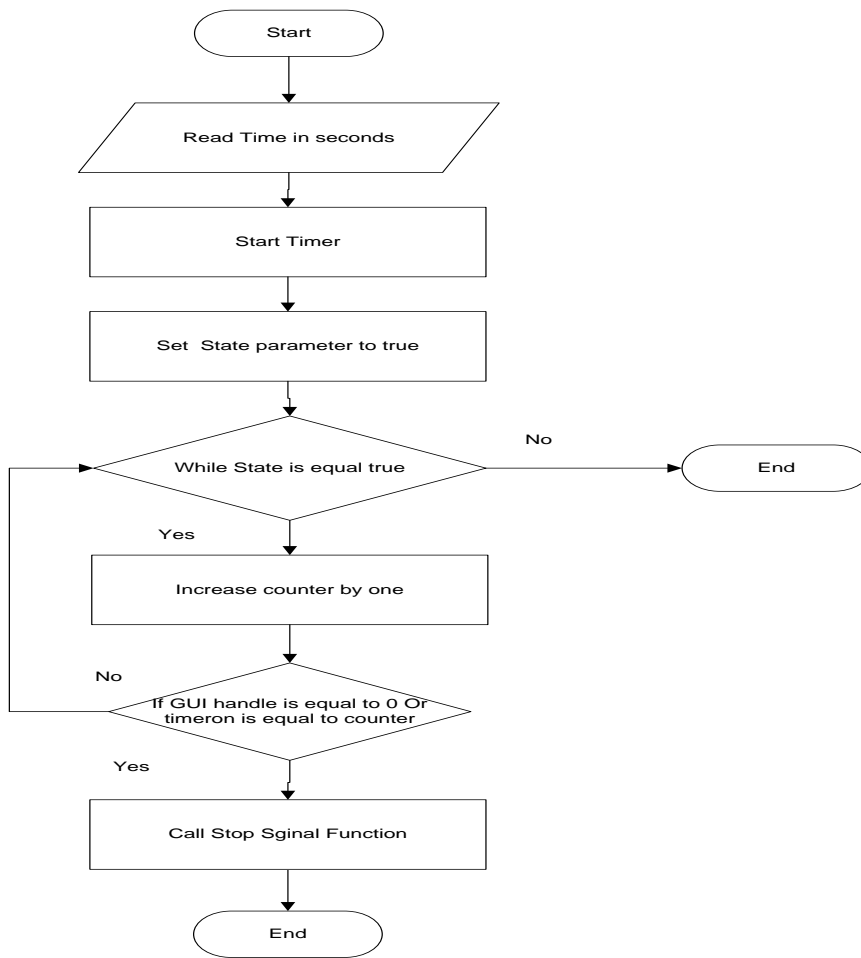


Figure 9.20 Flowchart that controls the time that the generator is ON

9.12. MRI Compatible Camera Control Panel

For monitoring the condition of a patient, the installation of an MRI compatible camera is needed. Therefore, in this section, the control of the MRI compatible camera is presented. MATLAB programming environment has the ability to call specific functions from the language that enables the user to control the MRC camera within a MATLAB window. The cameras perform the following operations: 1) preview of operation, 2) capture picture, 3) recording of video.

9.12.1. Parts for implementing camera control panel

Since the camera operates within the MRI scanner room, then the camera has to be MRI compatible (figure 9.21.A). The MRC camera consists of three parts. The camera will operate within the MRI scanner, the filter box (figure 9.21.B), and the video grabber (figure 9.21.C). The analogue signal coming from the camera will be transformed to digital signal using the video grabber. All parts are connected via cables (figure 9.21.D).

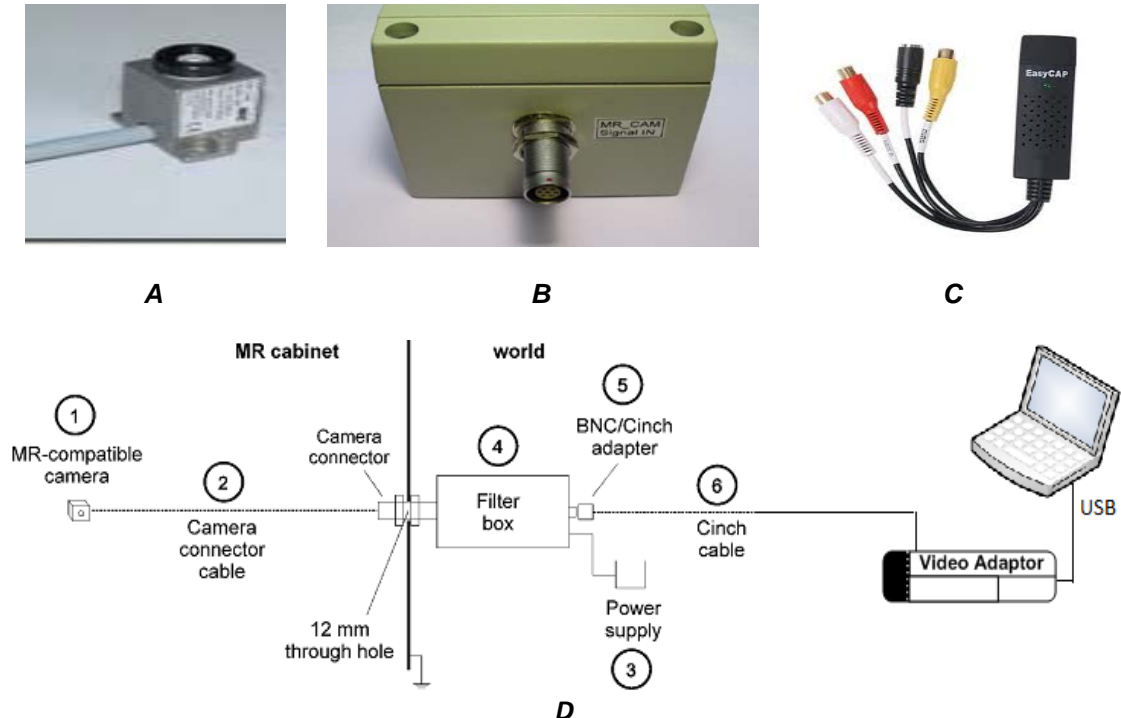


Figure 9.21 A: picture of MR Camera. B: Filter Box. C: Video crapper. D: Block diagram of MRI compatible camera.

MR camera setup consists of 6 parts. Figure 9.21 shows that MRI compatible camera (1) placed inside the MRI room and it is connected via camera cable to filter box (2) that is placed outside the MRI room. Filter box (4) is connected also with power cable to wall power socket (3). Additionally, filter box BNC/Cinch adapter (5) is connected via cinch cable (6) to video adaptor.

9.12.2. Parameters needed for implementing the camera control panel

The parameters needed to implement this part of the subprogram is the directory that camera saves the pictures and video files (*.jpg and *.avi format respectively). A folder browser command is used to implement this [179].

9.12.3. Functions developed for implementing the camera control panel

Lists of functions are needed to implement this operation. Some features of MATLAB are used. Firstly, folder browser function is required to call from the language abstract. This function calls a process from the windows operating system; a browser folder dialog appears.

Uigetdir('C\...');

The full name of this function is the '*user interface get directory*' command. This function is called by passing the full path directory as the first parameter to be predefined and the title of the dialog box as second. This function (method) is polymorphic. This means that, it can be called by passing either one parameter or two. The second function needed for this is the video input call.

videoinput('winvideo',1);

This function will create the object video. This object is used to enable the camera window. Also this object is used by a function named 'preview'.

Preview(Object video);

Another function uses to stop the camera. To do this, the object camera video has to be deleted by calling the following abstract function.

delete(Object video);

This function is called by passing the camera object as parameter. An additional task of the camera is to get snapshots inside the MRI scanner room. To achieve this, a frame is captured by using the following function:

getframe(ObjectCamera.snapshot);

The object camera has the ability to get pictures by using the snapshot attribute. The following function *'now'* and *'datestr'* [179] are used to build the name of the image. The function *'now'* is an embedded function that calls a windows operating system process. This process will return the current date and time:

datestr(now, 'mmm dd, yyyy HH.MM.SS.FFF AM');

The function *now* passes as parameter to embedded function *'datestr'*. This function converts the current date from date format to string format. The second parameter of the function *'datestr'* is the format of current date and time to be converted. In fact, this function returns the name of the image. After that, the function *'saveas'* will be called.

saveas(gcf, strdate, 'jpg');

The function named *'saveas'* [179] saves the image in a current directory. In this function the parameters accepted are: the image frame, the name of the file, and the extension of the image (*.jpg).

As it is shown in figure 9.22, in order to get a video from the camera the program need to get snapshots frame by frame within a loop. These frames will be merged at the end of the procedure and the file will be stored in the selected directory.

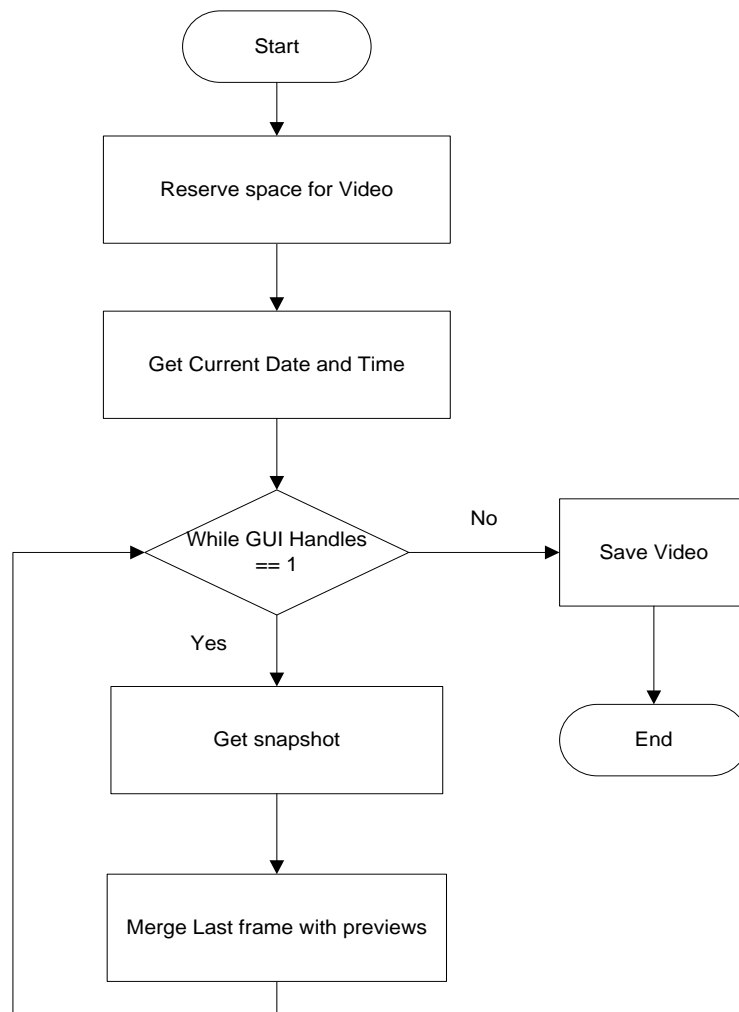


Figure 9.22 Recording Operation

9.13. MRI images

The software needs to control the images coming from the MRI scanner. The user has the opportunity to put side by side the images in two ways. One way is that, the user has the option to select from the list box the images needed. The other option is that the user can place all images side by side by pressing one button. Additionally, a slide show 'dicom' viewer is implemented. The slide show 'dicom' viewer displays the MRI images three by three with interval time at 3 seconds. A horizontal scroll bar is also enclosed on the viewer. The scroll bar helps to scan the images one by one.

9.13.1. Parameters needed for implementing MRI images panel

Parameters needed to implement the above talks are three. MRI made the images, the number of images that the user can see side by side and the size of the computer screen.

9.13.2. Functions used for implementing this MRI images panel

Functions needed to implement this part are called from the abstract. As mentioned above the images are transferred from the MRI scanner. The MRI scanner stores the images in *dicom* format (*.dcm). Therefore the program needs to have the ability to recognize the *.dcm format. To do this, the following functions are needed:

dicomread(file_path);

In order to call this function, the file name is concatenated together with the directory that the image is stored. This string has to be passed as parameter. After the function recognizes a *dicom* file, the file will be displayed on a figure window as MRI image. MRI images are displayed side by side in rows of three (figure 9.23). To do that, the size of the monitor has to be known. To find out the size of the monitor the following function will be used:

get(0,'ScreenSize');

Based on the given size, the program will calculate the position of the figure to be shown. The following flowchart demonstrates the operation in detail.

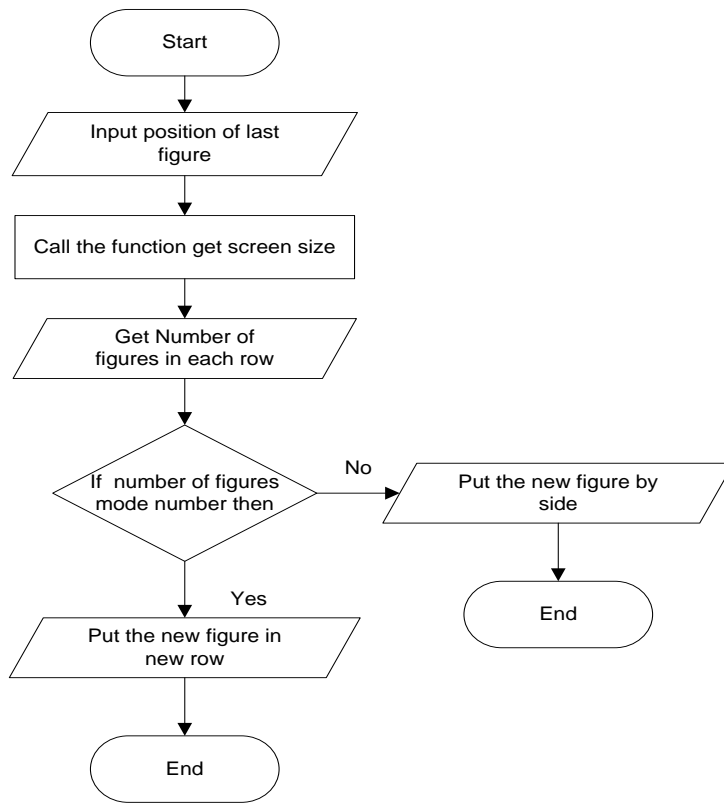


Figure 9.23 Open DICOM images in series of figures.

9.14. Parts for implementing robot movement actuation

9.14.1. Data acquisition board

In order to acquire data from the actuator, a data acquisition board is needed. In this case NI Instruments USB 6221 card (picture 9.1) is employed [180]. NI USB 6221 board has the ability of interfacing with MATLAB data acquisition tool box 9.3.



Picture 9:1 NI Instrument data acquisition card USB 6251

This card is connected with the computer using a USB interface. A special driver must be installed on the destination computer first, before the USB interface is plugged. The driver (NI DAQ mx 9.3) has been found from the manufacturer's supports web site [182]. By using the test panel software driver, the NI USB 6221 card can be tested and see if the card has been connected with the computer successfully.

MATLAB data acquisition toolbox 9.3 has the ability to connect with NI USB 6221 card by using two types of interfaces [180, 181 and 182]:

- a) Legacy Based Interface
- b) Session Based Interface

The legacy interface supports hardware from multiple vendors and all sound cards on 32-bit versions of MATLAB. According to the table below (Table 9.2), the legacy interface also supports voltage measurements of analog input, analog output, and digital I/O subsystems. The session-based interface supports analog input, analog output, and counter/timer subsystems on both

32-bit and 64-bit versions of MATLAB (The first version of the software has been developed using 32 bit version of MATLAB).

Table 9:2 MATLAB functionalities for controlling Data acquisition tool box

Functionality		Session-Based Interface	Legacy Interface
Analogue Input			
	Voltage	✓	✓
	Current	✓	
	Temperature	✓	
	Accelerometer	✓	
	Bridge	✓	
Analogue Output			
	Voltage	✓	✓
	Current	✓	
Counter/Timer Input and Output			
	Edge count	✓	
	Pulse width	✓	
	Frequency	✓	
	Position	✓	
Digital Input and Output			✓
Multi-device acquisition and generation		✓	
Simulink Blocks			✓

Therefore, the legacy based interface and digital input/output method has been used for the movements (backward and forward) of the motors and the session based interface has been used for acquire the counter value from rotary encoder by acquiring the 'Edge Counter' parameter. (Table 9.2, highlighted rows).

9.15. Functions used for implementing robot movements

9.15.1. Date acquisition Register Command

In order to use MATLAB data acquisition toolbox, 'daqregister' command has been called first (See code below). This command accepts as parameter the file name and path of a library named 'nwnidaq.dll'. This library gives us the ability to use all the commands available in MATLAB data acquisition toolbox. This library has been called inside the figure load event.

**daqregister('C:\Program Files
(x86)\MATLAB\R2011b\toolbox\daq\daq\private\mwnidaq.dll');**

9.15.2. Motor Movements (X – Θ axes)

Legacy based interface connection has been used for the robot movements. This is because; it supports digital input/output connection with the NI USB 6221 card. Digital input/output connection has been selected, because the motor has two states. The motor can be either ON or OFF. At the beginning, DIO (Digital Input Output) object has been created. The way of creating DIO objects is shown below:

dio=digitalio('nidaq','Dev2');

DIO object is initialized in a variable name “dio”. This object has been created by using the function named ‘*digitalio*’. ‘*Digitalio*’ function accepts the adaptor name (“nidaq”) and the hardware device ID (“Dev2”). After creating the DIO object, eight lines have been added to it.

In order to move the motor, eight lines represented by eight bit are required. To do this, *addline* function has been used. This function accepts three parameters which are the following: 1) dio object, 2) number of lines reserved, and 3) the mode of connection (in or out). The following code demonstrates how this done:

addline(dio,0:7,0,'out');

By using the above code, eight lines have been added. This means that, three motors can be controlled. Two lines used for backward and forward movements of a motor. All eight lines are initially set to one. By doing this, the motor has been commanded to stop because the ground is set to logical ‘1’ (not grounded). The following code demonstrates how the lines sent to output port:

**boarddata=logical([1 1 1 1 1 1 1 1]);
putvalue(dio,boarddata);**

A variable named “boarddata” initialised as array of logical series of eight bits (see line 1). After that a function named ‘*putvalue*’ (second line) has been

called to set the values to output port. This function accepts two parameters which are the DIO object and board data.

In order to move the motor need to set the proper line to logical '0'. By set a line to logical '0', the motor driver is grounded and starts moving. For instance, by setting the first line of '*boarddata*' to logical '0' and put the new values to output port, the motor starts moving. The following code demonstrates how motor start moving forward:

```
boarddata(1)=0;  
putvalue(dio,boarddata);
```

In the above code, the first element of the array is set to '0'. After that, the data is sent to the output port by using the function '*putvalue*' (see second line). Two lines are needed for each motor. So, by adding eight lines the program is capable to control four motors.

Finally, to stop the motor the first line of the board data is set to logical '1' again. The '*putvalue*' function has been used again to put the new values to output port. DIO object is no longer needed that's why it is removed from the memory by using the following two lines of code:

```
delete(dio);  
clear dio;
```

The above procedure is demonstrated in figure 9.24:

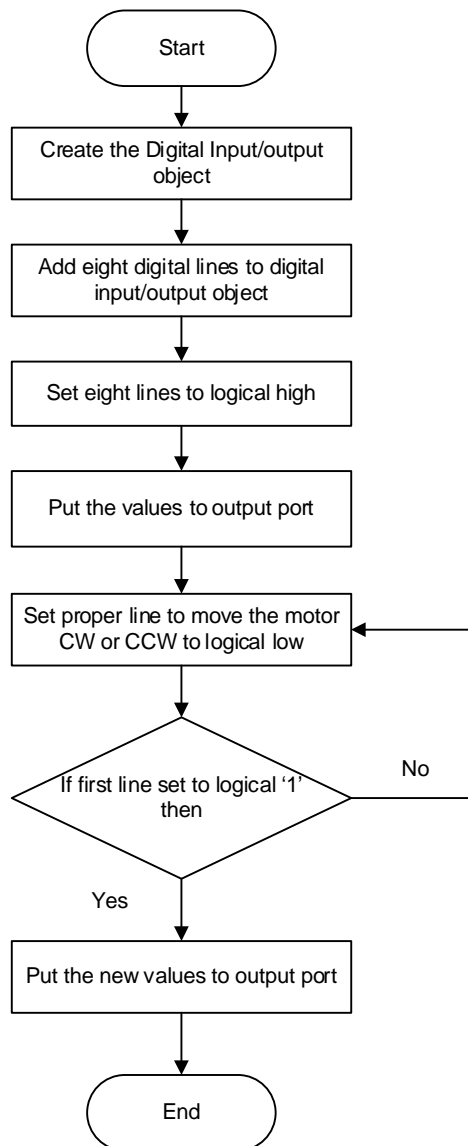


Figure 9.24 Function to move the motor in one direction

9.15.3. Motor – Get Counter Value

The counter value is acquired by the ‘Edge Count’ value from the NI instruments USB card. The ‘Edge Count’ value is the necessary feedback received from the motor in order to know the direction that the rotary encoder is on move. Software timers never take a precise measurement that’s why the feedback from the hardware is needed.

According to the NI instruments card user guide, the edge counter value is given from the pin 81 in digital input/output part of the data board. The MATLAB data acquisition toolbox 9.3 has the ability to connect with the NI

instrument card by using two interfaces. In order to get the edge counter value, the session based interface is employed (See Table 9.2). Session based interface supports DAQ (Data Acquisition) package.

A connection with NI card is required in order to get the edge count value. The DAQ package supports the 'get vendor' command. This command returns the vendor id and device id parameters. 'GetVendor' function is used only at a development time.

daq.getVendors();

'VendorID' parameter is passed to the function name 'createSession'. The code below demonstrates the use of 'createSession' function. Actually, the variable "s" is initialised as DAQ create session type. The vendor id parameter "ni" is passed as parameter to function *createSession*. "s" variable will be used from the following commands to extract the encapsulated functions from DAQ library.

s = daq.createSession('ni');

The following function is named 'addCounterInputChannel'. This function is responsible for getting the counter value form the NI card. The 'addCounterInputChannel;' accepts the following three parameters: 1) 'deviceid', 2) 'channelid' and 3) 'measurementtype'. The following code demonstrates how the counter channel is added to NI card:

s.addCounterInputChannel('Dev1', 'ctr0', 'EdgeCount');

As you can see in the above code, the device id is 'Dev1'. The name of the channel is 'ctr0'. The measurement type is 'Edge Count'. The details of the above parameters are found by using the NI card drivers test panel.

The following code demonstrates how the input signal is called. The function named 'inputSignleScan' immediately acquires a single scan from each input channel in the session and returns the data acquired in double format.

countervalue = s.inputSingleScan;

The input value is stored in the variable 'countervalue'. In order to get a new measurement, the reset of counter is needed.

s.resetCounters;

The counter is reset before the new value is stored. The above operation is demonstrated in figure 9.25.

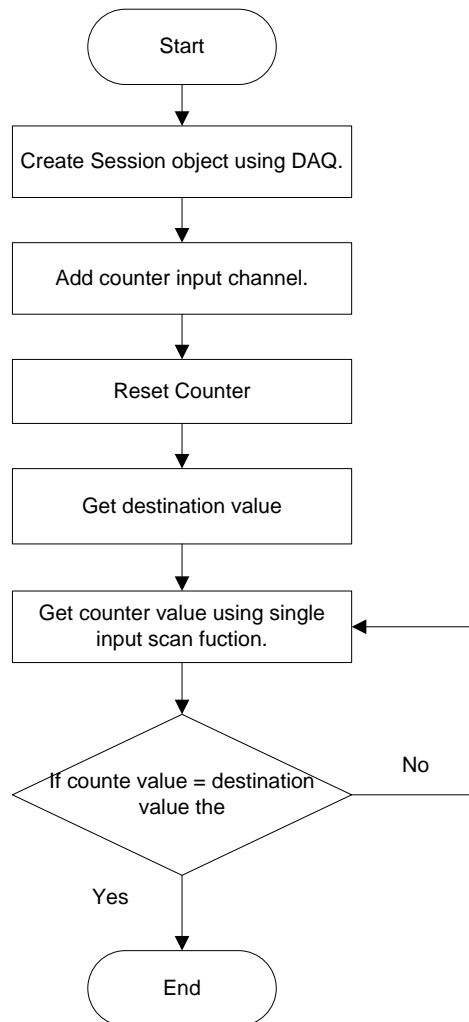


Figure 9.25 Flowchart for the Get Counter Value

In order to see the counter value that incremented during the motor movement, a MATLAB function named '*plot*' is used. Plot function generates a figure that displays a line chart of the edge counter value. Figure 9.26 shows a line chart. This chart compares the edge counter value together with voltage of the motor during the movement.

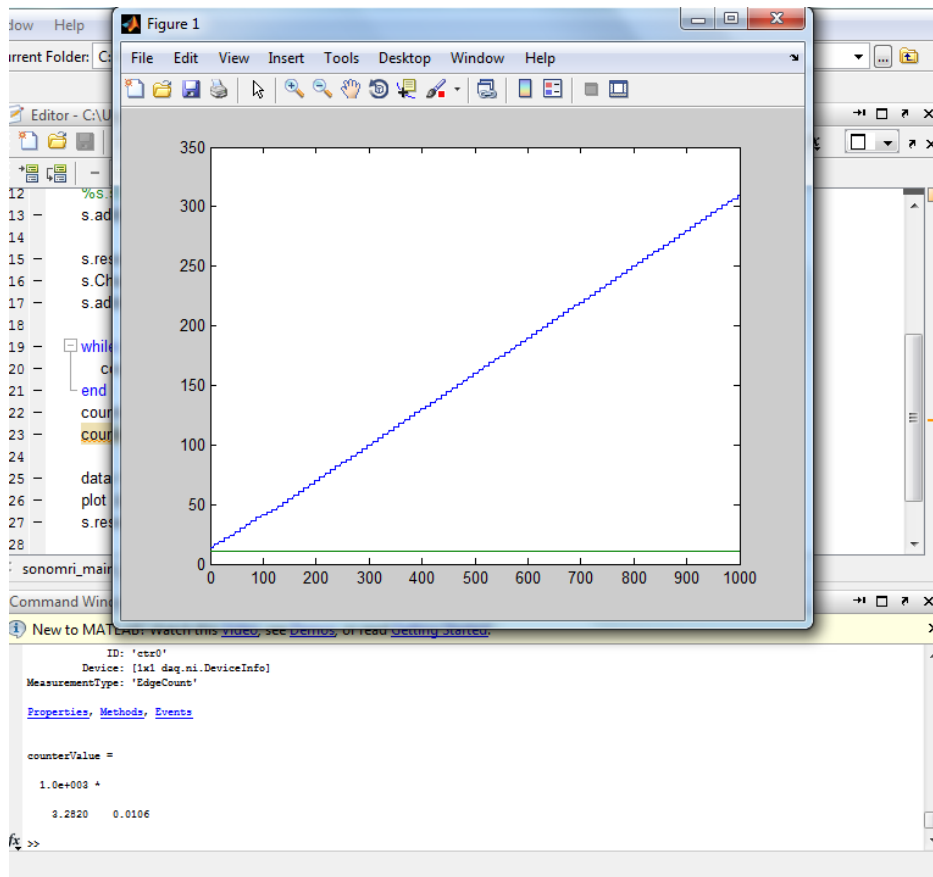


Figure 9.26 Edge Counter value compare with Voltage value

9.15.4. Robot initial and current position

Another part of the robot control is the initial position. The robot position must be initialized to zero in order to know how far the robot moved. This helps to know the precise position of the transducer. Two variables have been created into the GUI handles array. The names of the variables are X and Θ . The software automatically stores the robot position to these variables, after any motor movement, by adding or subtracting from the current value. The code below demonstrates how the variable X is initialised to zero (Line 1). In line 2, the variable X is increase by adding the distance that the robot move on X direction.

handles.x=0;

handles.x=handles.x+handles.xdistance;

In case that robot moves in reverse direction, the software decreases the variable X by subtracting the distance covered by the motor. In this way, the

end user is able to know the current position of the robot on X axis at any moment. The same procedure was followed also for the Θ axis.

9.16. Application Command History

9.16.1. Functions used for implementing command history

Application command history is a list box that is located in the upper right corner of the interface. This function helps us to follow what actions are used. Two fields are stored in the list box: the name of operation and the date/time. In order to get date/time from the system, a specific MATLAB function is called. The following code demonstrates how date/time is acquired from the system:

```
datestr(now, 'mmm dd, yyyy HH.MM.SS.FFF AM');
```

The above function named '*datestr*' accepts two parameters. The parameter '*now*' return the current date/time based on the system. After that, the format of the 'date/time' is passed in string format. The current 'date/time' is concatenated with name of the operation by using the following code:

```
strcat('Name of operation', strdate);
```

The concatenation function is used again by merging the existing content of the list box and the current record added.

9.17. Interconnection between the electronic devices

Firstly, the computer is connected with Agilent Signal generator in order to be able to control and deliver the HIFU therapy. Agilent generator is connected to the amplifier in order to verify the signal generator output. Additionally, a video grabber is connected with the computer. The video grabber converts the analog signal coming from the MR camera filter box to digital. The MR camera is connected to the filter box. The filter box collects the video signal from the camera in analog form. Last, data acquisition board is connected to the computer. DAQ board has the ability to send/get signals to/from rotary encoder motor via motor driver. The DAQ board is directly connected to motor driver via a cable. The motor driver is connected to a motor via cable by using the proper pins terminator. See wiring diagram in figure 9.27.

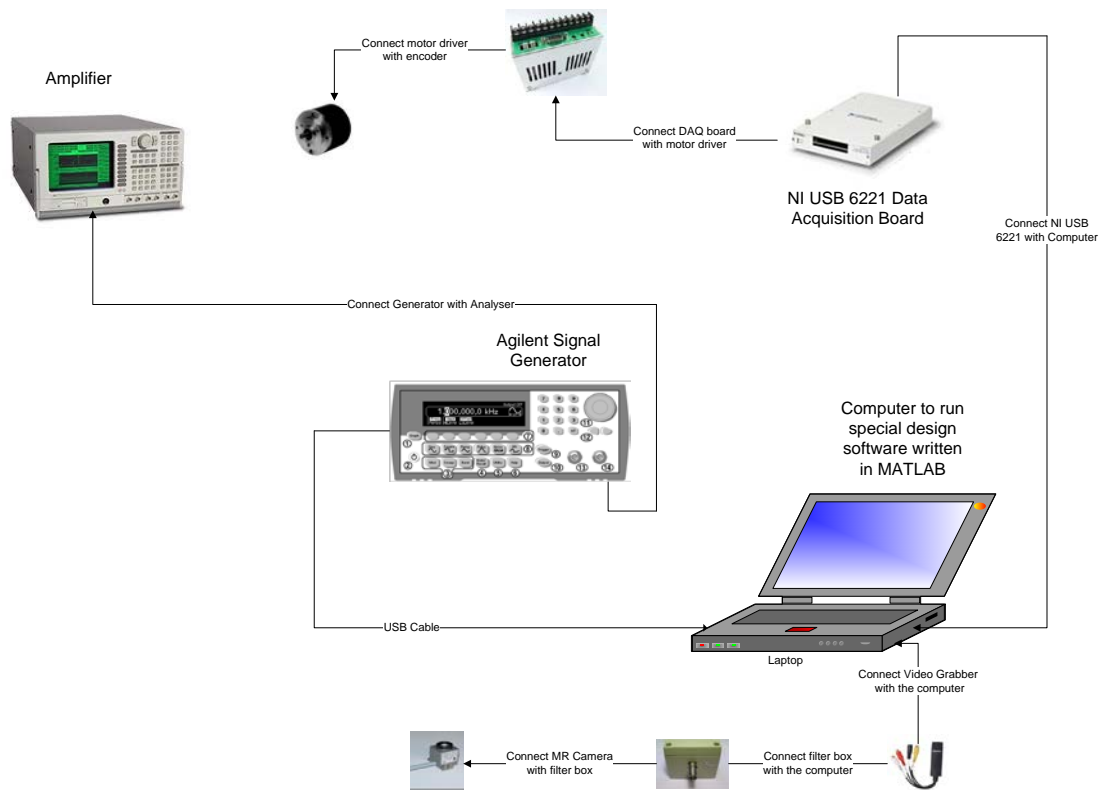


Figure 9.27 Wiring diagram of all electronic devices

9.18. Patient Data Form

In this subchapter a function that gives the ability to the user to store some useful information about the patient is presented. The end user can open a window that contains a menu with the following options:

- a) Enter patient information
- b) Enter information about a particular operation to a patient
- c) Search for a patient
- d) Edit data
- e) Delete data
- f) Navigate through all patients

In order to achieve the above tasks, a friendly form was developed by using VB .NET 2010 (Microsoft Visual Studio .NET Express 2010). MS Visual Studio was used, because is a proper choice of develop an application

database system. This is because Visual Studio has embedded libraries that give the ability of better quality interface design.

Also RDBMS (Relational Database Management System) software named Microsoft Access 2010 has been used. To establish a connection between these two platforms, a connection library named '**OLEDbConnection**' has been used. Two more libraries named '**bindingsource**' and '**bindingnavigator**' are also used.

9.18.1. Data files

In any relational database system, data is organized in tables (Table 9.3). In this particular case, the data is separated in two tables named '*patient*' and '*operations*'. Patient data table accepts the personal information about the patients and the operations tables accepts the details about the particular operation. So, two tables have been created in MS Office Access database system. In the table below, the data for each table are presented:

Table 9:3 MS Access Patient's Data

Patient Table		Operations Table	
Field	Data Type	Field	Data Type
ID	Text	Operation ID	Auto Number
Last Name	Text	ID	Text
First Name	Text	Operation	Date/Time
Address	Text	Description	Memo
City	Text		
Country	Text		
Phone	Text		
Age	Text		

9.18.2. Design of Patient Data GUI

According to the needs of this form, a list of GUI controls is located in the patient data form (figure 9.28). Text boxes, command buttons, labels, group boxes and a data grid are used. Text boxes are used to enter and display data. The labels describe what is bind to a text box. Group box separate the patient data and the operation data. Command buttons actually perform the operations and a data grid that displays the operation according to the selected patient.

The screenshot shows a MATLAB window titled "Patient Data" containing a "Patient Data Form". The form is divided into two main sections: "Patient's Information" and "Patient's Operations".

Patient's Information: This section contains several text input fields with the following data: ID: 689525, Last Name: Pavlos, First Name: Kyriacou, Address: 25th Street, M. Gitor, City: Limassol, Country: Cyprus, Phone: 35725663322, and Age: 75.

Patient's Operations: This section contains a table with the following data:

Operation ID	Patient ID	Date Of Operation	Discription
7	689525	16/2/2012	Liver Ablation
11	689525	30/03/2014	Prostate Ablation

Below the table are two buttons: "Add Operation" and "Refresh". At the bottom of the form are navigation buttons: "First", "Previous", "Next", "Last", "Add New", "Save", "Update", "Delete", and "Close". A search box labeled "Search By Patient ID:" is located in the top right corner.

Figure 9.28 Patient Data Form (Sample data)

Command buttons are grouped as follows in navigation buttons and action buttons. Navigation buttons allow us scroll through all records of. Navigation buttons are named as follow: 'First', 'Previous', 'Next' and 'Last record'. Action buttons allow us to perform operations on the table data. Actions buttons are named 'Add New', 'Save', 'Update', 'Delete'. The patient data form performs the group of operations that is named *CRUD* (Create, Read, Update, and Delete). A search text box located at the upper right corner allows the user to make a search for a particular patient. The above form will open within a MATLAB window.

9.18.3. OLEDB Connection

Two different platforms are used to implement this task. The first one is MS Access 2010 and the second one is MS Visual Basic. Firstly, the abstract class named '*OleDb*' has been imported as follows:

Imports System.Data.OleDb

The '*OleDb*' class allows us to generate dynamic object of the '*OleDbConnection*' class. An '*OleDbConnection*' object represents a unique connection to a data source. In this case data source is MS Access database file.

Dim Conn As OleDbConnection = New OleDbConnection()

The above code is used to initialize and generate a unique object of the class name '*OleDbConnection*'. The variable named "conn" has been used to call the encapsulated behaviors (functions) of the '*OleDbConnection*' class. Behavior 'Open' and 'connectionstring' have been used. The behavior named "Open" has been opened an instance connection to the data source. The behavior 'connectionstring' has been used to pass the data source connection provider as parameter to the connection. The data source provider was established the connection between two different platforms.

```
myconnectionstring = "Provider=Microsoft.Jet.OLEDB.4.0;Data  
Source=patientdata.mdb;User Id=admin;Password=";  
conn.ConnectionString = myconnectionstring  
conn.Open()
```

The code above, parameters source (file name), 'username', and 'password' have been passed together with data source provider. The behaviour named 'Open' has been used to open the connection with the data source.

9.18.4. Query Database

A database query is a piece of code that is sent to a database in order to get information back from the database. It is used as the way of retrieving the information from database. A database 'query' is basically a 'question' that you ask the database. The result of the query is the information that is returned by the database management system. Queries are usually

constructed using SQL (structured query language) which resembles a high-level programming language.

In order to execute a query using 'OLEDBConnection', another variable name 'mycommand' need to be declare. The code below shows how the variable was declared.

Dim myCommand As New OleDbCommand

The variable name 'mycommand' was declared as 'OLEDBCommand'. Two parameters have been assigned to this variable; the two parameters are shown below.

myCommand.Connection = Conn Line 1

myCommand.CommandText = qry Line 2

The parameter '**conn**' is for the connection and the parameter 'qry' is the 'sql' query statement. The 'sql' query is the question that has to be asked to the data source. In order to extract all the records from the table named patients, the following 'sql' command has been used:

“select * from patient”

The above command means, select all records from table patient. After extracting all the records needed in any particular case, the next step is to assign the data to the correct controls (text boxes). In order to achieve this, two more classes are needed to be called. The classes named '*OLEDBDataAdapter*' and '*DataTable*'. So, two variables declared. The variables named 'myAdapter' and 'myData' (See code below), are declared.

Dim myAdapter As New OleDbDataAdapter

Dim myData As New DataTable

The 'myAdapter' variable is responsible to accept the record set returned by the variable named 'mycommand'. The 'myData' variable get the record set from the Table Adapter (See code below)

myAdapter.SelectCommand = myCommand

myAdapter.Fill(myData)

After filling the variable name 'myData' (Table Adapter), two libraries named '*bindingsource*' and '*bindingnavigator*' are used. The control binding navigator gives the ability to see all the records extracted by the data source. (See code below)

BindingSource1.DataSource = myData
BindingNavigator1.BindingSource = BindingSource1

Finally, the extracted data has been assigned to the proper controls like the code below using the property 'Data Bindings':

```
Me.IDTextBox.DataBindings.Add(New Binding("Text", Me.BindingSource1, "id", True))
```

9.18.5. Query Language – SQL

SQL is a standard language for accessing and manipulating databases. It is the standard language for relational database management systems. SQL statements are used to perform tasks such as update data on a database, or retrieve data from a database. Some common relational database management systems that use SQL are: Oracle, Sybase, Microsoft SQL Server, Access, Ingres, etc. Although most database systems use SQL, most of them also have their own additional proprietary extensions that are usually only used on their system. However, the standard SQL commands such as 'Select', 'Insert', 'Update', 'Delete', 'Create', and 'Drop' can be used to accomplish almost everything that one needs to do with a database.

All the SQL statements consist of three parts: 1) the selected fields, 2) the tables that fields are selected from and 3) the conditions that must be filled by the records in order to be a part of the results (code below).

```
SELECT field1, field2, field3 FROM table1 t, table2 t2 WHERE field1 = 'criteria'
```

9.19. Development of software platform using C Sharp

The software platform was reprogrammed using C sharp under the framework of Visual Studio .NET 2010 Express Edition (Microsoft Corporation, USA). The software is written in C sharp in order to make the execution faster. Some serious problems were facing during the preliminary tests of the system, the problems are the following:

- a) slow loading speed
- b) slow communication speed with the DAQ device (accuracy problem – overhead)
- c) slow loading time of MRI images

Additional Options were added to the software:

- a) DAQ device can be selected from a list, more than one devices can be controlled
- b) Signal generator can be selected from a list of two devices (there is option to add additional devices).
- c) The command history can be saved and retrieved from a text file
- d) The command history list box can be cleared during the execution of the application.
- e) More than one robotic devices can be controlled (the proper device can be selected from a drop down list)

9.20. Control of the devices using C Sharp

Special libraries are supported by C sharp in .NET studio and manufacturers with the extension file *dll* (dynamic link library). The *dll* files are used from the software to communicate with the devices. The software uses two libraries to communicate with the NI DAQ device, '*NationalInstruments.Common.dll*' and '*NationalInstruments.DAQmx.dll*'. The idea of communicate with PFI (programmable interface function) on digital I/O part of the card pin outs is the same with MATLAB. An array of eight Boolean values, (integer values in MATLAB), is required for controlling the PUM motors. The exact syntax is presented on the Appendix.

In order to control the Agilent signal generator the '*VisaComLib.dll*' library was used to send and received commands form the signal generator. The commands were send in string format to the generator. Software platform controls the MRI compatible camera using the following library: '*DriectX.Capture.dll*' and '*DShowNET.dll*'. The '*Microsoft.Office.Interop.Excel.dll*' and the '*Office.dll*' are used to load the spreadsheet file with the type of HIFU transducers.

9.21. Control of HIFU Generator RFG 1000

The RFG_1000 (JJ&A Instruments, USA) [183] is an RF amplifier that it is used to generate HIFU. It is connected with the computer via a USB interface and can be controlled from the computer by sending commands in string format. This device combines a signal generator and an amplifier in one single device. The company provides the installation drives but it does not provide any driver compatible with C sharp.

In order to interchange string commands with device, a serial com port was opened. To do that, two libraries of C sharp were called from the language abstract.

```
using System.IO.Ports; //Open com Port
using System.Threading; //Open single threat
```

The communication with device was established by creating an instance of the Serial Port class like the following code line:

```
private SerialPort comPort = new SerialPort();
```

Open and close communication line with the device was established by using the following functions of the Serial Port class:

```
comPort.Open();  
comPort.Close();
```

The function '*GetPortNames*' was called in order to retrieve all the available port names that are connected to the computer at run time moment. The function was called from the serial port class like the following code. The com ports were stored in an array of string named *ports*. The array was listed in a list box control on the platform interface:

```
//Get a list of serial port names and store it in an array of  
strings  
string[] ports = SerialPort.GetPortNames();
```

The function was called by using the previous created instance named '*comPort*'. The method used to send the string commands to the device via the serial com port are the following:

```
//send the message to the port  
comPort.Write(msg + Delimiter); //Delimiter = "\r"
```

The variable '*msg*' was used to store the string command and the variable delimiter was used to store the command line terminator, both were send to the generator after concatenation was used. The function name '*ReadExisting*' was called in order to extract all the string commands was send by the generator to the computer.

```
comPort.ReadExisting();//Read data from the serial com port
```

The commands were came from the device stored in list box on the software interface. The string commands were send to the generator are shown in (Table 9.5):

Table 9:4 String commands were used to control the HIFU generator. The X, Y, and Z are integer parameter values

Command	Purpose
Set Freq X	Set the frequency parameter
Set pwr X	Set the power parameter in Watts
Set cw	Set the wave mode to continuous
Set mpn Xms, Yms, Z	Set the wave mode to pulse. X is the time on, Y is the time off, and Z is the number of cycles
run	Start the signal
stop	Stop the signal
mode	Review the parameters ware passed to the device

9.22. Temperature readings using thermocouple

The temperature reading subprogram communicate with NI DAQ analogue I/O part of the card pin-out. The card analogue pin-out is connected with a connector box. The connector box is connected with an Omega SMCJ-T Thermocouple (OMEGA Engineering INC, USA). Thermocouple gathers temperatures samples using copper wire. The negative wire (black) of the thermocouple is connected with pin number 3, the positive wire (red) is connected with pin number 4 and the negative wire (back) is grounded with pin number 5.

First, an analogue input channel was created. The analogue input channel was used to gather voltage, see the code below:

```
//initialize an analogue input channel
AIChannel myAIChannel;
```

A voltage input channel was assign to the analogue input channel. The constructor accepts six parameters. Device ID and terminal ID, the name of

the channel in string format (can be any), terminal configuration, minimum and maximum number of voltage, and the type of voltage units. See code below:

```
//create a voltage analogue input channel by passing the
appropriate parameters myAIChannel =
analogInTask.AIChannels.CreateVoltageChannel(deviceid +
"/ai1", "Temperature", AITerminalConfiguration.Differential,
0, 10, AIVoltageUnits.Volts);
```

Then, an analogue input channel reader was created using the proper constructor. The analogue input channel task was passed as parameter to channel reader constructor. See code below:

```
//create new analogue channel reader by passing the analogue
input stream
AnalogSingleChannelReader reader = new
AnalogSingleChannelReader(analogInTask.Stream);
```

Since, one degree Celsius is one thousand voltage, the following code converts the voltage to Celsius and store the result to a variable name 'analogDataIn'. The 'ReadingSingleSampe' method was called. See code below:

```
//1000 Volts for one degree C
double analogDataIn = 1000 * reader.ReadSingleSample();
```

The acquired value was stored in a text box control in format of real number and two decimal places precision. See code below:

```
//Temperature formatted into two decimal places in string
format
txtinputtemperature.Text = analogDataIn.ToString("0.00");
```

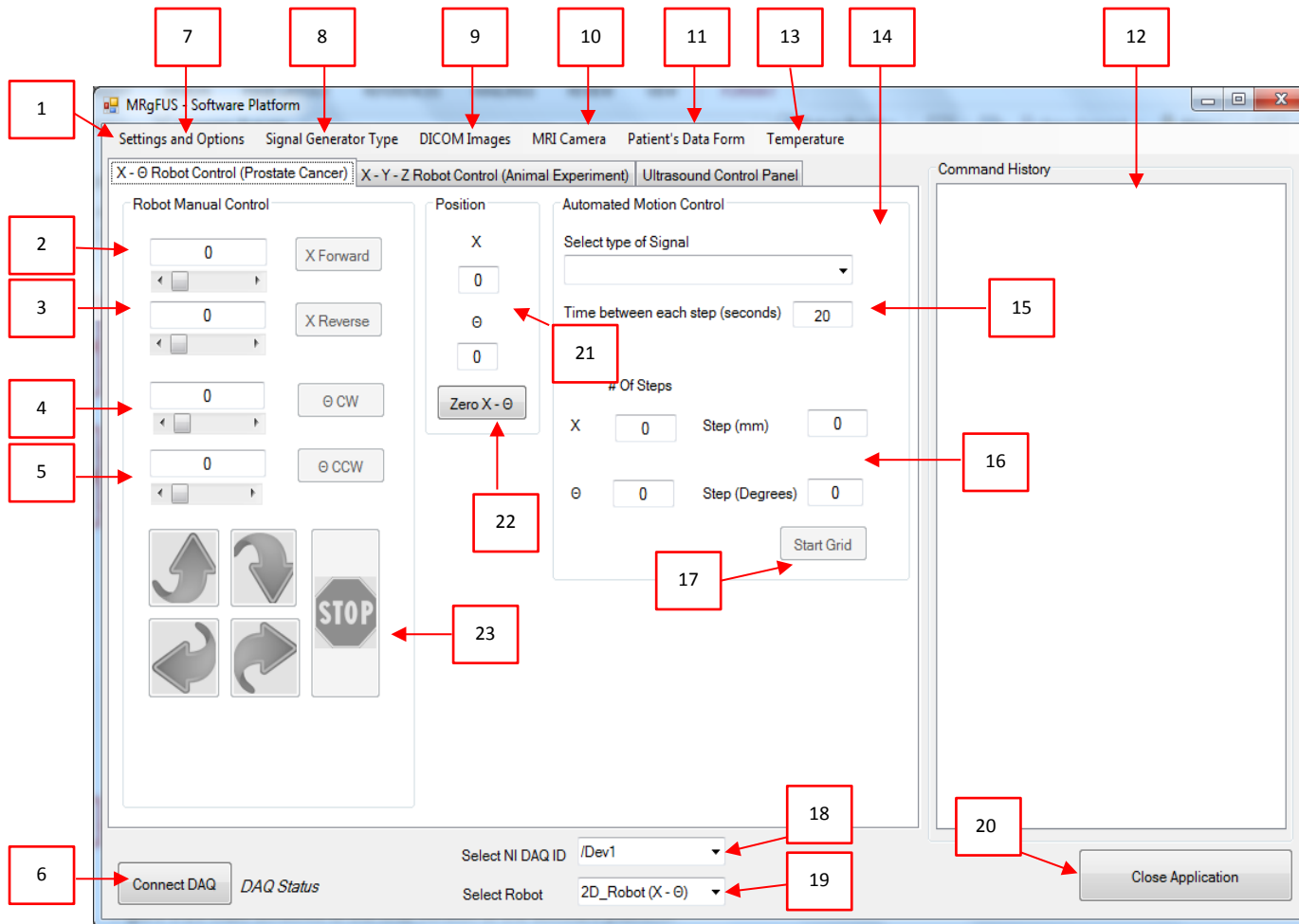
There is a graph chart on the user interface that it is updated real time during the temperature readings procedure. The code below add two values X and Y to the chart during the temperature measuring. The X value represents the interval time and the Y value represents the temperatures in Celsius.

```
//update the chart graph by passing time period to X axis
//values and temperature to Y axis values
chart1.Series["Series1"].Points.AddXY(Convert.ToDouble(txttime
period.Text), Convert.ToDouble(txtinputtemperature.Text));
```

The user has the ability to switch from Celsius to Fahrenheit and vice versa using a button on the thermocouple panel.

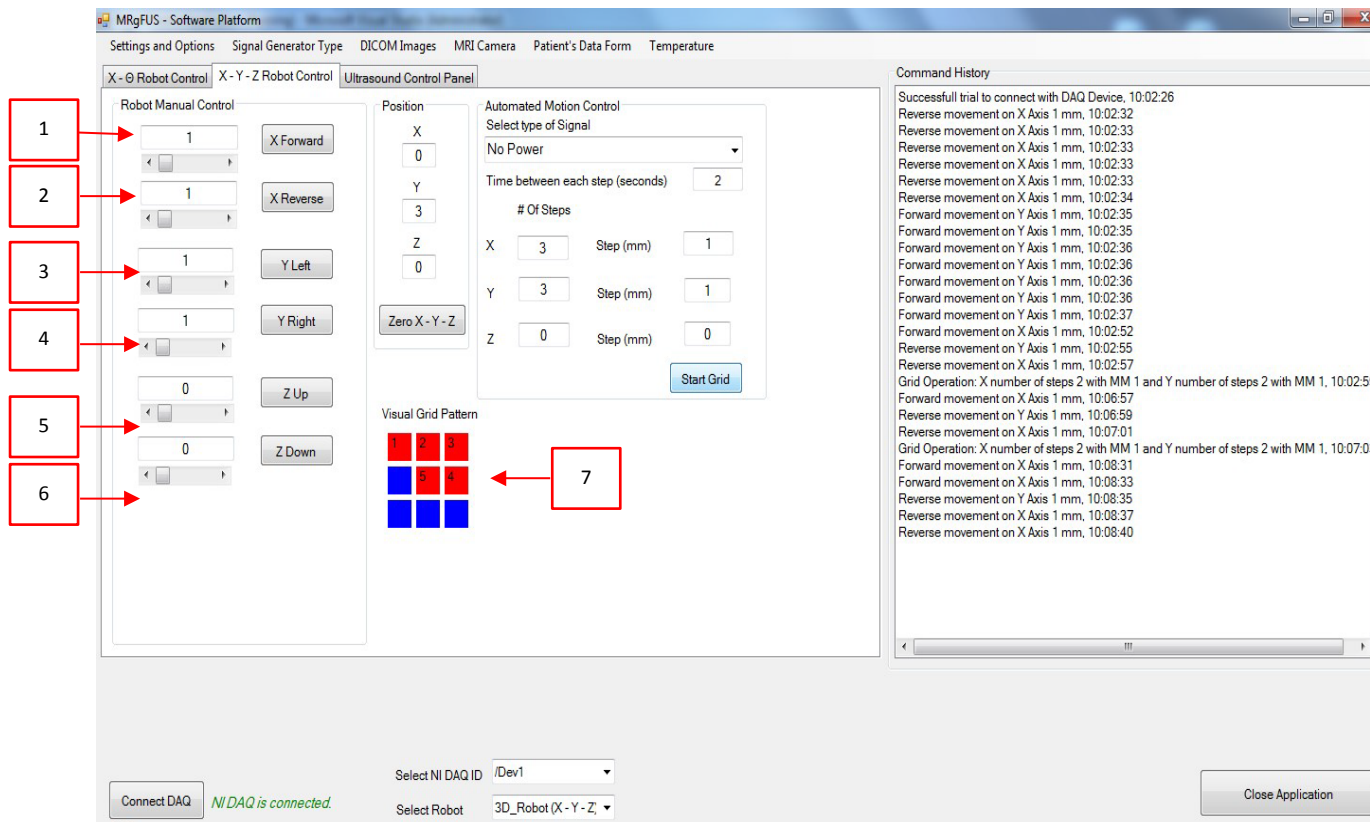
9.23. Final Version of the software platform

The design of the software underwent some improvements and modifications. The modifications are the following: a) there is a menu at the top of the form that consists of the settings and options, signal generator type (the application controls two types of signal generator), DICOM images, MRI camera, and patient's data form. b) The main window of the software platform was separated into three tabs (control of the prostate robot, control of a robot operating 3D and 2D linear stages respectively, ultrasound control panel). c) At the right hand side of the interface, there is a list box that lists all the commands that are executed during the execution of the application (figure 9.29). Detail explanation of the application is described in figures: 9.29, 9.30, 9.31, 9.32, 9.33, 9.34, and 9.35. d) Form that controls a thermocouple in order to gather temperature samples on regular intervals from HIFU focal point.



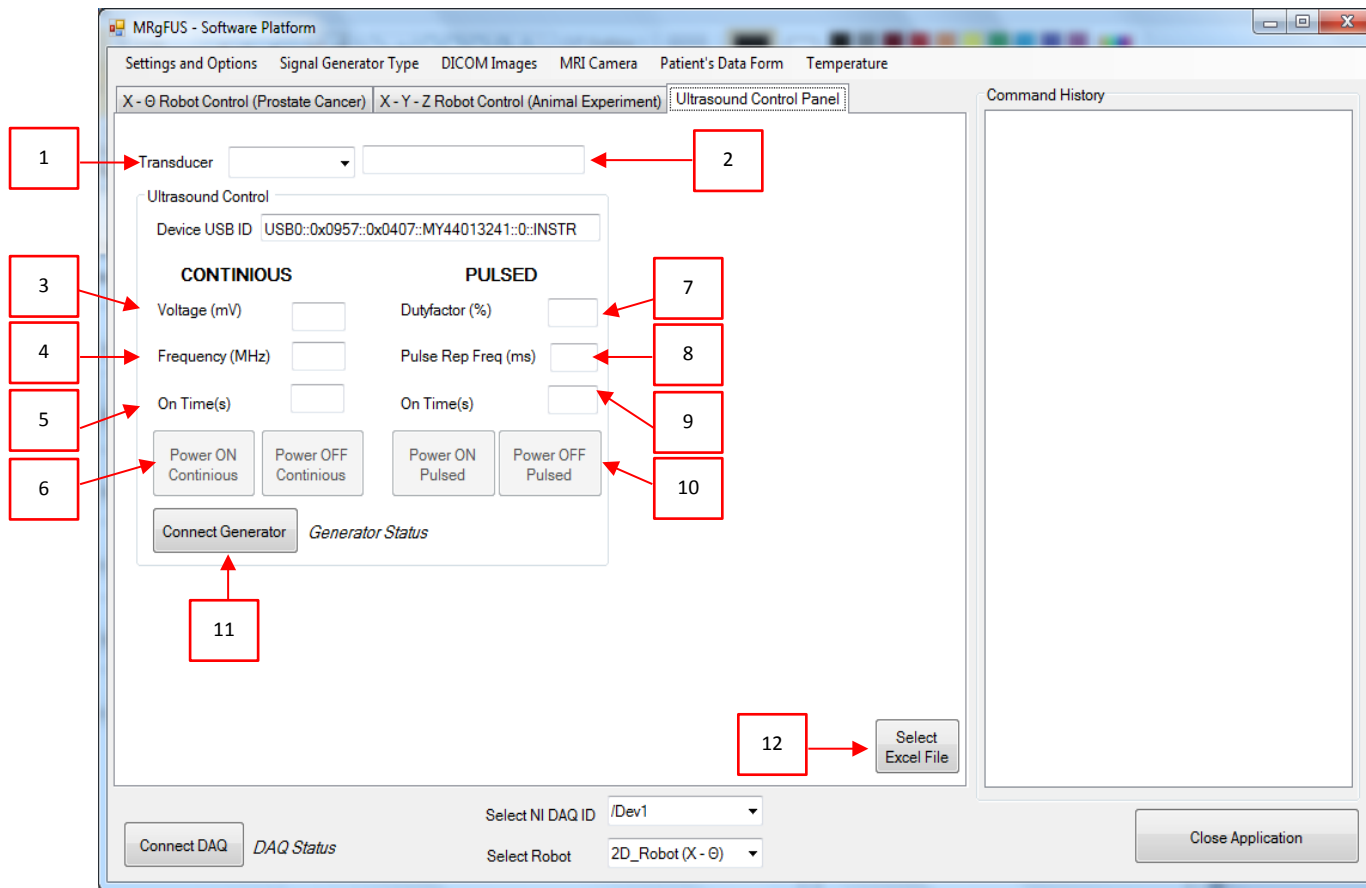
1. Main Menu
2. X Stage – Forward direction
3. X Stage – Reverse direction
4. Θ Stage – Clockwise direction
5. Θ Stage – Counter Clockwise direction
6. DAQ connection test
7. Setting and option menu (edit command history and DAQ devices)
8. Switch signal generator device
9. Open DICOM Viewer
10. Open MRI Camera window
11. Open Patient Data form
12. Command history list
13. Open Temperature Readings Form
14. Select HIFU signal type of automated motion control
15. Waiting time between ablations
16. Grid operation parameters
17. Start grid operation
18. Select robot type
19. Select DAQ device
20. Close the application
21. Current location of the transducer of x and Θ stage.
22. Set initial position to zero
23. Buttons for manual motion control of the robot.

Figure 9.29 Main windows of the final version of the software platform. The main options of the platform are separated into three tabs (tab Prostate Robot enabled).



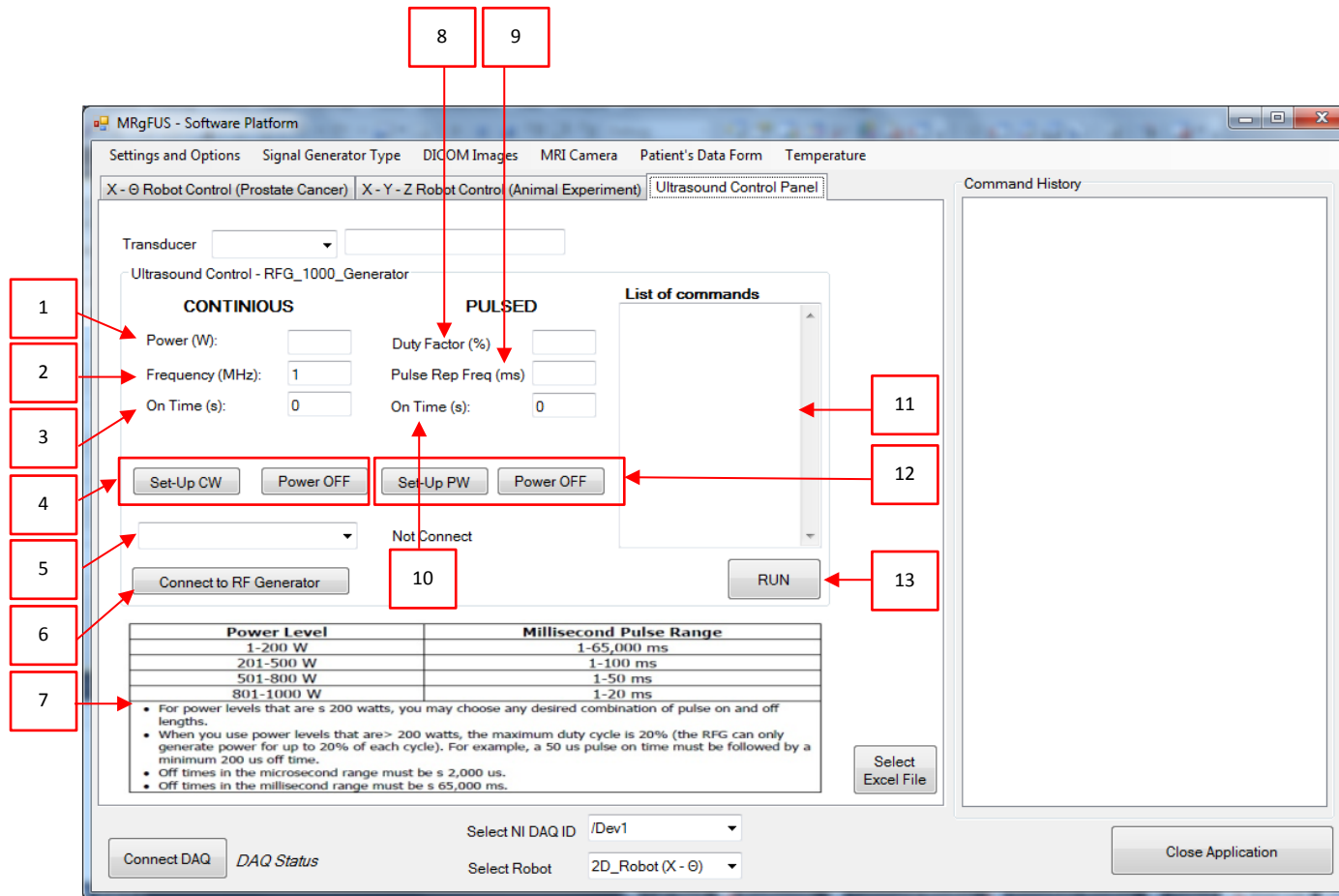
1. X Stage – Forward direction
2. X Stage – Reverse direction
3. Y Stage – Forward direction
4. Y Stage – Reverse direction
5. Z Stage – Forward direction
6. Z Stage – Reverse direction
7. Visual representation of the grid operation

Figure 9.30 Main windows of the software platform (X – Y – Z tab enabled)



1. Select transducer serial number from the drop down menu
2. Display transducer specifications
3. Power in millivolts
4. Frequency in MHz
5. ON Time for continuous signal
6. ON and Off buttons for continuous signal wave
7. Duty factor percentage for pulsed signal
8. Pulse Repetition Frequency – number of cycles in milliseconds
9. ON time for pulsed signal
10. ON and OFF buttons for pulsed US
11. Signal generator connection test
12. Select spreadsheet file with HIFU transducer specifications

Figure 9.31 Main windows of software– ultrasound control panel tab enabled (Agilent signal generator)



1. Set power level of the signal wave in watt
2. Set the frequency in MHz level of the signal wave
3. ON Time for continuous signal
4. Set continuous mode properties to generator and for the power OFF button turns of the signal wave
5. Select the com port
6. Button that checks the signal generator connection
7. Information about the range of acceptable cycles, for pulsed signal , per power level
8. Duty factor level percentage for pulsed US
9. Pulse Repetition Period– number of cycles in ms
10. ON time for pulsed signal
11. List of accepted commands by the generator
12. Set pulsed US properties to generator and for the power OFF button turns OFF the generator
13. Run button executes the last acceptable commands

Figure 9.32 Main windows of software platform – third tab enabled (RFG_1000 generator)

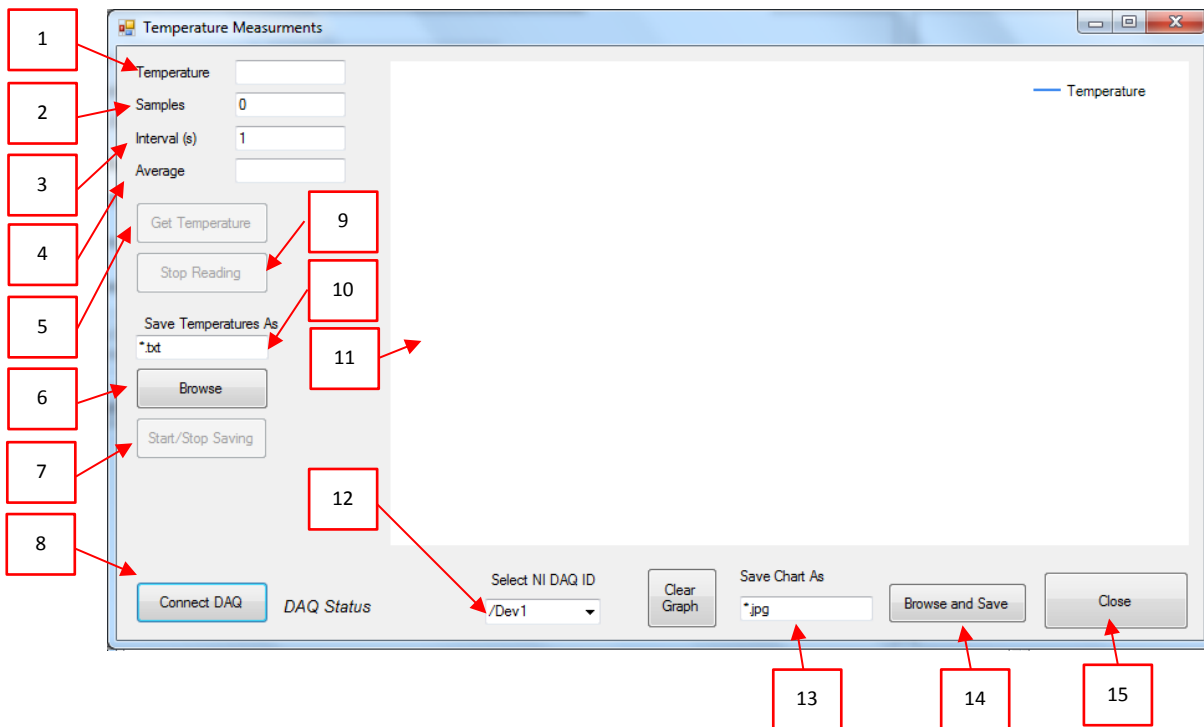


Figure 9.33 Temperature Readings Form. Gathering temperature measurements and creating real time graph chart

1. Temperature
2. The current sample of the temperature
3. User can selected the interval time for gathering the temperature
4. The current average temperature
5. Start read the temperature
6. Temperature file destination directory
7. Start or Stop writing the temperature
8. Connect with DAQ device
9. Stop read the temperature
10. File name of the temperature's text file
11. Real time graph chart
12. Select DAQ device
13. File name of the image graph chart
14. Find and save the destination directory
15. Close the form

Analysis of the main menu and submenus of the software is presented in figure 9.34, 9.35 and 9.36:

1. Open a text file that includes the name ID of the DAQ device. Delete, Addition and editing of a name ID is allowed
2. Open sub menu command history
3. Exit from the software
4. Save the current list of commands

5. Erase the current list from command history list box
6. Open the file that includes the command history

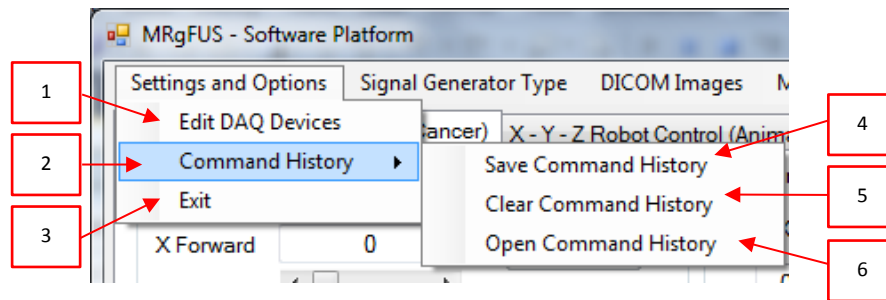


Figure 9.34 Explanation of main menu – Submenu: Settings and Options

1. Display Agilent generator control interface
2. Display RFG_1000 generator control interface

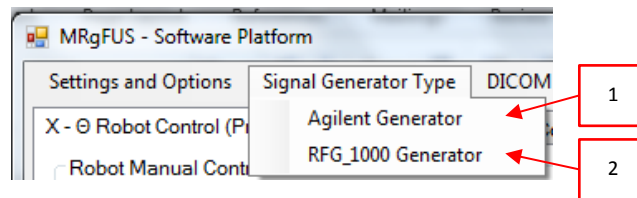


Figure 9.35 Explanation of main menu – Sub menu: Signal Generator Type

1. Open DICOM file transfer software
2. Open DICOM viewer
3. Import X and Θ dimensions from DICOM Viewer subprogram.

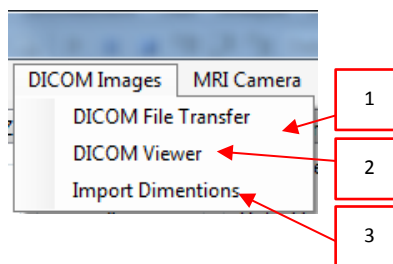


Figure 9.36 Explanation of main menu – Sub menu: DICOM Images

9.24. Discussion and Conclusion

The final version of software platform written in C Sharp has been developed in order to control an MRI guided Focused ultrasound. The software serves 6 main tasks through various windows or menus: a) MRI imaging, b) transducer movement (the user may move the robotic arm in a specific direction or customise the automatic movement of the robotic arm in any formation by specifying the pattern, the step and the number of steps), c) messaging (starting time, treatment time left etc), d) MRC Camera control, e) Patient data (age, weight, etc), f) Controlling the parameters and activation of signal generators). Accuracy motion feedback is provided using optical encoders. The software controls a positioning device which can be used to treat patients with prostate cancer.

Eventually, the version of software written in C Sharp was used instead of that version of software written in MATLAB for several reasons. The C Sharp version of the software solves some problems and malfunctions that were facing during the testing of the MATLAB version. C sharp has faster loading time than MATLAB, the application software can be loaded easily and fast. C sharp also provides more efficient distributable package (the executable setup includes installation packages of the external devices drivers). C sharp has faster communication speed with the DAQ device than MATLAB, so it provides better accuracy motion that is very important for the positioning device. C sharp provides more efficient functionalities for manipulating the 'dicom' images coming from the MRI. Also, images on c sharp are loaded faster.

Also, C sharp has several additional advantages over MATLAB such as: The language can be used for large projects with many members. The language can be used to develop applications that provide graphical user interface. The language provides reliable tools (libraries) that control external devices like HIFU generator, data acquisition boards and cameras. It is easy to debug programs when syntax or logic errors exist. It encourages writing reusable and easily maintainable code, easy to add additional functionalities when that is needed. Also, the language is suitable for real time applications. The

language can be used on another platform instead of windows by using different GUI libraries, such as UNIX or LINUX platforms.

Finally, the C Sharp version of the software created solves several problems that we were facing by using the MATLAB version of the software. The C Sharp version of the software provided significant improvement as it made the software more robust and reliable in controlling the MRI compatible ultrasound therapy system.

10. Chapter: Evaluation of 2D MR compatible positioning device for guiding a focused ultrasound system for trans-rectal treatment of prostate cancer.

10.1. Introduction

This chapter describes the evaluation of the MRI compatibility of the positioning device, the accuracy of the system, and the functionality of the MRgFUS system. It also includes evaluation of ablating capability, tested in tissue *in vitro* and commercially available gel phantoms.

10.2. Materials and Methods

10.2.1. Focused ultrasound system

In order to evaluate the accuracy of the positioning device discrete thermal lesions were created using focused ultrasound in a gel phantom and tissue *in vitro*. Overlapping lesions were created also demonstrating the functionality (ablation) of the positioning device. The focused ultrasound system consists of a signal generator (HP 33120A, Agilent technologies, Englewood, CO, USA), a RF amplifier (150 W, AR, Souderton, PA, USA), and a spherically shaped bowl transducer made from piezoelectric ceramic of low magnetic susceptibility (Etalon, Lebanon, IN, USA). The transducer operates at 3 MHz, has focal length of 4 cm and diameter of 3 cm. The frequency used is not the optimum frequency. This frequency has been shown by [184] and [185] that is very effective for the case of prostate. The transducer was attached on the arm that is mounted on the positioning device described in chapter 6.

10.2.2. MRI processing

The 2D positioning device and the transducer were tested inside an MRI scanner (Signa 1.5 T, by General Electric, Fairfield, CT, USA) for MRI compatibility. A spinal coil (USA instruments, Cleveland, OH, USA) was used to acquire the MRI signal. In order to test the MRI compatibility of the positioning device the DQA phantom (NiCl₂, H₂O) by GE-Dielectric Corporation (Menomonee Falls, WI, USA) was used.

The following parameters were used for T2-W FSE: TR: 2500 ms, TE=60 ms, Slice thickness=3 mm (gap 0.3 mm), Matrix = 256 x 256, FOV =16 cm, NEX = 3, ETL = 8.

The 2D positioning device was tested also on table of Magneto Symphony MRI scanner (1.5T and 3T, by Siemens, Germany), at the University Klinikum in Freiburg, Germany.

The following parameters were used in 1.5T for the noise test: Sequence: FLADH 2D, ST = 8mm, TR = 5ms, TE = 2.5ms, BW = 1953Hz/px, Flip angle voltage = 0V, FOV = 500x500mm, Matrix = 128x128, Frequency range = BW*Matrix in freq direction = 1953Hz/px * 128px = 250kHz.

The following parameters were used in 1.5T for the motor movement: Sequence: FLADH 2D, ST = 20mm, TR = 4.3ms, TE = 1.88ms, BW = 610Hz/px, Flip angle = 30°, FOV = 337x450, Matrix = 154x256.

The following parameters were used in 3T for the noise test: Sequence: FLADH 2D, ST = 8mm, TR = 5ms, TE = 2.5ms, BW = 1953Hz/px, Flip angle voltage = 0V, FOV = 500x500mm, Matrix = 128x128, Frequency range = BW*Matrix in freq direction = 1953Hz/px * 128px = 250kHz.

10.2.3. In vitro experiments

In vitro experiments were carried out in order to assess the repeatability of the positioning device. A polyacrylamide gel (ONDA Corporation, Sunnyvale CA, USA) was used to test the accuracy of the positioning device. For evaluating the functionality of the positioning device freshly-cut turkey tissue was used. The gel or turkey tissue under ablation was placed in a degassed saline tank. The gel or turkey was placed on top of an absorbing material in order to shield adjacent tissue from stray radiation from the bottom of the plastic water tank. The transducer was placed on the arm of the positioning device and was immersed in the saline tank, thus providing good acoustical coupling between the gel or turkey and transducer. Any bubbles that may have been collected under the face of the transducer face were removed in order to eliminate any reflections.

10.2.4. Experiment setup (Lab)

Figure 10.1 shows the photo of the experimental setup. The system includes a signal generator (Agilent 33220A) and an RF amplifier (AR 250W) for creating lesions. The system also includes the positioning device and electronic driving system establishing motion of the robot. The software was used to control the system was described on chapter 9.

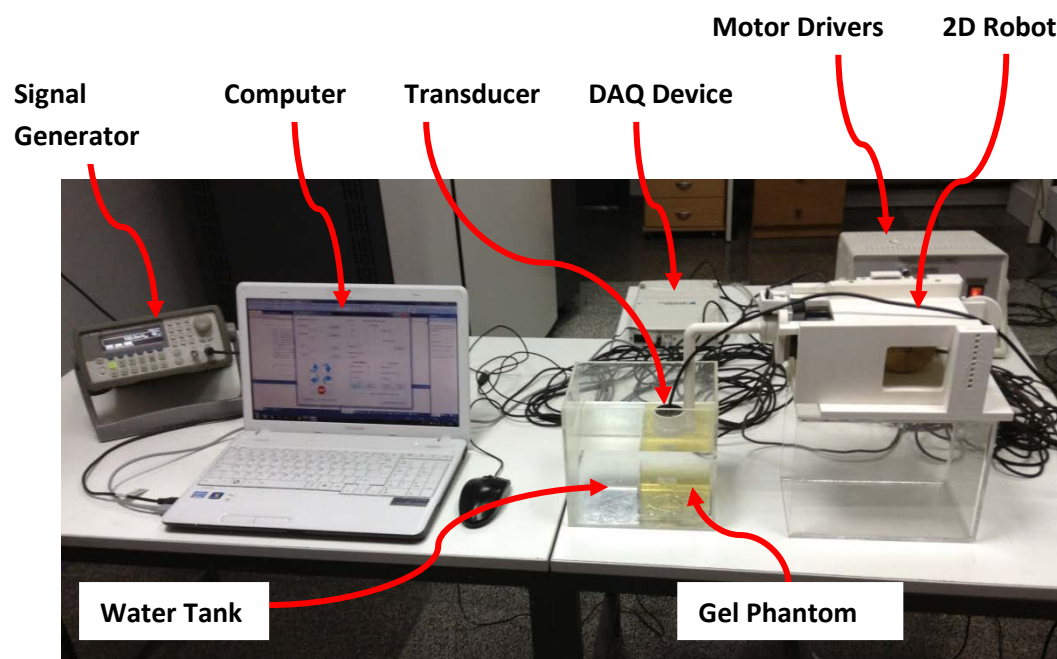


Figure 10.1 complete setup of the MRgFUS ultrasound system used for the experiments *in vitro* on dead tissues and gel phantoms

10.3. Results

Figure 10.3 shows the graph of measured distance of the encoder vs. the number of cycles of the encoder for the forward linear motion. The relationship between the measured distance (Y) and number of pulses of the number of encoder pulses (X) is linear. The relationship as extracted from this graph is:

$$Y=0.2+\alpha X.$$

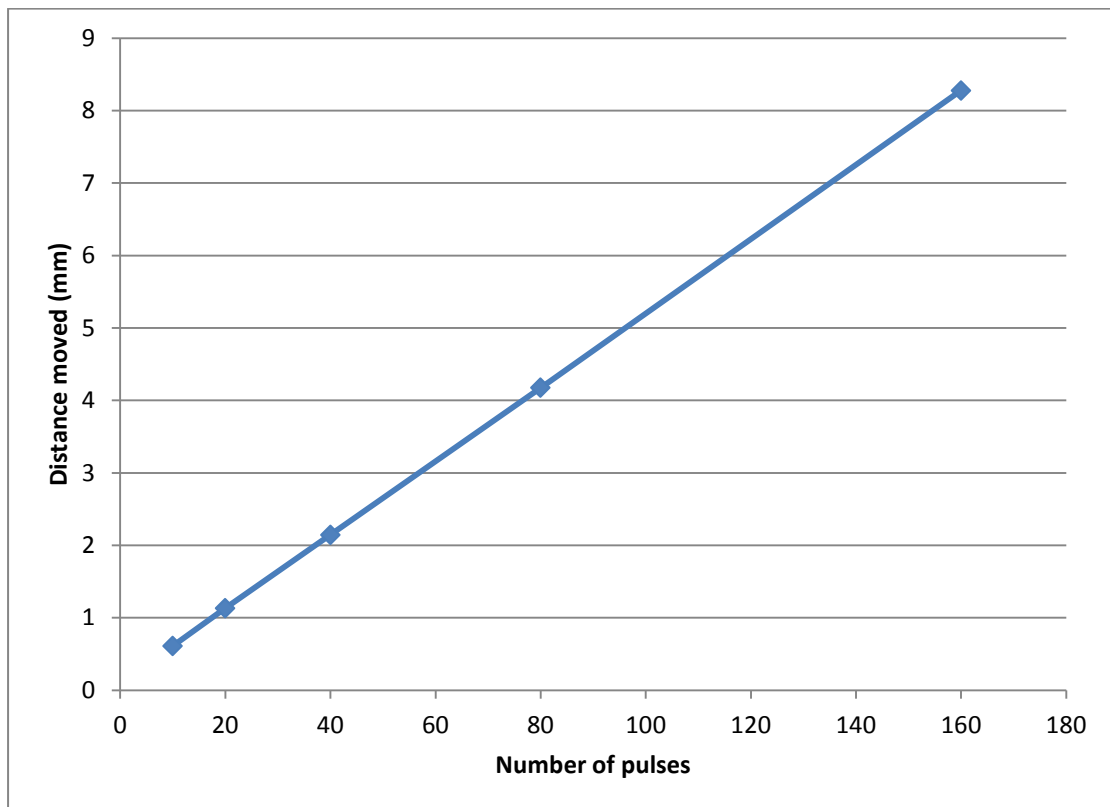


Figure 10.2 A line graph of the measured distance versus the number of cycles covered by the optical encoder. Graph demonstrates the linearity of the motor movement on X stage.

When the number of pulses is zero the distance moved is not zero. This is due to the fact that during the execution of the programming code in C, some overhead time is always needed and therefore Y is not zero for a zero pulse. Therefore, from this equation, as the user selects the distance to be moved (Y), the program extracts the number of pulses that the encoder has to measure. The constant α depends on the encoder type (for the linear encoder is 500 pulses per inch). During the evaluation test at any given X, twenty (20)

values of Y were measured. The average error measured for all steps was 20 μm . The amount of error was not related to the number of pulses (i.e. step size). Similar results were obtained when the linear stage was moved in reverse direction (average error 18 μm). The error for the angular stage was 13 μm . The relationship between pulses and distance is shown in the following equation:

$$Y = ((\alpha * X)/360) - 30.$$

Figure 10.4 shows the overhead time, in pulses per inch, of angular encoder compared with the distance covered. There are 20 pulses per inch overhead time about 3° motion using angular stage. The overhead time from 10 degrees and above is 30 pulses per inch. The overhead time for linear stage is standard for all steps.

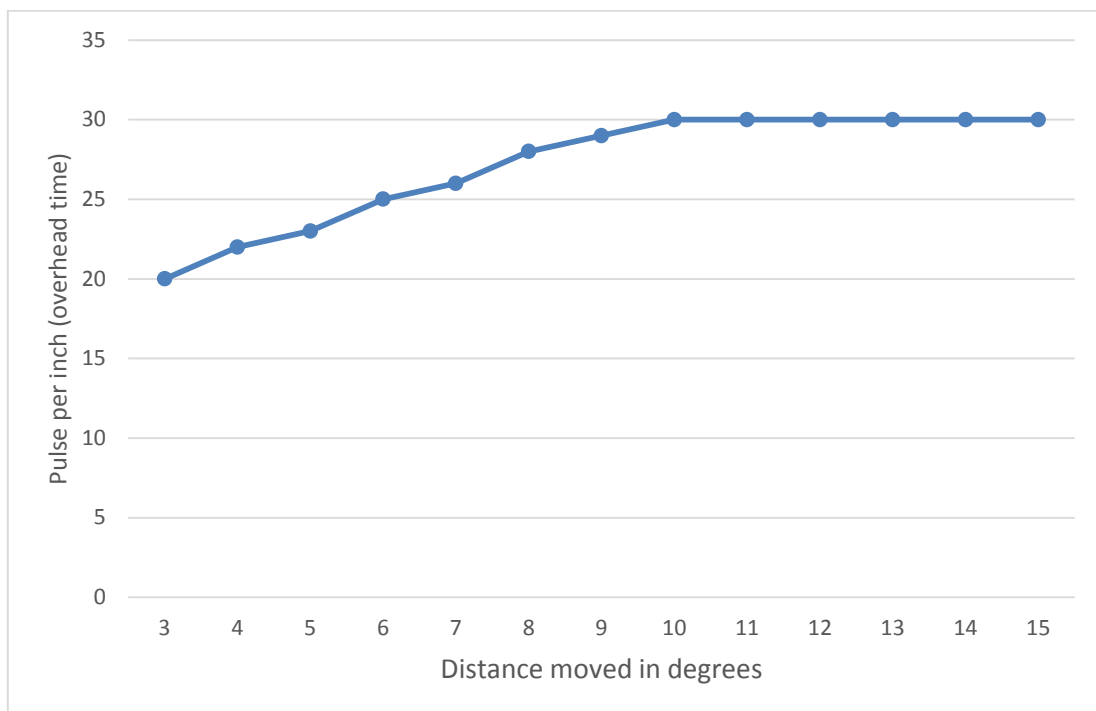


Figure 10.3 A line graph of the measured distance versus the number of cycles covered by the optical encoder (overhead time). Graph demonstrates the non-linearity (below 10 degrees) of the overhead time on Θ stage. From 10 degrees and above the overhead is standard.

During the evaluation test at any given X, thirty (30) values of Y were measured. The constant α depends on the encoder type (for angular is 2500 pulses per inch). The overhead time for the angular encoder is not the same

for all degrees. For 10 and above degrees, the overhead time is the same. For 10 and below degrees, the overhead time is a variable. The minimum motion that is valuable for the axis is 2 degrees.

The motion accuracy of the motor was evaluated using a digital calibre. One edge of the calibre was fixed on a stationary part of the positioning device and the other edge was fixed on a movable part. The movement of a specific step was measured using the incremental distance of the calibre. The resolution of the calibre was 10 μm .

10.3.1. MRI Compatibility Tests

Figure 10.5 shows a photograph of the positioning device placed on the table of the MRI scanner. The positioning device in this figure is placed on the top side of the lumbar spine coil. Figure 10.5 also shows the liquid phantom was used to evaluate the MRI compatibility of the system.

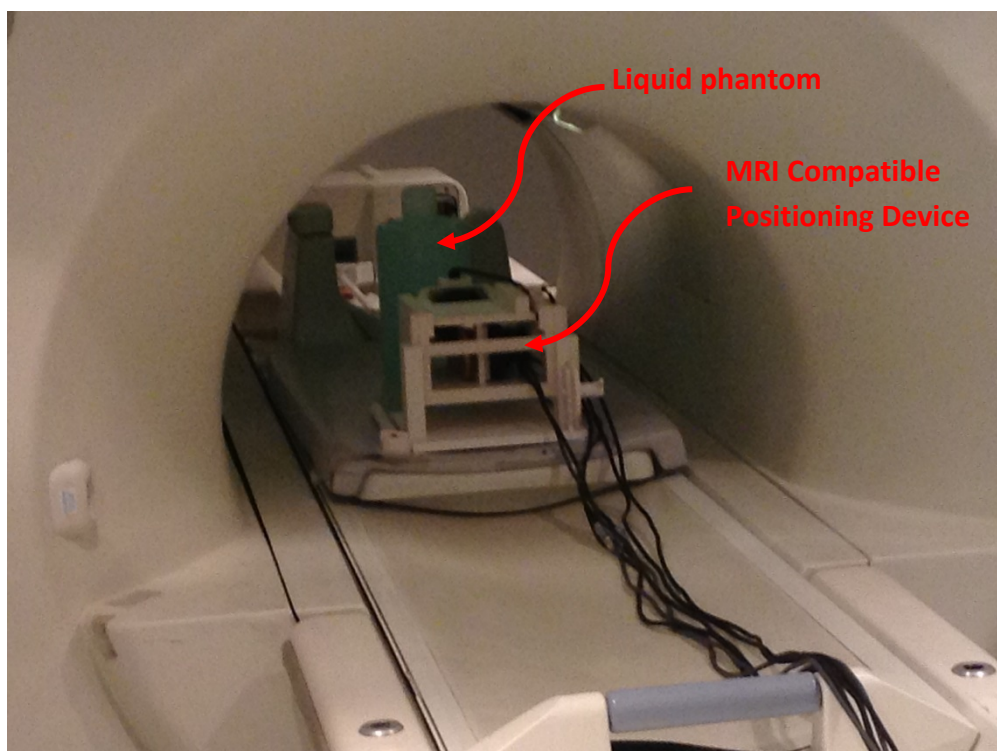


Figure 10.4 A photograph of the robot positioning device placed on the table of the MRI scanner

Figure 10.6 shows the test performed in order to evaluate the MR compatibility of the positioning device. Figure 10.6A shows the MRI image of T2W FSE without the activation of the motors and optical encoder. Figure 10.6B shows the MRI image of a liquid phantom using T2W FSE with the activation of the motors and optical encoder. The difference in the signal of the 2 images was in the same order as the noise of the images, demonstrating the excellent MRI compatibility of this positioning device.

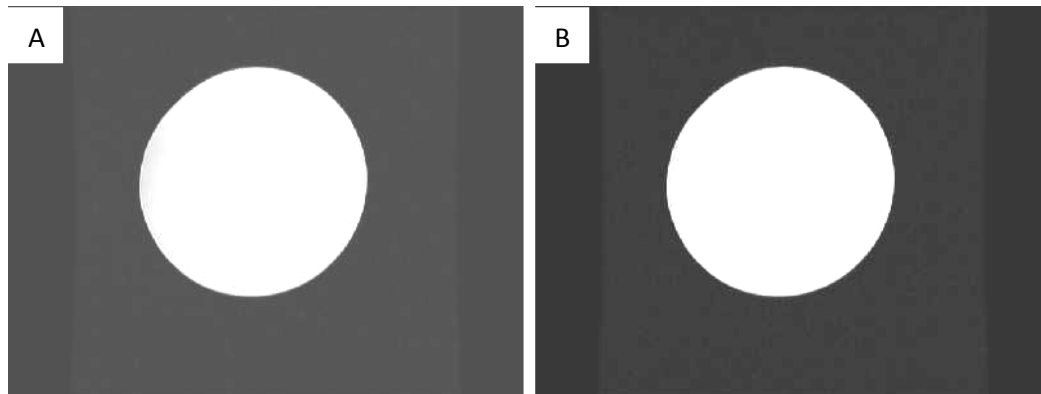


Figure 10.5 A. Image of the MRI compatible liquid phantom capture with the present of the robot positioning device. 10.5B image of the MRI compatible liquid phantom with the present and activation of the robot positioning device.

In vitro experiment was performed using a liquid marker. The experiment was done on a Siemens 1.5T and 3T MRI scanner in order to show the motion accuracy and functionality. Also, the experiment proved that the 2D positioning device is universal and it can be used in any commercial MRI scanner. Figure 10.7A shows the experiment setup and figure 10.7B shows the liquid marker attached on the positioning device.

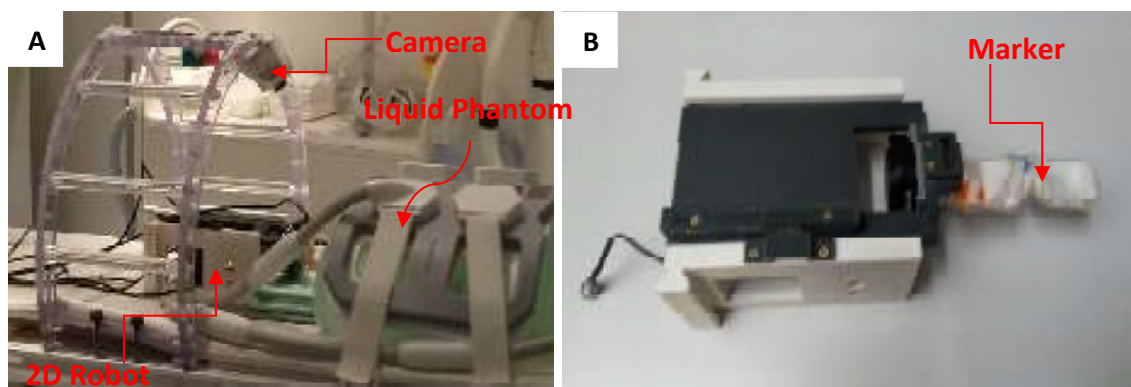


Figure 10.6: A photograph of the experiment setup on 3T MRI scanner. B. A photograph the liquid marker attached to the 2D positioning device, probe reception point.

The experiment on the 3T MRI scanner showed that the power supply is causing artefacts on the images. Figure 10.7A shows an MRI image with the power supply OFF, where figure 10.7B shows some artefacts on the image when the power supply was ON.

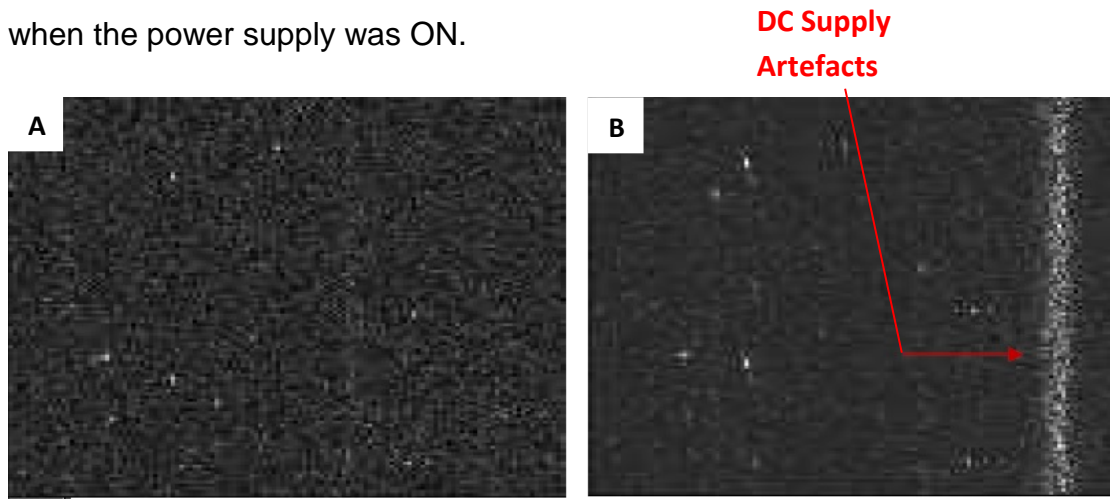


Figure 10.7: Image was taken with power supply OFF using 1.5Tesla. B. Image was taken with power supply ON using 1.5Tesla. The use of power supply was causing some artefacts on the image.

Figure 10.8A and 10.8B show linear motion of the system by moving the liquid marker on linear axis.

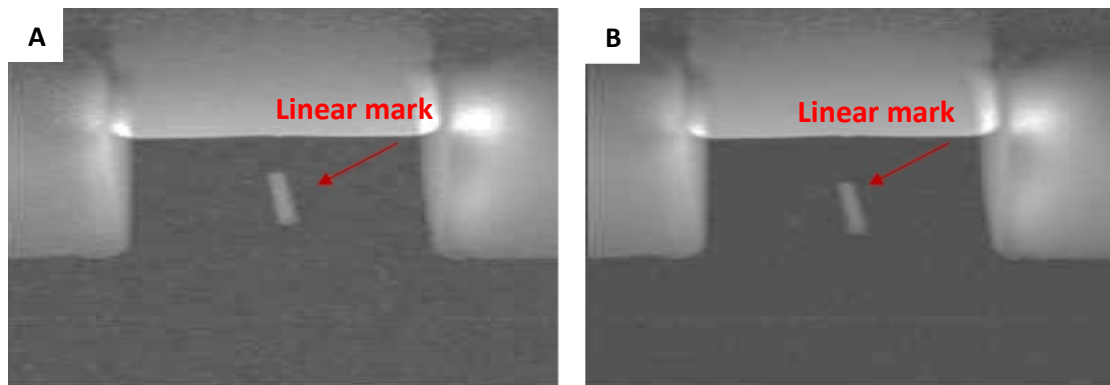


Figure 10.8: A. Image of a linear mark using 1.5Tesla. B. Image of a linear mark using 1.5Tesla.

Figure 10.9A and 10.9B show Θ motion of the system by moving the marker on the Θ axis. Figure 10.10A and 10.10B shows the functionality of Θ stage. The MRI image slicer was placed vertically on the marker, so only two points of the motion is visible.

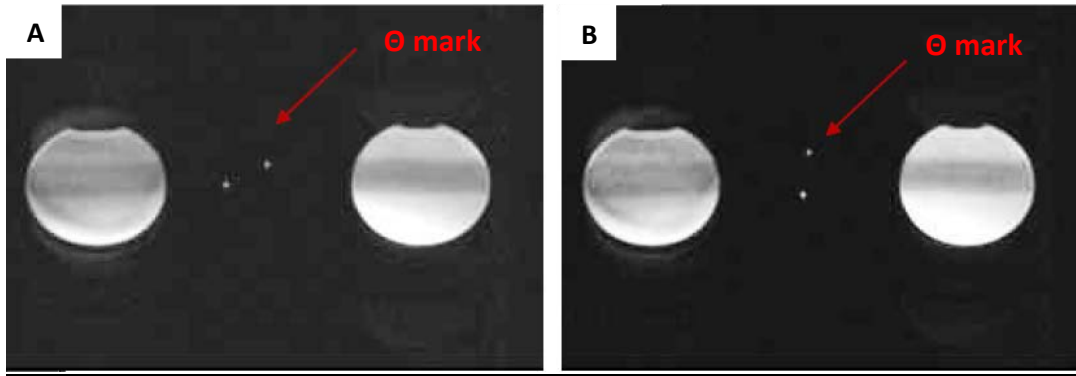


Figure 10.9: Image of a Θ mark using 1.5Tesla. B. Image of a Θ mark using 1.5Tesla.

Figure 10.10 A and B shows a Θ movement of the liquid marker in water. The image was taken before the motion was completed. The slicer was placed vertically on the marker so, only one dot is visible.

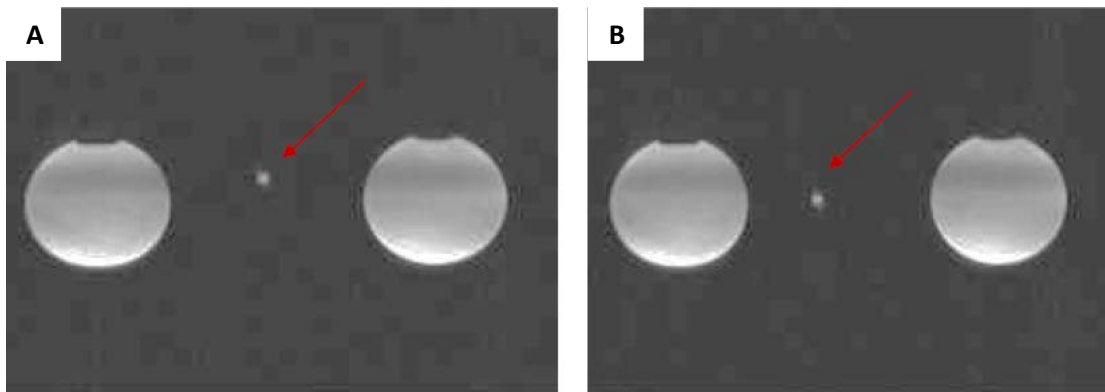


Figure 10.10: An image of Θ movement in water. B another image of Θ movement in water using 1.5Tesla

Figure 10.11 shows the liquid sign marker. The images were taken in 1.5 Tesla. The MRI image slicer was placed on top of the marker, so the marker was captured in top view.



Figure 10.11: Image of the marker using 1.5Tesla (top view).

Figures 10.12 and 10.13 shows images taken using the 3 Tesla MRI scanner. The 3T MRI scanner gives better quality images than the 1.5T scanner. Figure 10.12A and B shows the functionality of the Θ stage. Θ motion creates an arc that is valuable in the oval shape of prostate gland.

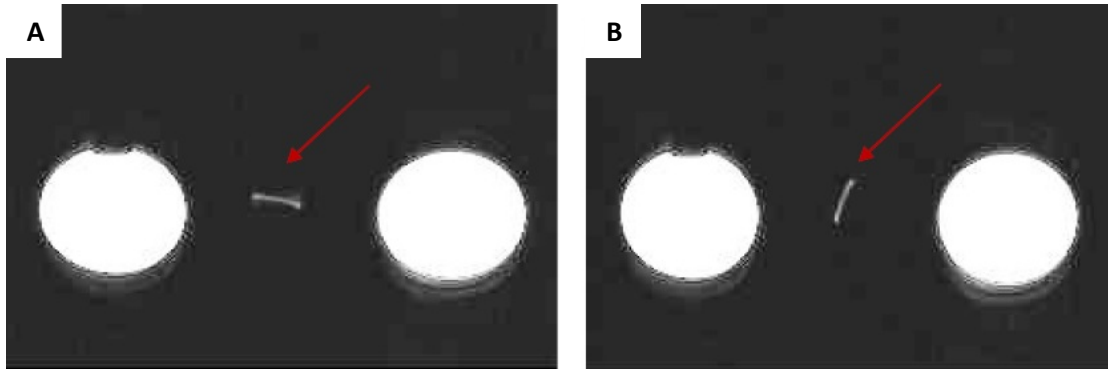


Figure 10.12: A and B shows two arcs were created using Θ movement using 3Tesla.

Figure 10.13A shows an image of the liquid marker in top view using a 3 Tesla MRI. The marker was rotated right using Θ stage. Figure 10.14B shows an image of the liquid marker using a 3 Tesla MRI scanner.

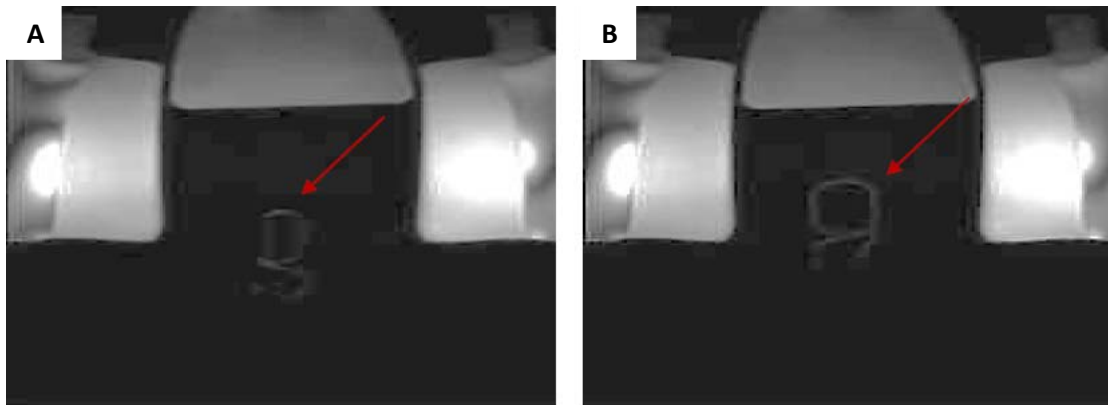


Figure 10.13: A and B shows images of the liquid marker using 3Tesla.

10.3.2. Positioning Device Accuracy Tests

Figure 10.14 shows discrete thermal lesions created in the gel phantom using the linear stage of the positioning device. The intensity used was 1500 W/cm² (spatial average in situ) for 10 sec. The spacing between the lesions was 10 mm. This figure clearly demonstrates the accuracy of moving the linear stage with the desired step.

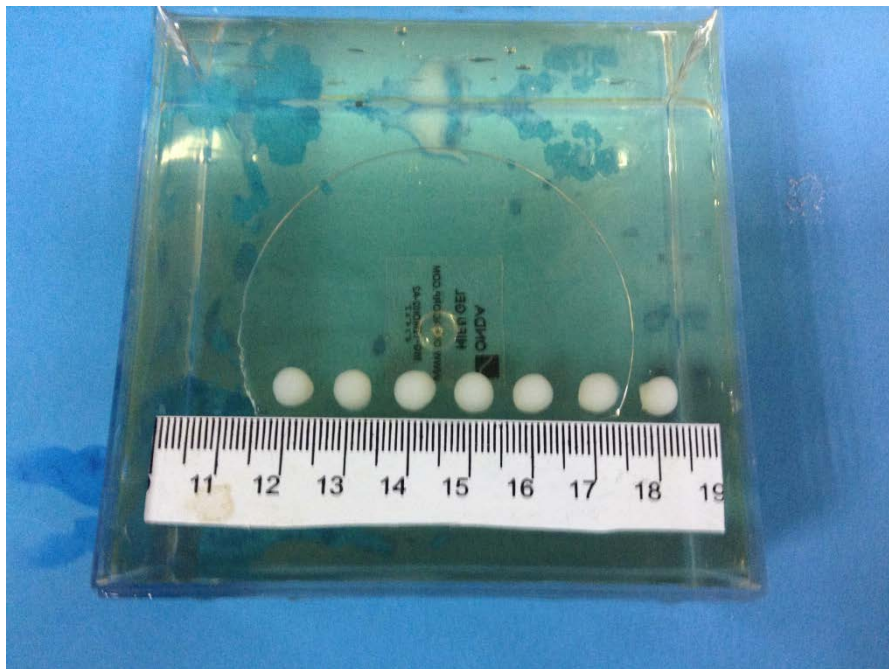


Figure 10.14 Thermal lesions created in the gel phantom using the linear stage of the positioning device. The seven lesions prove the excellent repeatability of the positioning device.

Figure 10.15 shows discrete thermal lesions created in the turkey dead tissue using the linear stage of the positioning device. The intensity used was 200 W/cm² (spatial average in situ) for 10 sec. The spacing between the lesions was 10 mm. This figure clearly demonstrates the accuracy of moving the linear stage with the desired step.

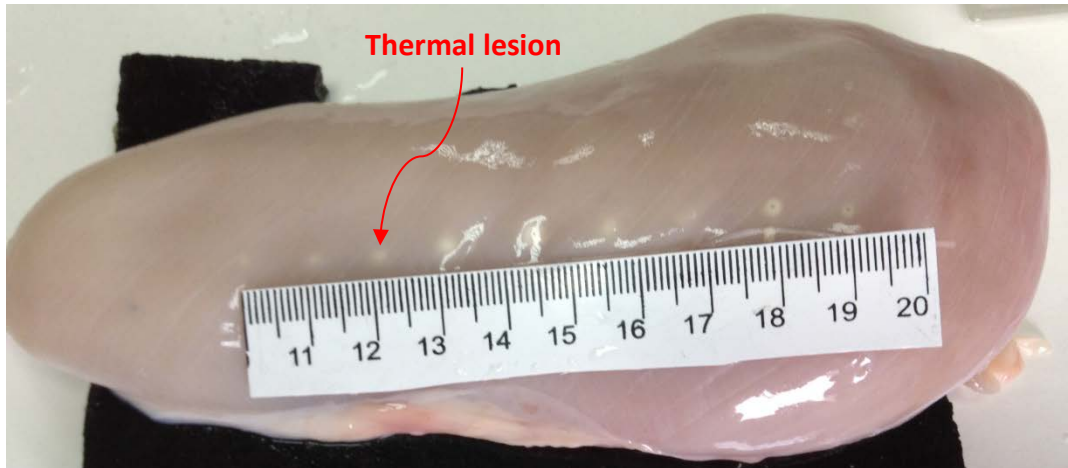


Figure 10.15 Thermal lesions created in the turkey dead tissue using the linear stage of the positioning device. The nine lesions proof again the excellent and robust repeatability of the positioning device.

Figure 10.16A and 10.16B shows discrete thermal lesions created in the pork tissue. The intensity used was 3000 W/cm² (spatial average in situ) for 10 sec. The spacing between the lesions was 2 mm. This figure also demonstrates the accuracy of creating overlapping lesions using the linear stage with the desired step.

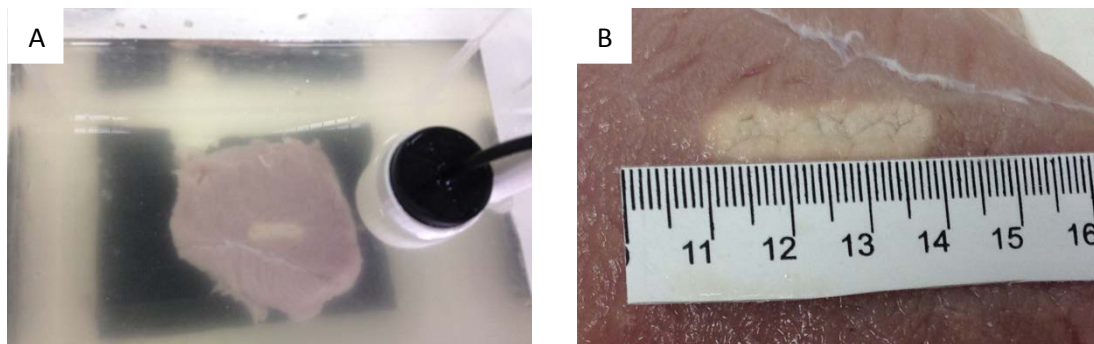


Figure 10.16A and B Thermal lesions created in the pork tissue using linear stage of the positioning device. Overlapping lesions were created successfully.

Figure 10.17 shows discrete thermal lesions on gel phantom using angular stage. This figure shows the excellent repeatability and functionality of the angular stage. Lesions were created using steps of 30 and the intensity used was at 1500 W/cm² for 10 sec. Also figure 10.13 shows the arc created by the Θ stage.

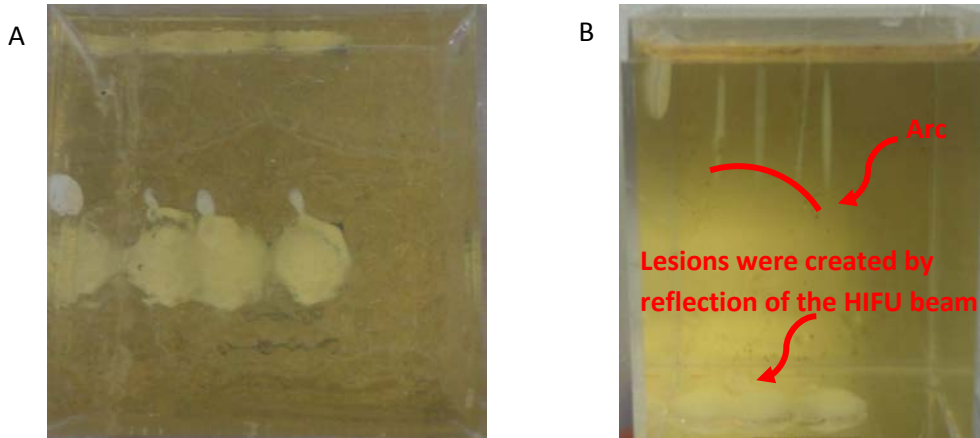


Figure 10.172A Gel phantom (top view) B A photograph of the gel phantom (side view), demonstration of Θ stage functionality. Some lesions caused by reflected beam are shown.

Figure 10.18 shows overlapping thermal lesions created in pork tissue in vitro using both the linear and angular stages of the positioning device. The intensity used was 1500 W/cm² (spatial average in situ) for 10 sec. The ablation grid was 5x5 with spacing between lesions of 2 mm for the linear stage and 3° for the angular stage. This figure clearly demonstrates the effectiveness of the positioning device for creating large lesions for the purpose of thermal ablation. The ablation grid was created using the automated motion control of the software platform.



Figure 10.18 Photograph of the overlapping thermal lesions created in pork tissue in vitro using both linear and angular stages of the positioning device. The ablation grid was 5x5 with spacing between lesions of 2 mm for the linear stage and 3° for the angular stage.

Figure 10.19A and 10.19B shows thermal lesions created in gel phantom using both the linear and angular stages of the positioning device. The intensity used was 1500 W/cm² (spatial average in situ) for 10 sec. The ablation grid was 5x3 with spacing between lesions of 2 mm for the linear stage and 3° for the angular stage. Figure 10.19A shows the grid ablation from the top view and the figure 10.19B shows the grid ablation from the side of the gel phantom.

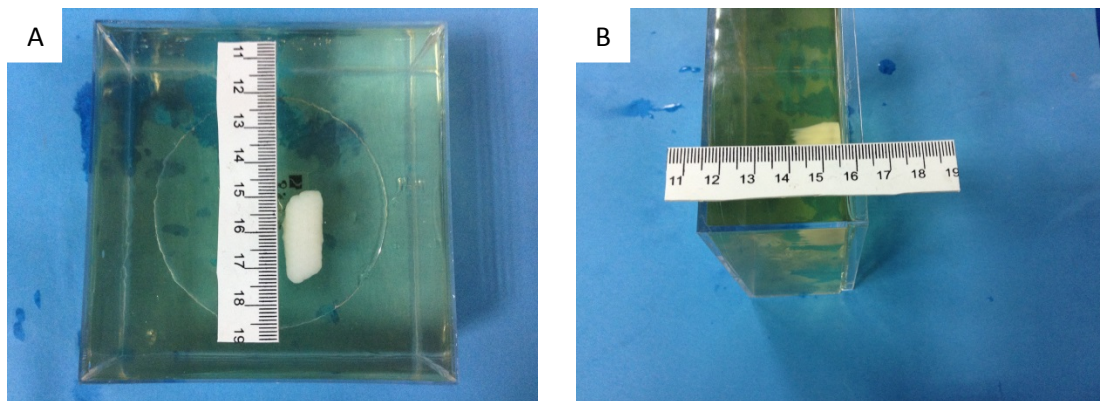


Figure 10.19A A photograph of the gel phantom (top view), B photograph of the gel phantom (side view).

The experiment on gel phantom was also performed on a clinical 1.5T MRI scanner. Figure 10.20A shows the experiment set up on MRI scanner's table. Figure 10.20B shows the transducer to gel coupling mechanism. The gel phantom was placed in a water tank with degassed water. The positioning device was moved the transducer holder above the gel.

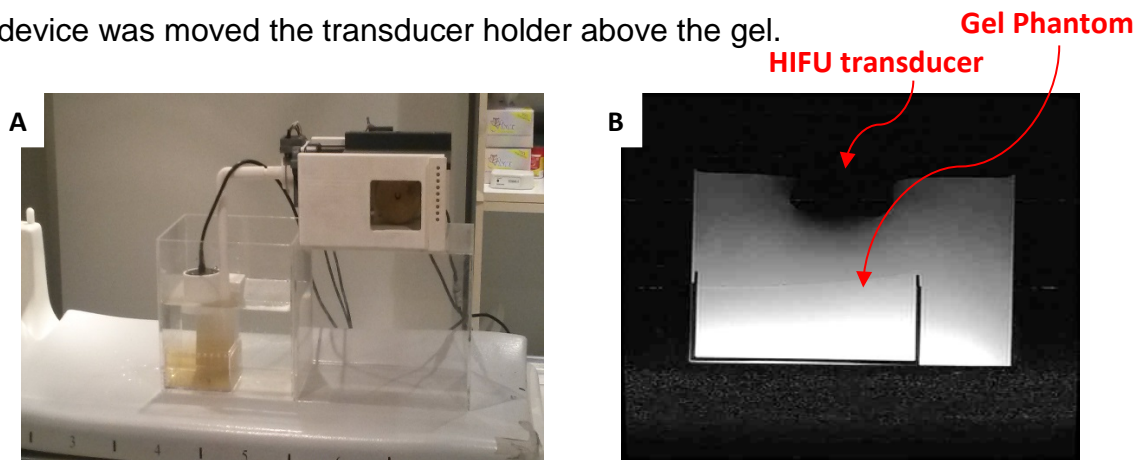


Figure 10.20 A. MRI compatible robot with test transducer holder and gel phantom demonstrates the transducer to gel coupling. B. MRI image of transducer to gel coupling.

Figure 10.21A and 10.21B shows discrete thermal lesions created in the gel phantom using the linear stage of the positioning device. The intensity used was 1500 W/cm² (spatial average in situ) for 10 sec. The spacing between the lesions was 10 mm. This figure clearly demonstrates the visibility of thermal lesions on the gel phantom using a T2W FSE on a 1.5T MRI scanner. Lesions on gel phantom were not visible using T1W FSE. Figure 10.21A proves that the operation of the optical encoders (EM1 US Digital, Vancouver, USA) is not effected by the MRI magnetic field.

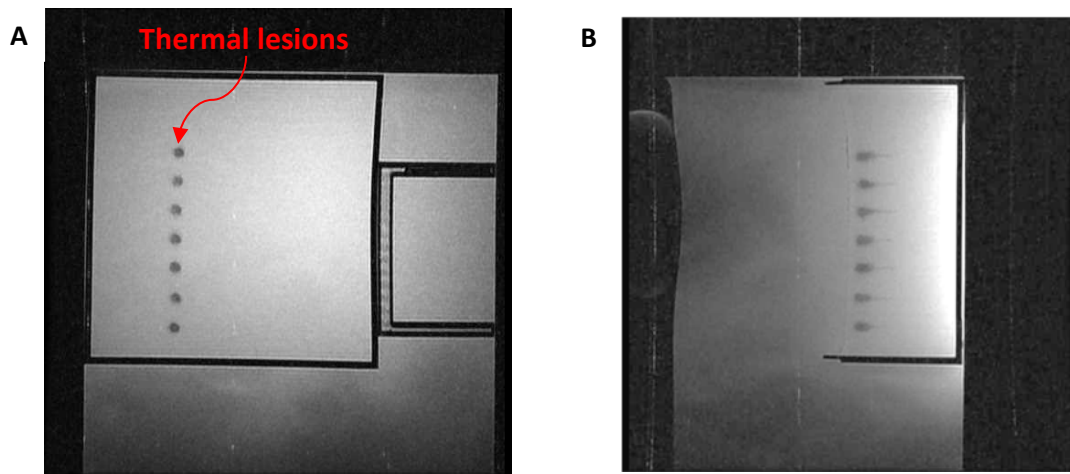


Figure 10.21 A T2W FSE image of the gel phantom (top view). B T2W FSE image of the gel phantom (side view)

10.4. Conclusion and discussion

The positioning device proposed can be comfortably placed on the table of the MRI scanner. Since the positioning device is placed on the table of the MRI scanner, this device can be used in all the available MRI scanners (i.e. it is a universal positioning device).

All the parts of the positioning device can be easily detached and this provides better portability but even more importantly is that any part of the robot can be redesigned and/or replaced easily and this will have no effect on the rest of the parts of the robot. It has been proven that the positioning device moves the transducer accurately and thus large thermal lesions can be produced reliably and repeatedly. This has been proven in both in vitro with gel phantom and in turkey tissue.

Following the evaluation it has been shown that the positioning device has a movement error of 20 μm for the linear stage and 13 μm for the angular stage. Also, it has been shown that the Z-stage can adjust the height of the positioning device at 1 cm steps. The variable Z-stage is needed since the entrance to the rectum varies from patient to patient. The data that we have in our disposal show that the height varies usually from 8 cm to 12 cm. It is possible that in some cases this height can be lower or higher. In case this system is used in the clinics, the design can easily be changed to cover these cases of rectal height as well.

10. CHAPTER: Conclusion and Future Expansions

10.1. Conclusion

The aim of this research was to design and manufacture a 2D MRI compatible positioning device with the capability to perform prostate cancer treatment using high intensity focus ultrasound. The prostate gland is a part of the male reproductive system and when is affected by a disease like cancer, functionality of the surrounding organs may be affected; therefore the quality of life is compromised. During the past few decades, several therapies were proposed and used for the treatment of prostate cancer. The existing therapies of the prostate are the following: Hormonal therapy, Active surveillance, Radical prostatectomy, Laparoscopic robotic prostatectomy, Branchy therapy (external and internal therapy)], Cryotherapy, Photodynamic therapy, Microwave thermal therapy, Transurethral ultrasound therapy and HIFU.

High intensity focused ultrasound (HIFU) has the potential to induce thermal changes in tissue, and therefore, it is used extensively for medical applications. Nowadays, HIFU is utilized to selectively heat biological tissues for oncological applications with minimal invasiveness by using magnetic resonance image (MRI) to provide, to the operator performing the procedure, images of a region within the subject being heated. HIFU was explored in almost every tissue that is accessible by ultrasound. The following represents some examples of some applications explored: eye [186], prostate [187], liver [188], brain [189, 190], kidney [191, 192, 193] and breast [194]. In commercial systems, HIFU is either guided by ultrasound or MRI. Ultrasonic imaging is the simplest and most inexpensive method to guide HIFU; however, MRI offers superior contrast than ultrasound, having the only disadvantage that is more expensive. HIFU has the ability to treat precise zones in tissues by focusing an ultrasound high energy beam in a target volume. In just a few seconds, HIFU causes the temperature to rise above 70°C in the focal zone of the transducer. The rapidity of this phenomenon induces a localized elementary coagulation necrosis lesion. Complete tumors can be treated using multiple elementary lesions placed side by side, so that the coagulated volumes overlap [195]. There are several advantages of using therapeutic

ultrasound as non-invasive surgery for the treatment of prostate cancer. The time is needed to complete the operation is less than the time is needed for the invasive surgery, therefore the patients do not necessary have to stay a number of days in the hospital.

The proposed device was manufactured using materials compatible with MRI magnetic field (the MRI is not affected from the operation of the device and the device is not affected from the strong MRI magnetic fields). The proposed device was manufactured using ABS plastic, brass screws and pinion, PUM motors, plastic optical encoders and strips. The positioning device was designed I such a way so it will be easy to place it on a table of any MRI scanner. The lower part is used to lift the robot up or down (Z axis) since the height of the rectum is variable. The movement is achieved manually using a rack and pinion which is placed in the main body of the positioning device. The main body includes a structure that provides guides for the X-plate (linear stage) movement. The base includes also a motor holder and a cover for the optical encoder. The X-axis plate also includes a motor holder for the Θ motion and a holder for the encoder plastic strip. The motor in the front of the x-plate established angular motion (Θ stage). An angular encoder is placed on the shaft of the motor and ensures accurate movement of the shaft. On the frontal part of the base a water enclosure can be attached. The positioning device system includes a data acquisition board for the purpose of interchange signals between the computer, the robot actuators and sensors.

The focus ultrasound system includes a signal generator and an amplifier. A spherical shape transducer made by piezoelectric ceramic, selected by low magnetic susceptibility was used for the evaluation of the developed device.

The custom made device has the following features which will enable the performance of the operation inside the MRI; tailor made software in order to control the system. The subprograms of the software that were implemented are: a) MRI imaging, b) transducer movement (the user may move the robot manually or automatically by specifying the pattern, the step and the number of steps), c) messaging (starting time, treatment time left etc.), d) Camera

control, e) Patient data (age, weight, etc.), f) Controlling the parameters and activation of a signal generator.

At the beginning of this research, the software was developed using MATLAB programming language. Preliminary control tests were performed using the software and some problems, mostly on communication speed, were encountered. The programme had too slow loading time and also it offered poor motion accuracy with height and unstable overhead time. The software was finally implemented using C Sharp programming language in order to eliminate all the problems that appeared during the control test.

The proposed system was evaluated for its motion accuracy and MRI compatibility. The motion accuracy of the device was evaluated using a digital caliper. The motion accuracy on linear stage was calculated at 20 μm and for angular at 13 μm . HIFU ablations were performed on gel phantoms and dead tissues by creating distinct and overlapping lesions using linear and angular stage. HIFU ablations clearly demonstrate the excellent accuracy, repeatability and functionality of the proposed system. Also, the 2D positioning device was tested using a MRI compatible marker that it was attached on the probe reception point. The marker's aim was to prove the functionality of the two stages of the device (X and Θ). The test proved that the positioning device can be used to cover the whole surface of the oval shape prostate gland.

The positioning device was evaluated also for its MRI compatibility. The positioning device was placed on a table near MRI compatible gel phantom on a clinical MRI scanner. The MRI compatibility of the device was tested using MRI scanners of two different manufacturers (Signa 1.5 T, by General Electric, Fairfield, CT, USA and Magneto Symphony 3 T, by Siemens Healthcare, Germany). The MRI compatible tests proved that the 2D positioning device can be operated perfectly without being affected by the strong MRI magnetic field. However, the MRI images were affected by the presence and operation of the power supply.

A simple, cost effective, portable positioning device has been developed which can be used in virtually any clinical MRI scanner since it can be placed

on the table of the MRI scanner. The uniqueness of this system is the ability to create thermal lesions inside the MRI with the intention to treat endorectally prostate cancer. The positioning device offers 20 μm on linear stage and 13 μm on angular stage accuracy that makes the device suitable for clinical use.

10.2. Future Expansions

The aim of the search was to develop a positioning device for the treatment of prostate cancer using therapeutic ultrasound. In order to archive this, the following task must be performed on future work:

- Attached an optimal HIFU transducer to the probe and proper registration marks inside the water enclosure.
- Obtaining regulatory approval for performing clinical trials and treatments on humans.
- Experiments in animals, especially in dogs (prostate dogs has similarities with male humans) for optimizing the HIFU protocol and treatment plans.

The following suggestions can be performed to improve the functionalities of the 2D positioning device:

- Add an additional linear stage internally to the probe enclosure to move the transducer up and down. This will make the deep of the focal length to be variable.
- Convert Z axis form manual driven to PC controlled.

Also, the following siggestions can be performed to improve the functionalities of the 2D positioning device:

- The positioning device can be expanded in order to use it for the prostate biopsy. This can be archived by replacing the probe with an MRI compatible needle biopsy.
- Modifications for the treatment of gynaecological diseases such as uterine fibroids.

Appendix

1. Publications

1.1. Journal publications

- Yiallouras C., Mylonas N., Damianou C., MR compatible positioning device for guiding a Focused ultrasound system for transrectal treatment of prostate cancer, Journal of Computer-Assisted Radiology and Surgery, 9(4):745-53. doi: 10.1007/s11548-013-0964-x. December 2013.
- Yiallouras C., Damianou C., Review of the MRI positioning devices for guiding Focused ultrasound systems, Journal of Computer-Assisted Radiology and Surgery, The International Journal Of Medical Robotics And Computer Assisted Surgery, 2014, DOI: 10.1002/rcs.1601, July 2014
- Yiallouras C., Ioannides K., Dadakova T, Pavlina M., Bock M., Damianou C. Three axis MR conditional robot for high intensity focused ultrasound for treating prostate diseases, Journal of Therapeutic Ultrasound, Accepted: December 2014.

1.2. Conference publications

- Yiallouras C, Ioakim M, Alexandrou A, Hadjisavvas V, Mylonas N, Damianou C., A software platform controlling an MRI guided focused ultrasound system, IEEE 12th International Conference on BioInformatics and BioEngineering November 11-13, 2012 Larnaca, Cyprus
- Yiallouras C., Mylonas N., Damianou C., MRI compatible positioning device for focused ultrasound prostate cancer treatment European Focused ultrasound surgery, Rome, October 10-11, 2013.
- Yiallouras C., Mylonas N., Damianou C., MRI compatible positioning device for high intensity focused ultrasound (HIFU) prostate cancer treatment. The 15th international conference on Biomedical engineering, ICBME 2013, Dec 4-7, 2013, Singapore.
- Yiallouras C., Mylonas N., Damianou C., MRI compatible positioning device for focused ultrasound prostate cancer treatment, ISTU 14, Las Vegas, USA, April 2-5, 2014.

- Yiannakou M., Yiallouras C., Mylonas N., Damianou C., MR-guided focused ultrasound robot for animal experiments', ISTU 14, Las Vegas, USA, April 2-5, 2014.

2. C Sharp coding

2.1. C sharp code requires the following libraries

```
//-----  
//Project --> Add Reference --> .NET  
//Add --> Microsoft.Office  
//Add --> Microsoft.Office.Interop.Excel  
//Add --> NationalInstruments.Common  
//Add --> NationalInstruments.DAQmx  
//Add --> VisaComLib  
//-----  
//National Instruments libraries  
using NationalInstruments;  
using NationalInstruments.DAQmx;  
//Visa connection library for agilent generator  
using Ivi.Visa.Interop;  
//office library for connecting with the excel application  
using Excel = Microsoft.Office.Interop.Excel;  
using System.Data.OleDb;  
//RFG_1000 Generator Reference  
using System.Management;  
using System.IO;  
using System.IO.Ports;  
using System.Threading;  
using System.Diagnostics;
```

2.2. C Sharp code that control the Agilent signal generator

The following code was developed under Microsoft Visual Studio Express Edition and C Sharp programming language. The program is responsible for controlling the signal generator and the HIFU protocol. The following code controls an Agilent Signal generator.

```
private void btnconnecttoagilent_Click(object sender, EventArgs e)  
{  
    try  
    {  
        string addr = null, msg = "";  
        //create the formatted io object  
        FormattedIO488 fg = new FormattedIO488();  
        //create the resource manager  
        ResourceManager mgr = new ResourceManager();  
        // For USB address  
        addr = txtagilentvisaID.Text;  
        // Open communication  
        fg.IO = (IMessage)mgr.Open(addr, AccessMode.NO_LOCK, 2000, "");  
        fg.WriteString("OUTPut " + "ON", true);  
        //writing strings to the generator  
        // Reset the instrument  
        fg.WriteString("*RST;*CLS", true);  
        // Wait for reset to complete  
        fg.WriteString("*OPC?", true);  
        msg = fg.ReadString();  
        fg.WriteString("OUTPut " + "OFF", true);  
        lblconnectionstatus.Text = "Agilent Generator is connected.";  
        btnconnecttoagilent.Enabled = false;  
        btnpoweroncont.Enabled = true;
```

```

        btnpoweronpulsed.Enabled = true;
        btnpoweroffcont.Enabled = true;
        btnpoweroffpulsed.Enabled = true;
        addCommandToHistoryList("Successful trial to connect with Signal Wave
        Generator, ");
    }
    catch (Exception ex)
    {
        MessageBox.Show(ex.ToString());
        lblconnectionstatus.Text = "Agilent Generator is not connected.";
        addCommandToHistoryList("Unsuccessful trial to connect with Signal
        Wave Generator, ");
    }
    finally
    {
        GC.Collect();
    }
}

private void turnONContinuous(double f, double v)
{
    string addr = null, msg;
    string Vstring = null, Fstring = null, PowerStringON = null;
    counter = 0;
    try
    {
        //create the formatted io object
        FormattedIO488 fg = new FormattedIO488();
        //create the resource manager
        ResourceManager mgr = new ResourceManager();
        // For USB address
        addr = txtagilentvisaID.Text;
        // Open communication
        fg.IO = (IMessage)mgr.Open(addr, AccessMode.NO_LOCK, 2000, "");

        //writing strings to the generator
        // Reset the instrument
        fg.WriteString("*RST;*CLS", true);
        // Wait for reset to complete
        fg.WriteString("*OPC?", true);
        msg = fg.ReadString();
        f = f * 1000000;
        //prepare the string for writing
        Fstring = "frequency " + Convert.ToString(f);
        Vstring = "VOLTage " + Convert.ToString(v) + "E-3";
        PowerStringON = "OUTPut " + "ON";
        //write the strings to the generator
        fg.WriteString(Fstring, true);
        fg.WriteString(Vstring, true);
        fg.WriteString(PowerStringON, true);
        //close connection
        fg.IO.Close();
    }
    catch (Exception e)
    {
        MessageBox.Show(e.Message + "\nin function: OpenPort", "VISACom");
    }
}

private void turnONPulsed(double df, double prf, int v, int f)
{
    string msg = null;
    string addr = null;

```

```

string BurstStringON = null, Vstring = null, PowerStringON = null,
burststringperiod = null, fstringpulsed = null;
double ncycles = 0;
counter = 0;
//create the formatted io object
FormattedIO488 fg = new FormattedIO488();
//create the resource manager
ResourceManager mgr = new ResourceManager();
// For USB address
addr = txtagilentvisaID.Text;
// Open communication
fg.IO = (IMessage)mgr.Open(addr, AccessMode.NO_LOCK, 2000, "");
try
{
    //writing strings to the generator
    // Reset the instrument
    fg.WriteString("*RST;*CLS", true);
    // Wait for reset to complete
    fg.WriteString("*OPC?", true);
    msg = fg.ReadString();
    f = f * 1000000;
    //calculate number of cycles
    ncycles = ((df / 100) * (prf * (10 ^ -3)) * (f * (10 ^ 6)));
    //prepare and send the string command about frequency
    fstringpulsed = "frequency " + Convert.ToString(f);
    fg.WriteString(fstringpulsed, true);
    //prepare strings for sending them to the generator
    Vstring = "VOLTage " + Convert.ToString(v) + "E-3";
    fg.WriteString(Vstring, true);
    burststringperiod = "BURSt:INTernal:PERiod " +
    Convert.ToString(Math.Abs(prf * (10 ^ -3)));
    fg.WriteString(burststringperiod, true);
    fstringpulsed = "BURSt:NCYCles " +
    Convert.ToString(Math.Abs(ncycles));
    fg.WriteString(fstringpulsed, true);
    BurstStringON = "BURSt:STATe " + "ON";
    fg.WriteString(BurstStringON, true);
    PowerStringON = "OUTPut " + "ON";
    fg.WriteString(PowerStringON, true);
    //close connection
    fg.IO.Close();
}
catch (Exception e)
{
    MessageBox.Show(e.Message + "\nin function: OpenPort",
    "VISACom");
}
}

private void turnOFFGenerator(int burst)
{
    string addr = null;
    string OFFstring = null, msg = null; ;
    try
    {
        //create the formatted io object
        FormattedIO488 fg = new FormattedIO488();
        //create the resource manager
        ResourceManager mgr = new ResourceManager();
        // For USB address
        addr = txtagilentvisaID.Text;
    }
}

```

```

// Open communication
fg.IO = (IMessage)mgr.Open(addr, AccessMode.NO_LOCK, 2000, "");
//writing strings to the generator
// Reset the instrument
fg.WriteString("*RST;*CLS", true);
// Wait for reset to complete
fg.WriteString("*OPC?", true);
msg = fg.ReadString();
//prepare the string for writing
OFFstring = "OUTPut OFF";
//write the strings to the generator
fg.WriteString(OFFstring, true);
if (burst == 1) //turn off burst function in case of pulse signal
{
    fg.WriteString("BURSt:StAte OFF", true);
    addCommandToHistoryList("Continious Signal with Agilent: " +
        "Voltage (mV): " + txtvoltage.Text + " Frequency (MHz): " +
        txtfrequency.Text + " Duty Factor (%): "+ txttdutyfactor.Text +
        " Pulsed Rep Period (ms): " + txtpulserepfreq.Text + " On Time
        (s): " + txtontimepulsed.Text);
    addCommandToHistoryList("Pulsed Signal with Agilent: Turn
        OFF");
}
else
{
    addCommandToHistoryList("Continious Signal with Agilent: " +
        "Voltage (mV): " + txtvoltage.Text + " Frequency (MHz): " +
        txtfrequency.Text + " On Time (s): " +
        txtontimecontinious.Text );
    addCommandToHistoryList("Continious Signal with Agilent: Turn
        OFF");
}

counter = 0;
timergeneratorC.Enabled = false;
timergeneratorC.Stop();
timergeneratorP.Enabled = false;
timergeneratorP.Stop();
}
catch (Exception e)
{
    MessageBox.Show(e.Message + "\nin function: OpenPort",
        "VISACom");
}
}
private void btnpoweroncont_Click(object sender, EventArgs e)
{
    counter = 0;
    turnONContinious(Convert.ToInt32(txtfrequency.Text),
        Convert.ToInt32(txtvoltage.Text));
    //start timer
    timergeneratorC.Enabled = true;
    timergeneratorC.Start();
}
private void btnpoweroffcont_Click(object sender, EventArgs e)
{
    //stop timer
    timergeneratorC.Enabled = false;
    timergeneratorC.Stop();
    //stop generator and continuous signal
    turnOFFGenerator(0);
}
}

```

```

private void btnpoweroffpulsed_Click(object sender, EventArgs e)
{
    //stop timer
    timergeneratorP.Enabled = false;
    timergeneratorP.Stop();
    //stop generator and pulse signal
    turnOFFGenerator(1);
}
//function timer for continuous signal
private void timergeneratorC_Tick(object sender, EventArgs e)
{
    counter = counter + 1;
    if (Convert.ToInt32(txtontimecontinious.Text) == counter)
    {
        counter = 0;
        turnOFFGenerator(0); //stop generator and cont signal
    }
}
//function timer for pulse signal
private void timergeneratorP_Tick(object sender, EventArgs e)
{
    counter = counter + 1;
    if (Convert.ToInt32(txtontimepulsed.Text) == counter)
    {
        counter = 0;
        turnOFFGenerator(1); //stop generator and pulse signal
    }
}
}

```

2.3. C Sharp code that control the RF_1000 generator

The program is responsible for controlling the signal generator and the HIFU protocol. The following code controls a RF_1000 generator.

```

private void btnconnect_Click(object sender, EventArgs e)
{
    string msg = string.Empty;
    OpenPort();
    try
    {
        //RFG command starting the generator
        msg = "RFG";
        //first make sure the port is open
        //if it is not open then open it
        if (!(comPort.IsOpen == true))
            comPort.Open();
        //send the message to the port
        comPort.Write(msg + Delimiter);
        //clear msg string variable
        msg = string.Empty;
        if (comPort.IsOpen)
        {
            lblconnectionstatusRFG.Text = "RFG_1000 is connected.";
        }
    }
    else
    {
        lblconnectionstatusRFG.Text = "RFG_1000 is not connected.";
    }
    System.Threading.Thread.Sleep(100);
}

```

```

        msg = string.Empty;//clear msg variable string
        txtreaddatainput.Text = txtreaddatainput.Text +
        comPort.ReadExisting();
        comPort.DiscardInBuffer();
    }
    catch (Exception ex)
    {
        MessageBox.Show(ex.Message);
        lblconnectionstatus.Text = "RFG_1000 is not connected.";
    }
}
public bool OpenPort()
{
    try
    {
        //first check if the port is already open
        //if its open then close it
        if (comPort.IsOpen == true)
            comPort.Close();
        //set the properties of our SerialPort Object
        comPort.BaudRate = int.Parse(_baudRate);    //BaudRate
        comPort.DataBits = int.Parse(_dataBits);    //DataBits
        comPort.StopBits = (StopBits)Enum.Parse(typeof(StopBits),
        _stopBits);//StopBits
        comPort.Parity = (Parity)Enum.Parse(typeof(Parity), _parity);
        //Parity
        comPort.PortName = _portName;    //PortName
        //now open the port
        comPort.Open();
        //display message
        //return true if the port is opened
        return true;
    }
    catch (Exception ex)
    {
        MessageBox.Show(ex.Message);
        return false; //return true if the port is not opened
    }
}
private void stopW()
{
    try
    {
        string msg = string.Empty;
        if (!comPort.IsOpen)
        {
            MessageBox.Show("Please open port!");
            return;
        }
        msg = "stop";//create stop command string
        comPort.Write(msg + Delimiter);//send stop command to
        generator via usb port
        System.Threading.Thread.Sleep(100);
        msg = string.Empty;//clear msg variable string
        txtreaddatainput.Text = txtreaddatainput.Text +
        comPort.ReadExisting();//read buffer and append it to listbox
        comPort.DiscardInBuffer();//clear the buffer
    }
    catch (Exception ex)
    {
        MessageBox.Show(ex.Message);
    }
}

```

```

}
private void btnoffcw_Click(object sender, EventArgs e)
{
    try
    {
        stopW();//stop the generator
        counter = 0; //clear the counter that is used by the timer
    }
    catch (Exception ex)
    {
        MessageBox.Show(ex.Message);
    }
}

private void btnonpw_Click(object sender, EventArgs e)
{
    try
    {
        string msg = string.Empty;
        //acquiring all the necessary parameters for the pulse signal
        voltage = int.Parse(txtvoltageRFG.Text);
        dutyfactor = int.Parse(txtdutyfactorRFG.Text);
        pulserepfreq = int.Parse(txtpulserepfreqRFG.Text);
        ontimepw = int.Parse(txtpwtineonRFG.Text);
        frequency = int.Parse(txtfrequencyRFG.Text);
        typeofsignal_RFG = false;
        //calculate the number of cycles for the next pulse signal
        ncycles = (ontimepw * 1000) / Math.Abs(pulserepfreq);
        //error controls to check if the calculated number of cycles
        //is acceptable from the RF_1000 generator
        if ((voltage >= 1) && (voltage <= 200))
        {
            if (ncycles > 65000)
            {
                MessageBox.Show("The Number of cycles is out of acceptable
range. \n The muximum
number of cycles for the current \n power level is 65000");
                return;
            }
        }
        else if ((voltage >= 201) && (voltage <= 500))
        {
            if (ncycles > 100)
            {
                MessageBox.Show("The Number of cycles is out of acceptable
range. \n The muximum number of cycles
for the current \n power level is 100");
                return; //exit function if ncycles is not acceptable
            }
            if(dutyfactor > 20)
            {
                MessageBox.Show("The Duty cycle is not acceptable. \n For
more than 200 Watts the muximum duty \n cycle is 20%");
                return;
            }
        }
        else if ((voltage >= 501) && (voltage <= 800))
        {
            if (ncycles > 50)
            {

```

```

        MessageBox.Show("The Number of cycles is out of acceptable
range. \n The maximum number of cycles for the current \n
power level is 50");
        return;
    }
    if (dutyfactor > 20)
    {
        MessageBox.Show("The Duty cycle is not acceptable. \n For
more than 200 Watts the maximum duty \n cycle is 20%");
        return;
    }
}
else if ((voltage >= 801) && (voltage <= 1000))
{
    if (ncycles > 20)
    {
        MessageBox.Show("The Number of cycles is out of
acceptable range. \n The maximum number of cycles for the
current \n power level is 20");
        return;
    }
    if (dutyfactor > 20)
    {
        MessageBox.Show("The Duty cycle is not acceptable. \n For
more than 200 Watts the maximum duty \n cycle is 20%");
        return;
    }
}
if (!comPort.IsOpen)
{
    MessageBox.Show("Please open port!");
    return;
}
//calculate frequency
frequency = frequency * 1000000;
msg = "set freq " + frequency.ToString();//create frequency
string
comPort.Write(msg + Delimiter);//send frequency to generator via
usb port
msg = string.Empty;//clear msg variable string
System.Threading.Thread.Sleep(100);
msg = string.Empty;//clear msg variable string
txtreaddatainput.Text = txtreaddatainput.Text +
comPort.ReadExisting();
msg = "set pwr " + voltage.ToString();//create power value
string
comPort.Write(msg + Delimiter);//send power value to generator
via usb port
System.Threading.Thread.Sleep(100);
msg = string.Empty;//clear msg variable string
txtreaddatainput.Text = txtreaddatainput.Text +
comPort.ReadExisting();
string sourceRes = GetLast(ncycles.ToString(), 2);//ge the last
two characters of the ncycles number
msg = "set mpn " + ((dutyfactor * pulserepfreq) / 100) + "ms, "
+ (Math.Abs(pulserepfreq - ((dutyfactor * pulserepfreq) / 100)))
+ "ms, " + ncycles + sourceRes + "";
comPort.Write(msg.Trim() + Delimiter);//send mpon to generator
via usb port
System.Threading.Thread.Sleep(100);
msg = string.Empty;//clear msg variable string

```

```

        txtreaddatainput.Text = txtreaddatainput.Text +
        comPort.ReadExisting();
        comPort.DiscardInBuffer();
        txtreaddatainput.AppendText("\n");
    }
    catch (Exception ex)
    {
        MessageBox.Show(ex.Message);
    }
}

private void btnoffpw_Click(object sender, EventArgs e)
{
    try
    {
        stopW(); //stop the generator
    }
    catch (Exception ex)
    {
        MessageBox.Show(ex.Message);
    }
}

private void btnmode_Click(object sender, EventArgs e)
{
    try
    {
        string msg = string.Empty; //local variable for store the string
        command temporally
        if (!comPort.IsOpen)
        {
            MessageBox.Show("Please open port");
            return;
        }
        msg = "run"; //run command for start transmitting
        comPort.Write(msg + Delimiter); //write run command to serial
        port
        msg = string.Empty; //empty msg variable string
        System.Threading.Thread.Sleep(100); //wait for serial port
        response
        txtreaddatainput.Text = txtreaddatainput.Text +
        comPort.ReadExisting(); //append to command list text box
        if (typeof(signal_RFG) == true)
        {
            timercw.Enabled = true;
        }
        else
        {
            timer.Enabled = true; //enable the timer
        }
        comPort.DiscardInBuffer(); //clear the buffer
    }
    catch (Exception ex) //catching the errors coming from the function
    {
        MessageBox.Show(ex.Message); //display the error on a message box
    }
}
}

```

2.4. C Sharp – Select Transducer

The following program was developed to open a spreadsheet file from Excel and display the details about a selected transducer from a list of serial numbers of a transducer list.

```
private void cmbselecttransducer_SelectedIndexChanged(object sender,
EventArgs e)
{
    //create an instance of Excel application
    Excel.Application xlApp = new Excel.Application();
    Excel.Workbook xlWorkbook = xlApp.Workbooks.Open(@" " +
    excelfilefullpath.Replace(" ", "")); //open the app using the pathname
    //assign data to sheet 1
    Excel._Worksheet xlWorksheet = xlWorkbook.Sheets[1];
    Excel.Range xlRange = xlWorksheet.UsedRange; //get the range of excel file
    int rowCount = xlRange.Rows.Count; //get the number of rows
    int colCount = xlRange.Columns.Count; //get the number of columns
    string specs = "";
    int myindex = 0;
    //get the selected index of the key field that is listed on the listbox
    myindex = cmbselecttransducer.SelectedIndex + 1;
    //nested loop for pass through rows and columns
    for (int i = 1; i <= rowCount; i++) //outer loop for row counter
    {
        if (i == myindex) //compare the current index with selected index
        {
            for (int j = 1; j <= colCount; j++) //inner loop for column count
            {
                //string concatenation of the selected row
                specs = specs + ", " + xlRange.Cells[i, j].Value.ToString();
            }
            txttransducerspecs.Text = specs; //display on the text box
            return; //stop the loops by exit the function
        }
    }
    xlWorkbook.Close(false, Type.Missing, Type.Missing); //close file
    xlApp.Quit(); //close the Excel application
    addCommandToHistoryList("Select a transducer "); //add to history
}
}
```

2.5. C Sharp code – Robot Movements

The following code was developed to control the movements of the 2D positioning device. The program moves the motors on forward and reverse direction. Also the program controls the accurate motion of the positioning device by acquiring feedback from the optical encoders.

```
//function to add or delete new DAQ devices using notepad. The program
recognise more than one devices
private void editDAQDevicesToolStripMenuItem_Click(object sender, EventArgs e)
{
    try
    {
        string adddevice;
        DialogResult result = openFileDialog.ShowDialog(); //open the dialog
        box
        if (result == DialogResult.OK) //check if the user press Ok
        {
```

```

        //temporary store the file to a variable
        adddevice = openFile.FileName.ToString();
        //display the file using notepad application
        System.Diagnostics.Process.Start("notepad.exe", adddevice);
    }
}
catch (Exception ex)//catch any errors during the execution of the try
block
{
    MessageBox.Show(ex.Message);//give the message in message box
}
}
//the function fills the combo box that list all the available DAQ devices
private void fill_ComboDeviceID()
{
    try
    {
        // Read each line of the file into a string array. Each element
        // of the array is one line of the file.
        string[] lines = System.IO.File.ReadAllLines(@"C:\DAQ_Device.txt");
        cmbdeviceid.Items.Clear();
        //write lines to the combobox
        foreach (string line in lines)
        {
            // add all lines from the text file to combobox.
            cmbdeviceid.Items.Add(line);
        }
    }
    catch (Exception ex)
    {
        MessageBox.Show(ex.Message);
    }
}
//button event used for checking the connection with NI DAQ
//The program can control more than one positioning devices of different
degrees of freedom
private void btnniconnect_Click(object sender, EventArgs e)
{
    Cursor.Current = Cursors.WaitCursor;
    try
    {
        using (Task digitalWriteTask = new Task())
        {
            //beta connection testing with NI DAQ
            deviceid = cmbdeviceid.Text;
            robottype = cmbrobotsection.Text;
            digitalWriteTask.DOChannels.CreateChannel(deviceid +
            "/Port0/line0:7", "",
            ChannelLineGrouping.OneChannelForAllLines);
            bool[] dataArray = new bool[8];
            dataArray[0] = true;
            dataArray[1] = true;
            dataArray[2] = true;
            dataArray[3] = true;
            dataArray[4] = true;
            dataArray[5] = true;
            dataArray[6] = true;
            dataArray[7] = true;
            DigitalSingleChannelWriter writer = new
            DigitalSingleChannelWriter(digitalWriteTask.Stream);
            writer.WriteSingleSampleMultiLine(true, dataArray);
        }
    }
}

```

```

lbldaqstatus.Text = "NI DAQ is connected.";
lbldaqstatus.ForeColor = Color.Green;
//enable the button used for control the DAQ device
if (robottype == "2D_Robot (X - 0)")
{
    btnxfw.Enabled = true;
    btnxrev.Enabled = true;
    btnthitacw.Enabled = true;
    btnthitaccw.Enabled = true;
    btnmxfw.Enabled = true;
    btnmcrev.Enabled = true;
    btnmcw.Enabled = true;
    btnmccw.Enabled = true;
    btnstartgrid.Enabled = true;
    btnstopnow.Enabled = true;
    //cmbdeviceid.Enabled = false;
}
else if (robottype == "2D_Robot (X - Y)")
{
    btnxforward_3d.Enabled = true;
    btnxreverse_3d.Enabled = true;
    btnyforward_3d.Enabled = true;
    btnyreverse_3d.Enabled = true;
    btnstart3dgrid.Enabled = true;
}
else if (robottype == "3D_Robot (X - Y - Z)")
{
    btnxforward_3d.Enabled = true;
    btnxreverse_3d.Enabled = true;
    btnyforward_3d.Enabled = true;
    btnyreverse_3d.Enabled = true;
    btnzforward_3d.Enabled = true;
    btnzreverse_3d.Enabled = true;
    btnstart3dgrid.Enabled = true;
}
else if (robottype == "1D_Robot (X)")
{
    lbl1Dtitle.Visible = true;
    lbl1Dtitle1.Visible = true;
    txt1Drepeats.Visible = true;
    txt1Dseconds.Visible = true;
    btn1Dgrid.Visible = true;
}
addCommandToHistoryList("Successfull trial to connect with
DAQ Device, ");
}
}
catch (DaqException ex)
{
    MessageBox.Show(ex.Message);
    lbldaqstatus.Text = "NI DAQ is not connected.";
    lbldaqstatus.ForeColor = Color.Red;
    addCommandToHistoryList("Unsuccessfull trial to connect with
DAQ Device, ");
}
finally
{
    Cursor.Current = Cursors.Default;
}
}

```

```

private void btnxfw_Click(object sender, EventArgs e)
{
    double mm = 0;//store the number of dots (line) required for completing
    the motion
    counter = 0;
    double availablespace = 0;
    //convert the millimeters in dot per inch and subtract the error
    constant (0.1)
    mm = Double.Parse(txtxfw.Text);
    availablespace = (110 - Convert.ToDouble(txtxposition.Text));
    if ((mm != 0) && (mm <= availablespace))
    {
        mm = ((mm - 0.1) / 25.4) * 500;//get the parameter in millimeters
        Cursor.Current = Cursors.WaitCursor;
        try//try block in order to catch errors if any without crashing the
        system
        {
            using (Task digitalWriteTask = new Task())//create digital writer
            task
            {
                //create a digital output channel by passing the correct
                paramtrs
                digitalWriteTask.DOChannels.CreateChannel(deviceid +
                "/Port0/line0:7", "",
                ChannellineGrouping.OneChannelForAllLines);
                //create an array of 8 boolean elements
                bool[] dataArray = new bool[8];
                //initialize the elements with the proper parameter
                //11011111
                dataArray[0] = true;
                dataArray[1] = true;
                dataArray[2] = false;//set the third element to false,
                because we need to move the robot fw
                dataArray[3] = true;
                dataArray[4] = true;
                dataArray[5] = true;
                dataArray[6] = true;
                dataArray[7] = true;
                //set the array to digital writer
                DigitalSingleChannelWriter writer = new
                DigitalSingleChannelWriter(digitalWriteTask.Stream);
                writer.WriteSingleSampleMultiLine(true, dataArray);
                //call the function edge counter value by passing two
                parameters, the number of lines covered and the direction
                //1 for forward direction
                getEdgeCounterValue(Convert.ToInt32(mm), 1);
            }
        }
        catch (DaqException ex)//catch the errors if any
        {
            MessageBox.Show(ex.Message);//display the errors in a msg box
        }
        finally//after completing the try block
        {
            Cursor.Current = Cursors.Default;//To return back the default
            behavior
        }
    }
    else
    {
        btnstopnow_Click(sender, e);//stop motors
    }
}

```

```

        MessageBox.Show("The number of millimetres can not be zero or
        more than 110 or \n there is no enough space to move. \n The
        available space is " + availablespace.ToString() + " mm", "Robot
        and Ultrasound Control Application", MessageBoxButtons.OK,
        MessageBoxIcon.Information);
    }
}

private void btnxrev_Click(object sender, EventArgs e)
{
    double mm = 0; //store the number of dots (line) required for completing
    the motion
    counter = 0;
    double availablespace = 0;
    //convert the millimeters in dot per inche and subtract the error
    constunt (0.1)
    mm = Double.Parse(txtxrev.Text);
    availablespace = (Convert.ToDouble(txtxposition.Text) - mm);
    if ((mm != 0) && ((availablespace >= 0)))
    {
        mm = ((mm - 0.1) / 25.4) * 500;
        Cursor.Current = Cursors.WaitCursor;
        try //try block in order to catch errors if any without crashing the system
        {
            using (Task digitalWriteTask = new Task())
            {
                //create a digital output channel by passing the correct parametrs
                digitalWriteTask.DOChannels.CreateChannel(deviceid +
                "/Port0/line0:7", "",
                ChannellineGrouping.OneChannelForAllLines);
                //create an array of 8 boolean elements
                bool[] dataArray = new bool[8];
                dataArray[0] = false;
                dataArray[1] = true;
                dataArray[2] = true;
                dataArray[3] = true; //set the fourth element to false,
                because we need to move the robot fw
                dataArray[4] = true;
                dataArray[5] = true;
                dataArray[6] = true;
                dataArray[7] = true;
                //set the array to digital writer
                DigitalSingleChannelWriter writer = new
                DigitalSingleChannelWriter(digitalWriteTask.Stream);
                writer.WriteSingleSampleMultiLine(true, dataArray);
                //call the function edge counter value by passing two
                parameters, the number of lines covered and the direction
                //0 for reverse direction
                getEdgeCounterValue(Convert.ToInt32(mm), 0);
            }
        }
        catch (DaqException ex)
        {
            MessageBox.Show(ex.Message);
        }
        finally
        {
            Cursor.Current = Cursors.Default;
        }
    }
    else
    {

```

```

        btnstopnow_Click(sender, e); //stop motors
        MessageBox.Show("The number of millimetres can not be zero or
more than 110 or \n there is no enough space to move. \n The
available space is " + availablespace.ToString() + " mm", "Robot
and Ultrasound Control Application", MessageBoxButtons.OK,
MessageBoxIcon.Information);
    }
}

private void btnthitacw_Click(object sender, EventArgs e)
{
    int edgccount = 0;
    int degress = 0;
    int availablespace = 0;
    degress = Int32.Parse(txtthitacw.Text); //get the parameter in degrees
    availablespace = 90 - Int32.Parse(txtthitaposition.Text);
    if ((degress != 0))
    {
        //in case of thita encoder the constant is variable
        if (degress >= 10)
        {
            edgccount = (int) (Math.Round((2500 * degress) / 360.0)) - 30;
        }
        else if (degress == 3)
        {
            edgccount = (int) Math.Round(((2500 * degress) / 360.0)) - 20;
        }
        else if (degress == 4)
        {
            edgccount = (int) Math.Round(((2500 * degress) / 360.0)) - 22;
        }
        else if (degress == 5)
        {
            edgccount = (int) Math.Round(((2500 * degress) / 360.0)) - 23;
        }
        else if (degress == 6)
        {
            edgccount = (int) Math.Round(((2500 * degress) / 360.0)) - 25;
        }
        else if (degress == 7)
        {
            edgccount = (int) Math.Round(((2500 * degress) / 360.0)) - 26;
        }
        else if (degress == 8)
        {
            edgccount = (int) Math.Round(((2500 * degress) / 360.0)) - 28;
        }
        else if (degress == 9)
        {
            edgccount = (int) Math.Round(((2500 * degress) / 360.0)) - 29;
        }
        else if ((degress == 1) || (degress == 2))
        {
            edgccount = (int) Math.Round(((2500 * degress) / 360.0));
        }
        counter = 0;
        Cursor.Current = Cursors.WaitCursor;
        try //try block for catching unexpected errors
        {
            using (Task digitalWriteTask = new Task())
            {

```

```

        digitalWriteTask.DOChannels.CreateChannel(deviceid +
        "/Port0/line0:7", "",
        ChannelLineGrouping.OneChannelForAllLines);
        //create an array of 8 boolean elements
        bool[] dataArray = new bool[8];
        dataArray[0] = true;
        dataArray[1] = true; //set the fourth element to false,
        because we need to move the robot cw
        dataArray[2] = false;
        dataArray[3] = true;
        dataArray[4] = true;
        dataArray[5] = true;
        dataArray[6] = true;
        dataArray[7] = true;
        //set the array to digital writer
        DigitalSingleChannelWriter writer = new
        DigitalSingleChannelWriter(digitalWriteTask.Stream);
        writer.WriteSingleSampleMultiLine(true, dataArray);
        //call the function edge counter value by passing two
        parameters, the number of lines covered and the direction
        //1 for cw direction
        getEdgeCounterValue(theta, edgecount, 1);
    }
}
catch (DaqException ex)
{
    MessageBox.Show(ex.Message);
}
finally
{
    Cursor.Current = Cursors.Default;
}
}
else
{
    MessageBox.Show("The number of degrees can not be zero
    degrees.", "Robot and Ultrasound Control Application",
    MessageBoxButtons.OK, MessageBoxIcon.Information);
}
}

private void btnthitaccw_Click(object sender, EventArgs e)
{
    int degress = 0, edgecount = 0;
    int availablespace = 0;
    degress = Int32.Parse(txtthitaccw.Text); //get the parameter in degrees
    availablespace = Int32.Parse(txtthitaposition.Text) - degress;
    if ((degress != 0))
    {
        //formula used to convert the given degrees into dots (lines)
        if (degress >= 10)
        {
            edgecount = (int)(Math.Round((2500 * degress) / 360.0)) - 30;
        }
        else if (degress == 3)
        {
            edgecount = (int)Math.Round(((2500 * degress) / 360.0)) - 20;
        }
        else if (degress == 4)
        {
            edgecount = (int)Math.Round(((2500 * degress) / 360.0)) - 22;
        }
    }
}

```

```

else if (degress == 5)
{
    edgecount = (int)Math.Round(((2500 * degress) / 360.0)) - 23;
}
else if (degress == 6)
{
    edgecount = (int)Math.Round(((2500 * degress) / 360.0)) - 25;
}
else if (degress == 7)
{
    edgecount = (int)Math.Round(((2500 * degress) / 360.0)) - 26;
}
else if (degress == 8)
{
    edgecount = (int)Math.Round(((2500 * degress) / 360.0)) - 28;
}
else if (degress == 9)
{
    edgecount = (int)Math.Round(((2500 * degress) / 360.0)) - 29;
}
else if ((degress == 1) || (degress == 2))
{
    edgecount = (int)Math.Round(((2500 * degress) / 360.0));
}
counter = 0;
Cursor.Current = Cursors.WaitCursor;
try//try block for catching unexpected errors
{
    using (Task digitalWriteTask = new Task())
    {
        //create a digital output channel by passing the correct parametrs
        digitalWriteTask.DOChannels.CreateChannel(deviceid +
        "/Port0/line0:7", "",
        ChannellineGrouping.OneChannelForAllLines);
        //create an array of 8 boolean elements
        bool[] dataArray = new bool[8];
        dataArray[0] = true;//set the fourth element to false,
        because we need to move the robot ccw
        dataArray[1] = true;
        dataArray[2] = true;
        dataArray[3] = false;
        dataArray[4] = true;
        dataArray[5] = true;
        dataArray[6] = true;
        dataArray[7] = true;
        //set the array to digital writer
        DigitalSingleChannelWriter writer = new
        DigitalSingleChannelWriter(digitalWriteTask.Stream);
        writer.WriteSingleSampleMultiLine(true, dataArray);
        //call the function edge counter value by passing two
        parameters, the number of lines covered and the direction
        //0 for ccw direction
        getEdgeCounterValuethita(edgecount, 0);
    }
}
catch (DaqException ex)
{
    MessageBox.Show(ex.Message);
}
finally
{
    Cursor.Current = Cursors.Default;
}

```

```

    }
}
else
{
    MessageBox.Show("The number of degrees can not be zero", "Robot and Ultrasound Control Application",
        MessageBoxButtons.OK, MessageBoxIcon.Information);
}
}

private void btnxthitaposition_Click(object sender, EventArgs e)
{
    //set initial robot position
    txtxposition.Text = "0";
    txtthitaposition.Text = "0";
    addCommandToHistoryList("Set Robot Initial Position to zero, ");
}

//get angular encoder value
private void getEdgeCounterValueTheta(int maxvaluetheta, int direction)
{
    Cursor.Current = Cursors.WaitCursor;
    try//try block for catching unnecessary errors
    {
        using (Task CounterReadTask = new Task())//create new Task and using it
        {
            deviceid = cmbdeviceid.Text;//store the selected the dev ID
            //create a counter read task by adding the parameters to the
            counter input channel
            CounterReadTask.CIChannels.CreateCountEdgesChannel(deviceid +
                "/ctr1", "", edgeType, Convert.ToInt64("0"),
                countDirection);//counter type and direction
            //set timing parameters to the counter reader task
            CounterReadTask.Timing.ConfigureSampleClock(deviceid + "/PFI3",
                Convert.ToDouble("100000.00"), SampleClockActiveEdge.Rising,
                SampleQuantityMode.FiniteSamples, Convert.ToInt32("100000"));
            runningTask = CounterReadTask;
            //create an instance of the counter reader configure above
            myCounterReader = new CounterReader(CounterReadTask.Stream);
            //initialize the variables to zero each time to call the function
            double data = 0;
            int currposition = 0;
            while (data < maxvaluetheta)//compare current value with required value
            {
                data = myCounterReader.ReadSingleSampleInt32();//getting an
                integer number of lines read so far during the motion
            }
            stopmotors();//stop the current motion
            //if block statement for choosing the correct direction of the
            motion and update the interface
            //1 for cw and 0 for ccw
            if (direction == 1)
            {
                currposition = Convert.ToInt32(txtthitaposition.Text) +
                    Convert.ToInt32(txtthitacw.Text);//calculate the current
                    position
                txtthitaposition.Text = currposition.ToString();//store the
                current position to the text box control
                addCommandToHistoryList("Clockwise rotation on 0 Axis " +
                    txtthitacw.Text + " degrees, ");
            }
        }
    }
}

```



```

        txtxposition.Text = Convert.ToString(currposition);//store
        the current position to the text box control
        addCommandToHistoryList("Forward movement on X Axis " +
        Convert.ToInt32(data) + " mm, ");
    }
    else
    {
        data = Convert.ToInt32((data * 25.4) / 500);
        currposition = Convert.ToInt32(txtxposition.Text) -
        data;//calculate the current position
        txtxposition.Text = Convert.ToString(currposition);//store
        the current position to the text box control
        addCommandToHistoryList("Reverse movement on X Axis " +
        Convert.ToInt32(data) + " mm, ");
    }
}
}
}
catch (DaqException ex)//catch any errors during the execution of the try block
{
    MessageBox.Show(ex.Message);//message after catching an error
}
finally
{
    Cursor.Current = Cursors.Default;
}
}
}

```

2.6. C Sharp code was developed for creating the command history

The following program add all commands that are executed by the program to a list box. The function is called at the end of the block statements of each function. Also, function to store, edit and retrieve commands are shown below.

```

//function to append commands into command history list
private void addCommandToHistoryList(string commandname)
{
    try
    {
        string format = "HH:mm:ss";//selected time format
        lstcommandhistory.Items.Add(commandname +
        DateTime.Now.ToString(format));//add command to listbox
    }
    catch (Exception ex)
    {
        MessageBox.Show(ex.ToString());//error message
    }
}

//function to append the commands list on a text file
private void writeCommandHistoryToTextFile(ListBox commandlist)
{
    try
    {
        //Open the File using new stream writer object
        System.IO.StreamWriter sw = new
        System.IO.StreamWriter(@"C:\MRgFUS_Command_History.txt", true,
        Encoding.UTF8);
        sw.Write(Environment.NewLine);//store the new line to stream
        writer
        //store the current data and time on the stream writer
    }
}

```

```

sw.Write(DateTime.Today + Environment.NewLine +
Environment.NewLine);
//Writeout all the elements on the command history listbox.
foreach (string item in commandlist.Items)
{
    //write the particular command on the stream writer object
    sw.Write(item + Environment.NewLine);
}
//close the file
sw.Close();
//inform us about saving of the commands
MessageBox.Show("The command history has been saved.", "Robot
and Ultrasound Control Application", MessageBoxButtons.OK,
MessageBoxIcon.Information);
}
catch (Exception e)
{
    Console.WriteLine("Exception: " + e.Message);
}
}

//function to retrieve the older commands for the text file
private void openCommandHistoryToolStripMenuItem_Click(object sender, EventArgs
e)
{
    try
    {
        string commandhistory;
        DialogResult result = openFileDialog.ShowDialog();//open the dialog box
        if (result == DialogResult.OK)//check if the user press Ok
        {
            //temporary store the commands on a variable
            commandhistory = openFileDialog.FileName.ToString();
            //display the commands using notepad application
            System.Diagnostics.Process.Start("notepad.exe", commandhistory);
        }
    }
    catch (Exception ex)//catch any errors during the execution of the try
        block
    {
        MessageBox.Show(ex.Message);//give the message in message box
    }
}
}

```

2.7.C Sharp code for Grid operation

The following program steers the robot to create two dimensional grid pattern. The program calls the signal generator function between the intermediate steps of the motion.

```

//button event for enable the grid operation
private void btnstartgrid_Click(object sender, EventArgs e)
{
    try
    {
        if (gbagilentgenerator.Enabled == true)
        {

```

```

//store the given parameters for the grid operation
double numofStepsx = Convert.ToInt32(txtnxgrid.Text);
double numofStepsthita = Convert.ToInt32(txtnthitagrid.Text);
double numofStepmmx = Convert.ToInt32(txtnxstep.Text);
double numofStepdegrees = Convert.ToInt32(txtnthitastep.Text);
if (numofStepsx != 0 || numofStepsthita != 0 || numofStepmmx !=
    0 || numofStepdegrees != 0)
{
    int timewait = 0;//wait for the generator to finished its
    operation
    int direction = 1;//motion direction
    int timewaitfornextsonication = 0;//time wait for next
    operation
    //set the values of motion duration
    txtxfw.Text = numofStepmmx.ToString();
    txtxrev.Text = numofStepmmx.ToString();
    txtthitacw.Text = numofStepdegrees.ToString();
    txtthitaccw.Text = numofStepdegrees.ToString();
    //neasted loop for perform grid operation
    for (int i = 0; i < numofStepsthita; i++)//external loop
    {
        if (i == 0)
        {
            //no action for thita for first column of the grid
        }
        else
        {
            btnthitacw_Click(sender, e);//call thita cw direction
            button event
        }
        for (int j = 0; j < numofStepsx; j++)//internal loop
        {
            if (cmbselectsignal.SelectedIndex == 0)
            {
                btnpoweroncont_Click(sender, e);
                //sleep the system and waiting the transducer to
                make the job done
                timewait = 1000 *
                Convert.ToInt32(txtontimecontinious.Text);
                System.Threading.Thread.Sleep(timewait);
                timewait = 0;
                //stop generator
                turnOFFGenerator(0);
                //waiting time for the next sonication
                timewaitfornextsonication = 1000 *
                Convert.ToInt32(txttimefornextsonication.Text);
                System.Threading.Thread.Sleep
                (timewaitfornextsonication);
            }
            else if (cmbselectsignal.SelectedIndex == 1)
            {
                btnpoweronpulsed_Click(sender, e);
                //sleep the system and waiting the
                transducer to make the job done
                timewait = 1000 *
                Convert.ToInt32(txtontimepulsed.Text);
                System.Threading.Thread.Sleep(timewait);
                timewait = 0;
                //stop generator
                turnOFFGenerator(1);
                System.Threading.Thread.Sleep(20000);
                //waiting time for the next sonication
            }
        }
    }
}

```

```

        timewaitfornextsonication = 1000 *
        Convert.ToInt32
        (txttimefornextsonication.Text);
        System.Threading.Thread.Sleep
        (timewaitfornextsonication);
    }
    else if (cmbselectsignal.SelectedIndex == 4)
    {
        //waiting time for the next sonication
        timewaitfornextsonication = 1000 *
        Convert.ToInt32
        (txttimefornextsonication.Text);
        System.Threading.Thread.Sleep
        (timewaitfornextsonication);
    }
    //even numbers for fw direction
    //odd numbers for rev direction
    if (direction % 2 != 0)
    {
        btnxfw_Click(sender, e); //call fw button event
    }
    else
    {
        btnxrev_Click(sender, e); //call rev button event
    }
}
direction += 1; //increase the steps
}
addCommandToHistoryList("Grid Operation: X number of steps " +
numOfStepsx + " with MM " + numOfStepmmx + " and 0 number of
steps " + numOfStepsthita + " with degrees " + numOfStepdegrees
+ ", ");
}
else
{
    MessageBox.Show("All the required parameters must be
filled.", "Robot and Ultrasound Control Application",
    MessageBoxButtons.OK, MessageBoxIcon.Information);
}
}
//.....Grid Operation using RFG_1000 generator
else if (gbrfg_1000.Enabled == true)
{
    //store the given parameters for the grid operation
    double numOfStepsx = Convert.ToInt32(txtnxgrid.Text);
    double numofStepsthita = Convert.ToInt32(txtnthitagrid.Text);
    double numofStepmmx = Convert.ToInt32(txtnxstep.Text);
    double numofStepdegrees = Convert.ToInt32(txtnthitastep.Text);
    if (numOfStepsx != 0 || numofStepsthita != 0 || numofStepmmx
    != 0 || numofStepdegrees != 0)
    {
        int timewait = 0; //wait for the generator to finished its
operation
        int direction = 1; //motion direction
        int timewaitfornextsonication = 0; //time wait for next
operation
        //set the values of motion duration
        txtxfw.Text = numofStepmmx.ToString();
        txtxrev.Text = numofStepmmx.ToString();
        txtthitacw.Text = numofStepdegrees.ToString();
        txtthitaccw.Text = numofStepdegrees.ToString();
        //nested loop for perform grid operation
    }
}

```

```

for (int i = 0; i < numOfStepsthita; i++)//external loop
{
    if (i == 0)
    {
        //no action for thita for first column of the grid
    }
    else
    {
        btnthitacw_Click(sender, e);//call thita cw
        direction button event
    }
    for (int j = 0; j < numOfStepsx; j++)//internal
    loop
    {
        if (cmbselectsignal.SelectedIndex == 2)
        {
            btnmode_Click(sender, e);
            //sleep the system and waiting the
            transducer to make the job done
            timewait = 1000 * Convert.ToInt32
            (txtcwtimeonRFG.Text);
            System.Threading.Thread.Sleep(timewait);
            timewait = 0;
            //stop generator
            stopW();
            //waiting time for the next sonication
            timewaitfornextsonication = 1000 *
            Convert.ToInt32
            (txttimefornextsonication.Text);
            System.Threading.Thread.Sleep
            (timewaitfornextsonication);
        }
        else if (cmbselectsignal.SelectedIndex == 3)
        {
            btnmode_Click(sender, e);
            //sleep the system and waiting the
            transducer to make the job done
            timewait = 1000 *
            Convert.ToInt32
            (txtpwtineonRFG.Text);
            System.Threading.Thread.Sleep(timewait);
            timewait = 0;
            //stop generator
            stopW();
            //waiting time for the next sonication
            timewaitfornextsonication = 1000*
            Convert.ToInt32
            (txttimefornextsonication.Text);
            System.Threading.Thread.Sleep
            (timewaitfornextsonication);
        }
        else if (cmbselectsignal.SelectedIndex == 4)
        {
            //waiting time for the next sonication
            timewaitfornextsonication = 1000 *
            Convert.ToInt32
            (txttimefornextsonication.Text);
            System.Threading.Thread.Sleep
            (timewaitfornextsonication);
        }
        //even numbers for fw direction
        //odd numbers for rev direction
    }
}

```

```

        if (direction % 2 != 0)
        {
            btnxfw_Click(sender, e); //call fw button event
        }
        else
        {
            btnxrev_Click(sender, e);
        }
        direction += 1; //increase the steps
    }
    addCommandToHistoryList("Grid Operation: X number of
steps " + numOfStepsx + " with MM " + numOfStepmmx +
" and  $\theta$  number of steps " + numOfStepsthita + " with
degress " + numOfStepdegrees + ", ");
}
else
{
    MessageBox.Show("All the required parameters must be
filled.", "Robot and Ultrasound Control
Application", MessageBoxButtons.OK,
MessageBoxIcon.Information);
}
}
}
catch (Exception ex)
{
    MessageBox.Show(ex.Message);
}
}
}

```

2.8. C Sharp code for temperature reading using thermocouple

The following program gather temperature measurements of the focal point of a HIFU transducer using copper wire that is placed inside the coupling mechanism. The program represents the temperature of the user given intervals and creates real time graph chart that can be saved on a selected directory. The temperature readings can be saved on a text file in csv format and can be opened using spreadsheet application. Also, the current average temperatures is demonstrated on the program user interface.

```

private void button4_Click(object sender, EventArgs e)
{
    Cursor.Current = Cursors.WaitCursor;
    try
    {
        //the following task is used for testing the NI DAQ connection
        using (Task temperatureTask = new Task()) //create new task for
        reading the voltage from the NI DAQ
        {
            deviceid = cmbdeviceid.Text; //get the device id
            AIChannel myAIChannel; //initialise an analogue channel
            //store a virtual analogue channel by passing the appropriate
            parameters
            myAIChannel =
            temperatureTask.AIChannels.CreateThermocoupleChannel
            (deviceid + "/ai0", "Temperature", 0, 100,
            AIThermocoupleType.J, AITemperatureUnits.DegreesC, 25);
        }
    }
}

```

```

        //create an analogue channel reader
        AnalogSingleChannelReader reader = new
        AnalogSingleChannelReader(temperatureTask.Stream);
        lbldaqstatus.Text = "NI DAQ is connected.");//update the
        status label
        lbldaqstatus.ForeColor = Color.Green;//change the font colour
        to green
        //enable the button used for control the DAQ device
        btngettemperature.Enabled = true;//enable the get temperature
        button
        btnstopreading.Enabled = true;//enable the stop reading
        button
    }
}
catch (DaqException ex)
{
    MessageBox.Show(ex.Message);
    lbldaqstatus.Text = "NI DAQ is not connected.");//update the
    status label
    lbldaqstatus.ForeColor = Color.Red;//change the font colour to
    red
}
finally
{
    Cursor.Current = Cursors.Default;
}
}

private void button2_Click(object sender, EventArgs e)
{
    Close();//close form
}

private void btngettemperature_Click(object sender, EventArgs e)
{
    tempInterval.Interval = Convert.ToInt32(txttimerinterval.Text) * 1000;
    //convert the selected interval into milliseconds
    chart1.ChartAreas[0].AxisX.MajorGrid.Interval =
    Convert.ToInt32(txttimerinterval.Text); //set major grid lines
    interval according to the given interval
    tempInterval.Enabled = true;//enable timer
    tempInterval.Start();//start timer
}

private void Form2_Load(object sender, EventArgs e)
{
    chart1.Series["Series1"].LegendText = "Temperature";//set the legend
    text property
    chart1.Series["Series1"].ChartType =
    System.Windows.Forms.DataVisualization.Charting.SeriesChartType.Line;
    //set the chart type into line
}

private void tempInterval_Tick(object sender, EventArgs e)
{
    Cursor.Current = Cursors.WaitCursor;
    try
    {
        //create analogue input task
        using (Task analogInTask = new Task())
        {
            //initialize an analogue input channel

```

```

    AICannel myAICannel;
    //create a voltage analogue input channel by passing the
    appropriate parameters
    //the cable is connected to AI1 pin
    //The name of the channel is Temperature (can be any)
    //capture values from 0 to 10
    //set voltage units to Volts
    myAICannel = analogInTask.AIChannels.
    CreateVoltageChannel(deviceid + "/ai1", "Temperature",
    AITerminalConfiguration.Differential, 0, 10,
    AIVoltageUnits.Volts);
    //create new analogue channel reader by passing the analogue
    input stream
    AnalogSingleChannelReader reader = new
    AnalogSingleChannelReader(analogInTask.Stream);
    //1000 Volts for one degree C
    double analogDataIn = 1000 * reader.ReadSingleSample();
    //Temperature formatted into two decimal places in string format
    txtinputtemperature.Text = analogDataIn.ToString("0.00");
    //keep the current sum
    tempsum = tempsum + Convert.ToDouble(txtinputtemperature.Text);
    //keep the current sample
    txttimeperiod.Text = Convert.ToString
    (Convert.ToInt32(txttimeperiod.Text) + 1);
    //update the chart graph by passing time period to X axis values
    and temperature to Y axis values
    chart1.Series["Series1"].Points.AddXY
    (Convert.ToDouble(txttimeperiod.Text),
    Convert.ToDouble(txtinputtemperature.Text));
    //calculate the average temperature
    txttemperatureaver.Text = Convert.ToString(tempsum /
    Convert.ToDouble(txttimeperiod.Text));
    //create new string line with the gathered data if the variable
    saveON is set to true
    if (saveON == true)
    {
        string newLine = string.Format("{0},{1}{2}",
        txttimeperiod.Text, txtinputtemperature.Text,
        Environment.NewLine);
        csv.Append(newLine);
    }
}
}
catch (DaqException ex)
{
    MessageBox.Show(ex.Message); //DAQ library error message
}
finally
{
    Cursor.Current = Cursors.Default;
}
}

private void btnstopreading_Click(object sender, EventArgs e)
{
    tempInterval.Enabled = false; //set timer to false
    tempInterval.Stop(); //stop timer
    tempsum = 0; //set the tempsum variable to 0 in order to calculate the
    current sum again if it is needed
    //store the csv line in string format to text file
    if (saveON == true)
    {

```

```

        //append csv object to the text file
        System.IO.File.AppendAllText(filefullpath, csv.ToString());
        button5.Enabled = true;
    }
}

private void button3_Click(object sender, EventArgs e)
{
    try
    {
        DialogResult result = fbDialog.ShowDialog();//open the dialog box
        if (result == DialogResult.OK)//check if the user press Ok
        {
            filefullpath = fbDialog.SelectedPath.ToString();//get the
            selected directory
            filefullpath = filefullpath + @"\\" + txtfilename.Text;//create
            the full file path name
            button5.Enabled = true;//enable the save button
        }
    }
    catch (Exception ex)//catch any errors during the execution of the try
    block
    {
        MessageBox.Show(ex.Message);//give the message in message box
    }
}

private void button1_Click(object sender, EventArgs e)
{
    try
    {
        DialogResult result = fbDialog.ShowDialog();//open the dialog box
        if (result == DialogResult.OK)//check if the user press Ok
        {
            filefullpath = fbDialog.SelectedPath.ToString();
            filefullpath = filefullpath + @"\\" + txtimagefilename.Text;
            chart1.SaveImage(filefullpath,
            System.Drawing.Imaging.ImageFormat.Jpeg);
        }
    }
    catch (Exception ex)//catch any errors during the execution of the try block
    {
        MessageBox.Show(ex.Message);//give the message in message box
    }
}

private void button5_Click(object sender, EventArgs e)
{
    saveON = true;
    button5.Enabled = false;
}

private void btncleargraph_Click(object sender, EventArgs e)
{
    //confirmation message in case of press the button accedentially
    if (MessageBox.Show("Are you sure you want to clear the graph data?",
        "Temperature Readings", MessageBoxButtons.YesNo) ==
        System.Windows.Forms.DialogResult.Yes)
    {
        chart1.DataBindings.Clear();//clear the chart graph
    }
}

```

```
}
```

2.9. C Sharp code for controlling the MRI Camera

The following program controls an MRI compatible camera. The program filters all the video input devices that are connected to the computer. The program can capture video and images.

```
private string filenameandpath = "";
// Capture using the first video
// and audio devices available
private static Filters f = new Filters();
Capture cap = new Capture(f.VideoInputDevices[0], null);
public frmcameraapp()
{
    InitializeComponent();
}

private void btnconnect_Click(object sender, EventArgs e)
{
    try
    {
        if (cap.PreviewWindow != null)
        {
            btnconnect.Text = "Start Camera"; //change the text property
            // Stop preview
            cap.PreviewWindow = null; //clear the preview window object
        }
        else
        {
            btnconnect.Text = "Stop Camera"; //change the text property
            // Start preview
            cap.PreviewWindow = picture_Box; //send the capture video to
            picture box
        }
    }
    catch (Exception ex)
    {
        MessageBox.Show(ex.ToString());
    }
}

private void btnselectforlder_Click(object sender, EventArgs e)
{
    try
    {
        DialogResult result = folderBrowserDialog.ShowDialog();//open the
        dialog box
        if (result == DialogResult.OK)//check if the user press Ok
        {
            //create the file name and path of the destination directory
            filenameandpath = folderBrowserDialog.SelectedPath.ToString();
            filenameandpath = filenameandpath + txtfilename.Text;
            cap.FileName = filenameandpath;//fill the filename method of the
            object cap
        }
    }
    catch (Exception ex)
    {

```

```

        MessageBox.Show(ex.ToString());
    }
}

private void btnstartvideo_Click(object sender, EventArgs e)
{
    try
    {
        cap.Start(); //start recording video by calling the method start
    }
    catch (Exception ex)
    {
        MessageBox.Show(ex.ToString());
    }
}

private void btnstopvideo_Click(object sender, EventArgs e)
{
    try
    {
        cap.Stop();//stop recording by calling the stop method
    }
    catch (Exception ex)
    {
        MessageBox.Show(ex.ToString());
    }
}

private void btntakepicture_Click(object sender, EventArgs e)
{
    try
    {
        using (Bitmap bmp = new Bitmap(cap.PreviewWindow.Width,
            cap.PreviewWindow.Width))
        {
            //create a bit map image from the preview window method of the
            //cap object
            cap.PreviewWindow.DrawToBitmap(bmp, new Rectangle(0, 0,
                bmp.Width, bmp.Height));
            picture_Box_takepicture.Image = bmp; //assign the image
            //property of the picture box the bit map
            bmp.Save(@" " + filenameandpath, ImageFormat.Bmp);//save the
            //bitmap on the selected directory
            MessageBox.Show("Saved Successfully.....");
        }
    }
    catch (Exception ex)
    {
        MessageBox.Show(ex.ToString());
    }
}
}

```

2.10. MATLAB and C Sharp Code – Control of MRI images

The following program opens ‘dicom’ images from a selected directory. The file names is listed on a text file. The images are displayed in a picture box. C Sharp code inports the coordinates from the dicom viewer.

```

DicomImageViewer.MainForm ap = new DicomImageViewer.MainForm();//global
instance of the dicom viewer
//the function imports coordinates X and Y form the MRI images
private void importDimentionsToolStripMenuItem_Click(object sender, EventArgs
e)
{
    double xdistance = 0;
    double ydistance = 0;

    try
    {
        //get the distance x and y from the dicom viewer object
        xdistance = double.Parse(ap.lbldistanceX .Text);
        ydistance = double.Parse(ap.lbldistanceY.Text);
        //display the coordinates on the proper interface x and theta
        stages
        if (ydistance < 0)
        {
            txtxfw.Text = Math.Abs(Math.Round(ydistance)).ToString();
        }
        else
        {
            txtxrev.Text = Math.Abs(Math.Round(ydistance)).ToString();
        }
        if (xdistance > 0)
        {
            txtthitacw.Text = Math.Abs(Math.Round(xdistance)).ToString();
        }
        else
        {
            txtthitaccw.Text = Math.Abs(Math.Round(xdistance)).ToString();
        }
    }
    catch (IOException ex)
    {
        MessageBox.Show(ex.ToString());
    }
}
}

```

```

function varargout = listofimages_Callback(h, eventdata, handles)
% hObject   handle to listofimages (see GCBO)
% eventdata reserved - to be defined in a future version of MATLAB
% handles   structure with handles and user data (see GUIDATA)

```

```

% Hints: contents = get(hObject,'String') returns listofimages contents as cell array
%         contents{get(hObject,'Value')} returns selected item from listofimages

```

```

try
    scrsz = get(0,'ScreenSize');
    counterlmg = 0;
    counterlmg = str2double(get(handles.countimageclicks, 'String'));
    counterlmg = counterlmg + 1;
    set(handles.countimageclicks, 'String', counterlmg);
    numberoffigures = get(handles.numoffigures, 'String');
    initx = 25;
    if counterlmg == 1
        inity = scrsz(4) - 250;
        set(handles.ypositionimage, 'String', inity);
    end
    x = get(handles.xpositionimage, 'String');
    y = get(handles.ypositionimage, 'String');

```

```

folder = get(handles.currdirectory, 'String');
if mod(str2double(get(handles.countimageclicks, 'String')), str2double(numberoffigures)
+ 1) == 0
    %set(handles.ypositionimage, 'String', inity);
    set(handles.xpositionimage, 'String', initx);
    x = get(handles.xpositionimage, 'String');
    y = get(handles.ypositionimage, 'String');
    index_selected = get(handles.listofimages, 'Value');
    list = get(handles.listofimages, 'String');
    item_selected = list{index_selected}; % Convert from cell array to string
    figure('position', [str2double(x), str2double(y) - 250,300,150]);%left, bottom, width,
height
    S = strcat(strcat(folder, '\'), item_selected);
    I = dicomread(S); % Reads image data
    imagesc(I); %displays image in colour map in outter frame
    colormap(gray); % Converts to gray scale
    axis off;
    set(handles.ypositionimage, 'String', (str2double(y)-250));
    set(handles.xpositionimage, 'String', (str2double(x)));
else
    index_selected = get(handles.listofimages, 'Value');
    list = get(handles.listofimages, 'String');
    item_selected = list{index_selected}; % Convert from cell array to string
    figure('position', [str2double(x), str2double(y),300,150]);%left, bottom, width, height
    S = strcat(strcat(folder, '\'), item_selected);
    I = dicomread(S); % Reads image data
    imagesc(I); %displays image in colour map in outter frame
    colormap(gray); % Converts to gray scale
    axis off;
    set(handles.ypositionimage, 'String', (str2double(y)));
    set(handles.xpositionimage, 'String', (str2double(x) + 325));
end
%Put action in history listbox
strdate = datestr(now, 'mmmm dd, yyyy HH.MM.SS.FFF AM');%get current date and
time and convert it to string format
str_part = strcat('Open MRI Images in figure ', strdate);
old_str = get(handles.historylist, 'String');
new_str = strvcats(old_str, str_part);
set(handles.historylist, 'String', new_str);
guidata(hObject,handles);
catch err
end

% -----
% Read the current directory and sort the names, and displays
% files in the listbox.
% -----
function load_listbox(dir_path,handles)

%Move to the selected directory
cd (dir_path);

%Gets name, date, bytes and isdir of the current directory.
% perharps date is usefull for date sorting.
dir_struct = dir(dir_path);

% Sorts name, First dot, then two dots, then numbers and then
% alphabetically.
[sorted_names,sorted_index] = sortrows({dir_struct.name});

```

```

% Stores file names in handles.
handles.file_names = sorted_names;

%If directory stores a 1, if a file it stores a 0.
handles.is_dir = [dir_struct.isdir];

% Stores index in handle
handles.sorted_index = [sorted_index];

%Saves handles data
guidata(handles.figure1,handles)

%Puts file names in the listbox
set(handles.listofimages,'String',handles.file_names,...
    'Value',1)

% Outputs the current directory to the text
%Pwd prints or displays working directory
set(handles.currdirectory,'String',pwd);

% --- Executes on slider movement. Show images one by one
function slider7_Callback(hObject, eventdata, handles)
% hObject    handle to slider7 (see GCBO)
% eventdata  reserved - to be defined in a future version of MATLAB
% handles    structure with handles and user data (see GUIDATA)

% Hints: get(hObject,'Value') returns position of slider
%       get(hObject,'Min') and get(hObject,'Max') to determine range of slider

%Put action in history listbox
strdate = datestr(now, 'mmm dd, yyyy HH.MM.SS.FF AM');%get current date and time and
convert it to string format
str_part = strcat('Load MRI Image ', strdate);
old_str = get(handles.historylist, 'String');
new_str = strvcats(old_str, str_part);
set(handles.historylist,'String', new_str);
%load image
file_list = get(handles.listofimages,'String');
guidata(hObject, handles);
list = get(handles.listofimages,'String');
indexvalue = get(hObject, 'Value');
S = char(strcat(strcat(get(handles.currdirectory, 'String'), '\'), list(int8(indexvalue))));
set(handles.dicomfilename, 'String', list(int8(indexvalue)));
colormap gray(256); % Converts to gray scale
I = dicomread(S); % Reads image data
imagesc(I, 'Parent', handles.mainview); %displays image in colour map in outer frame
axis off
figs = get(0, 'Children');
close(figs);

% --- Executes on button press in startshow.
function startshow_Callback(hObject, eventdata, handles)
% hObject    handle to startshow (see GCBO)
% eventdata  reserved - to be defined in a future version of MATLAB
% handles    structure with handles and user data (see GUIDATA)
try

```

```

%Put action in history listbox
strdate = datestr(now, 'mmmm dd, yyyy HH.MM.SS.FFF AM');%get current date and time and
convert it to string format
str_part = strcat('DICOM Viewer slide show ', strdate);
old_str = get(handles.historylist, 'String');
new_str = strvcats(old_str, str_part);
set(handles.historylist,'String', new_str);

dir_struct = dir(get(handles.currdirectory, 'String'));
set(handles.slider7, 'Enable', 'on');

% Sorts name, First dot, then two dots, then numbers and then
% alphabetically.
[sorted_names,sorted_index] = sortrows({dir_struct.name});
% Stores file names in handles.
file_names = sorted_names;

file_list = get(handles.listofimages,'String');

%Get number of total files in the directory
nimage=length(file_list);
guidata(hObject, handles);
list = get(handles.listofimages,'String');
set(handles.slider7, 'Value', 3);
set(handles.slider7, 'Max', nimage);
set(handles.slider7, 'Min', 3);
% Display all images
for k=3:nimage
    if k < nimage - 3
        S = char(strcat(strcat(get(handles.currdirectory, 'String'), '\'), list(k)));
        colormap gray(256); % Converts to gray scale
        I = dicomread(S); % Reads image data
        imagesc(I, 'Parent', handles.thumbnail1); %displays image in colour map in outer
frame
        axis off
        S = char(strcat(strcat(get(handles.currdirectory, 'String'), '\'), list(k+1)));
        colormap(gray); % Converts to gray scale
        I = dicomread(S); % Reads image data
        imagesc(I, 'Parent', handles.thumbnail2); %displays image in colour map in outer
frame
        axis off
        S = char(strcat(strcat(get(handles.currdirectory, 'String'), '\'), list(k+2)));
        colormap gray(256); % Converts to gray scale
        I = dicomread(S); % Reads image data
        imagesc(I, 'Parent', handles.thumbnail3); %displays image in colour map in outer
frame
        axis off
    else
        S = char(strcat(strcat(get(handles.currdirectory, 'String'), '\'), list(k)));
        colormap gray(256); % Converts to gray scale
        I = dicomread(S); % Reads image data
        imagesc(I, 'Parent', handles.thumbnail1); %displays image in colour map in outer
frame
        axis off
    end

    S = char(strcat(strcat(get(handles.currdirectory, 'String'), '\'), list(k)));
    colormap gray(256); % Converts to gray scale

```

```

    I = dicomread(S); % Reads image data
    imagesc(I, 'Parent', handles.thumbnail2); %displays image in colour map in outer
frame
    axis off;
    S = char(strcat(strcat(get(handles.currdirectory, 'String'), '\'), list(k)));
    colormap gray(256); % Converts to gray scale
    I = dicomread(S); % Reads image data
    imagesc(I, 'Parent', handles.thumbnail3); %displays image in colour map in outer
frame
    axis off;
    figs = get(0, 'Children');
    close(figs);
end
for n = 1:200000000
end
end
end

catch err

end

```

2.11. Visual Basic Code – Patient Data Form

The following program stores, retrieves, edits and search data from an access database file. The program manipulates information about a patient.

```

Imports System.Data.SqlClient 'import sql client library
Imports System.Data.OleDb 'import ole db library
Public Class frmpatientdata
'declare the variables needed to implement the application
'the following variables instantiate the proper class in each case
Dim myCommand As New OleDbCommand
Dim myAdapter As New OleDbDataAdapter
Dim myAdaptersub As New OleDbDataAdapter
Dim myAdaptersubfill As New OleDbDataAdapter
Dim myAdapteditfill As New OleDbDataAdapter
Dim myData As New DataTable
Dim myDataSub As New DataTable
Dim myDataedit As New DataTable
Dim myDataSubfill As New DataTable
Dim qry As String
Dim myconnectionstring As String
'Public conn As New SqlConnection
Dim Conn As OleDbConnection = New OleDbConnection()

Private Sub Button1_Click(ByVal sender As System.Object, ByVal e As
System.EventArgs) Handles Button1.Click
    Me.Close() 'close form
End Sub

Private Sub frmpatientdata_Load(ByVal sender As System.Object, ByVal e As
System.EventArgs) Handles MyBase.Load
    'store the necessary provider string to variable mycommand

```

```

myconnectionstring = "Provider=Microsoft.Jet.OLEDB.4.0;Data
Source=patientdata.mdb;User Id=admin;Password="
Conn.ConnectionString = myconnectionstring 'assign the provider proper
connection attribute
Try
    conn.Open() 'open the connection
    refreshData() 'call refresh data function to fill the binding source
Catch exerror As SqlException
    MsgBox("There was an error reading from the database: " &
        exerror.Message)
    Me.Close()
End Try
End Sub

'refresh data source
Private Sub refreshData()
    Try
        BindingSource1.DataSource = Nothing
        BindingNavigator1.BindingSource = Nothing
        qry = "select * from patient" 'select all records from table patient
        myCommand.Connection = Conn
        myCommand.CommandText = qry
        myAdapter.SelectCommand = myCommand
        myAdapter.Fill(myData)
        BindingSource1.DataSource = myData
        BindingNavigator1.BindingSource = BindingSource1
        'assign the data to proper control
        Me.IDTextBox.DataBindings.Add(New Binding("Text", Me.BindingSource1,
            "id", True))
        Me.FirstnameTextBox.DataBindings.Add(New Binding("Text",
            Me.BindingSource1, "firstname", True))
        Me.LastnameTextBox.DataBindings.Add(New Binding("Text",
            Me.BindingSource1, "lastname", True))
        Me.AddressTextBox.DataBindings.Add(New Binding("Text",
            Me.BindingSource1, "address", True))
        Me.CityTextBox.DataBindings.Add(New Binding("Text", Me.BindingSource1,
            "city", True))
        Me.CountryTextBox.DataBindings.Add(New Binding("Text",
            Me.BindingSource1, "country", True))
        Me.PhoneTextBox.DataBindings.Add(New Binding("Text", Me.BindingSource1,
            "phone", True))
        Me.AgeTextBox.DataBindings.Add(New Binding("Text", Me.BindingSource1,
            "age", True))
        'fill subform
        filtersubform(Me.IDTextBox.Text)
    Catch ex As Exception
        'MsgBox(ex.ToString)
    End Try
End Sub

Private Sub filtersubform(ByVal id As String)
    Try
        'fill subform
        myDatasub.Clear()
        'sql command to select all the operations according to the selected
        patient
        qry = "select (historicaldata) as 'Operation ID', (id) as 'Patient ID',
            (operationdate) as 'Date Of Operation', (discription) as 'Discription'
            from patienthistory where patienthistory.id = '" + id + "'"
        myCommand.Connection = Conn
        myCommand.CommandText = qry
    
```

```

        myAdaptersub.SelectCommand = myCommand
        myAdaptersub.Fill(myDatasub)
        Me.PatienthistoryDataGridView.DataSource = myDatasub
    Catch ex As Exception
        MsgBox(ex.ToString)
    End Try
End Sub
'button next help us to move one record next
Private Sub btnnext_Click(ByVal sender As System.Object, ByVal e As
    System.EventArgs) Handles btnnext.Click
    Try
        If BindingSource1.Position + 1 < BindingSource1.Count Then
            BindingSource1.MoveNext()
            filtersubform(Me.IDTextBox.Text)
        Else
            BindingSource1.MoveFirst()
        End If
        Me.Invalidate()
    Catch ex As Exception

    End Try
End Sub

Private Sub btnprevious_Click(ByVal sender As System.Object, ByVal e As
    System.EventArgs) Handles btnprevious.Click
    Try
        BindingSource1.MovePrevious()
        filtersubform(Me.IDTextBox.Text)
        Me.Invalidate()
    Catch ex As Exception

    End Try
End Sub

Private Sub btnfirst_Click(ByVal sender As System.Object, ByVal e As
    System.EventArgs) Handles btnfirst.Click
    Try
        BindingSource1.MoveFirst()
        filtersubform(Me.IDTextBox.Text)
    Catch ex As Exception

    End Try
End Sub

Private Sub btnlast_Click(ByVal sender As System.Object, ByVal e As
    System.EventArgs) Handles btnlast.Click
    Try
        BindingSource1.MoveLast()
        filtersubform(Me.IDTextBox.Text)
    Catch ex As Exception

    End Try
End Sub
'add new button, clear all the text boxes
Private Sub btnaddnew_Click(ByVal sender As System.Object, ByVal e As
    System.EventArgs) Handles btnaddnew.Click
    Try
        Me.IDTextBox.Text = ""
        Me.FirstnameTextBox.Text = ""
        Me.LastnameTextBox.Text = ""
        Me.AddressTextBox.Text = ""
        Me.CityTextBox.Text = ""
    End Try
End Sub

```

```

        Me.CountryTextBox.Text = ""
        Me.PhoneTextBox.Text = ""
        Me.AgeTextBox.Text = ""
        Me.IDTextBox.Focus()
    Catch ex As Exception

    End Try
End Sub

Private Sub btnsave_Click(ByVal sender As System.Object, ByVal e As
                        System.EventArgs) Handles btnsave.Click
    Try
        'sql command that insert a new patient to the table
        qry = "insert into patient (id, lastname, firstname, address, city,
country, phone, age) values ('" + Me.IDTextBox.Text + "', '" +
Me.LastnameTextBox.Text + "', '" + Me.FirstnameTextBox.Text + "', '" +
Me.AddressTextBox.Text + "', '" + Me.CityTextBox.Text + "', '" +
Me.CountryTextBox.Text + "', '" + Me.PhoneTextBox.Text + "', '" +
Me.AgeTextBox.Text + "')"
        myCommand.Connection = Conn
        myCommand.CommandText = qry
        If myCommand.ExecuteNonQuery() Then 'execute the insert query and
verify the insertion of data
            MsgBox("Patient data has been stored", vbOK, "By Patient Data
Form")
            refreshData()
            refreshData()
        Else
            MsgBox("Patient data has not been stored", vbOK, "By Patient Data
Form")
        End If
    Catch ex As Exception
        MsgBox(ex.ToString)
    End Try
End Sub

Private Sub btndelete_Click(ByVal sender As System.Object, ByVal e As
                        System.EventArgs) Handles btndelete.Click
    Try
        'sql command that delete a selected patient
        qry = "delete from patient where patient.id = '" + Me.IDTextBox.Text
myCommand.Connection = Conn
myCommand.CommandText = qry
        If myCommand.ExecuteNonQuery() Then
            MsgBox("Patient data has been deleted", vbOK, "By Patient Data
Form")
            refreshData()
            refreshData()
        Else
            MsgBox("Patient data has not been deleted", vbOK, "By Patient Data
Form")
        End If
    Catch ex As Exception
        MsgBox(ex.ToString)
    End Try
End Sub

Private Sub btnupdate_Click(ByVal sender As System.Object, ByVal e As
                        System.EventArgs) Handles btnupdate.Click
    Try
        'sql command that update the selected patient record

```

```

qry = "update patient set id='" + Me.IDTextBox.Text + "', lastname='"
+ Me.LastnameTextBox.Text + "', firstname='" +
Me.FirstnameTextBox.Text + "', address='" + Me.AddressTextBox.Text +
"', city='" + Me.CityTextBox.Text + "', country='" +
Me.CountryTextBox.Text + "', phone='" + Me.PhoneTextBox.Text + "',
age='" + Me.AgeTextBox.Text + "' where patient.id ='" +
Me.IDTextBox.Text + "'"
myCommand.Connection = Conn
myCommand.CommandText = qry
If myCommand.ExecuteNonQuery() Then
    MsgBox("Patient data has been updated", vbOK, "By Patient Data
    Form")
    refreshData()
    refreshData()
Else
    MsgBox("Patient data has not been updated", vbOK, "By Patient
    Data Form")
End If
Catch ex As Exception
    MsgBox(ex.ToString)
End Try
End Sub

Private Sub btnaddhistory_Click(ByVal sender As System.Object, ByVal e As
    System.EventArgs) Handles btnaddhistory.Click
    Try
        phgroup.Visible = True
        txthid.Text = "Auto Number"
        txtpid.Text = IDTextBox.Text
        txtdate.Text = Today.Date
        txtdiscription.Text = ""
        txtdiscription.Focus()
    Catch ex As Exception

    End Try
End Sub

Private Sub btnhsave_Click(ByVal sender As System.Object, ByVal e As
    System.EventArgs) Handles btnhsave.Click
    Try
        qry = "insert into patienthistory (id, operationdate, discription)
        values ('" + Me.txtpid.Text + "', '" + Me.txtdate.Text + "', '" +
        Me.txtdiscription.Text + "')"
        myCommand.Connection = Conn
        myCommand.CommandText = qry
        If myCommand.ExecuteNonQuery() Then
            MsgBox("Patient history data has been stored", vbOK, "By Patient
            Data Form")
            refreshData()
            refreshData()
            phgroup.Visible = False
        Else
            MsgBox("Patient history data has not been stored", vbOK, "By
            Patient Data Form")
        End If
    Catch ex As Exception
        MsgBox(ex.ToString)
    End Try
End Sub

Private Sub btnhdelete_Click(ByVal sender As System.Object, ByVal e As
    System.EventArgs) Handles btnhdelete.Click

```

```

Try
    qry = "delete from patienthistory where patienthistory.historicaldata
    = " + Me.txthid.Text + ""
    myCommand.Connection = Conn
    myCommand.CommandText = qry
    If myCommand.ExecuteNonQuery() Then
        MsgBox("Patient history data has been deleted", vbOK, "By Patient
        Data Form")
        refreshData()
        refreshData()
    Else
        MsgBox("Patient history data has not been deleted", vbOK, "By
        Patient Data Form")
    End If
Catch ex As Exception
    MsgBox(ex.ToString)
End Try
End Sub

Private Sub txtsearch_KeyDown(ByVal sender As Object, ByVal e As
    System.Windows.Forms.KeyEventArgs) Handles
    txtsearch.KeyDown
    If e.KeyCode = Keys.Enter Then
        Try
            qry = "select * from patient where patient.id='" +
            txtsearch.Text + ""
            myCommand.Connection = Conn
            myCommand.CommandText = qry
            myAdaptersubfill.SelectCommand = myCommand
            myAdaptersubfill.Fill(myDatasubfill)
            BindingSource1.DataSource = myDatasubfill
            BindingNavigator1.BindingSource = BindingSource1
            clearbindings()
            Me.IDTextBox.DataBindings.Add(New Binding("Text",
            Me.BindingSource1, "id", True))
            Me.FirstnameTextBox.DataBindings.Add(New Binding("Text",
            Me.BindingSource1, "firstname", True))
            Me.LastnameTextBox.DataBindings.Add(New Binding("Text",
            Me.BindingSource1, "lastname", True))
            Me.AddressTextBox.DataBindings.Add(New Binding("Text",
            Me.BindingSource1, "address", True))
            Me.CityTextBox.DataBindings.Add(New Binding("Text",
            Me.BindingSource1, "city", True))
            Me.CountryTextBox.DataBindings.Add(New Binding("Text",
            Me.BindingSource1, "country", True))
            Me.PhoneTextBox.DataBindings.Add(New Binding("Text",
            Me.BindingSource1, "phone", True))
            Me.AgeTextBox.DataBindings.Add(New Binding("Text",
            Me.BindingSource1, "age", True))

            'fill subform
            filtersubform(Me.IDTextBox.Text)
        Catch ex As Exception
            MsgBox(ex.ToString)
        End Try
    End If
End Sub

Private Sub clearbindings()
    Me.IDTextBox.DataBindings.Clear()
    Me.FirstnameTextBox.DataBindings.Clear()
    Me.LastnameTextBox.DataBindings.Clear()
    Me.AddressTextBox.DataBindings.Clear()

```

```

Me.CityTextBox.DataBindings.Clear()
Me.CountryTextBox.DataBindings.Clear()
Me.PhoneTextBox.DataBindings.Clear()
Me.AgeTextBox.DataBindings.Clear()
End Sub
Private Sub btnhupdate_Click(ByVal sender As System.Object, ByVal e As
    System.EventArgs) Handles btnhupdate.Click
    Try
        qry = "update patienthistory set id='" + Me.txtpid.Text + "',
            operationdate='" + Me.txtdate.Text + "', discription='" +
            Me.txtdiscription.Text + "' where patienthistory.historicaldata = "
            + Me.txthid.Text + ""
        myCommand.Connection = Conn
        myCommand.CommandText = qry
        If myCommand.ExecuteNonQuery() Then
            MsgBox("Patient history data has been updated", vbOK, "By
                Patient Data Form")
            refreshData()
            refreshData()
            phgroup.Visible = False
        Else
            MsgBox("Patient history data has not been updated", vbOK, "By
                Patient Data Form")
        End If
    Catch ex As Exception
        MsgBox(ex.ToString)
    End Try
End Sub

Private Sub btnrefresh_Click(ByVal sender As System.Object, ByVal e As
    System.EventArgs) Handles btnrefresh.Click
    Try
        refreshData()
        refreshData()
        filtersubform(Me.IDTextBox.Text)
    Catch ex As Exception
    End Try
End Sub
Private Sub PatienthistoryDataGridView_CellMouseDoubleClick(ByVal sender As
    Object, ByVal e As System.Windows.Forms.DataGridViewCellEventArgs) Handles
    PatienthistoryDataGridView.CellMouseDoubleClick
    Try
        If e.ColumnIndex > -1 AndAlso e.RowIndex > -1 AndAlso TypeOf
            sender.CurrentCell Is DataGridViewTextBoxCell Then 'AndAlso TypeOf
            sender.CurrentCell Is DataGridViewTextBoxCell

            phgroup.Visible = True
            qry = "SELECT * FROM(patienthistory) WHERE
                (((patienthistory.historicaldata)=" +
                sender.CurrentCell.EditedFormattedValue() + ")))"

            myCommand.Connection = Conn
            myCommand.CommandText = qry
            myAdaptereditfill.SelectCommand = myCommand
            myAdaptereditfill.Fill(myDataedit)
            BindingSource2.DataSource = myDataedit
            Me.txthid.DataBindings.Clear()
            Me.txtpid.DataBindings.Clear()
            Me.txtdate.DataBindings.Clear()
            Me.txtdiscription.DataBindings.Clear()
            Me.txthid.DataBindings.Add(New Binding("text", BindingSource2,
                "historicaldata", True))
    End Try
End Sub

```

```

Me.txtpid.DataBindings.Add(New Binding("text", BindingSource2,
"id", True))
Me.txtdate.DataBindings.Add(New Binding("text", BindingSource2,
"operationdate", True))
Me.txtdiscription.DataBindings.Add(New Binding("text",
BindingSource2, "discription", True))
End If
Catch ex As Exception
MsgBox(ex.ToString)
End Try

End Sub
End Class

```

3. Prostate Cancer Statistics

3.1. Average Testosterone Levels by Age in Men

The following tables demonstrate the average testosterone levels in men grouped by age.

Vermeulen, A. (1996). Declining Androgens with Age: An Overview . In Vermeulen, A. & Oddens, & B. J. (Eds.), <i>Androgens and the Aging Male</i> (pp. 3-14). New York: Parthenon Publishing.							
Measurements in SI Units (nmol/L)							
Age	Number of Subjects	Total Test	Stand. Dev.	Free Test	Stand. Dev.	SHBG	Stand. Dev.
25-34	45	21.38	5.90	0.428	0.098	35.5	8.8
35-44	22	23.14	7.36	0.356	0.043	40.1	7.9
45-54	23	21.02	7.37	0.314	0.075	44.6	8.2
55-64	43	19.49	6.75	0.288	0.073	45.5	8.8
65-74	47	18.15	6.83	0.239	0.078	48.7	14.2
75-84	48	16.32	5.85	0.207	0.081	51.0	22.7
85-100	21	13.05	4.63	0.186	0.080	65.9	22.8
Measurements in Conventional Units (ng/dl), SHBG in (nmol/L)							
Age	Number of Subjects	Total Test	Stand. Dev.	Free Test	Stand. Dev.	SHBG	Stand. Dev.
25-34	45	617	170	12.3	2.8	35.5	8.8
35-44	22	668	212	10.3	1.2	40.1	7.9
45-54	23	606	213	9.1	2.2	44.6	8.2
55-64	43	562	195	8.3	2.1	45.5	8.8
65-74	47	524	197	6.9	2.3	48.7	14.2
75-84	48	471	169	6.0	2.3	51.0	22.7
85-100	21	376	134	5.4	2.3	65.9	22.8

Normal Testosterone Levels in Men (Non-Diabetic)

Simon, D., Nahoul, K., & Charles M.A. (1996). **Sex Hormones, Aging, Ethnicity and Insulin Sensivity in Men: An Overview of the TELECOM Study.** In Vermeulen, A. & Oddens, and B. J. (Eds.), *Androgens and the Aging Male* (pp. 85-102). New York: Parthenon Publishing.

Measurements in SI Units (nmol/L)

Age	Number of Subjects	Mean Total Test	Stand. Dev.	Median Total Test	5th %	10th %	95th %
<25	125	23.97	5.48	24.15	14.15	16.22	33.12
25-29	354	23.18	7.14	22.08	13.46	15.18	34.84
30-34	330	21.53	6.72	20.70	12.07	13.46	33.81
35-39	212	20.70	6.55	19.66	11.39	13.46	32.77
40-44	148	20.70	6.87	20.70	11.04	13.11	32.43
45-49	154	18.91	5.66	18.28	11.39	12.42	29.32
50-54	164	18.87	6.49	17.94	10.01	12.07	32.43
55-59	155	19.14	6.04	18.97	11.04	11.73	30.01

Measurements in Conventional Units (ng/dl)

Age	Number of Subjects	Mean Total Test	Stand. Dev.	Median Total Test	5th %	10th %	95th %
<25	125	692	158	697	408	468	956
25-29	354	669	206	637	388	438	1005
30-34	330	621	194	597	348	388	975
35-39	212	597	189	567	329	388	945
40-44	148	597	198	597	319	378	936
45-49	154	546	163	527	329	358	846
50-54	164	544	187	518	289	348	936
55-59	155	552	174	547	319	338	866

3.2. Prostate Cancer Statistics

The following table demonstrates the prostate cancer statistics word-wild grouped by region. The statistics are separated into two categories, incidence and mortality.

Age-standardized incidence of prostate cancer (per 100,000) in the world [196]

Africa	Congo	29.0
	Kenya	16.6
	Senegal	7.5
	Uganda	38.0
	Zimbabwe	27.4
North America	Canada	78.2
	US	124.8
	US, White	107.8
	US, Black	185.4
Asia	China	1.7
	Taiwan	3.0
	Israel	47.5
	Japan	12.6
	Korea	7.6
	Thailand	4.5
Europe	Austria	71.4
	Austria, Tyrol	100.1
	Austria, Vorarlberg	66.4
	France	59.3
	Hungary	34.0
	Iceland	75.2
	Norway	81.8
	Spain	35.9
	Sweden	90.9
	Switzerland	77.3
	UK	52.2
Oceania	Australia	76.0
	New Zealand	100.9

Age-standardized mortality of prostate cancer (per 100,000) in the world [196]

Africa	South Africa	22.6
	Uganda	32.5
	Senegal	6.5
	Zimbabwe	23.5
Asia	China	1.0
	Israel	13.4
	Japan	5.7
Europe	Austria	18.4
	France	18.2
	Germany	15.8
	Hungary	18.4
	Iceland	23.0
	Italy	12.2
	Norway	28.4
	Spain	14.9
	Sweden	27.7
	UK	17.9
North America	US	15.8
	Canada	16.6
Oceania	Australia	17.7
	New Zealand	20.3

3.3. Accuracy measurements – Linear (Fwd) stage sample

	Forward	Forward	Forward	Forward	Forward	Forward	Forward
CPI	10	20	40	80	160	320	500
	0.62	1.17	2.19	4.18	8.31	16.34	25.52
	0.6	1.14	2.13	4.13	8.27		
	0.59	1.14	2.16	4.15	8.27		
	0.62	1.11	2.16	4.16	8.26		
	0.61	1.1	2.14	4.18			
	0.61	1.15	2.1	4.18			
	0.6	1.11	2.16	4.2			
	0.6	1.17	2.15	4.21			
	0.62	1.14	2.12				
	0.61	1.11	2.14				
	0.63	1.11	2.13				
Average	0.61	1.131818	2.143636	4.17375	8.2775	16.34	25.52
STDEV	0.011832	0.025226	0.024196	0.026152	0.022174	0	0

3.4. Measurements Prostates

Number	Volume Prostate (cc)	Anterior - Posterior (mm)	Apex - Base (mm)	Left - Right (mm)	Anus - Apex Prostate (mm)	Anus - Base Prostate (mm)	Table - Posterior Prostate (mm)	Rotate angle (°)
1	52	33.8	49.9	57.9	59.5	109.4	112.5	103
2	48	50.8	50.6	47.8	53	103.6	106.3	78.9
3	45	34.5	54.2	47.5	63.2	117.4	105.5	89.3
4	51	38.7	51.9	47.7	58.7	110.6	-	90.8
5	47	40.2	53.1	51	46.5	99.6	-	93.4
6	47	36.3	52.6	46.7	48.6	101.2	-	82.3
7	56	42.2	45	55	62.3	107.3	98.4	82.9
8	54	42.7	50	47.7	58.1	108.1	109.4	93.2
9	48	31	49.8	58.3	51	100.8	121.9	105
10	50	37.4	48.4	55	53.4	101.8	-	101
11	46	25	60.3	44.6	52.3	112.6	112.5	93.6
12	58	38.2	49.7	53.1	57.5	107.2	-	91.2
13	47	34.1	51.7	56.8	50.7	102.4	-	99.5
14	54	31.1	47.4	52.9	43.1	90.5	-	98.3
15	48	30.6	53.4	53.1	48.3	101.7	118	98.5
16	45	35.8	45.3	53.4	44.2	89.5	112.8	97.8
17	57	39	51.4	54.8	63.4	114.8	103.1	96.5
18	45	33.4	49.9	52.6	46.6	96.5	-	102
19	45	35.8	51	47.1	52.6	103.6	-	88.1
20	46	40.2	51.6	49	63.3	114.9	-	84.1
21	45	34	48.7	52.4	48	96.7	104.7	86.8
22	48	34.5	55	49.2	42.2	97.2	106	81.7
23	60	41	53.2	53	39.3	92.5	95.4	105

24	46	30.9	52	55.4	47.1	99.1	-	120
25	54	37	57.9	54.9	45	102.9	95.5	107
26	57	34.6	64.6	50.2	53.4	118	-	97.1
27	57	40.2	52.3	55.8	44.3	96.6	116.4	102
28	59	39.6	49.1	58.3	41.9	91	95.5	108
29	45	31.6	56	47.7	49.5	105.5	-	96.6
30	47	38.3	48.5	49.5	52.8	101.3	-	99
31	46	30.7	47.9	58.9	39.2	87.1	108.7	116
32	56	42.3	49.4	52	60.4	109.8	-	93.3
33	48	34.2	59.3	45.8	29.5	88.8	106.3	94.3
34	53	31	68	48.2	34.9	102.9	107.9	85.2
35	54	34.9	57.6	50.5	37.6	95.2	98.4	89.5
36	50	38.4	47.6	52.9	39.9	87.5	106.8	112
37	52	36.8	48.4	55.8	57.8	106.2	107.8	106
38	57	38.6	54.6	50.7	41.3	95.9	106.7	104
39	48	39	47.8	49	29.3	77.1	115.4	107
40	53	40.3	50.7	50.7	53.9	104.6	-	107
41	55	31.7	59.9	55	38.8	98.7	-	96.5
42	59	33.1	61.9	54.6	51.7	111.3	-	105
43	48	33.5	48.3	55.6	46.6	88.1	96.9	101
44	46	32.3	53.4	51.8	47.2	99.3	-	108
45	45	38.1	47.8	47.1	59	106.8	-	74.1
46	55	43.2	55.4	54.6	49.5	101.1	-	97.9
47	48	41.4	47.8	46.6	48.4	96.2	114.1	92.3
48	52	39.8	48.7	50.7	55	101.2	-	108
49	56	43.8	37.1	57.6	33.6	72.3	92.2	91.2

50	55	35.9	52.8	55.4	59.1	92.7	139.1	103
51	46	37.5	51.2	45.9	44.5	84.8	111	87.4
52	52	28.1	70.7	49.8	41.1	110.1	-	97
53	59	33	54.6	61.6	43.2	94.5	-	111
54	56	41.9	60	58.3	47.4	101.4	-	105
55	60	34.2	60.4	56.7	39.4	95.7	-	108
56	47	31.8	51.9	41.8	29	74.8	89.1	95.5
57	46	29.3	53.5	53.5	43.6	86.1	98.6	107
58	47	35.4	53	47.8	37.3	81.7	105.7	95.1
59	58	41.5	59.5	53.2	37.8	97.1	-	101
60	58	39.5	47	58.7	42.5	89.5	111.9	95.1
61	52	32.2	55.6	55.5	38	89.4	-	98.3
62	54	36.7	54.9	56	48.2	101.4	109.4	94.5
63	45	37.4	50.1	47	50.4	100	-	95.6
64	45	33	55.2	45.1	41	89.7	118.3	82.5
65	52	34.6	58.4	55.22	47.9	106.6	-	98.7
66	56	34.6	61	53.9	47.3	105.3	-	93.4
67	47	35	48.7	52.6	49.2	94	-	101
68	55	40.7	47	50.6	49.8	95.9	101.2	103
69	48	36.8	48.1	53.6	46.2	91.2	104.1	101
70	55	34.6	60.2	49.8	45	98.8	105	83.8
71	51	35	70	51.4	39	104.1	-	101
72	55	32.4	57.7	56.5	47.2	106.4	-	105
73	45	30.1	53.8	54.4	39.6	87.9	-	100
74	49	33.9	44.8	53.7	50.8	90.5	146.2	126
75	57	36.2	55.8	54.4	46.7	103.9	-	94.6

76	50	35.3	49.7	59.4	36	80	104.4	99.2
77	52	35.3	55.4	52.2	50.3	99.1	117.3	100
78	55	40	44.3	60	39.8	81.9	-	106
79	51	35	48.9	55	30.7	76.1	115.7	96.8
80	45	33	48	53.7	50	95.6	107.7	95.1
81	50	36.9	48.6	54.4	22	55.5	108.8	107
82	46	29	54.1	56.7	37.1	76.5	119.7	106
83	45	33.4	49.1	53.4	39.1	81.7	120.5	99.7
84	59	41.6	50.5	51.6	28.7	66.7	94.1	99.5
85	45	38.7	43.1	51.3	33.6	74.1	91.6	100
86	45	35	43.8	54.6	20.7	66.7	113.6	103
87	55	33	48.7	54	41.2	92.5	-	95.5
88	51	33.4	51.4	63.8	35.1	86.1	-	130
89	56	42.7	50	53.1	45.4	90.4	112.2	105
90	54	37	54.4	52.3	39.6	87.7	106.8	100
91	45	31.2	41.8	66	45.1	90.1	-	119
92	48	39.8	49.2	47	31.9	71.2	108.2	104
93	47	39	55.1	51.4	46.2	91.8	-	94.3
94	45	37.5	52.6	58.7	37.2	88.2	105.6	118
95	55	34.2	50.3	51.4	32.5	75.3	95	98.9
96	45	41	57.5	44.2	31.8	74.9	95	88.5
97	59	46.6	61.9	53.4	31.2	97	-	100
98	49	37.8	47.2	52.8	46.7	91.8	110.2	93.2
99	45	28.9	50.6	56.7	46.5	87.8	108.6	111
100	46	33.1	50.3	52.5	39.8	91.5	97.5	91.7

References

1. <http://www.cancerresearchuk.org/cancer-info/cancerstats/world/incidence/>
2. <http://www.cancer.gov/cancertopics/types/prostate>
3. <http://info.cancerresearchuk.org/cancerstats/types/prostate/incidence/>
4. <http://www.upmccancercenters.com/cancer/prostate/hormonetherapy.html>
5. <http://www.prostate-cancer.com/brachytherapy/treatment-description/prostate-brachytherapy.html>
6. Blana A, "First analysis of the long-term results with transrectal HIFU in patients with localized prostate cancer.", *Eur Urol*, 53:1194-1203, 2008.
7. Polascik TJ and Mouraviev V. "Focal therapy for prostate cancer.", *Curr Opin Urol*, 18:269-274, 2008.
8. Trachtenberg J, "Vascular-targeted photodynamic therapy with palladium bacterium pheophorbide photosensitizer for recurrent prostate cancer following definitive radiation therapy: Assessment of safety and treatment response.", *J Urol*, 178:1974-1979, 2007.
9. Trachtenberg J, "Vascular-targeted photodynamic therapy (padaporfin, WST09) for recurrent prostate cancer after failure of external beam radiotherapy: a study of escalating light doses.", *BJU Int*, 102:556-562, 2008.
10. Zacharakis E, "The feasibility and safety of high-intensity focused ultrasound as salvage therapy for recurrent prostate cancer following external beam radiotherapy". *BJU Int*, 102, 786-792, 2008.
11. Ahmed HU, "High-intensity focused ultrasound in the treatment of primary prostate cancer: the first UK series." *Br J Cancer*, 101:19-26, 2009.
12. N. A. Sanghvi, F. J. Fry, R. Bihrlé, R. S. Foster, M. H. Phillips, J. Syrus, A. V. Zaitsev, and C. W. Henninge, "Non invasive surgery of prostate tissue by high-intensity ultrasound.", *IEEE Trans. Ultrason., Ferroelect., Freq. Contr.*, vol. 43, pp. 1099-1110, 1996.
13. Kyle O. Rove, Kathryn F. Sullivan, E. David Crawford, "High –intensity focused Ultrasound Ready for Primetime.", 37(1):27-35, doi: 10.1016/j.ucl.2009.11.010, 2010.
14. Francois-Joseph Murat, MD, Laura Poissonnier, MD, Gilles Pasticier, MD, and Albert Gelet, MD, "High-Intensity Focused Ultrasound (HIFU) for Prostate Cancer.", Vol. 14, No. 3, 2007
15. Bihrlé R, Foster RS, Sanghvi NT, "High-intensity focused ultrasound in the treatment of prostatic tissue.", *Urology*, 43(2 Suppl):21–6, 1994

16. Gelet A, Chapelon JY, Margonari J, "Highintensity focused ultrasound experimentation on human benign prostatic hypertrophy.", *European Urology*, 23(Suppl 1):44–7, 1993
17. Gassert R., Burdet E., Chinzei K. "MRI-Compatible robotics– A Critical Tool for Image Guided Interventions.", *Clinical Diagnostics and Neuroscience. IEEE Engineering in Medecine and Biology*, 27: 12-14, 2008
18. Schenck JF. "The role of magnetic susceptibility in magnetic resonance imaging: MRI magnetic compatibility of the first and second kinds.", *Medical Physics*, 23(6): 815-850, 1996
19. Gassert R, Burdet E, Chinzei K. "Opportunities and challenges in MR-Compatible Robotics.", *IEEE Engineering in Medecine and Biology*, 27(3):15-22, 2008
20. Benjamin-Cummings Publishing Company, *Human anatomy and physiology*, Jun 22, 2010 - 1264 page
21. Klower Academic Publishers, *Prostate cancer: new horizons in research and treatment-*, Now York, Boston, Dordrecht, London, Moscow, 2002
22. Meredith W., Lorrie P., *Prostate Cancer: Nursing Assessment, Management, and Care*, 2002, Springer Series on Geriatric Nursing, ISBN: 0-8261-8745-5
23. Chapple C., William D., *Practical Urology: Essential Principles and Practice: Essential Principles*, 2002, John Lumley Series Edition, ISBN: 978-1-84882-033-0
24. Kai H. Hammerich, Gustavo E. Ayala, and Thomas M. Wheeler, *Anatomy of the prostate gland and surgical pathology of prostate cancer*
25. <http://www.siteman.wustl.edu/CancerDetails.aspx?mid=153&id=673&xml=CDR257530.xml>
26. http://en.wikipedia.org/wiki/File:Illu_prostate_lobes.jpg
27. <http://www.sciencephoto.com/media/153190/enlarge>
28. <http://www.sperlingprostatecenter.com/prostate-cancer>
29. <http://www.upmccancercenter.com/cancer/prostate/treatment.cfm>
30. Beth A. Hellerstedt, MD, Kenneth J. Pienta, MD, "The Current State of Hormonal Therapy for Prostate Cancer.", *CA Cancer J Clin*. 52:154-179, 2002
31. Suresh Bhat, M.K. Ramaprasad, M.S. Sachin Joseph, "Active Surveillance in Prostate Cancer", *American Medical Association*, Page 1 – 44, 2013
32. Ian M. Thompson, MD, Laurence Klotz, MD, *Active Surveillance for Prostate Cancer*, (Reprinted) *JAMA*, Vol 304, No. 21, 2010
33. Kai H. Hammerich, Gustavo E. Ayala, Thomas M. Wheeler, "Anatomy of the prostate gland and surgical pathology of prostate cancer.", *Cambridge University Press*, 978-0-521-88704-5, 2009
34. Anna Bill-Axelson, M.D., Lars Holmberg, M.D., Ph.D., Mirja Ruutu, M.D., Ph.D., Michael Haggman, M.D., Ph.D., Swen-Olof Andersson, M.D., Ph.D., Stefan

- Bratell, M.D., Ph.D., Anders Spangberg, M.D., Ph.D., "Radical Prostatectomy versus Watchful Waiting in Early Prostate Cancer.", *England journal of medicine*, 352;12, DOI: 10.1056/NEJMoa043739, 2005
35. Janet L. Stanford, PhD, Ziding Feng, PhD, Ann S. Hamilton, PhD, Frank D. Gilliland, PhD, Robert A. Stephenson, MD, J. William Eley, PhD, "Urinary and Sexual Function After Radical Prostatectomy for Clinically Localized Prostate Cancer.", *JAMA*, 283(3):354-360. doi:10.1001/jama.283.3.354, 2000
 36. Christian Bolenz, Amit Gupta, Timothy Hotze, Richard Ho, Jeffrey A. Cadeddu, Claus G. Roehrborn, Yair Lotan, "Cost Comparison of Robotic, Laparoscopic, and Open Radical Prostatectomy for Prostate Cancer.", *European Urology*, Volume 57, Issue 3, Pages 453-458, 2009
 37. Vincenzo Ficarra, Giacomo Novara, Walter Artibani, Andrea Cestari, Antonio Galfano, Markus Graefen, "Retropubic, Laparoscopic, and Robot-Assisted Radical Prostatectomy: A Systematic Review and Cumulative Analysis of Comparative Studies.", *European Urology*, Volume 55, Issue 5, Pages 1031-1033, 2009
 38. <http://journal.nzma.org.nz/journal/121-1287/3422/>
 39. Subir Nag, M.D., David Beyer, M.D., Jay Friedland, M.D., Peter Grimm, D.O., Ravinder Nath, Ph.D., "American Brachytherapy Society (Abs) Recommendations For Transperineal Permanent Brachytherapy Of Prostate Cancer.", *I. J. Radiation Oncology c Biology c Physics* Volume 44, Number 4, 1999
 40. Arthur T. Porter, MD, John C. Blasko, MD, Peter D. Grimm, DO, Sarada M. Reddy, MD, Haakon Ragde, MD, "Brachytherapy for Prostate Cancer.", Vol. 45 No. 3 may/june 1995
 41. Michael W. Kattan, Louis Potters, John C. Blasko, David C. Beyer, Paul Fearn, William Cavanagh, Steve Leibel, And Peter T. Scardino, "Pretreatment Nomogram For Predicting Freedom From Recurrence After Permanent Prostate Brachytherapy In Prostate Cancer.", ELSEVIER SCIENCE INC, 2001
 42. Hazel Templeton, "Prostate cancer –presentation,diagnosis and treatment: what does the literature say?", The Author. Journal compilation, 2007
 43. Moreira SG, Seigner JD, Ordorica RC, Marcet J, Pow-Sang JM, Lockhart JL, "Devastating complications after brachytherapy in the treatment of prostate adenocarcinoma.", *BJU International*; 93: 31–35, 2004.
 44. Alessandro Sciarra, Michele Innocenzi, Andrea Alfarone, Susanna Cattarino, Alessandro Gentilucci, Francesco Minisola, "Cryotherapy for Prostate Cancer.", *European Urological Review*, 7(1):17–23, 2012
 45. Joanne Cresswell, Susan Asterling, Moazzam Chaudhary, Naeem Sheikh And Damian Greene, "Third-generation cryotherapy for prostate cancer in the UK: a prospective study of the early outcomes in primary and recurrent disease.", Volume 97, Issue 5, pages 969–974, 2005

46. Caroline M Moore, Doug Pendse, and Mark Emberton, "Photodynamic therapy for prostate cancer – a review of current status and future promise.", 6, 18-30, 2008
47. Trachtenberg J, "Vascular-targeted photodynamic therapy with palladium bacterium pheophorbide photosensitizer for recurrent prostate cancer following definitive radiation therapy: Assessment of safety and treatment response.", Journal of Urology, 178:1974-1979, 2007.
48. Trachtenberg J, "Vascular-targeted photodynamic therapy (padaporfin, WST09) for recurrent prostate cancer after failure of external beam radiotherapy: a study of escalating light doses.", BJU Int, 102:556-562, 2008.
49. Caroline M Moore, Doug Pendse and Mark Emberton, "Photodynamic therapy for prostate cancer— a review of current status and future promise.", 6, 18-30, 2008
50. J. Trachtenberg, A. Bogaards, R. A. Weersink, M. A. Haider, A. Evans, S. A. McCluskey, "Vascular Targeted Photodynamic Therapy With Palladium-Bacteriopheophorbide Photosensitizer for Recurrent Prostate Cancer Following Definitive Radiation Therapy: Assessment of Safety and Treatment Response.", Vol. 178, 1974-1979, November 2007
51. M. Johannsen, U. Gneveckow, K. Taymoorian¹, B. Thiesen, N. Waldo Fner, R. Scholz, "Morbidity and quality of life during thermotherapy using magnetic nanoparticles in locally recurrent prostate cancer: Results of a prospective phase I trial.", 23(3): 315–323, 2007
52. Marian Devonec, M.D., Ph.D., N. Berger, M.D., And P. Perrin, M.D., "Transurethral Microwave Heating of the Prostate—Or from Hyperthermia to Thermotherapy.", Volume 5, 1991
53. Blana A, "First analysis of the long-term results with transrectal HIFU in patients with localized prostate cancer.", Eur Urol, 53:1194-1203, 2008.
54. Hazel Templeton, "Prostate cancer – presentation, diagnosis and treatment: what does the literature say.", International Journal of Urological Nursing, Volume 1, Issue 1, pages 6–17, 2007
55. Sebastien Crouzet, Francois J. Murat, Gilles Pasticier, Philippe, Cassier, Jean Y. Chapelon, And Albert Gelet, "High intensity focused ultrasound (HIFU) for prostate cancer: Current clinical status, outcomes and future perspectives.", Vol. 26, No. 8 , Pages 796-803, 2010
56. <http://urologyrbh.blogspot.com/2011/08/prostatitis.html>
57. <http://www.ultrasoundpaedia.com/normal-prostate/>
58. http://4urology.org/patient_information/conditions/prostate/
59. http://www.avantgardeurology.com/cryotherapy_of_prostate_cancer-en.html
60. http://www.avantgardeurology.com/cryotherapy_of_prostate_cancer-en.html
61. <http://www.hifu.ca/history-ablatherm-hifu.htm>

62. J E Kennedy, Mbbs, Mrcs, g R Ter Haar, Msc, Phd, Dsc And D CRANSTON, Dphil, FRCS, "High intensity focused ultrasound: surgery of the future?", *The British Institute of Radiology*, DOI: 10.1259/bjr/17150274, 590–599, 2003
63. Gail Ter Haar, & Constantin Coussios, "High intensity focused ultrasound: Physical principles and devices.", *Int. J. Hyperthermia*, 23(2): 89–104, 2007
64. Harvard Medical School, Brigham and Women's Hospital, Boston, MA 02115, USA, "Perspectives in clinical uses of high-intensity focused ultrasound" G.T. Clement, *Focused Ultrasound Laboratory, Department of Radiology*, 2004
65. Ahmed HU, "High-intensity focused ultrasound in the treatment of primary prostate cancer: the first UK series.", *Br J Cancer*, 101:19-26, 2009.
66. Blana A, Walter B, Rogenhofer S, Wieland WF, "High intensity focused ultrasound for the treatment of localized prostate cancer: 5 year experience.", *Urology*, 54: 273–277, 2004
67. Nathan McDannold, Mark Moss, Ron Killiany, Douglas L. Rosene, Randy L. King, Ferenc A. Jolesz, and Kullervo Hynynen, "MRI-Guided Focused Ultrasound Surgery in the Brain: Tests in a Primate Model.", Volume 49, Issue 6, pages 1188–1191, 2007
68. Hidemi Furusawa, FACS, Kiyoshi Namba, FACS, Sharon, Thomsen, Futoshi Akiyama, Achiude Bendet, Chiaki Tanaka, Yukiko Yasuda, Hiroshi Nakahara, "Magnetic Resonance–Guided Focused Ultrasound Surgery of Breast Cancer: Reliability and Effectiveness.", Volume 203, Issue 1, Pages 54–63, 2006
69. Polascik TJ and Mouraviev V. "Focal therapy for prostate cancer.", *Curr Opin Urol*, 18:269-274, 2008.
70. Trachtenberg J, "Vascular-targeted photodynamic therapy with palladium bacterium pheophorbide photosensitizer for recurrent prostate cancer following definitive radiation therapy: Assessment of safety and treatment response.", *Journal of Urology*, 178:1974-1979, 2007.
71. Trachtenberg J, "Vascular-targeted photodynamic therapy (padaporfin, WST09) for recurrent prostate cancer after failure of external beam radiotherapy: a study of escalating light doses.", *BJU Int*, 102:556-562, 2008.
72. Zacharakis E, "The feasibility and safety of high-intensity focused ultrasound as salvage therapy for recurrent prostate cancer following external beam radiotherapy.", *BJU Int*, 102, 786-792, 2008.
73. Ahmed HU, "High-intensity focused ultrasound in the treatment of primary prostate cancer: the first UK series.", *Br J Cancer*, 101:19-26, 2009.
74. Christakis Damianou, M. Pavlou, O. Velev, K. Kyriakou And M. Trimikliniotis, "High Intensity Focused Ultrasound Ablation Of Kidney Guided By MRI.", Volume 30, Issue 3, Pages 397–404, 2003
75. D. Germain, E. Vahala, G.J. Ehnholm, T. Vaara, M. Ylihautala, M. Savart, A. Laurent, J. Tantt, and H. Saint-Jalmes, "MR Temperature Measurement in

Liver Tissue at 0.23 T With a Steady-State Free Precession Sequence.”, Volume 47, Issue 5, pages 940–947, 2008

76. Chuan-Xing Li, Guo-Liang Xu, Zhen-You Jiang, Jian-Jun Li, Guang-Yu Luo, Hong-Bo Shan, Rong Zhang, Yin Li, “Analysis of clinical effect of high-intensity focused ultrasound on liver cancer.”, 10(15):2201-2204, 2008
77. Nicos Mylonas, Kleantlis Ioannides, Venediktos Hadjisavvas, Dimitris Iosif, Panayiotis A. Kyriacou, Christakis Damianou, “Evaluation of fast spin echo MRI sequence for an MRI guided high intensity focused ultrasound system for in vivo rabbit liver ablation.”, Volume 3, 241-246 2010
78. W. J. Fry, J. W. Barnard, F. V. Fry, R. F. Krunins, and J. F. Brennan, “Ultrasonic lesions in mammalian central nervous system,” *Science*, vol. 122, pp. 517-518, 1955.
79. Lizzi FL. “High-precision thermotherapy for small lesions.”, *European Urology* 23(Suppl. 1): 23-28, 1993
80. Ferenc A. Jolesz, Ion-Florin Talos, Richard B. Schwartz, Hatsuho Mamata, Daniel F. Kacher, MS, Kullervo Hynynen, Nathan McDannold, Pairash Saivironporn, Lei Zao, “Intraoperative magnetic resonance imaging and magnetic resonance imaging-guided therapy for brain tumors.”, 2002
81. Ballantine HT, Bell E, Manlapaz J. “Progress and problems in the neurological application of focused ultrasound.”, *J Neurosurg*, 17:858–76, 1960
82. Warwick R, Pond JB. “Trackless lesions in nervous tissues produced by HIFU (high-intensity mechanical waves).”, *J Anat*, 102:387–405, 1968
83. Lele PP. “Concurrent detection of the production of ultrasonic lesions.”, *Med Biol Eng*, 4:451–6, 1966
84. Burov AK, “High-intensity ultrasonic vibrations for action on animal and human malignant tumours.”, *Dokl Akad Nauk SSSR*, 106:239–41, 1956
85. Taylor KJW, Connolly CC. “Differing hepatic lesions caused by the same dose of ultrasound.”, *J Pathology*, 98:291–3, 1969
86. Bamber JC, Hill CR. “Ultrasonic attenuation and propagation speed in mammalian tissues as a function of temperature.”, *Ultrasound Medical Biology*, 5:149–57, 1979
87. Frizzell LA. “Threshold dosages for damage to mammalian liver by high-intensity focused ultrasound.” *IEEE Trans Ultrason Ferroelect Freq Cont*, 35:578–81, 1988
88. Linke CA, Carstensen EL, Frizzell LA, Elbodawi A, Fridd CW. “Localised tissue destruction by high-intensity focused ultrasound.”, *Arch Surg*, 107:887–91, 1973
89. Chen L, ter Haar GR, Hill CR, Dworkin M, Carnochan P, Young H. “Effect of blood perfusion on the ablation of liver parenchyma with high-intensity focused ultrasound.”, *Phys Medical Biology*, 38:1661–73, 1993
90. Lele PP, “Production of deep focal lesions by focused ultrasound current status.”, *Ultrasonics*, 5:105–12, 1967

91. Vallancien G, Chartier-Kastler E, Bataille N, Chopin D, Haroumi M, Bougaran J. "Focused extracorporeal pyrotherapy.", *Europe Urology*, 23(Suppl. 1):48–52, 1993.
92. Sibille A, Prat F, Chapelon JY, Abou el Fadil FA, Henry L, Theillere Y, "Extracorporeal ablation of liver tissue by high-intensity focused ultrasound.", *Oncology*, 50:375–9, 1993
93. Gelet A, Chapelon JY, Margonari J, Theillere Y, Gorry F, Souchon R., "High-intensity focused ultrasound experimentation on benign prostatic hyperplasia.", *European Urology*, 23(Suppl 1):44–7, 1993
94. Koehrmann KU, Michel MS, Fruhauf J, Volz J, Back W, Gaa J., "High-intensity focused ultrasound for noninvasive tissue ablation in the kidney, prostate and uterus.", *Journal of Urology*, 163(4 Suppl.):156, 2000
95. Uchida T, Ohkusa H, Yamashita H, Shoji S, Nagata Y, Hyodo T, Satoh T., "Five years' experience of transrectal high-intensity focused ultrasound using the Sonablate device in the treatment of localized prostate cancer.", *International Journal of Urology*, 13, 228–233, 2006
96. L.D. SULLIVAN, M.G. Mcloughlin, L.G. GOLDENBERG, M.E. GLEAVE And K.W. MARICH, "Early experience with high-intensity focused ultrasound for the treatment of benign prostatic hypertrophy.", *British Journal of Urology*, 79, 172–176, 1997
97. Chaussy C, Thuroff S, Zimmermann R. "Localized prostate cancer treated by transrectal high intensity focused ultrasound (HIFU). Outcome of 150 patients after 3 years.", *Journal of Urology*, 161:331, 1999
98. Gelet A, Chapelon JY, Margonari J, Theillere Y, Gorry F, Souchon R. "High-intensity focused ultrasound experimentation on benign prostatic hyperplasia.", *European Urology*, 23(Suppl 1):44–7, 1993
99. <http://www.wjgnet.com/2218-4333/index.htm>
100. Vladimir Turkevich, Sergey Kanaev, Aleksander Nosov, Andrei Mishchenko, Maxim Molchanov, Sergei Rozengard, "Preliminary Clinical Experience of Treating Low Risk Prostate Cancer with the use of the ExAblate Magnetic Resonance Guided Focused Ultrasound Surgery (MRgFUS).", 3rd International Symposium Focus Ultrasound 2012
101. Sangeet Ghai, Uri Lidner, Massom Haider, Walter Kucharczyk, Stuart McCluskey, Theodorus van der Kwast, John Trachtenberg, "Feasibility Study to Evaluate the Safety and Preliminary Effectiveness of Focal MR-Guided Focus Ultrasound Surgery (MRgFUS) for locally confined low risk prostate cancer: the first north American Experience.", 3rd International Symposium 2012
102. Tempany CM, Stewart EA, McDannold N, Quade B, Jolesz F, Hynynen K., "MRI Guided Focused Ultrasound Surgery (FUS) of Uterine Leiomyomas: A Feasibility Study.", *Radiology*, 227:897-905, 2003

103. Gassert R., Burdet E., Chinzei K., "MRI-Compatible robotics– A Critical Tool for Image Guided Interventions, Clinical Diagnostics and Neuroscience.", IEEE Engineering in Medecine and Biology, 27: 12-14, 2008
104. Schenck JF. "The role of magnetic susceptibility in magnetic resonance imaging: MRI magnetic compatibility of the first and second kinds.", Medical Physics, 23(6): 815-850, 1996
105. Gassert R, Burdet E, Chinzei K. "Opportunities and challenges in MR-Compatible Robotics.", IEEE Engineering in Medecine and Biology., 27(3):15-22, 2008
106. Chapuis D, Gassert R, Sache L, "Design of a simple MRI/fMR-compatible force/torque sensor.", Proceedings of the IEEE/RSJ International Conference on Intelligent Robots and Systems (IROS), Japan, 3: 2593–2599, 2004
107. K. Hynynen, A. Darkazanli, E. Unger, J.F. Schenck, "MRI-guided noninvasive ultrasound surgery", Medical Physics., 20(1), pp.107-15, 1993.
108. H.E. Cline, J.F. Schenck, K. Hynynen, R.D. Watkins, S.P. Souza, F.A. Jolesz, "MR-guided focused ultrasound surgery", J. Comput. Assist. Tomogr. 16, pp. 956–965, 1992.
109. Christakis Damianou, Kleanthis Ioannides, Nicos Milonas, "Positioning device for MRI-guided high intensity focused ultrasound system.", Volume 2, Issue 6, pp 335-345, 2008
110. T. Verghese, V. Palathinkara, M.B. Massat, J. McGill, M. Weichelt, "Innovation and Achievement in Advancing MR-guided Therapeutics", GE Signa Pulse, a GE Healthcare MR publication, pp.64-68, 2011.
111. Jolesz FA, Jakab PD., "Acoustic pressure wave generation within a magnetic resonance imaging system: potential medical applications.", J. Magn. Reson. Imag., 1(5):609-13, 1991
112. Hynynen K., Damianou C., Darkazanli A., Unger E., Schenck J., "The feasibility of using MRI to monitor and guide noninvasive ultrasound surgery", Ultrasound Med. Biol., Vol. 19 (1), pp. 91-92, 1992.
113. Hynynen K, Darkazanli A, Unger E, Schenck JF., "MRI-guided noninvasive ultrasound surgery.", Medical Physics, 20(1):107-15, 1993
114. Cline HE, Schenck JF, Hynynen K, Watkins RD, Souza SP, Jolesz FA., "MR-guided focused ultrasound surgery.", J. Comput Assist Tomogr., 16(6):956–965, 1992
115. Hynynen K, Darkazanli A, Damianou C, Unger E, Schenck JF., "The usefulness of a contrast agent and gradient-recalled acquisition in a steady-state imaging sequence for magnetic resonance imaging-guided noninvasive ultrasound surgery.", Invest Radiology, 29(10):897–903, 1994
116. Cline H, Ettinger R, Rohling K, Watkins R inventors General Electric Company, assignee. Magnetic resonance guided focussed ultrasound surgery. United States patent. US5247935. 1993.

117. Ettinger R, Cline H, Watkins R, Rohling K, inventors General Electric Company, assignee. Magnetic resonance guided ultrasound therapy system with inclined track to move transducers in a small vertical space. United States patent US5275165. 1994.
118. Cline H, Rohling K, Abeling W, inventors General Electric Company, assignee. Mechanical positioner for magnetic resonance guided ultrasound therapy. United States patent US5443068. 1995.
119. Yehezkeli O, Freundlich D, Magen N, Marantz C, Medan Y, Vitek S, Weinreb A, inventors, INSIGHTEC-TXSONICSLTD, assignee. Mechanical positioner for MRI guided ultrasound therapy system WO0209812. 2002.
120. Tempany CM, Stewart EA, McDannold N, Quade B, Jolesz F, Hynynen K., "MRI Guided Focused Ultrasound Surgery (FUS) of Uterine Leiomyomas: A Feasibility Study.", *Radiology*, 227:897-905, 2003
121. Stewart EA, Rabinovici J, Tempany C, Inbar Y, Regan L, Gostout B, Hesley G, Kim HS, Hengst S, Gedroyc W., "Clinical Outcomes of Focused Ultrasound Surgery for the Treatment of Uterine Fibroids, Fertility and Sterility.", 85(1):22-29, 2006
122. Kim HS, Baik JH, Pham LD, Jacobs MA., "MR-guided High-intensity Focused Ultrasound Treatment for Symptomatic Uterine Leiomyomata Long-term Outcomes.", *Acad Radiol.*, 18(8):970-6, 2011
123. Behera MA, Leong M, Johnson L, Brown H., "Eligibility and Accessibility of Magnetic Resonance guided Focused Ultrasound (MRgFUS) for the Treatment of Uterine Leiomyomas.", *Fertility & Sterility*, 94(5):1864-1868, 2010
124. Funaki K, Fukunishi H, Funaki T, Kawakami C. Mid-term Outcome of Magnetic Resonance-guided Focused Ultrasound Surgery for Uterine Myomas: From Six to Twelve Months After Volume Reduction, *J Minim Invasive Gynecol*, 2007;14(5):616-21.
125. Laveena Polina, Vinay Nyapathy, Anindita Mishra, Himabindu Yellamanthili, and Mythri P Vallabhaneni, "Noninvasive treatment of focal adenomyosis with MR-guided focused ultrasound in two patients.", *Indian J Radiol Imaging*, 22(2): 93–97, 2012
126. Rabinovici J, Inbar Y, Eylon-Cohen S, Schiff E, Hananel A, Freundlich D., "Pregnancy and live Birth after Focused Ultrasound Surgery for Symptomatic Focal Adenomyosis: A Case Report.", *Human Reproduction*, 21(5):1255-1259, 2006
127. Zini C, Elisabeth Hipp, Stephen Thomas, Alessandro Napoli, Carlo Catalano, Aytakin Oto., "Ultrasound- and MR-guided focused ultrasound surgery for prostate cancer.", *World J Radiology*, 28; 4(6): 247-252, 2012
128. Napoli A., Anzidei M., De Nunzio C., Cartocci G., Panebianco V, De Dominicis C, Catalano C, F Petrucci, C Leonardo, "Real-time Magnetic Resonance-guided High-intensity Focused Ultrasound Focal Therapy for Localised Prostate Cancer:Preliminary Experience.", *European Urology*, 395 – 398, 2013.

129. Gombos EC, Kacher DF, Furusawa H, Namba K., "Breast focused ultrasound surgery with magnetic resonance guidance.", *Top Magn Reson Imaging*, 17:181-188, 2006
130. Furusawa H, Namba K, Thomasen S, Akiyama F, Bendet A, Tanaka C, Yasuda Y, Nakahara H., "Magnetic resonance-guided focused ultrasound surgery of breast cancer: reliability and effectiveness." , *J Am Coll Surg*, 203(1):54-63, 2006
131. Khiat A, Gianfelice D, Amara M, Boulanger Y., "Influence of post-treatment delay on the evaluation of the response to focused ultrasound surgery of breast cancer by dynamic contrast enhanced MRI.", *The British Journal of Radiology*, 79:308-314, 2006
132. Gianfelice D, Abdesslem K, Boulanger Y, Amara M, Belblidia A., "MR imaging-guided focused ultrasound surgery of breast cancer: correlation of dynamic contrast-enhanced MRI with histopathologic findings.", *Breast Cancer Research and Treatment*, 82:93-101, 2003
133. Gianfelice D, Khiat A, Boulanger Y, Amara M, DES and Belblidia A., "Feasibility of magnetic resonance imaging-guided focused ultrasound surgery as an adjunct to tamoxifen therapy in high-risk surgical patients with breast carcinoma.", *Journal of Vascular and Interventional Radiology*, 14:1275-1282, 2003
134. Gianfelice D, Khiat A, Amara M, Belblidia A, Boulanger Y., "MR imaging-guided focused ultrasound surgery of breast cancer: correlation of dynamic contrast-enhanced MRI with histopathologic findings.", *Radiology*, 227(3):850-855, 2003
135. Hynynen K, Pomeroy O, Smith D, Huber P, McDannold N, Kettenbach J, Baum J, Singer S, Jolesz F., "MR imaging-guided focused ultrasound surgery of fibroadenomas in the breast: a feasibility study.", *Radiology*, 219:176-85, 2001
136. Okada A, Murakami T, Mikami K, Onishi H, Tanigawa, "A Case of Hepatocellular Carcinoma Treated by MR-guided Focused Ultrasound Ablation with Respiratory Gating.", *Magn Reson Med Sci.*, 5(3):167-71, 2006
137. Kopelman D, Inbar Y, Hanannel A, Dank G, Freundlic, "Magnetic Resonance-guided Focused Ultrasound Surgery (MRgFUS). Four Ablation Treatments of a Single Canine Hepatocellular Adenoma." *HPB*, 8:292-298, 2006
138. Napoli A, Anzidei M, Marincola BC, Brachetti G, Ciolina F, Cartocci G, Marsecano C, Zaccagna F, Marchetti L, Cortesi E, Catalano C., "Primary Pain Palliation and Local Tumor Control in Bone Metastases Treated With Magnetic Resonance-Guided Focused Ultrasound.", *Invest Radiology*, Volume48 – Issue 6, 2013
139. Lee JE, Yoon SW, Kim KA, Lee JT, Shay L, Lee KS., "Successful Use of Magnetic Resonance-Guided Focused Ultrasound Surgery for Long-Term Pain Palliation in a Patient Suffering from Metastatic Bone Tumor.", *J Korean Soc Radiol*, 65(2):133-138, 2011
140. Kopelman D, Inbar Y, Hanannel A, Pfeiffer RM, Dogadkin O, Freundlich D, Liberman B, Catane R., "Magnetic Resonance guided Focused Ultrasound

Surgery. Ablation of Soft Tissue at Bone – Muscle Interface in a Porcine Model.”, European Journal of Clinical Investigation, 38:268-275, 2008

141. Catane R, Beck A, Inbar Y, Rabin T, Shabshin N, Hengst S, Pfeffer RM, Hanannel A, Dogadkin O, Liberman B, Kopelman D., “MR-guided Focused Ultrasound Surgery (MRgFUS) for the Palliation of Pain in Patients with Bone Metastases-Preliminary Clinical Experience.”, *Annals of Oncology*, 18(1):163-7, 2006
142. Lipsman N., Schwartz M., Huang Y., Lee L., Sanka T., Chapman M., Hynynen K., Lozano A., “MR-guided focused ultrasound thalamotomy for essential tremor: a proof-of-concept study”, *Lancet Neurol*, 12: 462–68, 2013
143. Diederich CJ, Stafford RJ, Nau WH, Burdette EC, Price RE, Hazle JD. “Transurethral ultrasound applicators with directional heating patterns for prostate thermal therapy: In vivo evaluation using magnetic resonance thermometry.”, *Medical Physics*, 31:405–413, 2004
144. Pisani L, Ross A, Diederich C, Nau W, Sommer G, Glover G, Butts K, Effects of Spatial and Temporal Resolution for MR Image-guided Thermal Ablation of Prostate with Transurethral Ultrasound, *JMRI*, 2005 Jul;22(1):109-18.
145. Ross A, Diederich C, Nau W, Rieke V, Butts K, Sommer G, Curvilinear “Transurethral Ultrasound Applicator for Prostate Thermal Therapy Under MR Guidance.”, *Medical Physics*, 32(6):1555-65, 2005
146. Kinsey A, Diederich C, Tyreus PD, Nau W, Rieke V, Butts Pauly K, “Multisectored interstitial ultrasound applicators for dynamic angular control of thermal therapy.”, *Medical Physics*, 33(5):p1352-1363, 2006
147. Butts Pauly K, Diederich CJ, Rieke V, Bouley D, Chen J, Nau WH, Ross AB, Kinsey A, Sommer G, “MR-guided High Intensity Ultrasound Ablation of the Prostate, *Topics in Magnetic Resonance Imaging*.”, 17(3):p195-207, 2006
148. <http://www.healthcare.philips.com/main/products/mri/systems/sonalleve/applications.wpd>
149. Chopra R., Baker N., Choy V., Boyes A., Tang K., Bradwell D., and Bronskill M., “MRI-compatible transurethral ultrasound system for the treatment of localized prostate cancer using rotational control.”, *Medical Physics*, 35(4):1346-1357, 2008
150. Chopra R, Tang K, Burtnyk M, Boyes A, Sugar L, Appu S, Klotz L, Bronskill M. “Analysis of the spatial and temporal accuracy of heating in the prostate gland using transurethral ultrasound therapy and active MR temperature feedback.”, *Physics Medical Biology*, 54:2615–2633, 2009
151. Chopra R., Curiel L., Staruch R., Morrison L., Hynynen K., “An MRI-compatible system for focused ultrasound experiments in small animal models.” , *Medical Physics*, 36 (5),1867-1874, 2009.
152. McDannold M., Ziso H., Assif B., Hananel A., Vykhodtseva N., Gretton P., Pilatou M., Haker S., Tempany C., “MRI-guided focused ultrasound (MRgFUS)

system for thermal ablation of prostate cancer: Pre-clinical evaluation in canines, Energy-based Treatment of Tissue and Assessment V.", Thomas P. Ryan, Proc. of SPIE Vol. 7181 (February 23, 2009);

153. Chrsitos Yiallouras, Nicos Mylonas, Christakis Damianou, "MRI-compatible positioning device for guiding focus ultrasound system for transrectal treatment of prostate cancer.", DOI 10.1007/s11548-013-0964-x, 2013
154. C. Damianou, N. Milonas, K. Ioannides, "Positioning Device for MRI-guided high intensity focus ultrasound system.", CARS, 2:335-345, 2008
155. Mylonas N., and Damianou, C., "MR compatible positioning device for guiding a focused ultrasound system for the treatment of brain diseases.", Int. J. Med. Robotics Comput. Assist. Surg.. doi: 10.1002 /rcs.1501, 2013
156. www.imageguided.com
157. Krafft AJ, Jenne JW, Maier F, Stafford RJ, Huber PE, Semmler W, Bock M., "A long arm for ultrasound: a combined robotic focused ultrasound setup for magnetic resonance-guided focused ultrasound surgery.", Medical Physics, 37(5):2380-93, 2010
158. K. Chinzei, R. Kikinis and A. Jolesz, "MR Compatibility of Mechatronic Devices: Design Criteria: in Proc.", 2nd Int. Conf. Medical Image Computing and Computer –Assisted Interventions (MICCAI), pp.1020-1030, 1999
159. K. Chinzei, N. Hata, F.A. Jolesz, R. Kikinis, "MR Compatible Surgical Assist Robot: System Integration and Preliminary Feasibility Study.", Int Conf Med Image Comput Comput Assist Interv. (MICCAI), Pittsburgh, PA, USA, pp. 921-930, 2000
160. Hempel E, Fischer H, Gumb L, Höhn T, Krause H, Voges U, Breitwieser H, Gutmann B, Durke J, Bock M, Melzer A., "An MRI-compatible surgical robot for precise radiological interventions.", Comput. Aided. Surg., 8(40):180-191, 2003
161. Melzer A, Gutmann B, Remmele T, Wolf, R, Lukoscheck, A, Bock, M, Bardenheuer H, Fischer H., "INNOMOTION for percutaneous image-guided interventions: principles and evaluation of this MR- and CT-compatible robotic system.", IEEE Eng. Med. Biol. Mag., 27(3):66–73, 2008
162. Moche M, Zajonz D, Kahn T, Harald B., "MRI-guided procedures in various regions of the body using a robotic assistance system in a closed-bore scanner: preliminary clinical experience and limitations.", Jour. Magn. Reson. Imaging., 31(4):964–974, 2010
163. Li M Mazilu, D Horvath, KA., "Robotic system for transapical aortic valve replacement with MRI guidance.", Proc. of MICCAI '08 Lecture Notes in Computer Science. Springer, Vol.5242/2008, 476-484, 2008
164. Tsekos N, inventor. Regents of the University of Minnesota, assignee, MRI-guided interventional mammary procedures. United States patent. US 6,675,037. 2004.

165. Beyersdorff D, Winkel A, Hamm B, Lenk S, Loening SA, Taupitz M., "MR imaging-guided prostate biopsy with a closed MR unit at 1.5 T: initial results.", *Radiology*, 234:576–81, 2005
166. D'Amico AV, Tempany CM, Cormack R, "Transperineal magnetic resonance image guided prostate biopsy.", *Journal of Urology*, 164:385–7, 2000
167. Fischer GS, DiMaio SP, Iordachita II, Fichtinger G., "Robotic assistant for transperineal prostate interventions in 3 T closed MRI.", *Med Image Comput Comput Assist Interv Int Conf Med Image Comput Comput Assist Interv*, 10:425–33, 2007
168. Cleary K, Melzer A, Watson V, Kronreif G, Stoianovici D., "Interventional robotic systems: applications and technology state-of-the-art.", *Minim Invasive Ther Allied Technology*, 15:101–13, 2006
169. Stone NN, Roy J, Hong S, Lo YC, Stock RG., "Prostate gland motion and deformation caused by needle placement during brachytherapy." *Brachytherapy*, 1:154–60, 2002
170. Dattoli M, Waller K., "A simple method to stabilize the prostate during transperineal prostate brachytherapy.", *Int J Radiat Oncol Biol Phys*, 38:341–2, 1997
171. Stoianovici D, Song D, Petrisor D., "MRI stealth robot for prostate interventions.", *Minim. Invasive Ther. Allied Technol.* 16(4), 241–248, 2007
172. Mozer PC, Partin AW, Stoianovici D., "Robotic image-guided needle interventions of the prostate.2, *Rev. Urol.*, 11(1), 7–15, 2009
173. Zangos S, Herzog C, Eichler K., "MR-compatible assistance system for puncture in a high-field system: device and feasibility of transgluteal biopsies of the prostate gland.", *Eur. Radiol.*, 17(4), 1118–1124, 2007
174. Schouten MG, Ansems J, Renema WKJ, Bosboom D, Scheenen TWJ, Futterer JJ, "Introduction of a new method to image guided prostate biopsies: the MR-compatible transrectal prostate biopsy robot.", *Med. Phys.*, 2010
175. http://www.shinsei-motor.com/English/techno/ultrasonic_motor.html
176. <https://www.okw-web.com/products/desktop-eurocase/product/A0234670/>
177. <http://www.pewatron.com/en/products-solutions/power-supplies/>
178. Nobuhiko Hata, PhD, Masahiro Jinzaki, MD, Daniel Kacher, MS, Robert Cormak, PhD, David Gering, MS, Arya Nabavi, MD, Stuart G. Silverman, MD, Anthony V. D'Amico, MD, Ron Kikinis, MD, Ferenc A. Jolesz, MD, Clare M. C. Tempany, MD, "MR Imaging-guided Prostate Biopsy with Surgical Navigation Software: Device Validation and Feasibility.", *Radiology*, 220:263–268, 2001
179. A. Chanu, Student Member IEEE, E. Aboussouan, S. Tamaz and S. Martel, Member IEEE, "Sequence Design and Software Environment for Real-time Navigation of a Wireless Ferromagnetic Device using MRI System and Single

Echo 3D Tracking.”, Proceedings of the 28th IEEE EMBS Annual International Conference New York City, USA, Aug 30-Sept 3,2006

180. Junichi Tokuda, Gregory S. Fischer, Csaba Csoma, Simon P. DiMaio, David G. Gobbi, Gabor Fichtinger, Clare M. Tempany, and Nobuhiko Hata, “Software Strategy for Robotic Transperineal Prostate Therapy in Closed-Bore MRI.”, *Med Image Comput Comput Assist Interv.*, 11(Pt 2): 701–709, 2008
181. <http://www.mathworks.com/products/daq/> (Data Acquisition Toolbox)
182. <http://www.ni.com/pdf/products/us/371910b.pdf>
183. <http://jja-instruments.com/>
184. Madersbacher S, Marberger M., “High-energy shockwaves and extracorporeal high-intensity focused ultrasound.”, *J Endourology*, 17(8): 667–72, 2003
185. Saleh KY, Smith NB., “A 63 element 1.75 dimensional ultrasound phased array for the treatment of benign prostatic hyperplasia.”, *Biomed Eng Online*, 4(1):39, 2005
186. Lizzi F, Coleman J, Driller J, Franzen L, Jakobiec F, “Experimental, ultrasonically induced lesions in the retina, choroid, and sclera.”, *Invest Ophthalmol Visual Sci*, 205:350–360, 1978
187. Chapelon JY, Margonari J, Vernier F, Gorry F, Ecochard R, Gelet A, “In vivo effects of high-intensity ultrasound on prostatic adenocarcinoma.”, *Dunning R3327. Cancer Res*, 52(22):6353–6357, 1992
188. Ter Haar G, Sinnett D, Rivens I, “High intensity focused ultrasound: a surgical technique for the treatment of discrete liver tumors.”, *Phys Med Biol*, 34(11):1743–1750, 1989
189. Lele P, “A simple method for production of trackless focal lesions with focused ultrasound.”, *J Physiology*, 160:494–512, 1962
190. Vykhodtseva NI, Hynynen K, Damianou C, “Pulse duration and peak intensity during focused ultrasound surgery: theoretical and experimental effects in rabbit brain in vivo.”, *Ultrasound Med Biology*, 20(9):987–1000, 1994
191. Linke C, Carteensen EL, Frizzell LA, Elbdawi A, Fridd CW, “Localized tissue destruction by high intensity focused ultrasound.”, *Arch Surg*, 107(6):887–891, 1973
192. Hynynen K, Damianou CA, Colucci V, Unger E, Cline HH, Jolesz FA, “MR monitoring of focused ultrasonic surgery of renal cortex: experimental and simulation studies.”, *J Magn Reson Imag.*, 5(3):259–266, 1995
193. Damianou Christakis, PavlouM, Velev O, Kyriakou K, Trimikliniotis M., “High intensity focused ultrasound ablation of kidney guided by MRI.”, *J Ultrasound Medical Biology*, 30(3):397–404, 2004
194. Hynynen K, Pomeroy O, Smith DN, Huber PE, McDannold NJ, Kettenbach J, Baum J, Singer S, Jolesz FA., “MR imagingguided focused ultrasound surgery of

fibroadenomas in the breast: a feasibility study.”, *Radiology*, 219(1):176–185, 2001

195. J. Y. Chapelon, J. Margonari, Y. Theillkre, F. Gorry, F. Vernier, E. Blanc, and A. Gelet, “Effects of high-energy focused ultra- on kidney tissue in the rat and the dog,” *Eur. Urology*, VO~22. , pp. 147-152, 1992.

196. Gabriel H, Delongchamps N, Otis B, Ching W, Roza G, “The Worldwide Epidemiology of Prostate Cancer: Perspectives from Autopsy Studies.”, *Journal of Urology*, 15(1): 3866–3871, 2008